Effect of System Imperfections on the Performance of CDMA Receivers with CCI Cancellation

A Thesis

Submitted to the College of Graduate Studies and Research

in Partial Fulfillment of the Requirements

for the Degree of

Doctor of Philosophy

in the Department of Electrical Engineering

University of Saskatchewan

Saskatoon, Saskatchewan

By

P.C. John Panicker

Fall, 1996

UNIVERSITY OF SASKATCHEWAN
College of Graduate Studies and Research
SUMMARY OF DISSERTATION
Submitted in Partial Fulfillment
of the Requirements for the
DEGREE OF DOCTOR OF PHILOSOPHY
by

P.C. John Panicker
Department of Electrical Engineering
University of Saskatchewan
Fall 1996

Examining Committee:

Dr. S. Yannacopoulos	~~Dean/Associate Dean~~/Dean's Designate, Chair. College of Graduate Studies and Research
Dr. S.O. Kasap	Chair of Advisory Committee, Department of Electrical Engineering
Dr. S. Kumar	Supervisor, Department of Electrical Engineering
Dr. H.C. Wood	Department of Electrical Engineering
Dr. B. Daku	Department of Electrical Engineering
Dr. D. Eager	Department of Computational Science

External Examiner:
Dr. Paul H. Wittke
Department of Electrical Engineering
Queen's University, Kingston
Ontario K7L 3N6

Effect of System Imperfections on the Performance of CDMA Receivers with CCI Cancellation

Code Division Multiple Access (CDMA) is an emerging technology for future cellular and personal communication systems. Indoor radio communication is an integral part of personal communication systems. In an indoor CDMA system, the Co-Channel Interference (CCI) from other users of CDMA limits the system capacity and Bit Error Rate (BER) performance. Regeneration and cancellation of CCI from the received signal is an approach that improves capacity and BER performance.

CCI cancellation can be performed in single path correlator receiver and multipath combining RAKE receiver. In practice, there are system imperfections and their effect on the receiver performance has to be accurately evaluated. The power control error is modeled as log normal random variable. The estimate errors in channel parameters and spreading code phase are modeled as zero mean Gaussian random variables.

In this thesis, analysis is done initially on the effect of system imperfections on the BER performance of a CDMA system having correlator receiver and multipath combining RAKE receiver. The numerical results indicate that the BER performance degrades when the variance of normalized received power is above 0 dB, or the mean square of normalized estimate errors is above 0.01.

The effect of system imperfections on the performance of CCI canceling correlator and RAKE receiver is then analyzed. Numerical results indicate that significant improvement in system capacity is possible with two or three stages of CCI cancelers if the variance of the normalized received power is below 2 dB, or the mean square of normalized estimate errors is below 0.01. However, for CCI cancellation to be effective when all imperfections are present, the power control error and the estimate error has to be minimized. Computer simulations of indoor CDMA system are also performed to verify theoretical results. It is concluded that the simulated results are in agreement with the theoretical results for all practical values of signal to noise ratio. Simulation techniques based on importance sampling can be used to reduce considerably the computational burden involved in simulation of CDMA systems.

Copyright

Acknowledgements

I express my sincere gratitude to Professor Surinder Kumar, my research supervisor, who patiently guided this research and encouraged me during periods of frustration. Thanks are also due to other members of my research advisory committee, Professors Hugh Wood, Brian Daku, and Derek Eager for their keen interest and help during the preparation of this manuscript. I am grateful to all faculty members that I have come in contact with during my course work at University of Saskatchewan for the knowledge I have acquired from them.

I am indebted to my wife Annie for the many sacrifices she made and to my sons Aneesh and Praveen for bearing with me during the period of this research work. I thank my wife for making these years enjoyable. Also I express my gratitude and appreciation to my parents and brothers for their encouragement and moral support.

I gratefully acknowledge the financial support provided by the Canadian Commonwealth Scholarship and Fellowship Committee and I thank the committee for making my stay in Canada enjoyable and memorable. Finally, I wish to thank the management and staff of Telecommunication Research Labs, Saskatoon, Canada, for allowing me to use their facilities to carry out this research and for providing some financial support.

UNIVERSITY OF SASKATCHEWAN

Electrical Engineering Abstract 95A430

Effect of System Imperfections on the Performance of CDMA receivers with CCI Cancellation

Student: P.C. John Panicker

Supervisor: Dr. Surinder Kumar

Ph.D. Thesis Submitted to the

College of Graduate Studies and Research

January, 1996

Abstract

Code Division Multiple Access (CDMA) is an emerging technology for future cellular and personal communication systems. Indoor radio communication is an integral part of personal communication systems. In an indoor CDMA system, the Co-Channel Interference (CCI) from other users of CDMA limits the system capacity and Bit Error Rate (BER) performance. Regeneration and cancellation of CCI from the received signal is an approach that improves capacity and BER performance.

CCI cancellation can be performed in single path correlator receiver and multipath combining RAKE receiver. In practice, there are system imperfections and their effect on the receiver performance has to be accurately evaluated. The power control error is modeled as a log-normal random variable. The estimate errors in channel parameters and spreading code phase are modeled by zero mean Gaussian random variables.

In this thesis, analysis is done initially on the effect of system imperfections on the

BER performance of a CDMA system having correlator receiver and multipath combining RAKE receiver. Numerical results indicate that the BER performance degrades when the variance of normalized received power is above 0 dB, or the mean square of normalized estimate errors is above 0.01.

The effect of system imperfections on the performance of CCI canceling correlator and RAKE receiver is then analyzed. Numerical results indicate that significant improvement in system capacity is possible with two or three stages of CCI cancelers if the variance of normalized received power is below 2 dB, or the mean square of normalized estimate errors is below 0.01. However, for CCI cancellation to be effective when all imperfections are present, the power control error and the estimate error have to be minimized. Computer simulations of indoor CDMA system are also performed to verify theoretical results. It is concluded that the simulated results are in agreement with the theoretical results for all practical values of signal to noise ratio. Simulation techniques based on importance sampling can be used to reduce considerably the computational burden involved in simulation of CDMA systems.

Table of Contents

List of Figures

List of Tables

List of Abbreviations

AMPS	Advanced Mobile Phone Services
AWGN	Additive White Gaussian Noise
BER	Bit Error Rate
BLFSR	Binary Linear Feedback Shift Register
BPSK	Binary Phase Shift Keying
CCI	Co-Channel Interference
CDMA	Code Division Multiple Access
CT2	Cordless Telecommunication (second generation)
CT3	Cordless Telecommunication (third generation)
DECT	Digital European Cordless Telecommunication
DMF	Digital Matched Filter
DS	Direct Sequence
FCC	Federal Communication Commission
FDM	Frequency Division Multiplexing
FDMA	Frequency Division Multiple Access
IDS	Interference from Desired Signal
IS	Interim Standard
IS	Importance Sampling
ISI	Intersymbol Interference
MAI	Multiple Access Interference

MLSRS	Maximal Length Shift Register Sequence
MSE	Mean Square of normalized Error
PCS	Personal Communication Systems
PN	Pseudo-Noise
PSD	Power Spectral Density
RF	Radio Frequency
SNR	Signal to Noise Ratio
SS	Spread Spectrum
TDMA	Time Division Multiple Access
TPC	Transmitter Power Control
TIA	Telecommunication Industry Association
UPDC	Universal Portable Digital Communication
VLSI	Very Large Scale Integration
XOR	Exclusive-OR

1. Introduction

1.1 Background

The invention of the telegraph and telephone in the nineteenth century were the first steps towards shattering the barriers of space and time in communication between individuals. The next step was the successful deployment of radio communications. However most people are still restricted to telephone sets or "fixed wireline" equipment for communication and therefore the location barrier has not been yet surmounted fully. The astonishing success of cellular radio in the last decade in providing telecommunication services with mobile and hand held portable units has paved the way towards breaking location barriers in telecommunications. At the beginning of 1990, there were approximately 4.5 million cellular telephones, 6.5 million pagers and 25 million cordless telephones in the United States [1]. By the end of 1992, the number of cellular telephones in the US had risen to 11 million, an increase of 150% in three years. Total worldwide shipment of cordless units could exceed 200 million annually by the turn of the century and 300 million by 2010 [2]. The ultimate goal of Personal Communication Services (PCS) is to provide instant communication any time between individuals located anywhere in the world. Realization of pocket sized telephone units and subsequent wrist-watch phones are major communication frontiers. Industry and research organizations worldwide are

collectively facing great challenges in providing PCS.

An important consideration in successful implementation of a PCS is indoor radio communication which involves the transmission of voice and data to and from people moving inside buildings. Indoor radio communication covers a wide variety of situations ranging from communication with individuals walking in residential or office buildings, supermarkets or shopping malls, to fixed stations sending messages to robots in motion in assembly lines and factory environments of the future [3].

Network architectures for in-building communications are evolving rapidly. Systems such as Digital European Cordless Telecommunication (DECT), and the Cordless Telecommunications second and third generations (CT2 and CT3), are primarily in-building communication systems. Universal Portable Digital Communication (UPDC) in the US calls for unification of indoor and outdoor communication into an overall integrated system. Practical portable radio communication requires low power and light weight units. Digital communication technology can meet this requirement in addition to offering many other advantages.

In an indoor wireless communication system, a fixed antenna (base station antenna) installed in an elevated position communicates with a number of portable radios inside the building. As a result of reflection, refraction and scattering of radio waves by structures inside a building, the transmitted signal often reaches the receiver by more than one path, resulting in a phenomenon known as multipath fading. In narrow-band transmission, the multipath effect causes fluctuations in the received signal envelope and phase. In wide-band transmission, the effect is to pro-

duce a series of delayed and attenuated pulses for each transmitted pulse. Multipath fading seriously degrades the performance of communication systems operating inside buildings. If the multipath environment is well characterized, the transmitter and receiver can be designed to match the channel and thus the effect of multipath disturbances can be reduced.

As wireless services are developed for indoor environments, the potential demand increases dramatically. Thousands of active users per square kilometer are possible in core urban areas where multilevel office buildings are in abundance. Under such conditions, the bandwidth issues become acute and new technologies are needed to utilize efficiently the available bandwidth.

1.2 Multiple Access Techniques

The term "multiple access" refers to the situation where many users share a common facility or channel. Wireless multiple access communication systems generally fall into one of the following three categories:

- FDMA(Frequency Division Multiple Access): The available bandwidth is divided into channels by frequency. Each channel continuously occupies a fraction of the total bandwidth. Advanced Mobile Phone Service (AMPS), the first generation of mobile radio services, is an example of a system that employs FDMA.

- TDMA (Time Division Multiple Access): The available bandwidth is divided into slots by time. Each channel occupies the entire available bandwidth for a

fixed fraction of the time within each time period. The second generation of mobile radio services based on Interim Standard (IS)-54-B employs TDMA.

- CDMA (Code Division Multiple Access): This system is more commonly known as spread spectrum multiple access and in such a system all channels occupy the entire available bandwidth simultaneously. Unique codes are used by transmitters to spread the information signal over a large frequency range. Receivers use a synchronized version of these codes to de-spread the information signal. By de-spreading, the interfering signals from other channels appear as wide-band noise to the de-spread narrow-band desired information signal. The choice of CDMA is attractive because of potential capacity increase, low power requirement, privacy, and the capability to avoid multipath fading [4]-[8]. Recently, the Telecommunication Industry Association (TIA) has developed a standard, IS-95, for mobile cellular spread spectrum communication systems [9]. Field trials suggest that the capacity can be increased by a factor of 10 over a conventional AMPS system [10].

1.3 Indoor CDMA System

Basically, an indoor CDMA system consists of portable transmitters, indoor channels, and receivers. Each portable transmitter in a cell is given a unique spreading code. Using this code, each portable transmitter spreads the information (voice or data) signal so that it will occupy the entire system bandwidth. This is commonly done using the Direct Sequence Spread Spectrum (DS SS) technique. At

the receiver, signals other than the desired user signal act as interference signals and such signals are collectively referred to as the Co-Channel Interference (CCI). The co-channel interference results from the cross-correlation between the spreading codes of the desired and interfering users. Cross-correlation among the codes is an important criterion in the selection of the code set for CDMA. Gold sequences [11] and Kasami codes [12] have low cross-correlation values, so these particular codes are extensively used in CDMA applications. Spreading codes, their generation, and their cross-correlation properties are described further in Chapter 2.

Portable units communicate with one another through a base station. The communication link from the base station to a portable is referred to as the "forward link", or the "down link", and the link from a portable to the base station is referred to as the "reverse link", or the "up link". One significant problem in the reverse link is that of the "near-far" effect. This relates to the problem of very strong signals at the base station receiver from nearby portables predominating over the weaker signals from far away portables. To avoid the "near-far" problem, elaborate power control techniques are employed to control the transmitter power level of the portables so that a portable's signal arrives at the base station with the required amount of Signal to Noise Ratio (SNR). In IS-95, both open loop and close loop power control techniques are employed. Power control is discussed further in Chapter 2.

1.3.1 Indoor Channel

The DS SS signal transmitted from a portable transmitter propagates through the indoor channel before it is received by the base station receiver. Due to the presence of reflectors and scatterers of electromagnetic waves (such as walls, doors, ceilings, and people) in the indoor environment, signals reach the base station through multiple propagation paths. Three most important multipath issues for the digital cellular system designer are the following:

1. Random phase shift, which creates rapid fluctuations in signal strength known as Rayleigh fading.

2. Random frequency modulation due to different Doppler shifts for different paths.

3. Delay spread of the received signal.

In indoor channels, the Doppler shift in frequency of the received signal is generally less than that in land mobile channels because of the much lower speed of the mobiles. The indoor channel is, therefore, referred to as a slowly varying channel. The coherence bandwidth of a channel is approximately defined as the reciprocal of the delay spread. The channel is frequency selective if the signal bandwidth is greater than the coherence bandwidth of the channel. A DS SS modulated signal in an indoor channel can be considered frequency selective. A slowly varying frequency selective indoor channel model is used in this thesis for analysis and simulation.

An advantage of using direct sequence spread spectrum is that two paths with a propagation delay difference greater than the reciprocal of the spread spectrum bandwidth can be resolved at the receiver in the time domain. These resolved paths have independent fading and can be suitably processed by the receiver to improve SNR. This method is commonly referred to as spread spectrum diversity reception. As described in the next subsection, CDMA receiver structures differ in the method of processing these signals.

1.3.2 CDMA Receiver Structures

There are two principal types of CDMA receivers: correlator receivers that suppress the effects of multipath signals and multipath combining RAKE receivers that take full advantage of the diversity offered by spread spectrum modulation. A correlator receiver is aligned to one of the multipath signals, and signals from any other path with a time delay of one spreading code chip duration or more are suppressed. Correlator receiver structures are simple, but they are inferior in performance. In a RAKE receiver, all path signals are combined so as to accentuate credible signals and suppress signals which are less credible. RAKE receivers are complex because they require channel parameter estimation. RAKE receivers are generally superior in performance.

It is desirable to have an indoor CDMA system with capacity as high as possible. Methods for improving the capacity are discussed in the next subsection.

1.3.3 Methods of Improving CDMA Capacity

There are several methods available for increasing the capacity of a CDMA system. Some of these methods are as follows:

- Cell Size Reduction: The capacity of a CDMA cellular system and any system based on cell architecture can be increased by reducing the cell size. In order to accommodate high user densities in indoor environments, 'micro' cells or 'pico' cells are required. A fortuitous and desirable characteristic of small cell size is the reduced power required by the portables. This extends battery life and allays concerns about the health risks associated with high power electromagnetic radiations. The main drawbacks of small cell size are the increased number of base stations required, and the increased number of hand-offs required as a portable moves from cell to cell.

- Cell Sectorization: A method of organizing cells suited for CDMA applications in particular, is to divide the cell into a number of sectors and to use highly directive antennas to receive the signal from portables in each sector. This scheme reduces the interference signal received in each sector antenna and this results in more cell capacity.

- Voice Activity Monitoring: A major share of interference in a CDMA system is created by the users of the same cell utilizing the same bandwidth. If transmitters cease transmitting during periods of silence (voice inactivity), the co-user interference can be reduced and more users can be accommodated

into the given bandwidth.

- Co-Channel Interference (CCI) Regeneration and Cancellation: Another approach for increasing system capacity, still in the research stage, is the regeneration of CCI signals and their subsequent cancellation at the receiver input. This technique is especially suited to the reverse link where the near-far effect considerably reduces link capacity. CCI regeneration and cancellation alleviates the need for stringent power control techniques and has the potential of increasing the capacity significantly. This method of improving capacity is examined in detail in Chapters 4-6.

1.3.4 System Imperfections

In order to realize maximum capacity and the best possible Bit Error Rate (BER) performance, CDMA systems would require ideal conditions of operation. These ideal conditions of operation include:

- perfect transmitter power control so that all user signals arrive at the base station with equal power,
- perfect estimation of the spreading code phase of each user, and
- perfect channel parameter estimates (path amplitudes and phases) for multipath combining at the receiver.

One or more of these factors can be imperfect in a realistic indoor mobile environment. It is of practical importance to include the effect of system imperfections

in the analysis of the performance of CDMA receivers. Such an analysis will give more accurate and realistic results on the BER performance and capacity.

1.4 Literature Review

There is considerable literature on the BER performance and capacity of CDMA systems with two commonly used receivers known as the single path correlator, and the multipath combining RAKE receiver. An analysis of phase-coded CDMA communication in a single path channel has been presented by Pursley [13]. In this analysis, emphasis is placed on average performance and the result reveals the spreading code parameters that have the greatest impact on communication system performance. These code parameters are analyzed and previously known bounds and computational techniques for such parameters are surveyed by Sarwate [14]. The effect of multipath fading on the performance of DS CDMA systems has been analyzed by Turin [15]. It is shown that for single path non-fading links using DS CDMA, Differential Phase Shift Keying (DPSK) modulation, and power control, the maximum number of simultaneous users is 10-20% of the spreading gain at a BER of $10^{-3} - 10^{-5}$. It is also shown that in a multipath fading channel, without power control, the number of simultaneous users falls to 1-5% of the spreading gain even with ideal multipath combining receivers. A binary DS CDMA communication system with coherent correlation receiver is analyzed by Lehnert [16]. An approach for obtaining arbitrarily tight upper and lower bounds on the average probability of error is described in this reference.

Lehnert [17] has developed a method of analysis for multipath combining receiver for DS CDMA communications through a specular multipath channel. The performance of a multipath combining receiver is determined for the case of a single transmitter and also for the case of multiple transmitters. The performance is determined in terms of parameters of the signature sequences. Chase [18] has analyzed the performance of a DS SS scheme employing random orthogonal codes over a fading multipath indoor channel. It is illustrated that the RAKE receiver structure can exploit the implicit spread spectrum diversity, but knowledge of the channel is necessary to prevent excessive complexity. The effects of RAKE receiver structure, multiple users, power control, and code length on the average probability of error are also analyzed in this reference.

Similarly, a large body of information is available about CCI canceling receivers. Theoretical analysis of a CCI canceling CDMA receiver based on Digital Matched Filtering (DMF) in a single path channel is presented by Mowbray [19]. It is shown that at a BER of 10^{-4}, single and two stage cancellation receivers have 40% and 50% capacity respectively, compared to 10% capacity with conventional DMF receivers.

Yoon [20] has analyzed a CDMA correlator receiver with post-correlation cancellation of CCI in a multipath fading channel. Perfect power control and spreading code phase acquisition has been assumed, but the effect of path amplitude and phase estimation error has been considered. Kaul [21] has presented a closed form BER formula for a multi-stage interference cancellation scheme in a single path channel using a standard Gaussian approximation for multiple access interference. Analysis

of a simple successive interference cancellation scheme in a DS CDMA system with coherent BPSK modulation is presented by Patel [22]. It is shown that a simple successive interference cancellation scheme can effectively estimate and cancel a DS CDMA signal and thus substantially reduce the near-far effect and increase the capacity. The author stresses the need for further work to analyze the processing delay involved in the scheme and also to assess the sensitivity of the scheme to system errors. An enhanced version of DS CDMA referred to as CDMA-IC has been proposed by Everbring [23]. The method is to detect signals in a decreasing order of signal strength and during that process subtract the already detected signals from the received signal. By using this technique an estimated capacity of 40 times that of AMPS is claimed. Cascaded CCI canceling and diversity combining for CDMA over a multipath fading channel has been analyzed by Kohno [24] assuming perfect conditions of system operation. The results show that, with perfect channel estimates and power levels within ± 1 dB of a required standard level, the BER performance of the RAKE receiver approaches that of the single user case, with two stages of CCI cancelers.

The topic of BER performance prediction using computer simulation is also widely reported [25]-[31]. In [25] and [26], tutorial expositions of the different techniques for estimating BER in simulations of a digital communication system are given. A modified Monte-Carlo simulation technique based on importance sampling for an AWGN channel is given by Shanmugam [27]. An improved form of importance sampling is proposed by Lu [28] for use in AWGN channels. Problems

involved in the use of importance sampling for complex systems involving a number of inputs and error sources are considered by Hahn [29]. Some of the simulation issues for future wireless modems for mobile communication are addressed by Woerner [30]. Some reduced computational complexity techniques for CDMA systems are also mentioned in this reference. Results from Monte-Carlo simulation of DS SS for indoor radio communication in a Rician fading channel are given by Misser [31]. This paper points out that the difference in BER obtained using analysis using a standard Gaussian approximation and that obtained using simulation is small and concludes with the observation that standard Gaussian approximation can be used to obtain the performance analytically because this method is much faster compared to full simulation of CDMA systems.

From the above literature review, it is clear that the analysis of the effect of combined imperfections in power control, channel estimation and spreading code phase acquisition on the performance of correlator and multipath combining receivers in frequency selective indoor channels has not been reported. These types of imperfections are present in a practical system and an analysis that accurately estimates the effect of such imperfections on the performance of the two most commonly used receiver structures, the correlator and multipath combining receivers, will provide results that are representative of the expected performance in practice.

Similarly, analysis of the effect of system imperfections on the performance of another type of interference cancellation receiver namely, the parallel pre-correlation CCI canceling DS CDMA receiver, has not been reported in the literature. The ef-

fect of these system imperfections on the performance of a CCI canceling DS CDMA receiver with multipath diversity combining has also not been analyzed. Such an analysis will address the question of the magnitude of power control imperfections such a CCI cancellation scheme can tolerate and still provide the desired capacity improvement. It will also provide limits on the mean square error in channel estimation and spreading code phase estimation for the CCI regeneration and cancellation to be effective.

From the literature review, it is clear that the results of simulation have not been reported on the effect of system imperfections on BER performance of CDMA systems operating in a frequency selective Rayleigh faded indoor channel. Similarly, no comprehensive strategy for the use of the importance sampling technique to BER performance evaluation of an indoor CDMA system has been developed.

1.5 Research Objectives

The objectives of the research work reported in this thesis are the following:

1. Analyze the effect of imperfections in transmitter power control, carrier phase estimation, and spreading code phase estimation on the BER performance of a CDMA correlator receiver in a frequency selective slow Rayleigh fading indoor channel.

2. Analyze the effect of imperfections in transmitter power control, channel parameter estimation, and spreading code phase estimation on the BER per-

formance of a multipath combining CDMA RAKE receiver in a frequency selective slow Rayleigh fading indoor channel.

3. Develop an analysis for the BER performance of a pre-correlation CCI canceling CDMA correlator receiver with imperfections in power control, channel parameter estimation, and spreading code phase estimation in a frequency selective slow Rayleigh fading indoor channel.

4. Analyze the effect of imperfections in transmitter power control, channel parameter estimation, and spreading code phase estimation on the BER performance of a CCI canceling multipath combining CDMA RAKE receiver in a frequency selective slow Rayleigh fading indoor channel.

5. Develop simulation programs using Monte-Carlo and importance sampling methods to evaluate BER performance of indoor CDMA receiver structures and to verify the analytical results.

1.6 Thesis Outline

In addition to this introductory chapter, this thesis contains six more chapters. In Chapter 2, the transmitter, the channel, and the receiver for an indoor CDMA system are described in detail. The system imperfections and the models adopted to take into account these imperfections in the analysis are also explained in this chapter. In Chapter 3, the effects of system imperfections on the BER performance of a simple CDMA correlator and multipath combining CDMA RAKE receiver are analyzed. The BER is computed to evaluate the effect of each system imperfection

individually as well as in combination. The concept of co-channel interference regeneration and cancellation in a CDMA system is introduced in Chapter 4. The performance analysis for a CDMA correlator receiver with pre-correlation cancellation of CCI is also developed in this chapter. The effects of system imperfections on the performance of such a receiver are included in the analysis. The BER is computed to evaluate the performance of such a receiver with and without system imperfections. In Chapter 5, the effect of system imperfections on the performance of a CCI canceling CDMA RAKE receiver is analyzed. Numerical computations of BER are included to evaluate the performance of such receivers with and without system imperfections. Chapter 6 contains a simulation study of indoor CDMA system BER performance. This chapter also includes the methodology of using importance sampling for BER evaluation. The BER results of receivers with and without CCI cancellation, and in the presence and absence of system imperfections, are included in this chapter. Finally, conclusions and directions for future work are given in Chapter 7.

2. Indoor CDMA Systems

The need for indoor CDMA wireless communication was identified in Chapter 1. In this chapter, digital modulation and spread spectrum concepts are briefly discussed. This is followed by an examination of spreading codes used for CDMA and their cross-correlation properties. A brief description of the indoor radio channel and various factors that degrade the transmitted signals in such channels are included. Different receiver structures used in CDMA applications are also considered. Finally, the system imperfections and their effect on the receiver performance are discussed.

2.1 Digital Modulation

Digital modulation is the process by which digital symbols are transformed into signal waveforms that are compatible with the characteristics of the channel. In the case of baseband modulation, these waveforms are pulses. In the case of bandpass modulation, the information signal modulates a sinusoidal signal waveform called a carrier. Use of a high frequency carrier can reduce the dimensions of the antenna used for radiating the radio frequency signal into space. Bandpass modulation results in other important advantages such as:

1. Different information signals may be separated by using different frequency signals. Such a method is termed Frequency Division Multiplexing (FDM).

2. Bandpass modulation can be used to place an information signal in a frequency band where design requirements, such as filtering and amplification, can be easily met.

3. Modulation techniques such as spread spectrum modulation can also be used to minimize the effects of interference.

Two types of digital modulation techniques that are relevant to the CDMA system study in this thesis are Spread Spectrum (SS) modulation and Binary Phase Shift Keying (BPSK) modulation. BPSK is explained in the next subsection. SS modulation is considered in Section 2.2.

2.1.1 Binary Phase Shift Keying

In bandpass modulation, an RF carrier signal's amplitude, frequency, phase or a combination of them is varied in accordance with the digital information to be transmitted. A carrier signal can be written as

$$s(t) = A(t)\cos\left(\omega_o t + \phi\left(t\right)\right), \tag{2.1}$$

where $A(t)$ is the time varying amplitude, ω_o is the radian frequency, and $\phi(t)$ is the phase. In phase modulation, the phase $\phi(t)$ is varied in accordance to the digital symbol. Binary phase shift keying is the simplest form of phase shift keying; in binary phase shift keying, binary symbols '1' and '0' are used to select the phase $\phi(t)$ of the carrier in Equation (2.1) to be 0 degrees and 180 degrees respectively.

Thus for a binary symbol of duration T, the BPSK modulated carrier signal may be written as

$$s(t) = \pm A(t)\cos(\omega_o t + \phi), \tag{2.2}$$

for $0 \leq t \leq T$. The waveform in Figure 2.1(a) shows a typical BPSK waveform with its abrupt phase changes at symbol transitions. This figure illustrates the situation when the modulating data stream is 1011 with symbol duration T. Initial phase of the carrier, ϕ is assumed to be zero at $t = 0$ in this figure. The schematic in Figure 2.1(b) shows the signal vectors s_1 and s_2 corresponding to digital symbols '1' and '0'. The truth table for phase transition is shown in Figure 2.1(c). At the receiver the signal arrives with an arbitrary initial phase. When the phase of the RF carrier is recovered and then used for the detection process, it is referred to as coherent detection. When the receiver does not utilize such phase information, the process is called noncoherent detection. Coherent detection generally leads to better performance.

2.2 Spread Spectrum Communication Systems

In a large number of radio communication systems, the receiver thermal noise is a major source of performance degradation. Such systems are usually designed to be power and bandwidth efficient which means that minimum signal power and bandwidth necessary to achieve the desired performance is employed. In Spread Spectrum (SS) communication systems [32] - [35], the information signal is spread over a bandwidth much wider than that required to achieve communication when

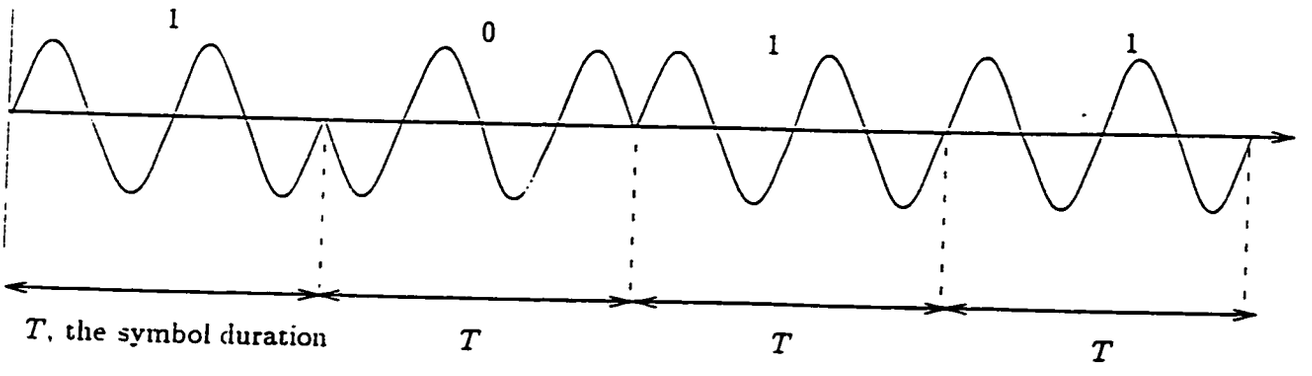

(a)

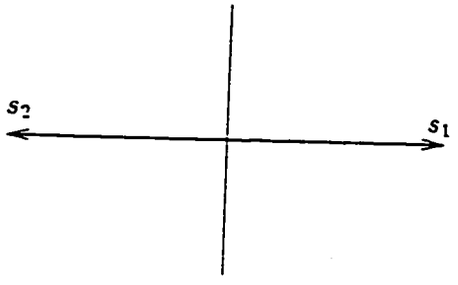

(b)

Digital symbol	Phase of the carrier
1	0
0	π

(c)

Figure 2.1 Binary phase shift keying (BPSK) modulation. (a) BPSK signal waveform. (b) BPSK signal vector representation. (c) Table defining the phase transition.

only thermal noise is present. This is also done to overcome other impairments such as intentional jamming, multipath propagation etc. A formal definition that reflects the basic characteristics of SS is given as [35]:

> Spread spectrum is a means of transmission in which signal occupies a bandwidth much in excess of the minimum necessary to send the information; the spreading is accomplished by means of a code which is independent of data. Synchronized reception with the code at the receiver is used for de-spreading and subsequent data recovery.

Experiments on transmission of signals using noise-like waveforms were performed by Mortimer and Rogoff [36] in the late 1940s and early 50s; the early spread spectrum communication systems were developed in the mid 1950s for military applications. Because of defense applications, there was a considerable amount of secrecy involved and spread spectrum technology was not widely available. Recently, some of the potential of SS in commercial applications such as indoor and mobile communication has been realized [4, 5, 7]. Interest in these applications has been spurred by the ruling of the U.S. Federal Communications Commission (FCC) that permits the use of SS in the 900 MHz, 2 GHz, 4.4 GHz and 5.725 GHz bands without a formal license [3]. A SS signal spread over a wide bandwidth has low power density. If different users employ different codes to spread the information signal, spread signals from all these users can co-exist in the same bandwidth. This technique is referred to as Code Division Multiple Access (CDMA).

2.2.1 Direct Sequence Spread Spectrum

In a typical DS SS, the bipolar information signal $b(t)$ is spread in bandwidth by using a bipolar Pseudo-Noise (PN) spreading code, $a(t)$. This is followed by BPSK carrier modulation resulting in the transmitted signal given by

$$s(t) = \sqrt{2P}b(t)a(t)\cos\omega_o t, \tag{2.3}$$

where P is the power of the carrier signal and ω_o is its radian frequency. This process is illustrated in Figure 2.2(a). The phase values of the carrier for various combinations of information signal $b(t)$ and PN code $a(t)$ are shown in Figure 2.2(b). The bandwidth of the transmitted signal $s(t)$ is much larger than the minimum bandwidth required to transmit the information signal $b(t)$, assuming that the bandwidth of the spreading signal $a(t)$ is much larger than the bandwidth of $b(t)$. The received signal contains the desired signal as well as the interference caused by other users in the system and the white Gaussian noise. With a transmission delay of T_d, the received signal may be written as

$$\begin{aligned} r(t) &= A\sqrt{2P}b(t-T_d)a(t-T_d)\cos[\omega_o(t-T_d)+\phi] + \text{interference} + n(t), \\ &= A\sqrt{2P}b(t-T_d)a(t-T_d)\cos[\omega_o t+\psi] + n'(t), \end{aligned} \tag{2.4}$$

where A represents the attenuation in the channel, $\psi = \omega_o T_d + \phi$ and $n'(t) = n(t) + \text{interference}$. The received signal is multiplied by a carrier $\cos(\omega_o t + \hat{\psi})$ where $\hat{\psi}$ is an estimate of ψ. It is then filtered and de-spread by correlating with

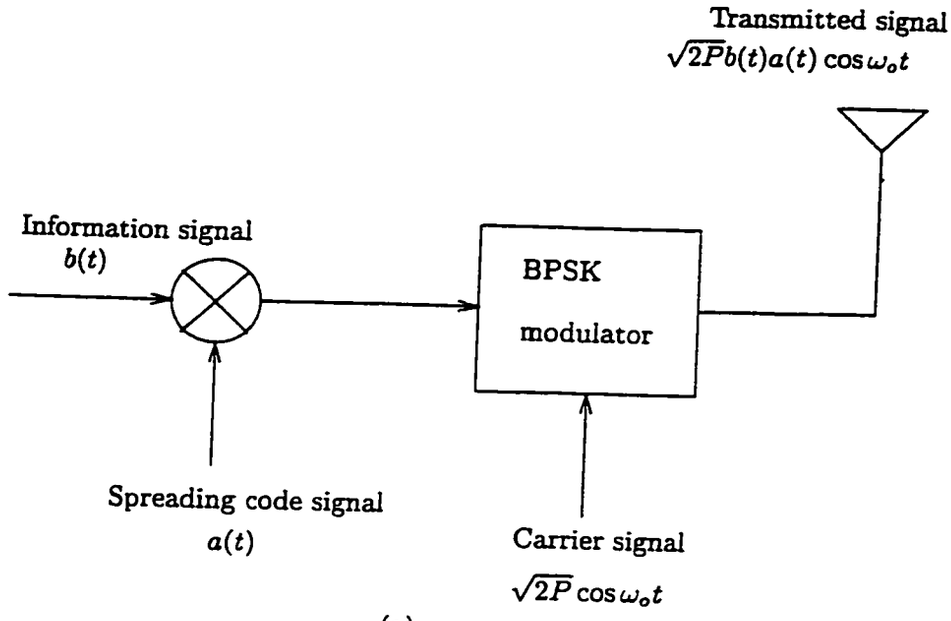

(a)

$b(t)$	$a(t)$	Phase of the carrier
-1	-1	0
1	-1	π
-1	1	π
1	1	0

(b)

Figure 2.2 (a) Simplified block diagram of DS SS transmitter. (b) Phase of the carrier signal for the combination of information and spreading code signal.

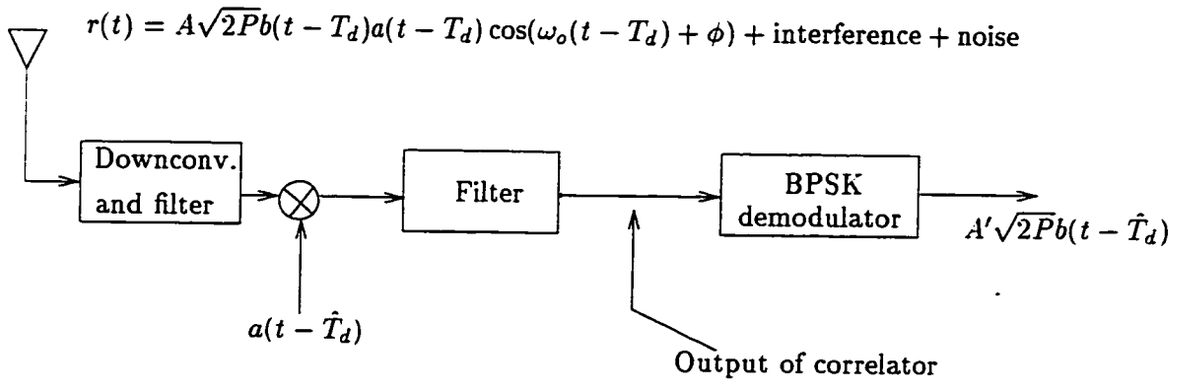

Figure 2.3 A simplified block diagram of DS SS receiver.

a synchronized replica of the spreading code $a(t-\hat{T}_d)$ where $\hat{T}_d$ is an estimate of T_d. This process is illustrated in Figure 2.3. De-spreading also results in separation of the desired signal from other user signals. This is then followed by BPSK data demodulation. When $\hat{\psi} = \psi$ and $\hat{T}_d = T_d$, the ouput signal is equal to $A'\sqrt{\frac{P}{2}}b(t-T_d)$, the transmitted information signal with a scaling factor.

Signal spectra in Figure 2.4 provide further insight into the spreading and de-spreading processes. The spectrum of the spread information signal and the spectrum of deliberate interference, called a jammer signal, are shown in Figure 2.4(a). The spectrum of the information signal is de-spread into a small bandwidth as shown in Figure 2.4(b) while the jammer signal remains spread over a wide frequency band. Only a small amount of spread jammer signal is present in the information signal bandwidth. It is thus easier to recover the signal from interference.

Spreading of the signal results in many useful properties. Some of these are the following:

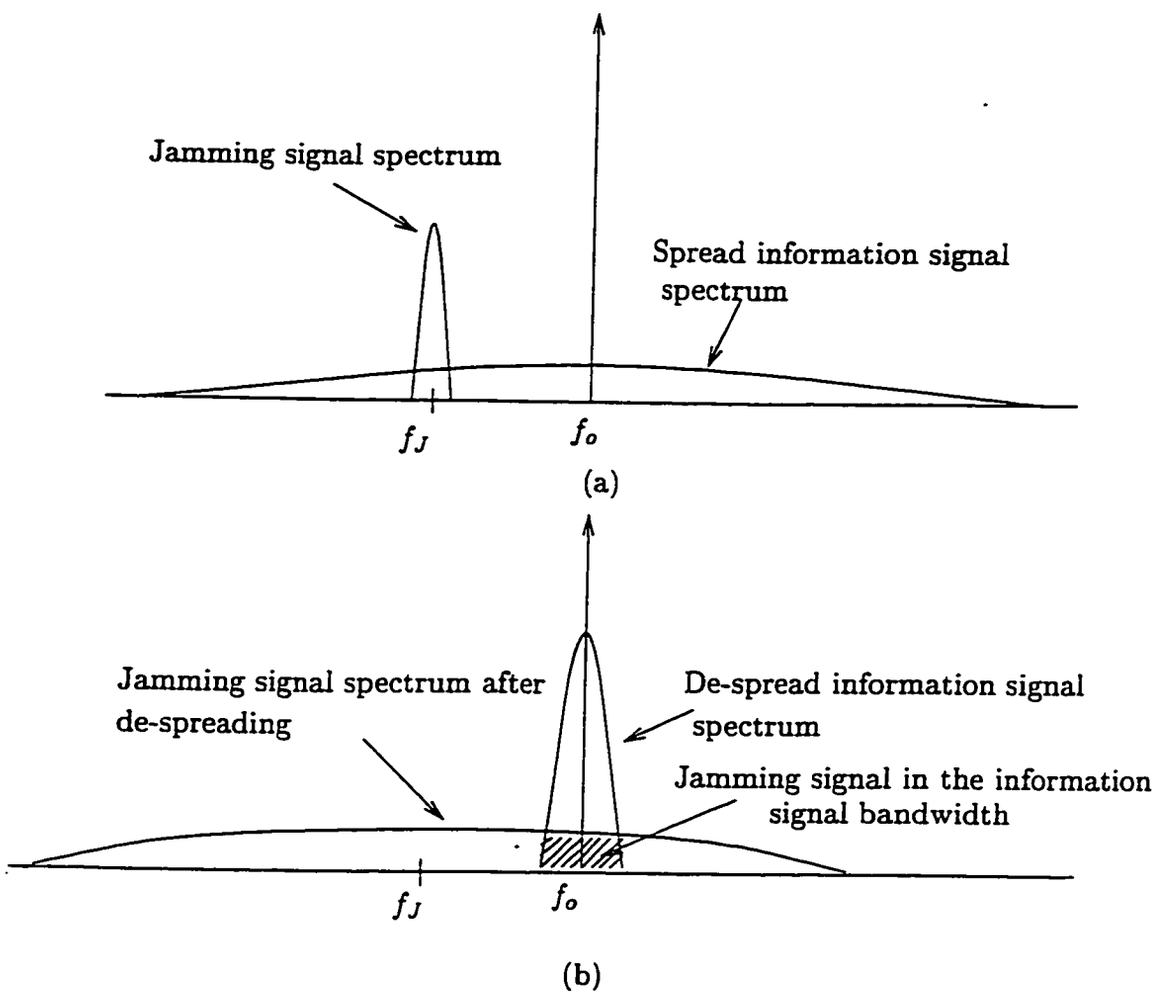

Figure 2.4 Power spectra of the desired signal and the jamming signal in a spread spectrum system. (a) Received signal spectrum. (b) Spectrum after de-spreading.

- Anti-jamming and anti-interference: Intentionally produced interference is referred to as jamming. Unintentional interference which is referred to simply as interference includes self interference caused by multipath propagation and cross interference caused by other users of the same bandwidth. Anti-jamming and anti-interference properties of SS result from spreading at the transmitter and subsequent de-spreading in the receiver. A jamming signal is generally a high power narrow bandwidth radio frequency signal. When a received signal containing a jammer signal is multiplied by the de-spreading code in the receiver, the spectrum of the desired signal is collapsed to the narrow information bandwidth whereas the spectrum of the jamming signal is spread over a wide bandwidth. As a result, the de-spread jamming signal has little energy remaining in the information bandwidth. In contrast to jamming, interference is a wide-band signal having the same bandwidth as the required signal. The interference signal will not be de-spread to a narrow bandwidth unless a synchronized spreading code corresponding to that of the wide-band interference signal is used in the receiver. This results in a major portion of the energy in the information bandwidth being due to the desired signal, and only a small portion being due to interference.

- Multipath diversity: A spread spectrum signal is a wide-band signal. Usually, the bandwidth is larger than the reciprocal of the difference between path time delays in an indoor environment. This means that by using SS modulation the individual paths in a multipath channel can be resolved in time. These

resolved paths will have independent fading and can be combined in a diversity combining receiver, known as a RAKE receiver, to improve the signal to noise ratio. The RAKE receiver is explained in a subsequent section.

- Privacy and secrecy: If the spreading code used is not known to anyone other than the desired user, de-spreading and subsequent information recovery by others is not possible. This aspect of SS provides some security for the communication, however, it is not as secure as using encryption because the spreading code can be recovered from the signal using some sophisticated signal processing.

- Multiple access: As stated before, spread spectrum modulation can be used to implement CDMA. In contrast to FDMA and TDMA, in CDMA all the users of the system occupy the whole bandwidth all the time. This thesis deals with CDMA application of spread spectrum, and the principle of CDMA is described in greater detail in the next section.

2.2.2 Code Division Multiple Access

The need for multiple access arises when a number of independent users are required to convey their messages through a common facility. An example is an indoor mobile wireless communication system where the portable transceivers must communicate with a central base station. FDMA and TDMA are two classical methods of providing multiple access; CDMA is accomplished by means of SS. In this system, each user is assigned a particular code for spreading the information

signal. Different codes for each user enables separation of messages at the receiving point.

A DS CDMA is shown in Figure 2.5. An attractive feature of CDMA is that, unlike in TDMA, it does not require network synchronization. Adding users to the system is relatively easy. In contrast to FDMA and TDMA, CDMA does not have a sharply defined system capacity. As the number of users increases, the signal to interference ratio decreases and there is a gradual degradation in performance until the SNR falls below some threshold value. Thus the system can tolerate significant amounts of overload if users are willing to tolerate poorer performance. Another factor that favors CDMA is the need, in addition to multiple access, for some type of external interference rejection capability. This interference may arise because of the multipath nature of the channel, because of other users or because of jamming signals. In indoor multipath channels, the choice of CDMA as a multiple accessing technique is appropriate because the same signal design allows both simultaneous users and improved performance of each user in a multipath channel environment.

An important consideration in CDMA is the number of users that can be accommodated simultaneously. This is dependent on the cross-correlation properties of the PN codes used by different users for spreading their information signal bandwidth. More information about PN codes is presented in the next section to bring out this important aspect of CDMA systems.

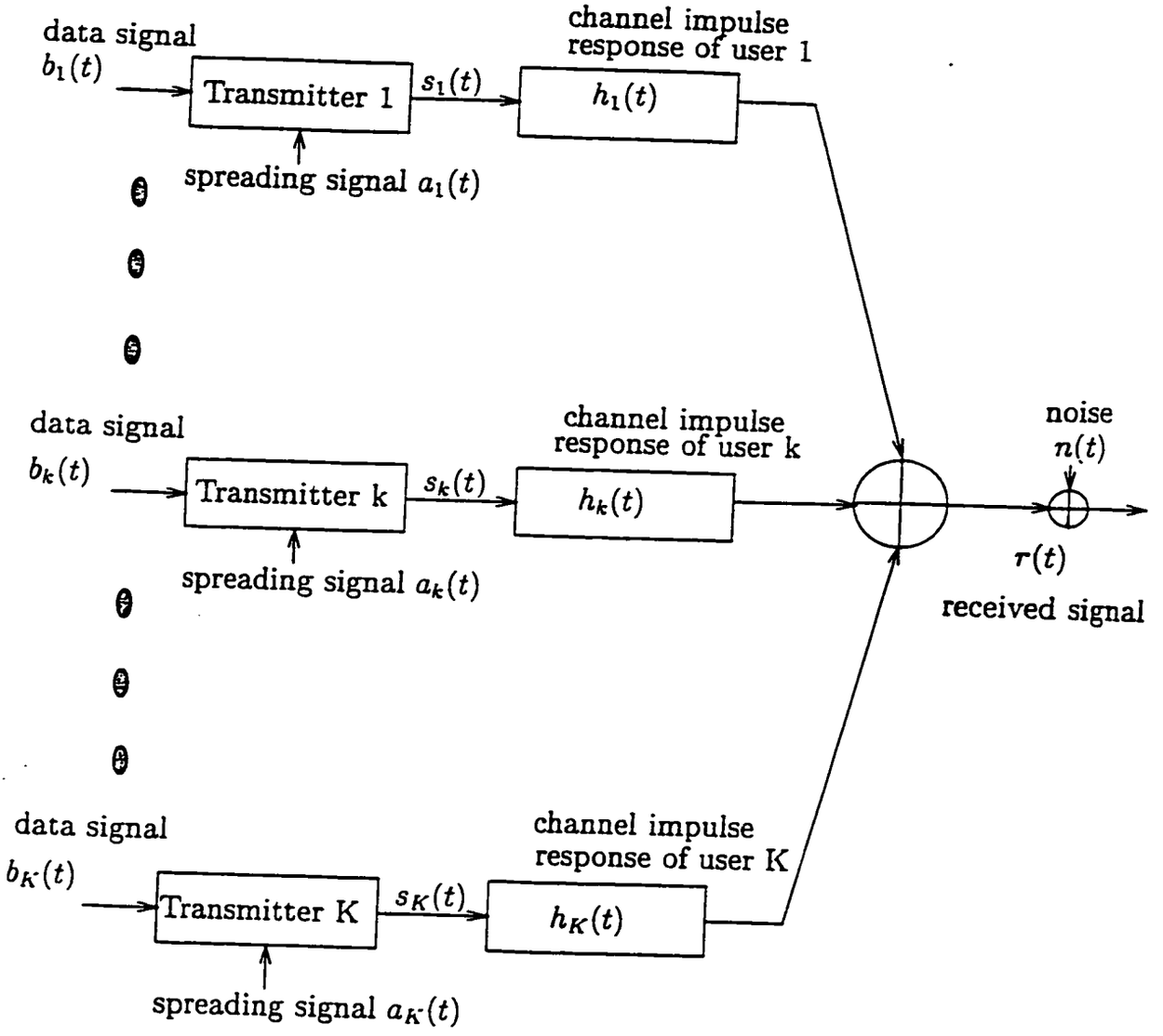

Figure 2.5 Code division multiple access system with direct sequence spread spectrum.

2.3 Codes for Spectrum Spreading

The spreading code used to spread and de-spread a data signal is usually a binary sequence generated with shift registers. For efficient operation, this binary sequence is selected to possess certain desirable properties. In a CDMA communication system, a set or a group of binary sequences or spreading codes is needed. In this case, the binary sequence is required to have the following properties:

1. Easy to generate.

2. The sequence is periodic. The period depends on system requirements.

3. Each sequence in the set is easy to distinguish from a time shifted version of itself.

4. Each sequence in the set is easy to distinguish from every other spreading code in the set.

Let $x(t)$ be a periodic sequence signal of period $T = NT_c$ where N is the number of chips (rectangular pulses) per period and T_c is one chip duration. Property (3) requires distinguishability of $x(t)$ and $x(t+\tau)$ for all $\tau \in (0, T)$. Consequently, it is the magnitude of the autocorrelation function

$$\theta_{x,x}(\tau) = \int_0^T x(t)x(t+\tau)dt, \tag{2.5}$$

that is of interest. Let $x(t)$ and $y(t)$ be two different sequence signals of period NT_c. Property (4) requires distinguishability of $x(t)$ and $y(t+\tau)$ for all $\tau \in (0, T)$. In

this case it is the magnitude of the cross-correlation function

$$\theta_{x,y}(\tau) = \int_0^T x(t)y(t+\tau)dt, \tag{2.6}$$

that is of importance. For periodic sequences, autocorrelation and cross-correlation functions are also periodic.

One important class of sequences is known as the Maximal Length Shift Register Sequences (MLSRS), also called m-sequences. They are called maximal length because these sequences have the maximum period for a given length of the shift register. These basic sequences are discussed in the next section. The Gold code which can be constructed using the m-sequences is discussed in Section 2.3.2. The mathematical background for this subject is widely available [32, 34, 37] and therefore not discussed here.

2.3.1 M-Sequences

As mentioned above, m-sequences are generated by using Binary Linear Feedback Shift Registers (BLFSR). The shift register is conveniently described by its polynomial. The m-sequences of period N are generated by BLFSR which correspond to primitive polynomials of degree n, where $N = 2^n - 1$, and n is equal to the length of the shift register. Primitive polynomials of degree n exist for every n. In Table 2.1, one primitive polynomial $h(x)$ for each value of n is given for $n \leq 20$. This table may be used to generate sequences of length $2^{20} - 1$. The binary representation for

Table 2.1 Some primitive polynomials of degree up to 20. From [37].

degree	$h(x)$	degree	$h(x)$
1	$x+1$	11	$x^{11}+x^2+1$
2	x^2+x+1	12	$x^{12}+x^7+x^4+x^3+1$
3	x^3+x+1	13	$x^{13}+x^4+x^3+x^2+1$
4	x^4+x+1	14	$x^{14}+x^{12}+x^{11}+x+1$
5	x^5+x^2+1	15	$x^{15}+x^1+1$
6	x^6+x+1	16	$x^{16}+x^5+x^3+x^2+1$
7	x^7+x+1	17	$x^{17}+x^3+1$
8	$x^8+x^6+x^5+x+1$	18	$x^{18}+x^7+1$
9	x^9+x^4+1	19	$x^{19}+x^6+x^5+x+1$
10	$x^{10}+x^3+1$	20	$x^{20}+x^3+1$

the n-stage linear shift register which corresponds to the polynomial

$$h(x) = h_0 x^n + h_1 x^{n-1} + ... + h_{n-1} x + h_n \tag{2.7}$$

is the binary vector $[h_0, h_1, ..., h_n]$ of length $n + 1$. In this vector $h_0 = h_n = 1$, and for $1 \leq i \leq n$, $h_i = 1$ if there is a feedback tap connection to the output of the ith stage and $h_i = 0$ otherwise. The register shown in Figure 2.6(a) corresponds to the primitive polynomial

$$h(x) = x^4 + x + 1, \tag{2.8}$$

which may be written in binary form as [1 0 0 1 1] or as 23 in octal. The rectangles represent shift registers and a circle with plus sign represents the exclusive-OR operation. The initial register loading is specified by the binary vector of length n which is given by $[a_0\ a_1\ a_2\ a_3]$ as shown in Figure 2.6(a). Any one of the initial register loadings except the all zero state results in the same state cycle sequence as that shown in Figure 2.6(b). Because all possible states, except the all zero state, appear once in the state cycle, the period of the output sequence $\mathbf{a}$ is the maximum possible. The output sequence consisting of {0, 1} can be transformed to the sequence that consists of {-1, +1} by mapping $0 \rightarrow -1$ and $1 \rightarrow +1$. The periodicity of the output sequence may be expressed by $\mathbf{a}_i = \mathbf{a}_{N+i}$ for any i. The spreading waveform $\mathbf{a}(t)$ derived from this sequence is periodic with period $T = NT_c$ and is specified by

$$\mathbf{a}(t) = \sum_{i=-\infty}^{+\infty} \mathbf{a}_i p(t - iT_c), \tag{2.9}$$

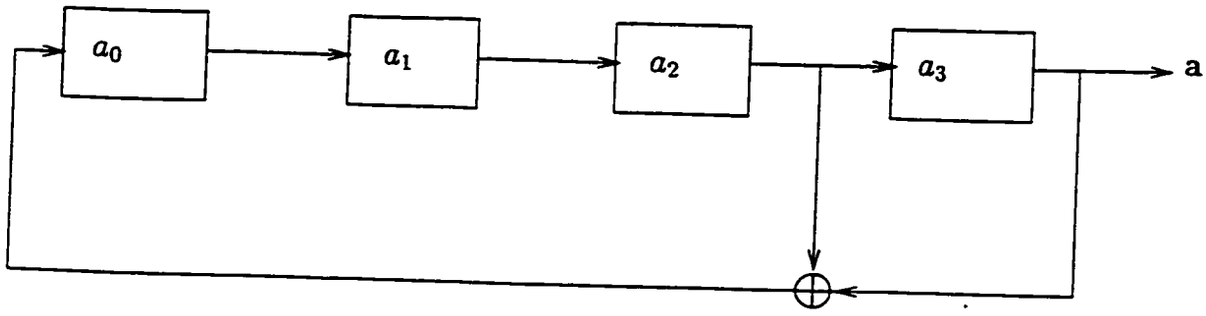

(a)

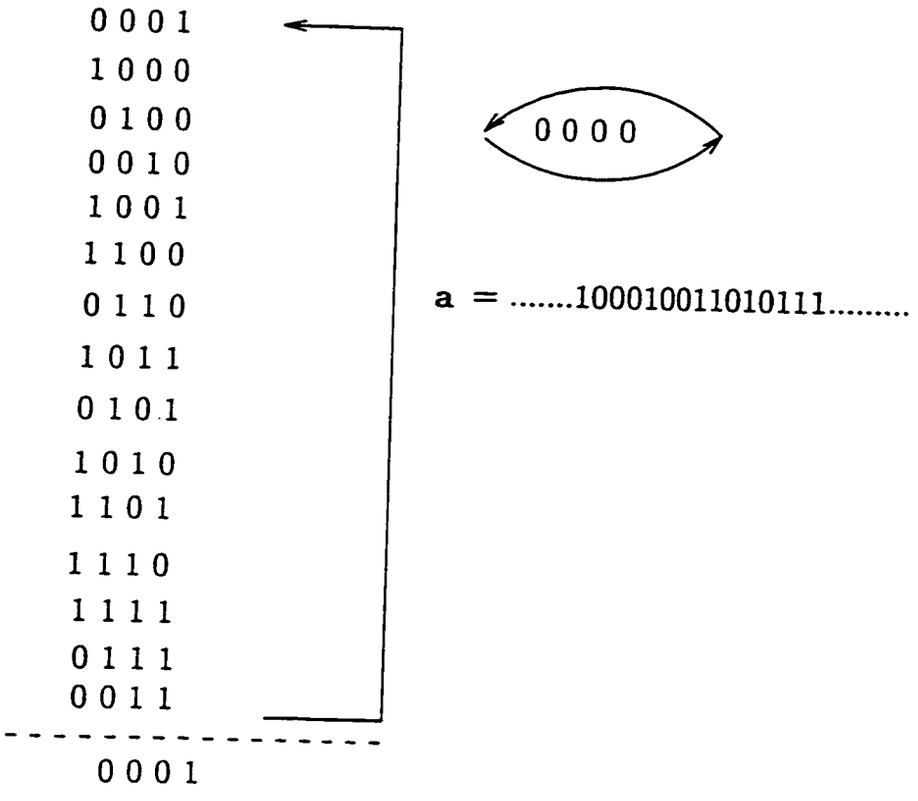

(b)

Figure 2.6 (a) Shift register configuration corresponding to polynomial $h(x) = x^4 + x + 1$. (b) Shift register sequence.

where $\mathbf{a}_i = \pm 1$ and $p(t)$ is the shaping signal over time 0 to T_c.

The autocorrelation function of a sequence of period N may be written as

$$\theta_{\mathbf{a}}(k) = \sum_{i=0}^{N-1} \mathbf{a}_i \mathbf{a}_{i+k}, \tag{2.10}$$

for $k = 0, \pm 1, \pm 2, ..$ For an m-sequence, the autocorrelation function may be written as

$$\theta_{\mathbf{a}}(k) = \begin{cases} N & k = iN \\ -1 & k \neq iN, \end{cases} \tag{2.11}$$

where i is any integer and N is the sequence period. The m-sequences are almost ideal in terms of autocorrelation properties.

In CDMA, cross-correlation properties of code sequences are as important as autocorrelation properties. The cross-correlation between two m-sequences $\mathbf{a}$ and $\mathbf{b}$ of period N can be defined as

$$\theta_{\mathbf{a},\mathbf{b}}(k) = \sum_{i=0}^{N-1} \mathbf{a}_i \mathbf{b}_{i+k}, \tag{2.12}$$

for $k = 0, \pm 1, \pm 2, ..$ Ideally, the sequences used by different users in a CDMA system should be mutually orthogonal to keep the level of interference experienced by any one user due to other user signals to a minimum. The cross-correlation function between any pair of m-sequences of the same period can have relatively large peak values as shown in Table 2.2. In Table 2.2, n is the length of shift registers used for the sequence generation, N is the sequence period and M is the number of

Table 2.2 Peak cross-correlations of m-sequences and Gold sequences. From [50].

n	$N = 2^n - 1$	M	θ_{max}	$\frac{\theta_{max}}{\phi(0)}$	$t(n)$	$\frac{t(n)}{\phi(0)}$
3	7	2	5	0.71	5	0.71
4	15	2	9	0.60	9	0.60
5	31	6	11	0.35	9	0.29
6	63	6	23	0.36	17	0.27
7	127	18	41	0.32	17	0.13
8	255	16	95	0.37	33	0.13
9	511	48	113	0.22	33	0.06
10	1023	60	383	0.37	65	0.06
11	2047	176	287	0.14	65	0.03
12	4095	144	1407	0.34	129	0.03

possible sequences. Quantities θ_{max} and $\phi(0)$ are the peak magnitudes of the cross-correlation function and autocorrelation function respectively; $t(n)$ is defined in the next section on Gold codes. It may be seen that for most sequences the peak magnitude θ_{max} of the cross-correlation function is a large percentage of the peak value of the autocorrelation function, $\phi(0)$. Although it is possible to select a small subset of m-sequences that have relatively smaller cross-correlation peak values, the number of sequences in the set is usually too small for CDMA applications.

PN sequences with better periodic cross-correlation properties than the m-sequences were proposed by Gold [11] and are referred to as Gold codes. These codes are ex-

plained in the next section.

2.3.2 Gold Codes

Gold codes [11] are derived from certain pairs of m-sequences of length $N = 2^n - 1$, that exhibit a three valued cross-correlation function with values {-1, $-t(n)$, $t(n)$-2} where

$$t(n) = \begin{cases} 2^{(n+1)/2} + 1 & \text{odd values of } n, \\ 2^{(n+2)/2} + 1 & \text{even values of } n. \end{cases} \tag{2.13}$$

Such m-sequences are referred to as the preferred sequences. From a pair of preferred sequences **a** and **b**, a set of N sequences of length N can be constructed by taking the modulo-2 sum of **a** with the N cyclically shifted versions of **b** or vice versa. Including **a** and **b** also in this set, the $N + 2$ sequences constructed in this manner are called Gold sequences or Gold codes.

The set of Gold sequences are not maximum length shift register sequences of length N, except for **a** and **b**, so their autocorrelation values are not two-valued. It can be shown [11] that the cross-correlation function for any pair of sequences from the set of $N + 2$ Gold sequences is three-valued with possible values {-1, -$t(n)$, $t(n)$-2} where $t(n)$ is given by Equation (2.13).

It is useful to compare the peak cross-correlation function of Gold codes with the lower bound on peak cross-correlation between any pair of binary sequences. A lower bound on θ_{max}, the peak cross-correlation between any pair of binary sequences of

period N in a set of M sequences, is given by [38]

$$\theta_{max} \geq N\sqrt{\frac{M-1}{MN-1}}. \tag{2.14}$$

This is termed as Welch's bound. It can be approximated as $\sqrt{N}$ for large values of M and N. For $N = 2^n - 1$, and $M = N + 2$, the lower bound is $\approx 2^{n/2}$. Comparing this value with the upper bound on peak cross-correlation $t(n)$ for Gold codes given in Equation (2.13), it is seen that Welch's bound is lower by $\sqrt{2}$ for n odd, and by 2 for n even.

Gold codes are used as the user codes for analyzing the performance of the proposed CDMA receivers in this thesis. Two sets of codes with period, $N = 31$ and 127 are employed. They are generated from primitive polynomials of degree $n = 5$ and 7 respectively. For $n = 5$, polynomials represented by vectors [1 0 0 1 0 1], (45 in octal) and [1 1 1 1 0 1], (75 in octal) are a preferred pair of primitive polynomials. The method of Gold code generation using these polynomials is shown in Figure 2.7(a). This will provide a set of 33 code sequences of period 31. In Figure 2.7(b), the method of generation of Gold sequences of period 127 using primitive polynomials [1 0 0 0 1 0 0 1], (211 in octal) and [1 0 0 0 1 1 1 1], (217 in octal) is shown. These two code sets are used as the spreading codes for the performance evaluation of CDMA receivers.

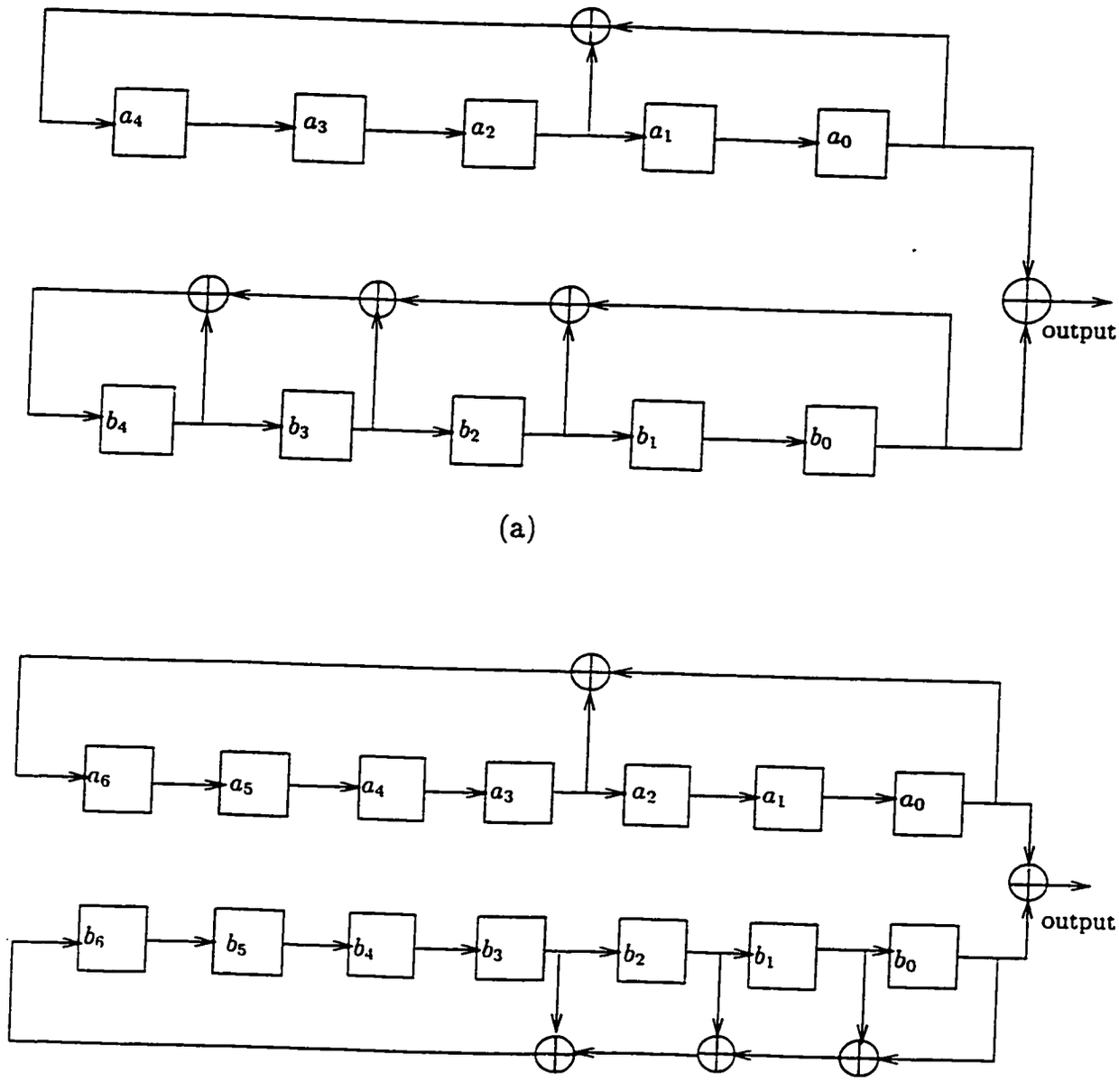

Figure 2.7 Generation of Gold codes. (a) $N = 31$, MLSR sequences obtained using polynomials x^5+x^2+1 and $x^5+x^4+x^3+x^2+1$. (b) $N = 127$, MLSR sequences obtained using polynomials x^7+x^3+1 and $x^7+x^3+x^2+x+1$.

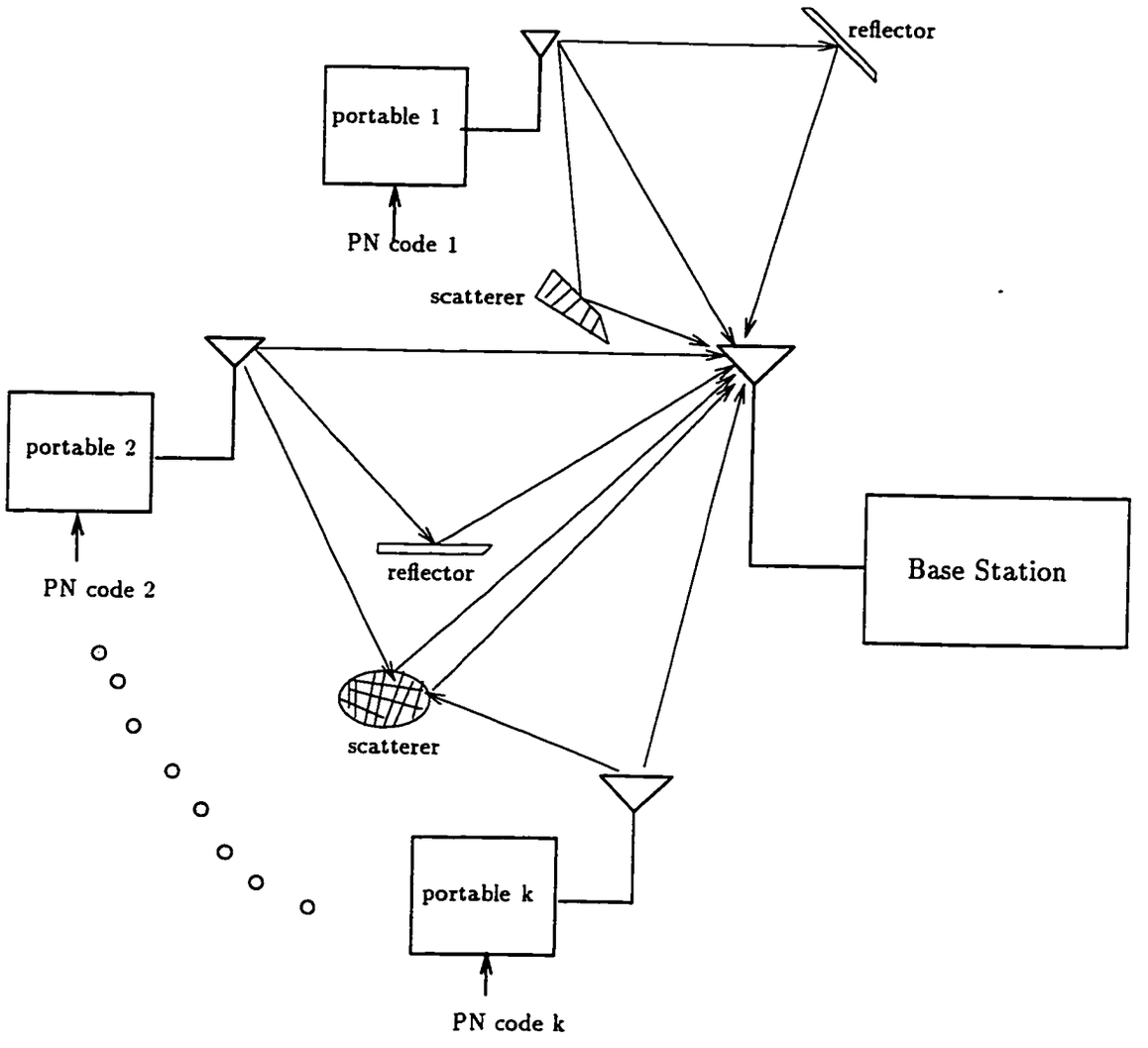

Figure 2.8 CDMA system in an indoor multipath channel.

2.4 Indoor Channel

A typical indoor system may consist of one or more fixed base stations and a number of portable units. Depending on the size of the building and the transmit power levels involved, the coverage area may be divided into a number of cells. Figure 2.8 illustrates one such cell and the nature of the multipath channel. There may be many different propagation paths between the portable and the base station

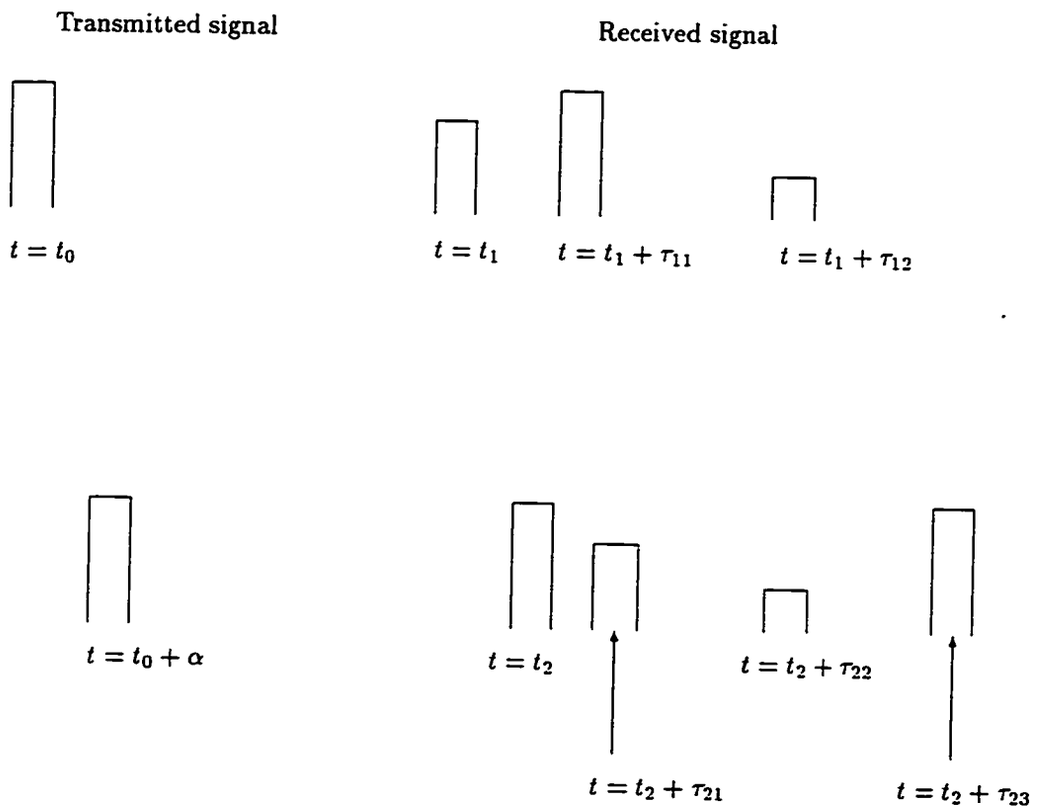

Figure 2.9 Impulse response of an indoor channel.

and these paths may or may not include a line of sight path. The multiple paths arise from reflections, diffractions, and scattering due to the structure, contents, and physical surroundings of the building. For brevity these phenomena will be collectively referred to as reflections and their sources as reflectors. In reality there may be a continuum of multipath components.

2.4.1 Impulse Response

If an impulse is transmitted over a multipath channel with L paths, the received signal appears as a series of L impulses. Because the paths have different lengths and attenuation, the received pulses arrive at different times and with different amplitudes as shown in Figure 2.9. The portables are free to move, and some signal

reflectors (e.g., doors, people etc.) are often not stationary. In general the channel is time-variant. The amplitude and delay associated with path l at time t are denoted by $a_l(t)$ and $\tau_l(t)$ respectively. Figure 2.9 illustrates the time-variant nature of the multipath channel with example responses for impulses transmitted at times $t = t_0$ and $t = t_0 + \alpha$.

A common method used to model this random time-varying indoor propagation channel is to use the concept of impulse response. For each point in the three-dimensional space, the channel is a linear time varying filter with impulse response given by

$$h(t,\tau) = \sum_{k=0}^{L(\tau)-1} a_k(t)\delta[\tau - \tau_k(t)]e^{j\theta_k(t)}, \tag{2.15}$$

where t and τ are the observation time and application time of the impulse, respectively. $L(\tau)$ is the number of multipath components, $\{a_k(t)\}, \{\tau_k(t)\}$ and $\{\theta_k(t)\}$ are the random time varying amplitude, arrival time and phase respectively and δ denotes the delta function. The channel is completely characterized by these path variables. This mathematical model is illustrated in Figure 2.10. Because of its generality, this model has the advantage that it can be used to obtain the response of the channel to the transmission of any transmitted signal $x(t)$ by convolving $x(t)$ with $h(t,\tau)$ and adding noise. For a stationary (time-invariant) channel, Equation (2.15) reduces to

$$h(t) = \sum_{k=0}^{L-1} a_k\delta(t - t_k)e^{j\theta_k}. \tag{2.16}$$

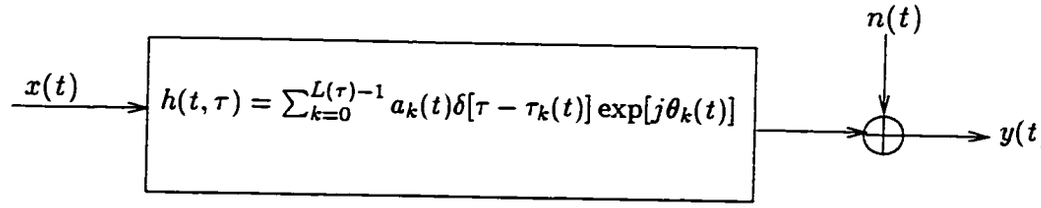

$$y(t) = \int_{-\infty}^{\infty} x(\tau)h(t,\tau)d\tau + n(t)$$

Figure 2.10 Mathematical model of the indoor channel.

2.4.2 Signal Fading

With the mathematical model of an indoor channel given by Equation (2.16), if signal $x(t) = \mathrm{Re}\{s(t)\exp(j\omega_o t)\}$ is transmitted through this channel (where $s(t)$ is any low-pass signal and ω_o is the radian carrier frequency), the signal $y(t) = \mathrm{Re}\{\rho(t)\exp(j\omega_o t)\}$ is received where

$$\rho(t) = \sum_{k=0}^{L-1} a_k s(t - t_k)e^{j\theta_k}. \tag{2.17}$$

When an unmodulated carrier is transmitted, $s(t) = 1$ and

$$\rho(t) = \sum_{k=0}^{L-1} a_k e^{j\theta_k}. \tag{2.18}$$

The low-pass equivalent signal $\rho(t)$ is the sum of L vectors with phase θ_k and amplitude a_k. The phase of each multipath component depends upon the path delay and the carrier frequency. At carrier frequencies of interest, θ_k can change by 2π radians

with small changes in path length. Thus $\rho(t)$ can be modeled as a random process. The vector phase θ_k being random, at certain time instants the vectors will add in phase resulting in a strong signal, while at other times, they will tend to add out of phase resulting in a weak signal. These fluctuations are called signal fading, and are a direct result of the multipath characteristics of the channel.

With a large number of paths, the central limit theorem can be applied and the summation $\rho(t)$ can be modeled as a zero mean complex valued Gaussian random process. Such a process is comprised of two real-valued, jointly stationary independent Gaussian processes and it may be given by

$$\rho(t) = \rho_r(t) + j\rho_i(t). \tag{2.19}$$

The envelope of such a complex-valued process may be written as

$$y(t) = |\rho(t)| = \sqrt{\rho_r^2(t) + \rho_i^2(t)}. \tag{2.20}$$

It is well known [50] that the envelope of a zero mean complex-valued Gaussian random process has a Rayleigh probability density given by

$$f(y) = \frac{y}{\alpha^2} e^{-\frac{y}{2\alpha^2}} U(t), \tag{2.21}$$

where $\alpha^2 = \sigma_r^2 = \sigma_i^2$ (the variances of the two real-valued processes) and $U(t)$ is the unit step function. A multipath channel that can be modeled by a zero

mean, complex-valued Gaussian random process is therefore said to exhibit Rayleigh fading.

2.4.3 Delay Spread

Because the received signals follow different paths and some of the paths are longer than the others, multipath signals arrive with slight differences in time delay. The multipath time delay structure in an indoor radio transmission can be measured by transmitting wide-band pulse-like signals between base station and portable locations [40] - [49]. Figure 2.11 illustrates two multipath delay profiles obtained from such a measurement at 1.5 GHz made in two rooms in a large building [49]. It is also called the power-delay profile. Comparison of these two figures illustrates the gross differences between profiles measured for different transmitter-receiver locations. The range of values of time delay over which the measured power is essentially non-zero is called the multipath delay spread, Δ, of the channel. A measure of the widths of such profiles is needed to determine limits on digital transmission rates possible over such radio channels. One simple parameter that is useful in describing the overall characteristic of the multipath profile is the root mean square (r.m.s) delay spread. The r.m.s delay spread σ_τ can be written as [49]

$$\sigma_\tau = \sqrt{\bar{\tau^2} - \bar{\tau}^2}, \tag{2.22}$$

where

$$\bar{\tau^n} = \frac{\sum_\lambda \tau_\lambda^n g_\lambda^2}{\sum_\lambda g_\lambda^2}. \tag{2.23}$$

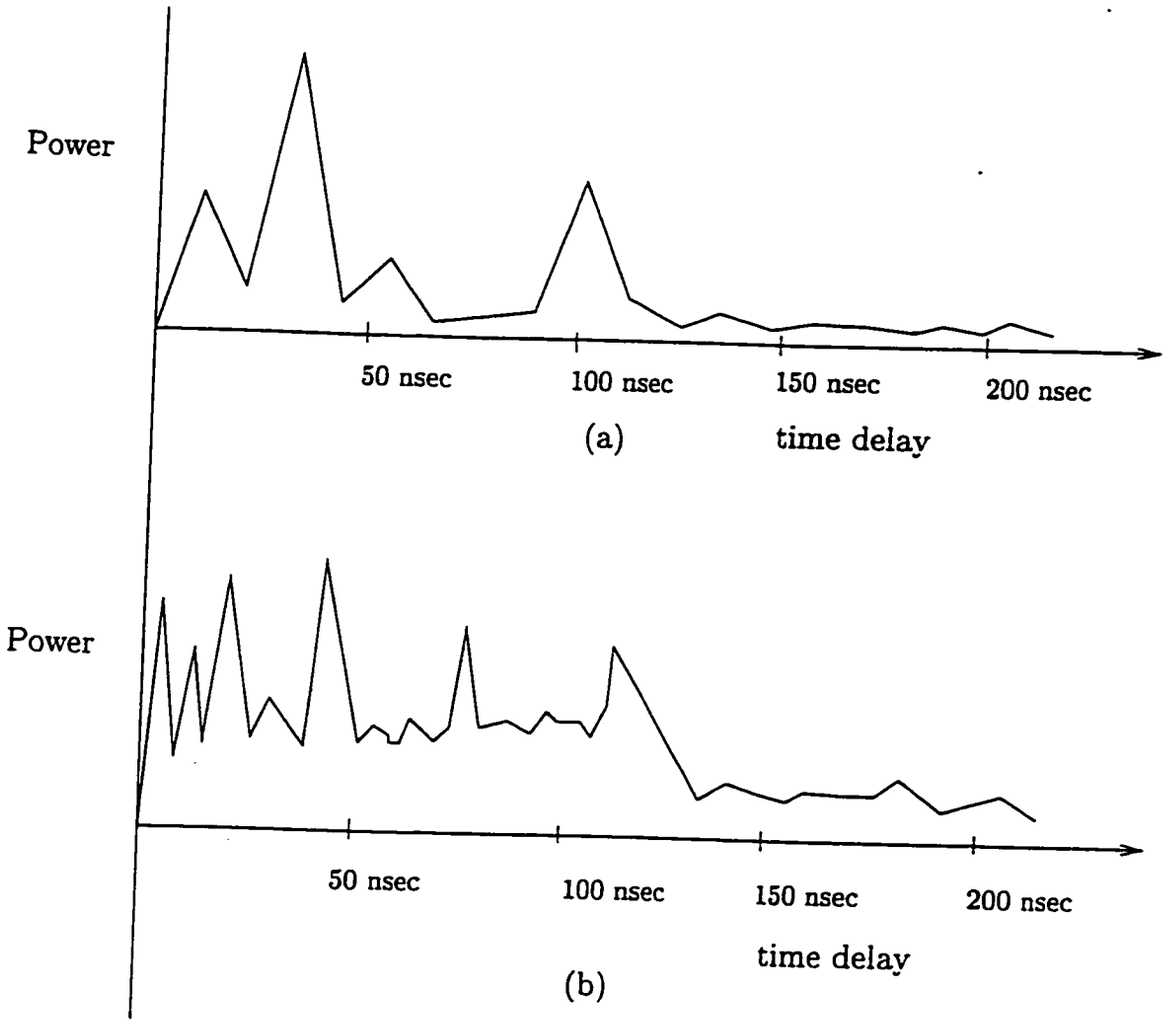

Figure 2.11 Average relative power received as a function of time delay for an 1.5 GHz probing transmitter and receiver located in different places in a large building. Plots (a) and (b) are for two different places in the building. From [49].

In Equation (2.23), the pair $(\tau_\lambda, g_\lambda)$ is the delay and gain of the λth path, respectively.

In a digital system, particularly one operating at a high bit rate, the delay spread causes each symbol to overlap with the preceding and following symbols, producing Intersymbol Interference (ISI). Therefore, the width of the signaling pulses transmitted over the channel should be much greater than the r.m.s delay spread to avoid ISI. In effect, delay spread sets a limit on the symbol transmission rate in an indoor digital system. Root mean square delay spreads in the 25-200 nsec range are widely reported for indoor channels [40]-[49].

2.4.4 Doppler Shift

Radio transmissions are frequency shifted due to the relative motion of portable units and reflectors in the indoor environment. This variation in the frequency of the received signal is known as Doppler shift. Moreover, the Doppler shift affects all multiple propagation paths, some of which may exhibit a positive shift and some a negative shift at the same instant. This shift introduces random frequency modulation in the received signal. Doppler shift can be quite high in a land mobile channel. At a vehicle speed of 40 km/hour and at a carrier frequency of 1.5 GHz, Doppler shift can be as high as 100 Hz. In indoor portable communications at 1.5 GHz, the Doppler shift is significantly lower (approximately 10-15 Hz).

2.4.5 Coherence Bandwidth

The coherence bandwidth of the channel is approximately defined as the reciprocal of the multipath delay spread [50]. Two sinusoids with frequency separation greater than the coherence bandwidth are affected differently by the channel. When an information bearing signal is transmitted through the channel, and the coherence bandwidth is small in comparison with the bandwidth of the transmitted signal, the channel is said to be frequency selective. If the coherence bandwidth is large in comparison with the bandwidth of the information bearing signal, the channel is said to be frequency non-selective. For practical CDMA systems, the indoor channel is frequency selective. The large bandwidth of CDMA signals allows multipath to be resolved in time with a time resolution equal to the reciprocal of the CDMA signal bandwidth. Because each resolved path is independently affected by the channel, these paths can be combined to improve signal to noise ratio. This form of diversity technique is referred to as spread spectrum diversity or multipath diversity.

2.4.6 Coherence Time

The coherence time of a channel is approximately defined as the reciprocal of the Doppler shift. A slowly varying channel has a large coherence time or, equivalently, a small Doppler shift. The indoor channel can be considered to be slowly varying at the bit rate of 1 Mbps.

2.5 CDMA Receivers

As stated in Chapter 1, CDMA receivers can be broadly classified as those that do not take advantage of the implicit spread spectrum diversity, such as the correlator receiver, and those that do take advantage of the multipath diversity offered by spread spectrum, such as the RAKE receiver. The principle of operation of these two types of receivers is described in the next two subsections.

2.5.1 Correlator Receiver

A correlator type base station receiver is shown in Figure 2.12. As shown in this figure, the received signal $r(t)$ is initially down converted and then de-spread by multiplying it with the transmitter code which is in phase with the received signal code. The correlator is aligned with one of the multipaths in the received signal. This can be the first path signal received or the strongest path signal. Aligning to the strongest path will result in better performance. This requires complex multipath tracking circuit. Multipath tracking is relatively easy when the first path signal is selected. The phase of the carrier signal used for down conversion is the phase of the path signal to which the correlator is aligned. Similarly the phase of the spreading code used at the receiver for de-spreading the signal should correspond to the code phase of the selected path signal. The de-spread signal is integrated over a symbol duration to obtain the decision variable to detect the information signal.

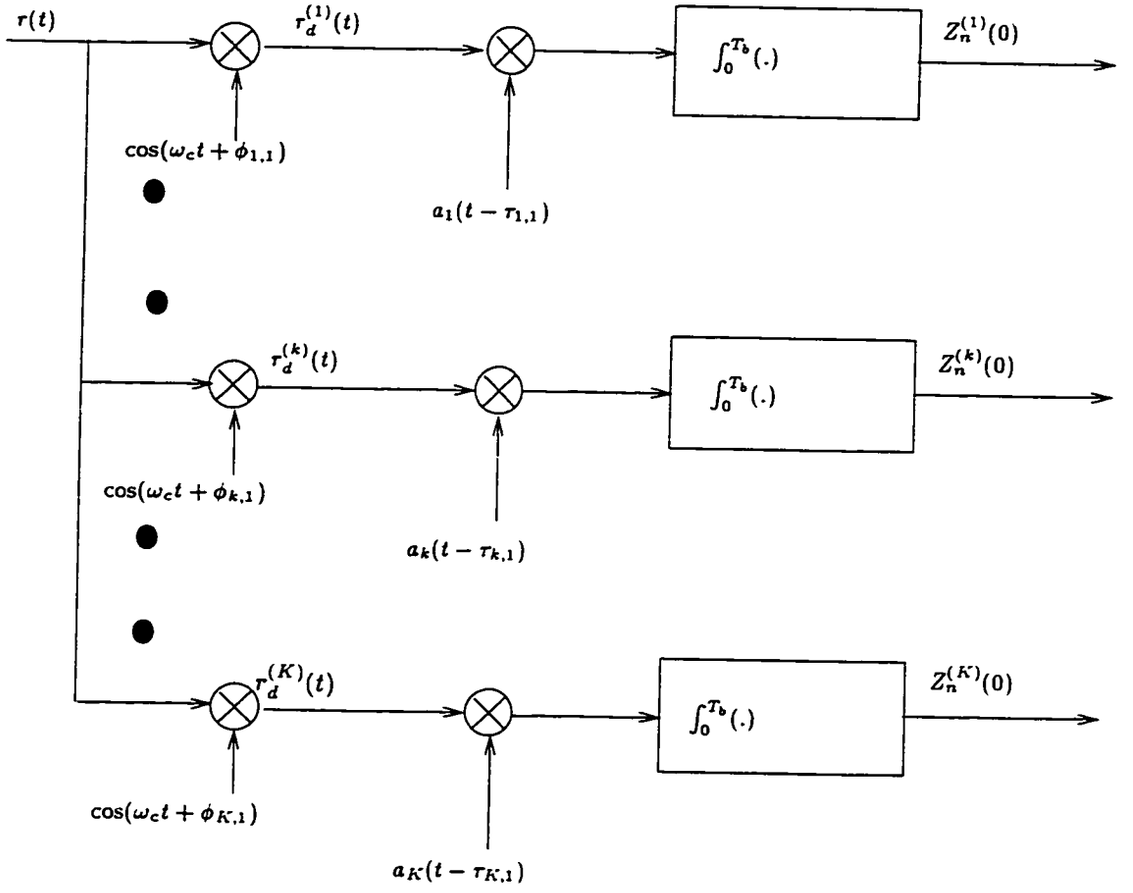

Figure 2.12 Correlator receiver for CDMA application.

2.5.2 RAKE Receiver

To improve performance, diversity combining techniques (time, frequency or space) are often used in a fading multipath environment. For CDMA systems, with DS SS operating in a multipath environment, signals of paths with a propagation delay difference of more than the spreading code chip duration can be separated in the receiver. As these paths have independent fading patterns, their signals can be combined to mitigate the effects of fading. In some cases, the path with the highest signal power is selected and paths with weaker signals are discarded. When multipaths are combined, one of the following two combining techniques can be applied.

- Equal gain combining: Signals of all received paths are added equally.
- Maximum ratio combining: Received signals from individual paths are combined in a way to accentuate credible signals and suppress less credible ones.

The maximum ratio combining method is more effective than the other two. A RAKE receiver with maximum ratio combining is shown in Figure 2.13. The received signal is down converted initially by a carrier signal and then passed through a Matched Filter (MF). An example of the output of MF looks like that shown in Figure 2.14(a). RAKE combining is realized by using a Transversal Filter (TF). TF is a delay line with a maximum delay equal to Δ, the multipath delay spread of the channel. The delay line is divided into L_k segments, where L_k denotes the number of significant paths for the kth user. The number of significant paths is decided by

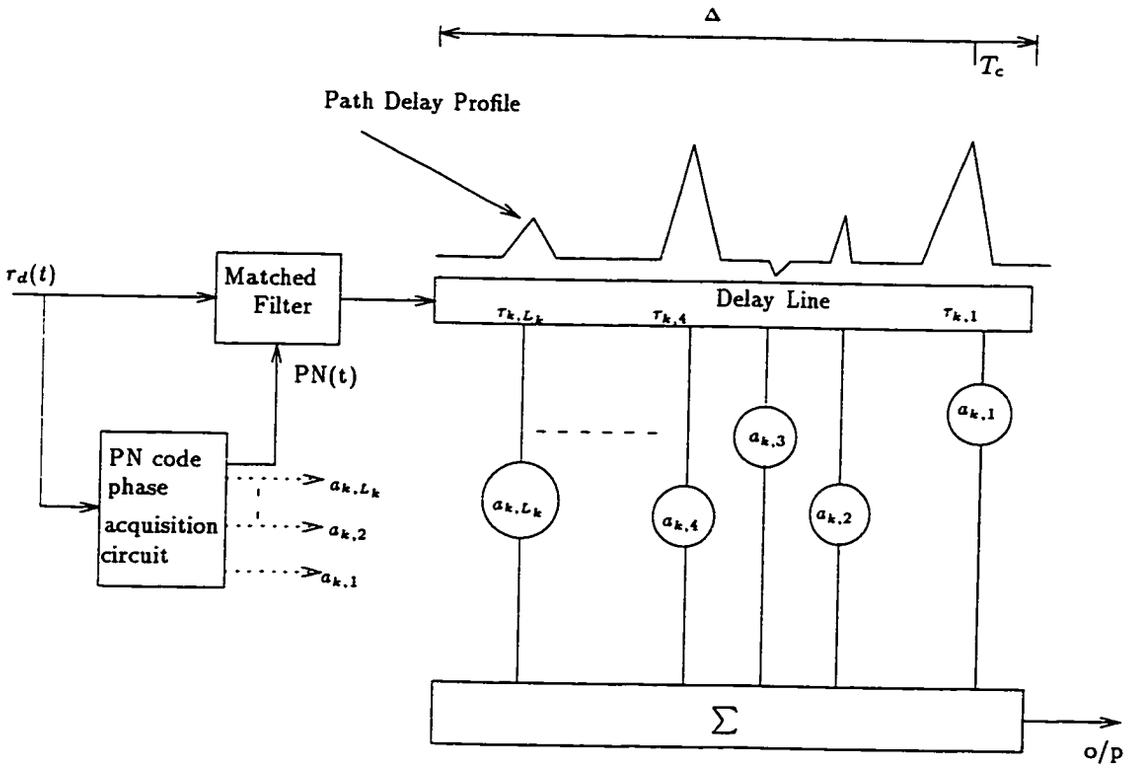

Figure 2.13 A diversity combining RAKE receiver.

the multipath tracking circuit. Each segment has a delay T_c, the spreading code chip duration. The signal values in each segment is multiplied by a weighting factor $a_{k,\lambda}$ proportional to $(g_{k,\lambda}e^{j\phi_{k,\lambda}})^*$, $1 \leq \lambda \leq L_k$, where $g_{k,\lambda}$ and $\phi_{k,\lambda}$ correspond to the amplitude and phase of the λth path of user k and * denotes complex conjugation. The impulse response of the RAKE combiner is the time reversal of the channel impulse response and is shown in Figure 2.14(b). The combiner output shown in Figure 2.14(c) is the convolution of the matched filter output and the combiner impulse response. The desired peak of the output occurs at $t = (L_k - 1)T_c$ and it is proportional to $\sum_{\lambda=1}^{L_k} g_{k,\lambda}^2$.

Diversity combining RAKE receivers achieve a significant improvement over non-combining single path correlator receivers. However, to realize this performance improvement, the channel parameters (path amplitudes $g_{k,\lambda}$ and path phases $\phi_{k,\lambda}$), have to be estimated with high precision.

2.5.3 Co-channel Interference in CDMA Receivers

As stated before, the same bandwidth is occupied by all users of a CDMA system. To each user, the signal from every other user of the system is an interference and this is referred to as the CCI. The CCI arises due to the cross-correlation among the spreading codes of different users. In an indoor CDMA system with a correlator receiver, other than the desired path signals of the same user, and all the path signals of all other users, contribute to CCI. In a diversity combining RAKE receiver, all path signals of all other users contribute to CCI. The CCI is the major

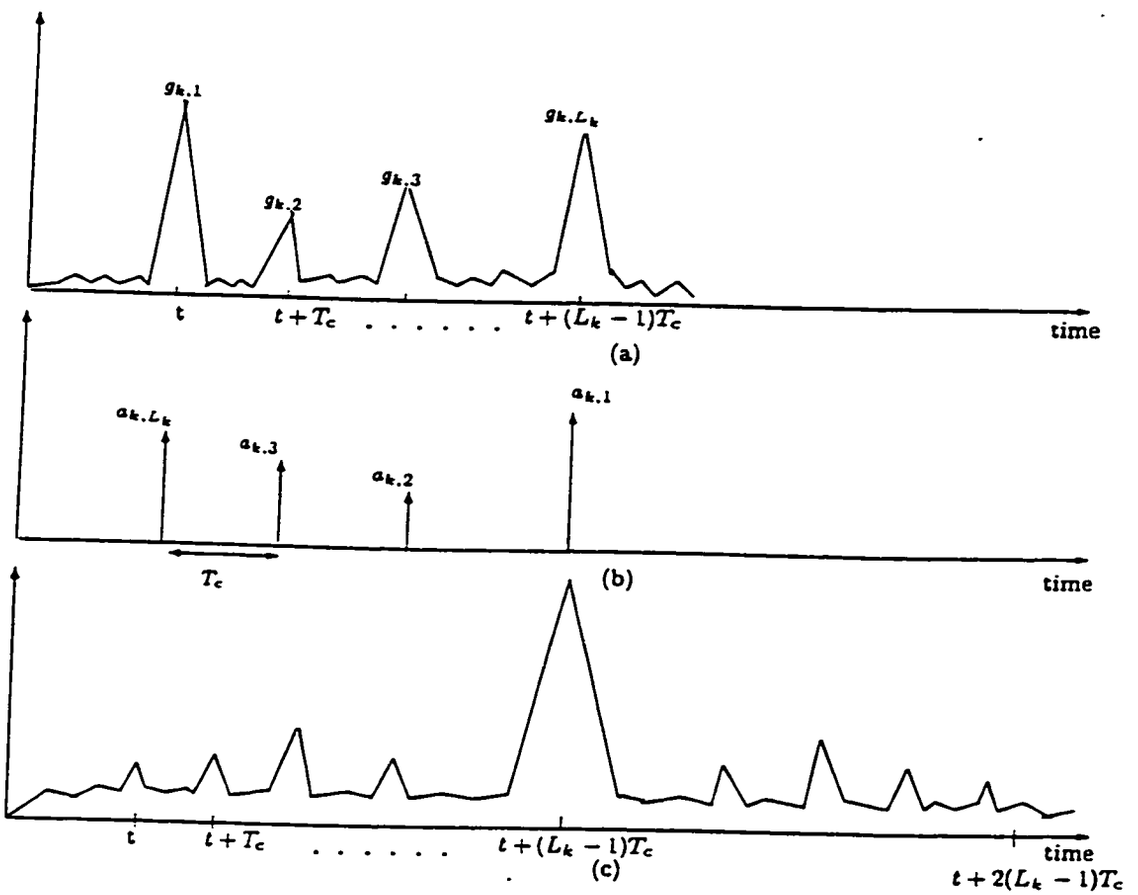

Figure 2.14 Time domain response of the channel impulse response convolved by RAKE combiner impulse response. (a) Output of the matched filter and input to RAKE combiner. (b) Impulse response of the RAKE combiner. (c) RAKE combiner output.

source of interference in a CDMA receiver and this interference limits the number of simultaneous users that can be accommodated in a CDMA system.

One method of improving the capacity of the CDMA system is to employ cancellation of CCI at the receiver. The concept of CCI cancellation in a CDMA receiver is explained in the next subsection.

2.5.4 CDMA Receivers with Co-channel Interference Cancellation

The CCI is a serious problem in the reverse link (portables to base station) of a cellular system. The signal received from a portable close to the base station will be much stronger than that received from a portable at the cell boundary. This becomes a serious problem for an indoor channel as the path loss exponent with distance is 3.7 to 4 [49] instead of 2 as it is for free space. Therefore, a more distant user will be dominated by the close-in portables. This is referred to as the near-far effect. As stated in Chapter 1, power control techniques are commonly used to alleviate this problem. However, due to imperfections in power control, the capacity of an indoor cellular system with traditional correlator or RAKE receivers is considerably reduced due to the near-far effect.

The CCI signals have the property that they are deterministic and can be regenerated at the receiver provided the symbol timing, incoming signal level, data content, spreading code, and channel parameters can be correctly estimated for all co-user signals. As shown in Figure 2.15, the receiver can achieve an improved per-

formance on a desired channel if additional receiver stages are incorporated for all interfering channels. Such stages are used to estimate parameters mentioned above. In a cellular system, this kind of receiver can be advantageously used at the base station to detect all multiple access signals. Once this is done, the interfering signals can be accurately regenerated at the receiver. These signals can then be used to cancel the interfering signals in the desired channel as shown in Figure 2.15. Cancellation of interfering signals from the received signal at the front end of the receiver will permit improved detection of autocorrelation peaks for the weaker signals in a subsequent receiver stage. The total cancellation of all known interfering signals from the received signals at the input of the receiver will also help the acquisition of spreading code phase and estimation of channel parameters. CDMA receivers with CCI regeneration and cancellation are analyzed in Chapters 4 and 5.

2.6 System Imperfections

It is clear that a traditional or a CCI canceling receiver will yield the best performance when all the parameters are perfectly estimated, however, it is often difficult to provide ideal conditions in indoor mobile communications for such an optimum performance. The primary focus of this research is to investigate the effect of three system imperfections on the performance of traditional and CCI canceling CDMA receivers. This is done by modeling these imperfections and using these models for analysis and simulation of the BER performance. The particular system imperfections considered are:

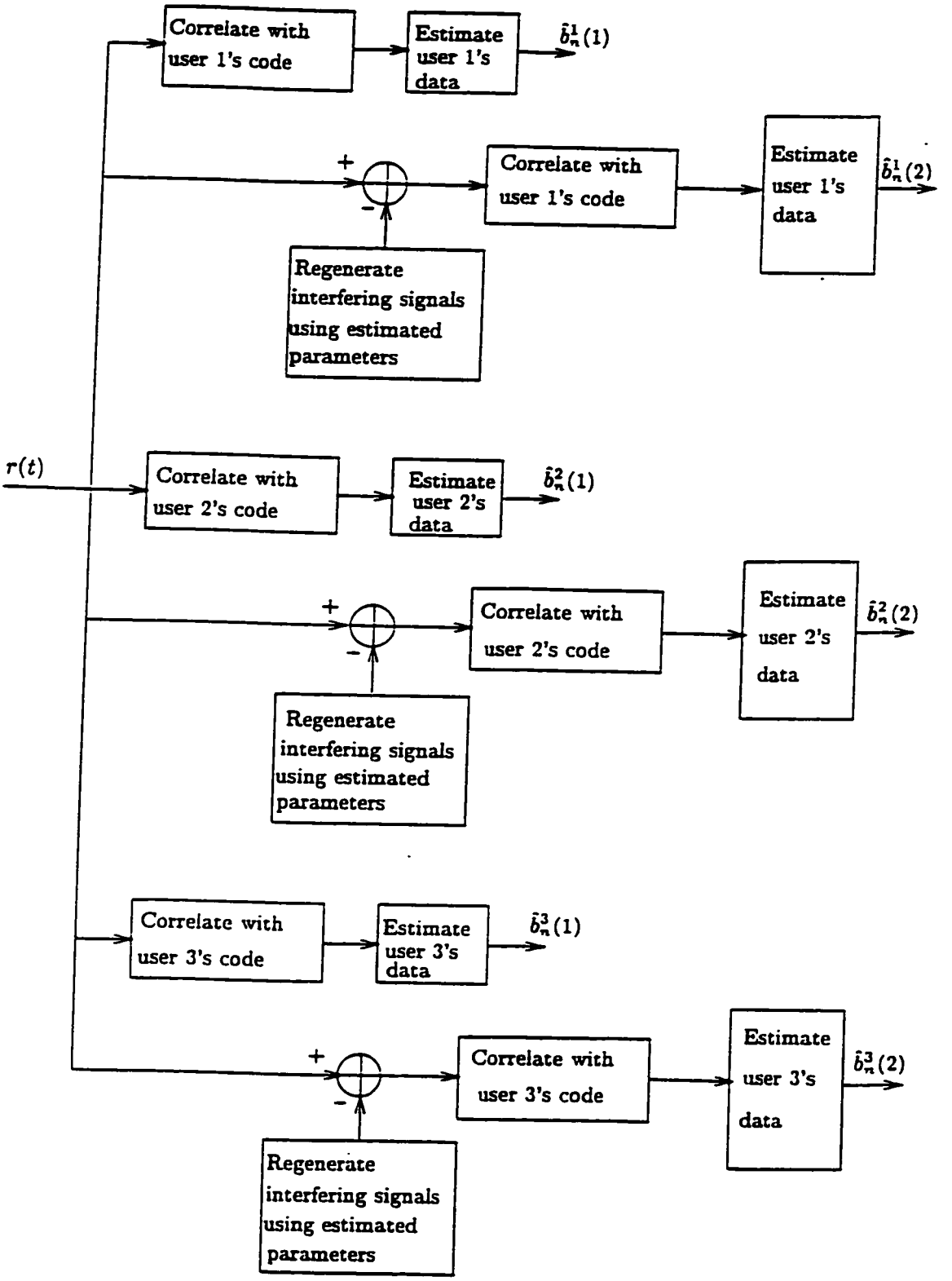

Figure 2.15 A CDMA receiver that uses successive data estimation and interference cancellation.

- Power control imperfections.
- Channel estimate imperfections.
- Spreading code phase estimate imperfections.

A brief review of the three types of imperfections is presented in the next three subsections.

2.6.1 Imperfections in Power Control

It is desirable to maximize the number of allowed simultaneous users in a given system bandwidth. This system capacity is maximized if the transmitted power of each portable is controlled so that its signal arrives at the base station with the minimum required signal to interference ratio. Any power below this results in an unacceptable BER. If the received power is too high, the performance of this portable is good, but interference to all other portables that are sharing the channel is increased. This may result in unacceptable performance for other portables. These problems can be overcome by power control measures.

The North American dual-mode CDMA cellular system standard, commonly referred to as interim standard 95 or IS-95, specifies open loop and close loop power control in the reverse link. In the open loop scheme, each portable unit attempts to estimate the path loss from the base station to the portable by measuring the power level of a pilot signal from the base station. In the case of a sudden change in channel conditions, as would happen when a portable moves in and out of shadow

zones, open loop power control provides for a very rapid response over a period of a few microseconds. For a full-duplex facility, separate frequency bands are allocated for forward and reverse links. When frequency separation is more than the coherence bandwidth of the channel, fading on the forward and the reverse paths is independent. The above simple method of power control is insufficient, and the portable transmitter power must also be controlled by a separate signal from the base station. Each base station demodulator measures the received signal to noise ratio for each portable, and the measured SNR is compared with the desired SNR for that portable so that a power adjustment command can be issued to that portable unit. This closed loop power adjustment command is combined with the portable's open loop estimate to set the mobile's transmit power.

Imperfections in such a Transmitter Power Control (TPC) can be due to faulty TPC, finite dynamic range of TPC, and propagation effects. Field trials for an outdoor cellular system show that even with power control, the normalized received power from the mobile unit is a log-normal variable with a variance of 1-2 dB [10]. The TPC imperfections of the same order can be assumed for an indoor CDMA system. In the subsequent analysis, the normalized received power from the portable is taken as a log-normal random variable. The normalization is obtained by dividing the received power from the portable by the set or the desired power. The set or the desired power is the power obtained from the portable if perfect power control is available. The variance of this log-normal random variable is a measure of the magnitude of TPC imperfections.

2.6.2 Imperfections in Channel Parameter Estimation

Channel parameter estimates (multipath amplitudes and phases) are required in CCI canceling receivers to regenerate the co-user signals which are then canceled from the desired signal. Many channel estimation algorithms use the principle of minimizing the mean squared error in the estimates [66]. This results in a finite error in the estimates. In some other channel estimations, an averaging process is used. Using long averaging periods, such a system suppresses the influence of noise efficiently. On the other hand, long averaging intervals lead to systematic errors in the estimated channel parameters since the channel is time-variant. No experimental studies on the distribution of channel estimate errors have been reported so far in the literature. However, the path amplitude and the path phase errors have been modeled as zero mean Gaussian in [20]. Because the estimate error is due to a combination of several independent factors like CCI, time variation of channel and AWGN, it is reasonable to assume the error as a zero mean Gaussian random variable. Therefore, in the performance analysis of CDMA receivers (traditional and CCI canceling) reported in this thesis, the channel estimate errors are modeled by zero mean Gaussian random variables. The path amplitude estimate error is normalized by one volt and the path phase estimate error is normalized by π radians. The normalization of these estimate errors permits the use of a single mean square value to represent the second moment of these estimate errors. The mean square of the normalized estimate errors is used as a measure of the estimate imperfections.

2.6.3 Imperfections in Spreading Code Phase Estimates

An estimate of the received spreading code phase is required to implement despreading in a spread spectrum receiver. In CCI canceling receivers, synchronized spreading codes are also required to regenerate the co-user signals which are then subtracted from the received signal. Phase acquisition strategy used in the receiver provides the code phase with an accuracy of $\pm \frac{1}{2}$ chip. This is followed by a code tracking circuit which provides a more accurate phase estimate of the spreading code. Co-user signals with different spreading codes which have a finite cross-correlation with the desired user spreading code cause error in the code phase estimation. Similar to the case of channel estimate error, no experimental studies on the distribution of spreading code phase estimate error have been reported in literature. With the reasoning used in the case of channel estimate errors, the code phase estimate error is also modeled by a zero mean Gaussian random variable. The standard deviation of the normalized code phase estimate error is used as a measure of code phase estimate imperfection. Normalization is obtained by dividing the error by the spreading code chip duration.

A detailed analysis of the effect of these three system imperfections on both CCI canceling and non-CCI canceling receivers is developed in the next three chapters.

2.7 Summary

Some basic concepts of an indoor CDMA system and the terminology used in the analysis were introduced in this chapter. BPSK modulation and spread spectrum

were briefly described. This was followed by a description of maximal length shift register and Gold spreading codes and their cross-correlation properties. A brief description of the impairments in an indoor radio channel was included. Traditional and CCI canceling CDMA receiver structures were introduced. Finally, the imperfections in power control, channel estimates, and spreading code phase estimates were discussed along with the models for representing them in analysis.

3. Effect of System Imperfections on the Performance of Correlator and RAKE Receivers

In this chapter, the effect of system imperfections on the BER performance of an indoor CDMA radio system using correlator and RAKE receivers is analyzed theoretically. Special emphasis is placed on the analysis of the combined effect of imperfections in power control, path amplitude and phase estimation, and spreading code phase estimation on the system BER. The indoor channel is modeled as a frequency selective slow Rayleigh fading channel with three paths on average. The effect of Additive White Gaussian Noise (AWGN) is also included in the analysis. Expressions for the probability of error are derived using a Gaussian approximation model for the Multiple Access Interference (MAI). By using a more complex and computationally intensive improved Gaussian approximation, it is shown that the simpler Gaussian approximation is reasonably accurate for the range of SNR values encountered in a practical system.

The CCI canceling CDMA receiver configurations presented in Chapters 4 and 5 are logical extensions of the correlator and RAKE receiver configurations considered in this chapter. The analysis presented in this chapter sets the stage for analysis of CCI canceling receivers in Chapters 4 and 5.

3.1 System Description

The transmitter and channel models are presented in this section. These models are also applied for the analysis and simulation in Chapters 4-6. The communication system considered is the reverse link (portables to the base station) in a microcellular system operating in an indoor environment. There are K portables transmitting asynchronously over their individual multipath fading channels to the base station receiver. Such a scheme is illustrated in Figure 3.1.

3.1.1 Transmitter

Each station transmits using BPSK modulation for a DS SS system. The kth transmitter generates data bits at a rate of $\frac{1}{T_b}$ bits per second, where T_b is the bit duration. Its data signal $b_k(t)$ and spreading signal $a_k(t)$ with chip duration T_c are defined as

$$b_k(t) = \sum_{n=-\infty}^{\infty} {b_n}^{(k)} p_{T_b}(t - nT_b) \tag{3.1}$$

and

$$a_k(t) = \sum_{n=-\infty}^{\infty} {a_n}^{(k)} p_{T_c}(t - nT_c), \tag{3.2}$$

where unit rectangular pulse $p_T(t)$ is defined as

$$p_T(t) = \begin{cases} 1 & 0 \leq t < T \\ 0 & \text{otherwise.} \end{cases} \tag{3.3}$$

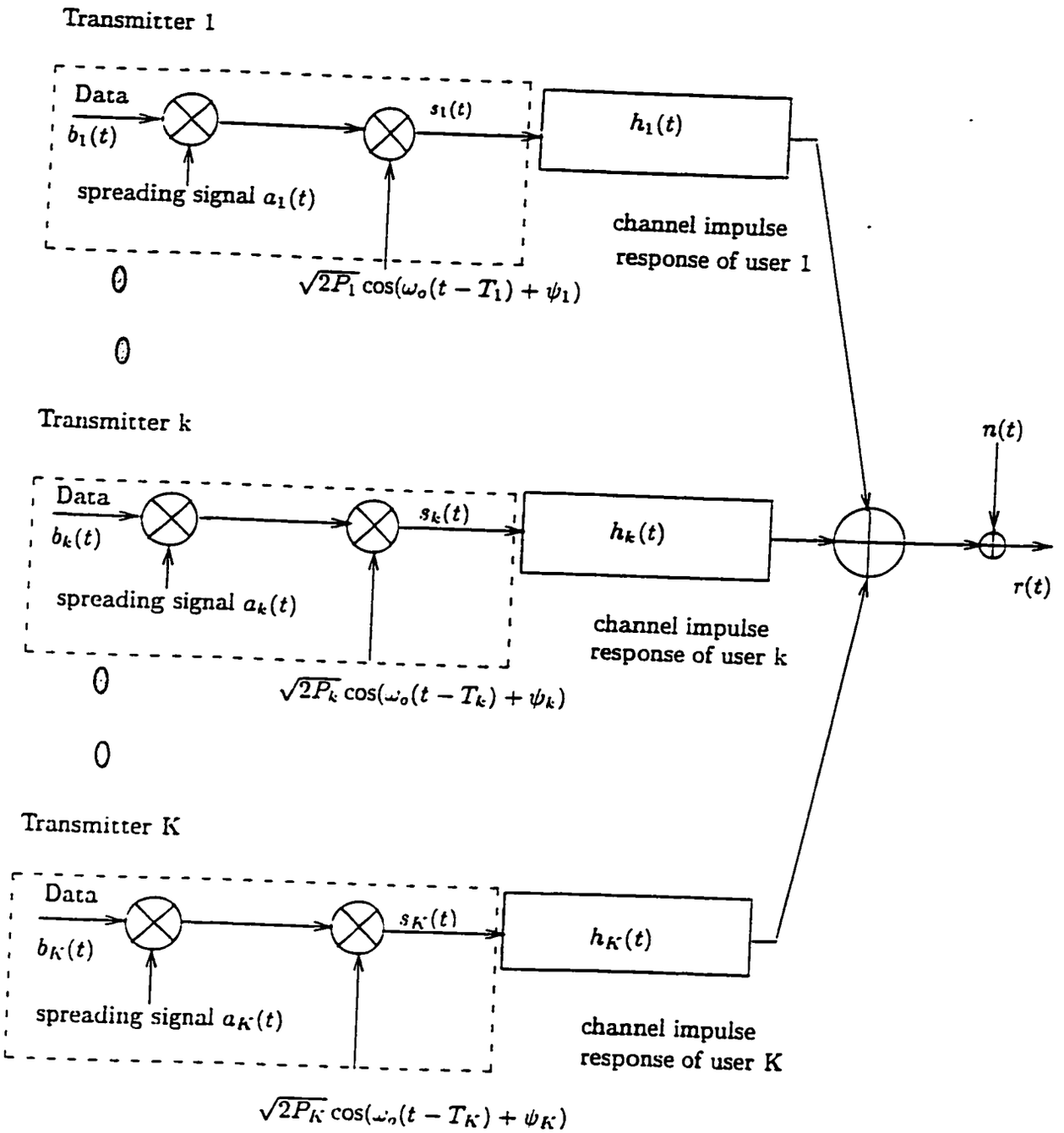

Figure 3.1 Received signal at the base station. Received signal in CDMA contains the multiple user signals and AWGN.

The data symbols $b_n^{(k)}$ are considered to be independent and identically distributed (i.i.d) sequences with $\Pr[b_n^{(k)} = +1] = \Pr[b_n^{(k)} = -1] = 0.5$. The spreading sequence $a_n^{(k)}$ has a period of N and $T_b = NT_c$. The equivalent low-pass bandwidth of the channel, W, is assumed to be equal to $1/T_c$. The data signal is first multiplied by the spreading signal to produce the baseband signal $u_k(t)$, where

$$u_k(t) = b_k(t)a_k(t). \tag{3.4}$$

With carrier modulation, the transmitted signal becomes

$$s_k(t) = \sqrt{2P_k}u_k(t - T_k)cos[\omega_c(t - T_k) + \psi_k], \tag{3.5}$$

where ω_c is the radian frequency, T_k is the kth user's transmitter delay, and ψ_k is its phase offset. T_k and ψ_k are uniformly distributed over $[0, T_b]$ and $[0, 2\pi]$ respectively for all k. P_k represents the received power of the kth user's signal such that $P_k = E_{b,k}/T_b$, where $E_{b,k}$ represents the energy per bit for user k. As mentioned before, perfect power control is difficult in a fading multipath mobile environment. In this thesis, imperfect power control is assumed.

3.1.2 Channel

The random and time varying indoor propagation channel of the kth user can be modeled as a linear time varying filter with an impulse response given by [41]

$$h_k(t,\tau) = \sum_{\lambda=1}^{L_k(\tau)} g_{k,\lambda}(t)\delta[\tau - \tau_{k,\lambda}(t)]e^{j\theta_{k,\lambda}(t)}, \tag{3.6}$$

where t and τ are the observation time and application time of the impulse respectively. $L_k(\tau)$ is the number of multipath components in the kth user's propagation channel. Quantities, $\{g_{k,\lambda}(t)\}$, $\{\tau_{k,\lambda}(t)\}$, $\{\theta_{k,\lambda}(t)\}$ are the random time varying amplitude, arrival time and phase sequence respectively and δ represents the delta function. With β defined as the time increment, the impulse responses $h_k(t,\tau)$ and $h_k(t+\beta,\tau)$ are similar when $\beta << T_{coh}$, T_{coh} being the coherence time of the channel. With velocity v of the portable unit and the wavelength λ_0 at center frequency, T_{coh} can be approximated by [51]

$$T_{coh} \approx \frac{\lambda_0}{2v}. \tag{3.7}$$

With a λ_0= 0.2 meter and v = 5 km/hr, T_{coh} for an indoor channel is $\approx$ 70 msec. With a symbol duration T_b = 1 microsecond, a channel can be considered to be time invariant for several data symbol durations. Thus, a slow fading channel is assumed in this analysis. This implies that the channel parameters remain invariant over the duration of several bits [49]. The multipath amplitudes and phases can be estimated fairly accurately in a slow fading indoor radio channel.

For a quasi-static channel like the one described above, Equation (3.6) reduces to

$$h_k(t) = \sum_{\lambda=1}^{L_k} g_{k,\lambda}\delta(t - t_{k,\lambda})e^{j\theta_{k,\lambda}}. \tag{3.8}$$

The number of paths, L_k, in link k has a Binomial distribution [52]. For this distribution

$$\Pr[\lambda = L_k] = \binom{N_\Delta}{L_k} {P_b}^{L_k}(1 - P_b)^{N_\Delta - L_k}, \tag{3.9}$$

where N_Δ is the number of bins that can be formed by dividing the delay spread, Δ into intervals of one chip period such that $N_\Delta = \lfloor \frac{\Delta}{T_c} \rfloor$; $\lfloor x \rfloor$ being the integer part of the real number x. The maximum possible value of L_k is N_Δ and $L_k \in \{1, 2, ..., N_\Delta\}$. P_b is the probability that a path exists in any one of the bins.

Paths are counted as different paths only if

$$|t_{k,\alpha} - t_{k,\lambda}| > \frac{1}{W} \tag{3.10}$$

for all $\alpha \neq \lambda$. Distinct paths in the physical medium that violate this resolvability condition are not counted separately, since they cannot be distinguished in a system with a bandwidth of W. These unresolvable "subpaths" present within a chip duration add vectorially. Mathematically, if $|t_{k,\alpha_i} - t_{k,\alpha_j}| < \frac{1}{W}$, for $i, j = 1, ..., n$, where n is the number of subpaths within a chip duration, then

$$g_{k,\alpha}e^{j\theta_{k,\alpha}} = \sum_{i=1}^{n} g_{k,\alpha_i}e^{j\theta_{k,\alpha_i}} \tag{3.11}$$

is the resolved multipath component [40].

Although the gains of adjacent multipath components $\{g_{k,\lambda},\ \lambda = 1, 2, ..., L_k\}$ are likely to have some correlation, the existence or the degree of this type of correlation has not yet been established. However, measurements indicate that two components can be considered to have uncorrelated gains if their time delay difference is more than 25 nanoseconds [41]. With a data rate of 1 megabits per second (Mbps) and a chip rate of 31 megachips per seconds (Mcps), the resolvable path delay is equal to 33 nanoseconds in the CDMA system under consideration. Thus the assumption of uncorrelated amplitudes of the resolvable paths is just valid in this case.

The following assumptions are made in the analysis that follows. (i) The path amplitude $g_{k,\lambda}$ is Rayleigh distributed, the path phase $\theta_{k,\lambda}$ is uniformly distributed over $[0, 2\pi]$ and the path time delay, $t_{k,\lambda}$ is uniformly distributed over $[0, \Delta]$. (ii) The sets $\{t_{k,\lambda}\}$, $\{g_{k,\lambda}\}$, $\{\theta_{k,\lambda}\}$ and $\{L_k\}$ are mutually independent and members within each set are i.i.d random processes for all k and λ.

3.2 Performance of Correlator Receiver

As explained in Chapter 2, an attractive feature of correlator receivers is their simplicity. Because of this, they find applications in many practical systems. In this section, the BER performance of a correlator receiver is analyzed for an indoor CDMA system. In particular, the effect of imperfections in power control, carrier phase estimation and spreading code phase estimation on the performance of such receivers is investigated. The components of the received signal at the base station

are examined and models to analyze the effect of system imperfections are developed in Section 3.2.1. An expression for receiver output data estimate is developed in Section 3.2.2. It is followed by BER analysis and numerical results in Section 3.2.3 and 3.2.4 respectively.

3.2.1 The Received Signal

The received signal, which is the sum of all the signals arriving from each user and path in addition to the thermal noise, can be written as

$$r(t) = \sum_{k=1}^{K} \int_{-\infty}^{\infty} h_k(\tau) s_k(t-\tau) d\tau + n(t), \tag{3.12}$$

where $n(t)$ is the white zero mean Gaussian thermal noise process with a two sided noise power spectral density of $\frac{N_o}{2}$ at the receiver input. It is to be noted that, due to imperfections in power control, the received signal $r(t)$ consists of user signals with a log-normal distribution of power. The variance of the distribution can be up to 2 dB. Using Equations (3.5) and (3.8), $r(t)$ may be written in the form

$$r(t) = \sum_{k=1}^{K} \sum_{\lambda=1}^{L_k} \sqrt{2P_k} g_{k,\lambda} a_k(t-\tau_{k,\lambda}) b_k(t-\tau_{k,\lambda}) \cos(\omega_c t + \phi_{k,\lambda}) + n(t). \tag{3.13}$$

The net time delay, $\tau_{k,\lambda}$, and the net phase offset, $\phi_{k,\lambda}$, are obtained by summing their respective transmitter and channel parts so that $\tau_{k,\lambda} = T_k + t_{k,\lambda}$ and $\phi_{k,\lambda} = (\psi_k + \theta_{k,\lambda} - \omega_c \tau_{k,\lambda})$ modulo 2π. $\tau_{k,\lambda}$ and $\phi_{k,\lambda}$ are modeled to be uniformly distributed over $[0, T_b + \Delta]$ and $[0, 2\pi]$ respectively. The correlator receiver for the ith $(1 \leq i \leq K)$

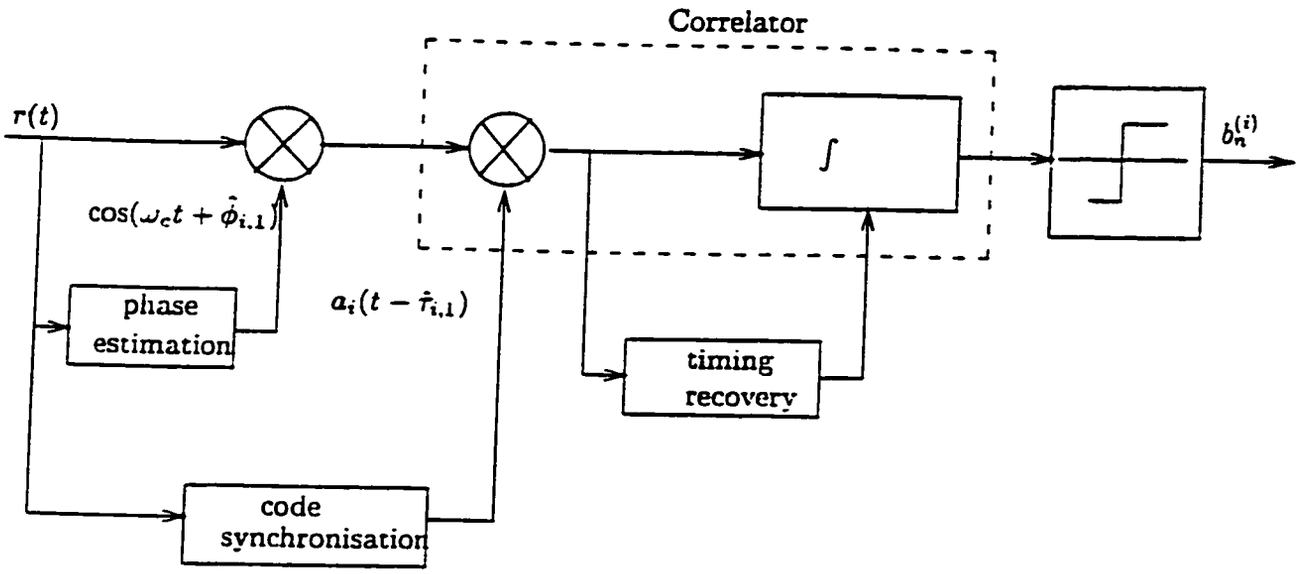

Figure 3.2 A functional block diagram of correlator receiver for demodulating the desired data from CDMA received signal.

user shown in Figure 3.2 is aligned with the signal arriving in the first path. The first step in the receiver is down conversion to the baseband signal $r_d(t)$. This is done by multiplying $r(t)$ by $\cos(\omega_c t + \hat{\phi}_{i,1})$. where $\hat{\phi}_{i,1}$ is the estimate of phase $\phi_{i,1}$ of the signal arriving in the first path. Estimation of this phase angle cannot be assumed to be perfect. The estimated phase $\hat{\phi}_{i,1}$ can be written as

$$\hat{\phi}_{i,1} = \phi_{i,1} + \Delta\phi_{i,1}. \tag{3.14}$$

where $\Delta\phi_{i,1}$ is the error in the estimation of $\phi_{i,1}$ and is assumed to be a zero mean Gaussian random variable with a variance of $\sigma^2_{\Delta\phi_{i,1}}$. The down converted and low-pass filtered signal for the desired user i. can be written as

$$\begin{aligned} r_d(t) &= \sqrt{\frac{P_i}{2}} g_d(i,i,1) a_i(t-\tau_{i,1}) b_i(t-\tau_{i,1}) \\ &\quad + \sqrt{\frac{P_i}{2}} \sum_{\lambda=2}^{L_i} g_d(i,i,\lambda) a_i(t-\tau_{i,\lambda}) b_i(t-\tau_{i,\lambda}) \\ &\quad + \sum_{k=1,k\neq i}^{K} \sum_{\lambda=1}^{L_k} \sqrt{\frac{P_k}{2}} g_d(i,k,\lambda) a_k(t-\tau_{k,\lambda}) b_k(t-\tau_{k,\lambda}) \\ &\quad + n_d(t). \end{aligned} \tag{3.15}$$

where $g_d(i,k,\lambda) = g_{k,\lambda}\cos(\phi_{k,\lambda} - \hat{\phi}_{i,1})$ and $n_d(t)$ is the lowpass filtered component of the down converted noise signal $n(t)\cos(\omega_c t + \hat{\phi}_{i,1})$. In Equation (3.15), the first term corresponds to the desired path signal for the ith user. The second component is the Interference from the Desired Signal (IDS) due to the multipaths in the ith user signal. The third component represents the Multiple Access Interference (MAI)

from other users of the CDMA system and the fourth term is due to the Additive White Gaussian Noise (AWGN).

The receiver must acquire the phase of the spreading sequence corresponding to the first path signal of the desired transmitter. Because of the multiple spread spectrum signals transmitted in the same bandwidth by other users of the CDMA system. this acquisition process is difficult. The presence of multiple access interference results in an error in the acquired code phase. The error in code phase acquisition results in a path delay estimation error, $\Delta\tau_{i,1}$, such that

$$\hat{\tau}_{i,1} = \tau_{i,1} + \Delta\tau_{i,1}. \tag{3.16}$$

where $\hat{\tau}_{i,1}$ denotes the estimated delay of the first path signal of the ith user. The error in code phase acquisition results in a spreading code $a_i(t - \hat{\tau}_{i,1})$ being fed to the correlator shown in Figure 3.2. The path delay estimation error is modeled as a zero mean Gaussian random variable with a variance of $\sigma^2_{\Delta\tau_{i,1}}$. It is assumed that $\Delta\tau_{i,1}$ and $\Delta\phi_{i,1}$ are mutually independent random variables.

3.2.2 Analysis of Data Estimates

At time $t = nT_b + \hat{\tau}_{i,1}$, the correlator output $Z_n^{(i)}$ for the nth symbol is given by

$$\begin{aligned} Z_n^{(i)} &= \int_{(n-1)T_b+\hat{\tau}_{i,1}}^{nT_b+\hat{\tau}_{i,1}} r(t)a_i(t - \hat{\tau}_{i,1})\cos(\omega_c t + \hat{\phi}_{i,1})dt \\ &= D_n^{(i)} + F_n^{(i)} + I_n^{(i)} + \zeta_n^{(i)}. \end{aligned} \tag{3.17}$$

where $\hat{\tau}_{i,1}$ and $\hat{\phi}_{i,1}$ have been defined previously. In Equation (3.17), $D_n^{(i)}$ denotes the desired output of the correlator, $F_n^{(i)}$ corresponds to the interference output due to other path signals of the desired user and $I_n^{(i)}$ is the output due to signals of other simultaneous users of the CDMA system. The quantity, $\zeta_n^{(i)}$ is the correlator output due to AWGN. By substituting for $r(t)$ and performing the integration, it is straightforward to show that

$$D_n^{(i)} = \sqrt{\frac{P_i}{2}} b_n^{(i)} g_d(i,i,1) R_{i,i}(\Delta\tau_{i,1}) T_b, \tag{3.18}$$

$$F_n^{(i)} = \sum_{\lambda=2}^{L_i} \left[\sqrt{\frac{P_i}{2}} g_d(i,i,\lambda) \left\{ b_{n-1}^{(i)} R_{i,i}(\tau(i,i,\lambda)) + b_n^{(i)} \hat{R}_{i,i}(\tau(i,i,\lambda)) \right\} \right]. \tag{3.19}$$

$$I_n^{(i)} = \sum_{k=1,k\neq i}^{K} \sum_{\lambda=1}^{L_k} \left[\sqrt{\frac{P_k}{2}} g_d(i,k,\lambda) \left\{ b_{n-1-m}^{(k)} R_{k,i}(\tau(i,k,\lambda)) + b_{n-m}^{(k)} \hat{R}_{k,i}(\tau(i,k,\lambda)) \right\} \right] \tag{3.20}$$

and

$$\zeta_n^{(i)} = \int_{(n-1)T_b+\hat{\tau}_{i,1}}^{nT_b+\hat{\tau}_{i,1}} n(t) a_i(t-\hat{\tau}_{i,1}) \cos(\omega_c t + \hat{\phi}_{i,1}) dt. \tag{3.21}$$

where $g_d(i,k,\lambda)$ has been previously defined. Other notations used in Equations (3.18) - (3.20) are explained below. Quantity $R_{i,i}(\Delta\tau_{i,1})$ denotes the autocorrelation function of the spreading code of the desired user, i. The counter m is defined as

$$m = \lfloor \frac{\tau_{k,\lambda} - \hat{\tau}_{i,1}}{T_b} \rfloor, \tag{3.22}$$

and it specifies the relative bit shift in user k's bit sequence arriving over its λth path with respect to user i's bit sequence arriving over its first path. This is required to

determine the overlapping paths. The functions $R_{k,i}(\tau(i,k,\lambda))$ and $\hat{R}_{k,i}(\tau(i,k,\lambda))$ represent the time continuous partial correlation between the spreading signal of user k's λth path and that of user i, defined as [13]

$$R_{k,i}(\tau(i,k,\lambda)) = \int_0^{\tau(i,k,\lambda)} a_k(t-\tau(i,k,\lambda))\, a_i(t)dt \tag{3.23}$$

and

$$\hat{R}_{k,i}(\tau(i,k,\lambda)) = \int_{\tau(i,k,\lambda)}^{T_b} a_k(t-\tau(i,k,\lambda))\, a_i(t)dt, \tag{3.24}$$

for $0 \leq \tau(i,k,\lambda) \leq T_b$. The time delay $\tau(i,k,\lambda)$ between two signals is introduced to perform a modulo T_b operation. This ensures that the arguments of $R_{k,i}(\tau(i,k,\lambda))$ and $\hat{R}_{k,i}(\tau(i,k,\lambda))$ satisfy $0 \leq \tau(i,k,\lambda) \leq T_b$. It is given by

$$\tau(i,k,\lambda) = (\tau_{k,\lambda} - \hat{\tau}_{i,1}) - mT_b. \tag{3.25}$$

A hard decision on the correlator output $Z_n^{(i)}$ provides a data estimate of ith user's nth symbol as

$$\hat{b}_n^{(i)} = \mathrm{sgn}(Z_n^{(i)}). \tag{3.26}$$

This data estimate variable is used in the BER analysis presented in the next section.

3.2.3 BER Analysis

It is difficult to obtain the exact BER of the DS/CDMA system because analysis is often intractable. In many practical cases the analytical expression for the proba-

bility of error cannot be evaluated exactly. A great deal of work has gone into finding efficient methods for computation of the BER of CDMA systems [13, 14, 16, 17], [53]-[55]. These include approximations and bounds. The BER analysis presented here utilizes the standard Gaussian approximation [13] and the improved Gaussian approximation [54] to model the effect of multiple access interference.

Standard Gaussian Approximation

A computationally simple approximation is the standard Gaussian approximation. In this approximation the interference signals $F_n^{(i)}$ and $I_n^{(i)}$ from all paths of all users are assumed to have a joint Gaussian distribution which implies unconditional independence among the components of the multiple access interference within a desired data bit duration.

In Equation (3.17), an expression for the decision variable $Z_n^{(i)}$ was developed. Because the symbol $b_n^{(i)}$ is equally likely, the system BER $p_e^{(i)}$ for the ith user is then given by

$$p_e^{(i)} = 0.5\Pr(Z_n^{(i)} < 0 | b_n^{(i)} = +1) + 0.5\Pr(Z_n^{(i)} \geq 0 | b_n^{(i)} = -1). \qquad (3.27)$$

Because of symmetry, one can write

$$\Pr(Z_n^{(i)} \geq 0 | b_n^{(i)} = -1) = \Pr(Z_n^{(i)} < 0 | b_n^{(i)} = +1). \qquad (3.28)$$

Therefore

$$p_e^{(i)} = \Pr(Z_n^{(i)} \geq 0 | b_n^{(i)} = -1). \tag{3.29}$$

Specifically, one can write

$$\begin{aligned} p_e^{(i)} &= \Pr(F_n^{(i)} + I_n^{(i)} + \zeta_n^{(i)} \geq D_n^{(i)} | b_n^{(i)} = -1) \\ &= \Pr(\frac{F_n^{(i)} + I_n^{(i)} + \zeta_n^{(i)}}{\sqrt{\mathrm{Var}(F_n^{(i)}) + \mathrm{Var}(I_n^{(i)}) + \mathrm{Var}(\zeta_n^{(i)})}} \geq \sqrt{SNR_n^{(i)}}). \end{aligned} \tag{3.30}$$

where

$$SNR_n^{(i)} = \frac{E([D_n^{(i)}]^2)}{\mathrm{Var}(F_n^{(i)}) + \mathrm{Var}(I_n^{(i)}) + \mathrm{Var}(\zeta_n^{(i)})}. \tag{3.31}$$

A straightforward application of the central limit theorem then indicates that $p_e^{(i)} \rightarrow Q(\sqrt{(SNR_n^{(i)}})$ where

$$Q(x) = \frac{1}{\sqrt{2\pi}} \int_x^\infty e^{-\frac{u^2}{2}} du. \tag{3.32}$$

The central limit theorem is applicable when no single or asymptotically small proportion of users contribute to a major share of interference. This condition holds true in the case of perfect power control and also in the case of imperfect power control with a variance of 1-2 dB in the normalized received power. However, in the case of no power control, a weak signal may experience high power interference from a portable close to the base station. Under such a condition, the central limit theorem cannot hold and the standard Gaussian approximation is not accurate.

Using computer simulations, histograms of the MAI are obtained corresponding

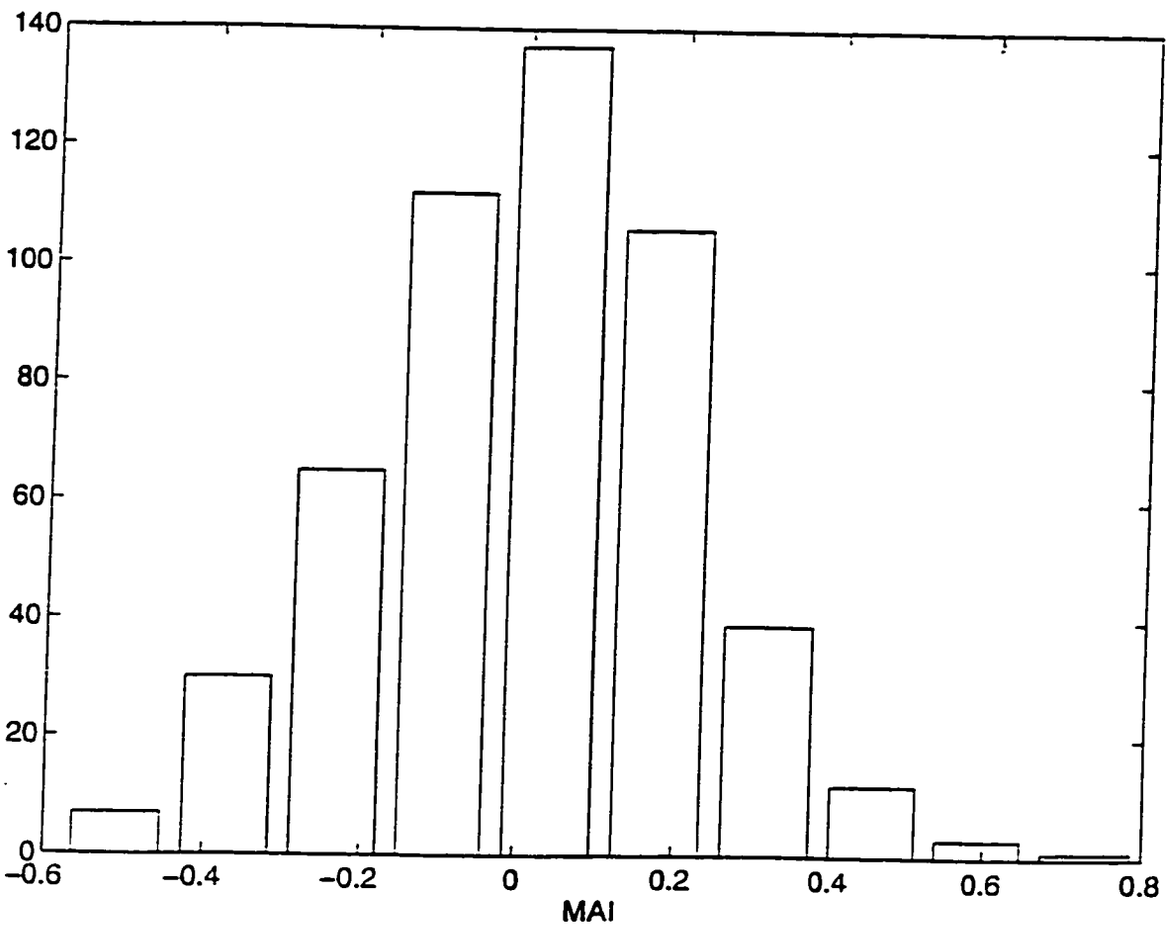

Figure 3.3 Histogram of the multiple access interference using 512 data points with $N = 31$, number of co-users $= 2$, $\bar{L} = 3$, and perfect power control.

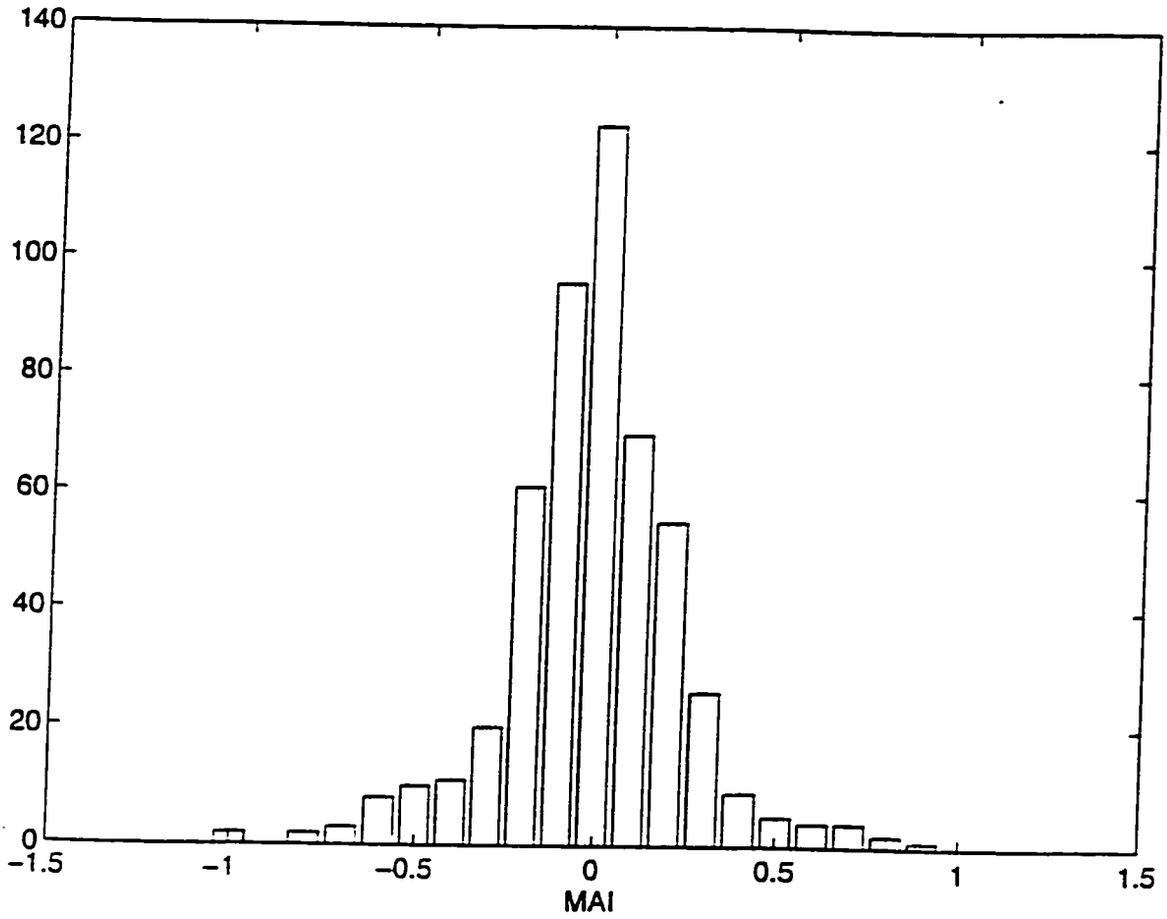

Figure 3.4 Histogram of the multiple access interference using 512 data points with $N = 31$, number of co-users $= 2$, $\bar{L} = 3$ and 2 dB variance in normalized received power.

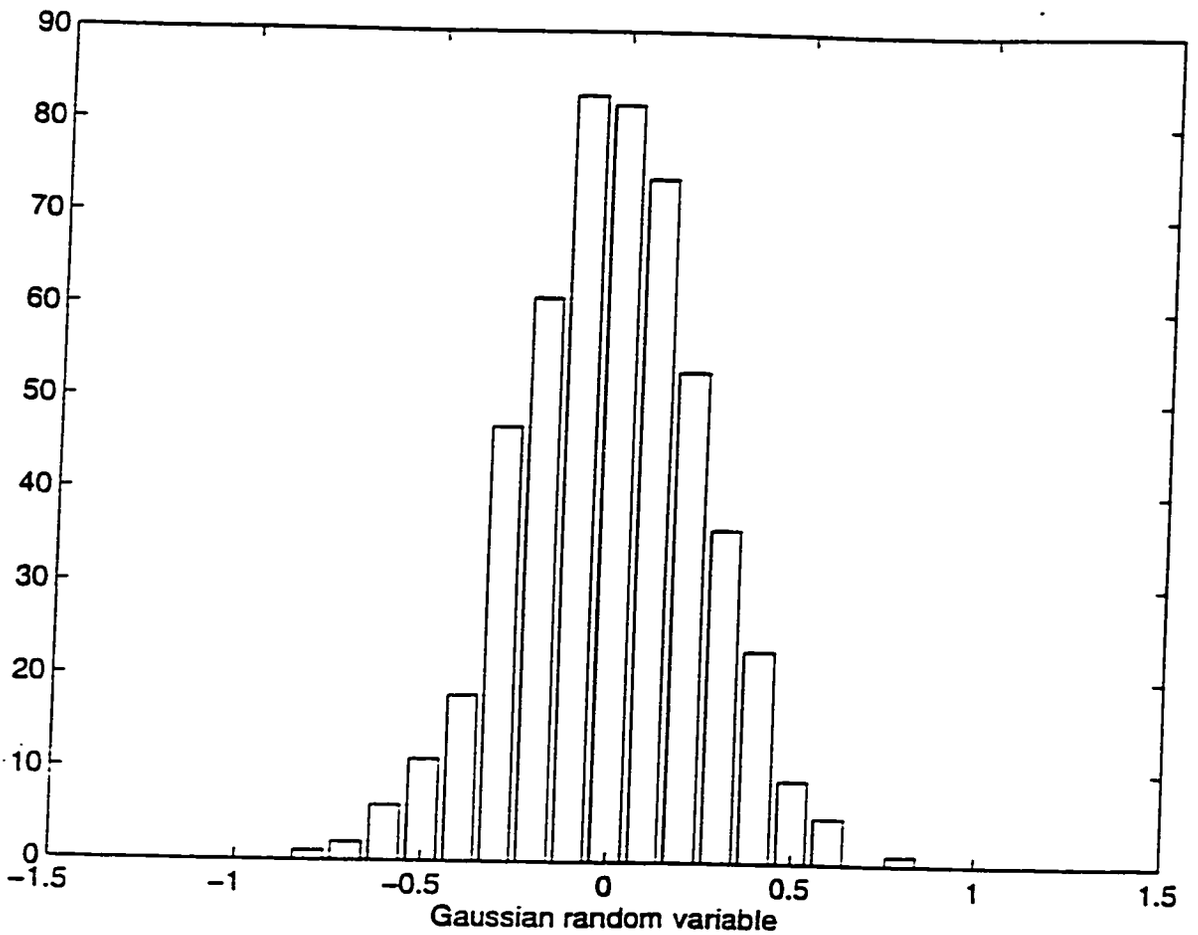

Figure 3.5 Histogram of the Gaussian random variable vector of size 1 X 512 generated by MATLAB.

to perfect power control and imperfect power control situations. These are shown in Figures 3.3 and 3.4. For comparison, the Gaussian random variable generated by the simulation software MATLAB is shown in Figure 3.5. As may be seen, with imperfect power control, the MAI is not very different from Gaussian.

The BER at the output of the receiver is calculated using standard Gaussian approximation. To do this, expressions for the expected desired signal strength and the variances of interferences and thermal noise at the output of the receiver have to be derived. From Equation (3.18), by taking the expected value of the mutually independent random variables, the average desired signal strength of the nth symbol of the ith user can be written as

$$E\left\{\left[D_n^{(i)}\right]^2\right\} = \frac{1}{4}E\{P_i\}T_b^2 E\left\{g_{i,1}^2\right\}\left[1+\exp(-2\sigma^2_{\Delta\phi_{i,1}})\right]E\left\{R^2_{i,i}(\Delta\tau_{i,1})\right\}. \qquad (3.33)$$

where $E\{[b_n^{(i)}]^2\} = 1$ has been utilized. Note that in deriving Equation (3.33), the fact that for a zero mean Gaussian random variable x with variance σ_x^2, $E\{\cos bx\} = \exp(-\frac{b^2\sigma_x^2}{2})$, where b is a constant, has been used. The components of the set of received power $\{P_k,\ 1 \le k \le K\}$ are independent and log-normally distributed random variables [10].

In Equation (3.33), $E\left\{R^2_{i,i}(\Delta\tau_{i,1})\right\}$ has to be evaluated. This is done as follows. In a practical synchronization system, most likely values of the error $\Delta\tau_{i,1}$ lie between $+T_c$ and $-T_c$. During this interval the autocorrelation function of the spreading

code may be written approximately as

$$R_{i,i}(\Delta\tau_{i,1}) = \begin{cases} 1 - \frac{|\Delta\tau_{i,1}|}{T_c}: & |\Delta\tau_{i,1}| \leq T_c \\ 0 & \text{otherwise.} \end{cases} \tag{3.34}$$

$E\left\{R_{i,i}^2(\Delta\tau_{i,1})\right\}$ of this random variable is given by

$$E\left\{R_{i,i}^2(\Delta\tau_{i,1})\right\} = 1 - \frac{2}{T_c}\sqrt{\frac{2}{\pi}}\sigma_{\Delta\tau_{i,1}} + \frac{1}{T_c^2}\sigma_{\Delta\tau_{i,1}}^2. \tag{3.35}$$

Using Equation (3.35), Equation (3.33) is written as

$$\begin{aligned} E\left\{\left[D_n^{(i)}\right]^2\right\} &= \frac{1}{4}E\{P_i\}T_b^2 E\left\{g_{i,1}^2\right\}\left[1 + \exp(-2\sigma_{\Delta\phi_{i,1}}^2)\right]. \\ &\quad (1 - \frac{2}{T_c}\sqrt{\frac{2}{\pi}}\sigma_{\Delta\tau_{i,1}} + \frac{1}{T_c^2}\sigma_{\Delta\tau_{i,1}}^2). \end{aligned} \tag{3.36}$$

The variance of the $F_n^{(i)}$ term given by Equation (3.19) can be similarly obtained as

$$\begin{aligned} \mathrm{Var}(F_n^{(i)}) &= \frac{1}{2}E\{P_i\}(\bar{L}_i - 1)E\left\{g_d^2(i,i,\lambda)\right\}. \\ &\quad E\left\{R_{i,i}^2(\tau(i,i,\lambda)) + \hat{R}_{i,i}^2(\tau(i,i,\lambda))\right\}. \end{aligned} \tag{3.37}$$

where $\bar{L}_i$ is the average number of paths of the ith user. To evaluate Equation (3.37), the probability density function of $\tau(i,i,\lambda)$ has to be obtained. It can be shown that in the case of perfect synchronization, the probability density function of $\tau(i,i,\lambda)$

is $\frac{1}{\Delta - T_c}$ within the interval T_c to Δ. In the case of imperfect synchronization, the probability density function of $\tau(i,i,\lambda)$ as given by Equation (3.25) is obtained as the convolution of the uniformly distributed delay and the Gaussian distributed error in path delay $\Delta\tau_{i,1}$. This density function is given by

$$f(\tau(i,i,\lambda)) = \frac{1}{2(\Delta - T_c)}\left[\mathrm{erf}(\frac{\tau(i,i,\lambda) - T_c}{\sqrt{2}\sigma_{\Delta\tau_{i,1}}}) - \mathrm{erf}(\frac{\tau(i,i,\lambda) - \Delta}{\sqrt{2}\sigma_{\Delta\tau_{i,1}}})\right]. \qquad (3.38)$$

where $\mathrm{erf}(x)$ is defined as

$$\mathrm{erf}(x) = \frac{2}{\sqrt{\pi}}\int_0^x e^{-t^2}dt. \qquad (3.39)$$

The density function in Equation (3.38) is plotted in Figure 3.6.

Similarly, the variance of the $I_n^{(i)}$ term (interference from all paths of other users), in Equation (3.20) may be obtained as

$$\begin{aligned}\mathrm{Var}(I_n^{(i)}) &= \sum_{k=1,k\neq i}^{K}\left[\frac{1}{2}E\{P_k\}\bar{L}_k E\left\{g_d^2(i,k,\lambda)\right\}.\right. \\ &\quad \left. E\left\{R_{k,i}^2(\tau(i,k,\lambda)) + \hat{R}_{k,i}^2(\tau(i,k,\lambda))\right\}\right]. \qquad (3.40)\end{aligned}$$

To evaluate Equation (3.40), the probability density function of $\tau(i,k,\lambda)$ has to be obtained. For perfect synchronization, the probability density function of $\tau(i,k,\lambda)$ is $\frac{1}{\Delta + T_b}$ within the interval $-T_c$ to $\Delta + T_b - T_c$. In the case of imperfect synchronization, the probability density function of $\tau(i,k,\lambda)$ is obtained as the convolution of the uniformly distributed delay and the Gaussian distributed error $\Delta\tau_{i,1}$ in path delay.

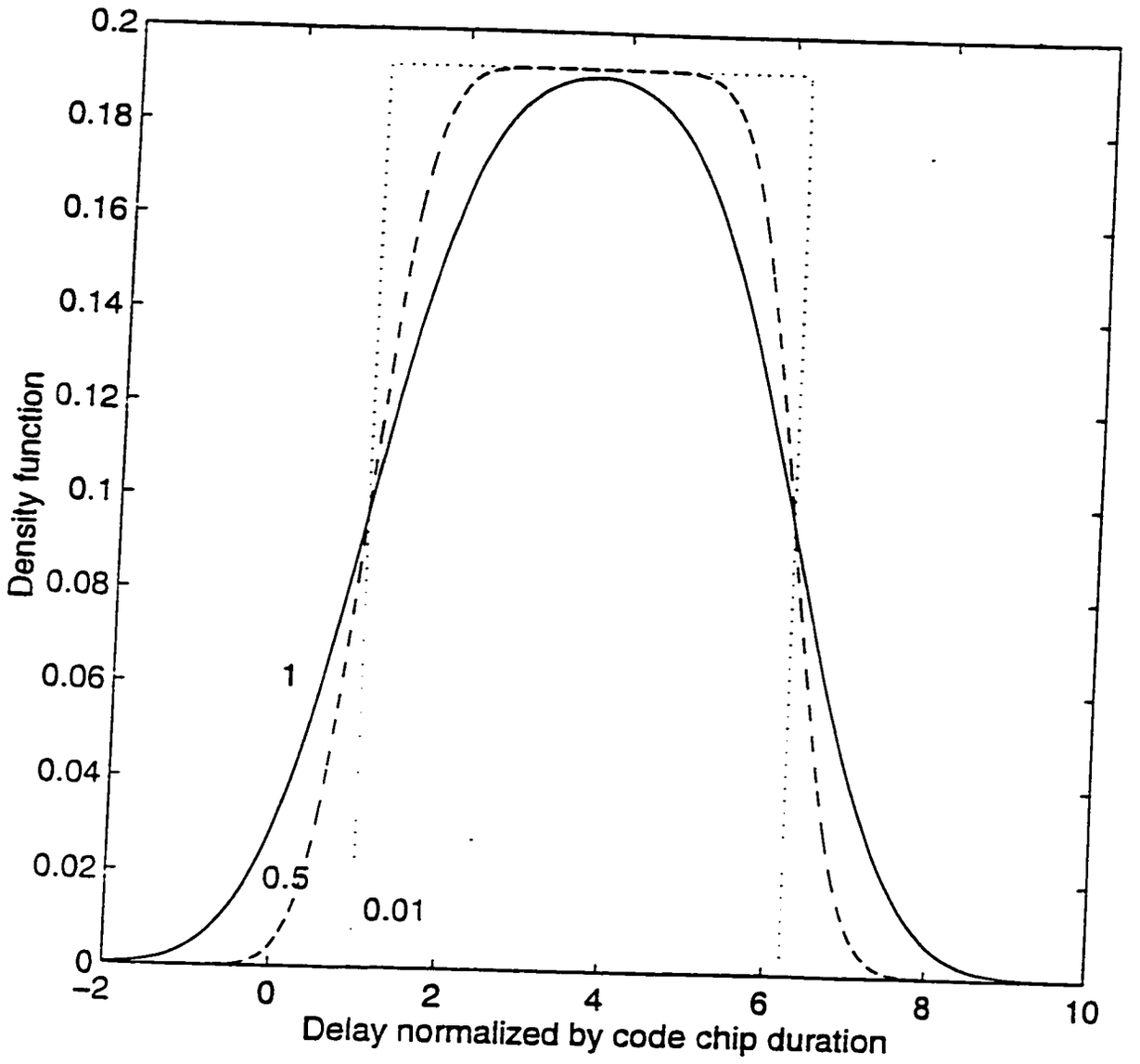

Figure 3.6 The plot of density function in Equation (3.37) for standard deviations of 0.01, 0.5 and 1 in normalized estimation error. The path delays are normalized by chip duration

This density function is then given by

$$f(\tau(i,k,\lambda)) = \frac{1}{2(\Delta+T_b)}\left[\mathrm{erf}(\frac{\tau(i,k,\lambda)+T_c}{\sqrt{2}\sigma_{\Delta\tau_{i,1}}}) - \mathrm{erf}(\frac{\tau(i,k,\lambda)+T_c-\Delta-T_b}{\sqrt{2}\sigma_{\Delta\tau_{i,1}}})\right]. \quad (3.41)$$

To obtain the variances of $F_n^{(i)}$ and $I_n^{(i)}$, the values of $R_{i,i}^2$, $\hat{R}_{i,i}^2$ and $R_{k,i}^2$, $\hat{R}_{k,i}^2$ are required. The time continuous partial cross-correlation functions $R_{k,i}$ and $\hat{R}_{k,i}$ are defined in terms of discrete aperiodic cross-correlation function of the spreading codes as [13]

$$R_{k,i}(\tau) = C_{k,i}(l-N)T_c + [C_{k,i}(l+1-N) - C_{k,i}(l-N)](\tau - lT_c) \quad (3.42)$$

and

$$\hat{R}_{k,i}(\tau) = C_{k,i}(l)T_c + [C_{k,i}(l+1) - C_{k,i}(l)](\tau - lT_c). \quad (3.43)$$

for $0 \le lT_c \le \tau \le (l+1)T_c \le T_b$. In Equations (3.42) and (3.43), the discrete aperiodic cross-correlation function $C_{k,i}$, for the code sequences $(a_j^{(k)})$ and $(a_j^{(i)})$ of the kth and ith user is given by

$$C_{k,i}(l) = \begin{cases} \sum_{j=0}^{j=N-1-l} a_j^{(k)} a_{j+l}^{(i)}: & 0 \le l \le N-1 \\ \sum_{j=0}^{j=N-1+l} a_{j-l}^{(k)} a_j^{(i)}: & 1-N \le l < 0 \\ 0: & |l| \ge N \end{cases} \quad (3.44)$$

where N is the code period. The discrete aperiodic autocorrelation function may

be obtained by putting $k = i$ in Equation (3.44).

$E\left\{R_{i,i}^2(\tau(i,i,\lambda)) + \hat{R}_{i,i}^2(\tau(i,i,\lambda))\right\}$ and $E\left\{R_{k,i}^2(\tau(i,k,\lambda)) + \hat{R}_{k,i}^2(\tau(i,k,\lambda))\right\}$ are now easily evaluated using numerical integration.

The mean and variance of the noise in Equation (3.21) are given by .

$$E\{\zeta_n^{(i)}\} = 0 \tag{3.45}$$

and

$$\mathrm{Var}(\zeta_n^{(i)}) = \frac{N_o T_b}{4}. \tag{3.46}$$

Then from Equations (3.36),(3.37),(3.40) and (3.46), the ith user's signal to noise ratio may be written as.

$$SNR_n^{(i)} = \frac{E\{[D_n^{(i)}]^2\}}{\mathrm{Var}(F_n^{(i)}) + \mathrm{Var}(I_n^{(i)}) + \mathrm{Var}(\zeta_n^{(i)})}. \tag{3.47}$$

The data bit error probability is then given by

$$p_e^{(i)} = Q\left(\sqrt{SNR_n^{(i)}}\right), \tag{3.48}$$

where the Q function has been defined previously.

Improved Gaussian Approximation

Standard Gaussian approximation is an accurate approximation for SNR values up to 10 to 12 dB. This approximation becomes very optimistic as N, the spreading

code period, increases and for small values of the number of co-users [54]. In such a situation, improved Gaussian approximation is used to obtain accurate results.

The difference between the standard Gaussian approximation and the improved Gaussian approximation is on the distribution function of the MAI. In the standard Gaussian approximation the MAI is assumed to have unconditional Gaussian distribution whereas in the improved Gaussian approximation MAI is assumed to have a conditionally Gaussian approximation. To develop an expression for the BER using the improved Gaussian approximation, a conditional variance for the MAI is first derived to obtain a conditional SNR. The Q function of this conditional SNR is then averaged over the density function of the variance to obtain an accurate value of BER. An analysis to obtain an expression for the BER using improved Gaussian approximation is developed as follows.

It is easy to understand that the terms $F_n^{(i)}$ and $I_n^{(i)}$ are not unconditionally Gaussian as assumed in the standard Gaussian approximation. For example, consider two terms in $F_n^{(i)}$ for $\lambda = 2$ and 3

$$F_2 = \sqrt{\frac{P_i}{2}} g_{i,2} \cos(\phi_{i,2} - \phi_{i,1}) \left\{ b_{n-1}^{(i)} R_{i,i}(\tau(i,i,2)) + b_n^{(i)} \hat{R}_{i,i}(\tau(i,i,2)) \right\}. \qquad (3.49)$$

and

$$F_3 = \sqrt{\frac{P_i}{2}} g_{i,3} \cos(\phi_{i,3} - \phi_{i,1}) \left\{ b_{n-1}^{(i)} R_{i,i}(\tau(i,i,3)) + b_n^{(i)} \hat{R}_{i,i}(\tau(i,i,3)) \right\}. \qquad (3.50)$$

Quantities $g_{i,\lambda}$, $\phi_{i,\lambda}$, b_n, b_{n-1} and $\tau_{i,\lambda}$ are all independent random variables. For

a given value of $\phi_{i,1}$ and $\tau_{i,1}$, the interference terms. F_2 and F_3 are independent. Therefore, the actual interferences from all paths of all users are only conditionally independent, the condition being that the phase and the delay of the first path signal be known. This, of course, assumes that deterministic spreading sequences are used for all users and the transmitted code phases of all users are known.

A conditional variance Ψ for the multiple access interference from all paths of all users can be derived by conditioning on the relative delays and phases of all interfering signals. Then each outcome $\Psi = \psi$ is produced by a specific outcome of τ and ϕ. For notational simplicity, τ and ϕ are defined as $\tau = \{\tau(i,k,\lambda);\ 1 \leq k \leq K,\ 1 \leq \lambda \leq L_k\}$ and $\phi = \{\phi(i,k,\lambda);\ 1 \leq k \leq K,\ 1 \leq \lambda \leq L_k\}$, where $\phi(i,k,\lambda) = \phi_{k,\lambda} - \phi_{i,1}$. Without considering the effect of AWGN, BER is given by $Q(\sqrt{\frac{P_{av}}{\psi}})$, where P_{av} is the average desired signal power. This provides an accurate expression for probability of error for a particular value of ψ [54] . Therefore, the probability of error can be calculated by averaging over the density function of ψ as

$$p_e^{(i)} = \int_0^\infty Q(\sqrt{\frac{P_{av}}{\psi}}) f_\Psi(\psi) d\psi. \tag{3.51}$$

Obtaining the value of $f_\Psi(\psi)$ is quite complex, especially when there are numerous signals from various paths of all users of the CDMA, each of which has infinite possible values of τ and ϕ [54].

A method of evaluating Equation (3.51) with greatly reduced computational complexity, given in [55], is based on the fact that Equation (3.51) is the expectation of

the function of the random variable w. That is

$$\begin{aligned} p_e^{(i)} &= \int_0^\infty Q(\sqrt{\frac{P_{av}}{w}}) f_w(w) dw \\ &= E\left\{ Q(\sqrt{\frac{P_{av}}{w}}) \right\}. \end{aligned} \tag{3.52}$$

With this method, no distribution functions are needed, provided some distributional analysis is done. It is then possible to calculate the value of Equation (3.51) with first and second moments of w. Including the effect of AWGN and using the method described in [55], $p_e^{(i)}$ may be written as

$$\begin{aligned} p_e^{(i)} &\approx \frac{2}{3} Q(\sqrt{\frac{P_{av}}{\mu + \sigma_T}}) \\ &+ \frac{1}{6} Q(\sqrt{\frac{P_{av}}{\mu + \sqrt{3}\sigma + \sigma_T}}) \\ &+ \frac{1}{6} Q(\sqrt{\frac{P_{av}}{\mu - \sqrt{3}\sigma + \sigma_T}}). \end{aligned} \tag{3.53}$$

where μ and σ^2 are the mean and variance of w and σ_T^2 is the variance of AWGN.

For the sake of comparison, the probability of bit error is derived using the improved Gaussian approximation for a simple case. Firstly, an expression for the conditional variance of multiple access interference is obtained. Then μ and σ^2 are calculated and are substituted in Equation (3.53) for the BER computation.

The interference terms in $F_n^{(i)}$ and $I_n^{(i)}$ are all zero mean and conditionally independent. By using the fact that the variance of the sum of zero-mean, independent random variables is the sum of their second moments, and assuming perfect power

control so that $P_1 = P_2 = ... = P$.

$$\begin{aligned}
\Psi &= \mathrm{Var}\left[\left(F_n^{(i)}|\phi,\tau\right) + \left(I_n^{(i)}|\phi,\tau\right)\right] \\
&= \mathrm{Var}\left[F_n^{(i)}|\phi,\tau\right] + \mathrm{Var}\left[I_n^{(i)}|\phi,\tau\right] \\
&= E\left[\left(F_n^{(i)}\right)^2|\phi,\tau\right] + E\left[\left(I_n^{(i)}\right)^2|\phi,\tau\right] \\
&= E\left[\left(\sum_{\lambda=2}^{L_i}\sqrt{\frac{P}{2}}g_{i,\lambda}\cos\phi\left\{b_{n-1}^{(i)}R_{i,i}\left(\tau\left(i,i,\lambda\right)\right) + b_n^{(i)}\hat{R}_{i,i}\left(\tau\left(i,i,\lambda\right)\right)\right\}\right)^2|\phi,\tau\right] + \\
&\quad E\left[\left(\sum_{k=1,k\neq i}^{K}\sum_{\lambda=1}^{L_k}\sqrt{\frac{P}{2}}g_{k,\lambda}\cos\phi\left\{b_{n-1-m}^{(i)}R_{k,i}\left(\tau\left(i,k,\lambda\right)\right) + \right.\right.\right. \\
&\quad \left.\left.\left. b_{n-m}^{(i)}\hat{R}_{k,i}\left(\tau\left(i,k,\lambda\right)\right)\right\}\right)^2|\phi,\tau\right] \\
&= \Psi_F + \Psi_I. \qquad (3.54)
\end{aligned}$$

The conditional variance Ψ_F of $F_n^{(i)}$ with respect to the variables ϕ and τ is given by

$$\begin{aligned}
\Psi_F &= \frac{P}{2}\sum_{\lambda=2}^{L_i}E\{g_{i,\lambda}^2\}E\{\cos^2\phi|\phi\}E\{R_{i,i}^2\left(\tau\left(i,i,\lambda\right)\right) + \hat{R}_{i,i}^2\left(\tau\left(i,i,\lambda\right)\right)|\tau\} \\
&= \frac{P}{4}G\sum_{\lambda=2}^{L_i}\left[\left(1+\cos 2\phi\right)E\{R_{i,i}^2\left(\tau\left(i,i,\lambda\right)\right) + \hat{R}_{i,i}^2\left(\tau\left(i,i,\lambda\right)\right)\}\right]. \qquad (3.55)
\end{aligned}$$

where $E\{g_{i,\lambda}^2\} = G$ for all i and λ. By using a similar procedure, the conditional variance Ψ_I of $I_n^{(i)}$ with respect to the variables ϕ and τ can be obtained as

$$\Psi_I = \frac{P}{4}G\sum_{k=1,k\neq i}^{K}\sum_{\lambda=1}^{L_k}\left[\left(1+\cos 2\phi\right)E\{R_{k,i}^2\left(\tau\left(i,k,\lambda\right)\right) + \hat{R}_{k,i}^2\left(\tau\left(i,k,\lambda\right)\right)\}\right]. \qquad (3.56)$$

The mean μ of the conditional variance Ψ can be obtained by taking the expectation

of Ψ with respect to o which is uniformly distributed in $[0, 2\pi]$. Thus

$$\begin{aligned}\mu &= \mu_F + \mu_I \\ &= \frac{P}{4}G(\bar{L}-1)E\{R^2_{i,i}(\tau(i,i,\lambda)) + \hat{R}^2_{i,i}(\tau(i,i,\lambda))\} + \\ &\quad \frac{P}{4}G\sum_{k=1,k\neq i}^{K}\bar{L}E\{R^2_{k,i}(\tau(i,k,\lambda)) + \hat{R}^2_{k,i}(\tau(i,k,\lambda))\}. \end{aligned} \tag{3.57}$$

where the average number of paths per user $\bar{L}_k = \bar{L}$ for all users.

The variance σ^2 of Ψ may be defined as

$$\sigma^2 = \sigma_F^2 + \sigma_I^2. \tag{3.58}$$

where σ_F^2 is the variance of Ψ_F and σ_I^2 is that of Ψ_I. With $\Psi_{F,l}$ and $\Psi_{F,j}$ as two components of Ψ_F, σ_F^2 is given by

$$\sigma_F^2 = (\bar{L}-1)\left[E\left(\Psi_{F,l}{}^2\right) - E(\Psi_{F,l})^2 + (\bar{L}-2)\mathrm{Cov}(\Psi_{F,l},\Psi_{F,j})\right]. \tag{3.59}$$

By evaluating the expectations and covariances in Equation (3.59), σ_F^2 is obtained as

$$\sigma_F^2 = P^2G^2(\bar{L}-1)\left\{\frac{1}{32} + \frac{(\bar{L}-2)}{32}\right\}\left[E\{R^2_{i,i}(\tau(i,i,\lambda)) + \hat{R}^2_{i,i}(\tau(i,i,\lambda))\}\right]^2. \tag{3.60}$$

By using a similar procedure, σ_I^2 is evaluated as

$$\begin{aligned}\sigma_I^2 = & \frac{3P^2G^2\bar{L}}{32}\sum_{k=1,k\neq i}^{K}\left\{\left[E\{R_{k,i}^2(\tau(i,k,\lambda))+\hat{R}_{k,i}^2(\tau(i,k,\lambda))\}\right]^2\right\}- \\ & \frac{P^2G^2\bar{L}}{16}\sum_{k=1,k\neq i}^{K}\left\{\left[E\{R_{k,i}^2(\tau(i,k,\lambda))+\hat{R}_{k,i}^2(\tau(i,k,\lambda))\}\right]^2\right\}+ \\ & \frac{P^2G^2\bar{L}}{32}\sum_{k=1,k\neq i}^{K}\sum_{l=1,l\neq k}^{K}\left[E\{R_{k,i}^2(\tau(i,k,\lambda))+\hat{R}_{k,i}^2(\tau(i,k,\lambda))\}\right]. \\ & \left[E\{R_{l,i}^2(\tau(i,l,\lambda))+\hat{R}_{l,i}^2(\tau(i,l,\lambda))\}\right]. \end{aligned} \tag{3.61}$$

The value of σ is

$$\sigma = \sqrt{\sigma_F^2+\sigma_I^2}. \tag{3.62}$$

The values of μ and σ are then substituted in Equation (3.53) to obtain $p_e^{(i)}$.

The BER obtained using standard Gaussian and improved Gaussian for various values of N, K and E_b/N_o are computed in Section 3.2.4.

3.2.4 Numerical Results

Performance results are computed for a system that uses a carrier frequency of 1.5 GHz and a data rate of 1 Mbps. Gold sequences of length N = 31 are used as the spreading codes. Each user's link is modeled with the same parameter values. Maximum path delay Δ is set to 200 nanoseconds thereby making the number of resolvable bins $N_\Delta = 6$. The probability that a path exists in a resolvable bin, P_b, is 0.5 so that $\bar{L}$ equals to 3. With $E\{\delta^2\}$ defined as the Mean Square of normalized Error (MSE), the variance of the carrier phase estimate error is $\sigma_{\Delta\phi_{i,l}}^2 = \pi^2 E\{\delta^2\}$.

and the variance of the code phase estimate error is $\sigma^2_{\Delta\tau_{i,1}} = T_c^2 E\{\delta^2\}$, where T_c is the chip duration. To take into account the effect of power control imperfections, as stated in Section 2.6, the normalized received power from each portable transmitter is modeled as a log-normal random variable with a variance of 1-2 dB. A variance of 0 dB denotes perfect power control.

In Figures 3.7 - 3.10, BER versus E_b/N_o obtained using the standard Gaussian approximation and the improved Gaussian approximation are plotted for various combinations of N and K. It may be seen that the standard Gaussian approximation provides very optimistic BER performance at high values of E_b/N_o with $N = 127$ and $K = 3$ as in Figure 3.7. With $N = 127$ and $K = 8$, the difference between the two BERs reduces considerably, as in Figure 3.8. The difference between the two BERs obtained using the standard Gaussian approximation and the improved Gaussian approximation are not so large for $N = 31$, even for low values of K, as in Figures 3.9 and 3.10. In all these cases, the BER performance obtained using these two approximations are quite close for commonly encountered practical values of E_b/N_o (up to about 12 dB). The BER results reported hereafter are derived using the standard Gaussian approximation to model CCI.

Numerical results on the effect of system imperfections on the BER performance of a CDMA correlator receiver are presented for various combination of factors. The individual effect of various system imperfections on BER performance is shown in Figures 3.11 - 3.13. Their combined effect is presented in Figure 3.14. In these figures the number of users, $K = 3$ and the spreading code sequence period, $N = 31$.

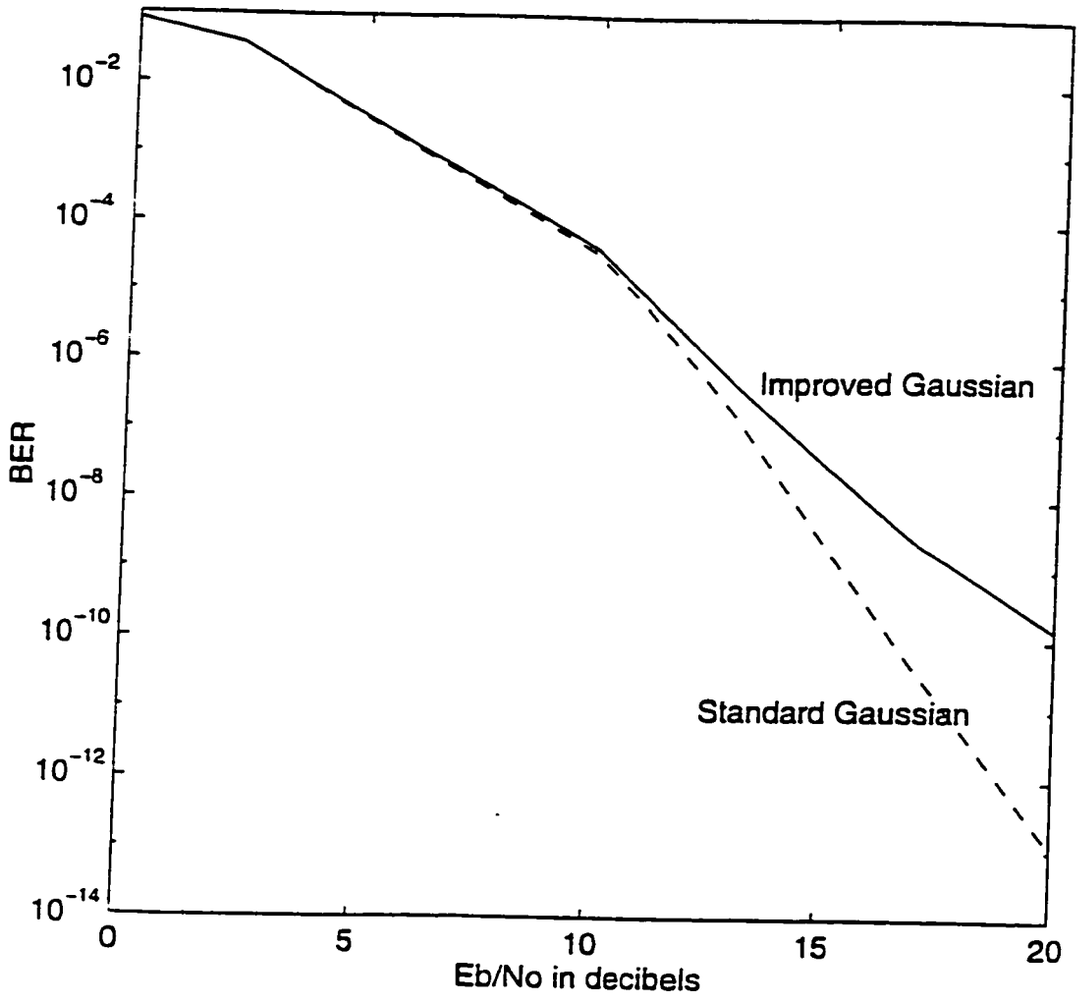

Figure 3.7 BER versus Eb/No for a correlator receiver. Perfect power control, spreading code phase estimation and carrier phase estimation; K = 3; $\bar{L} = 3$; $N = 127$.

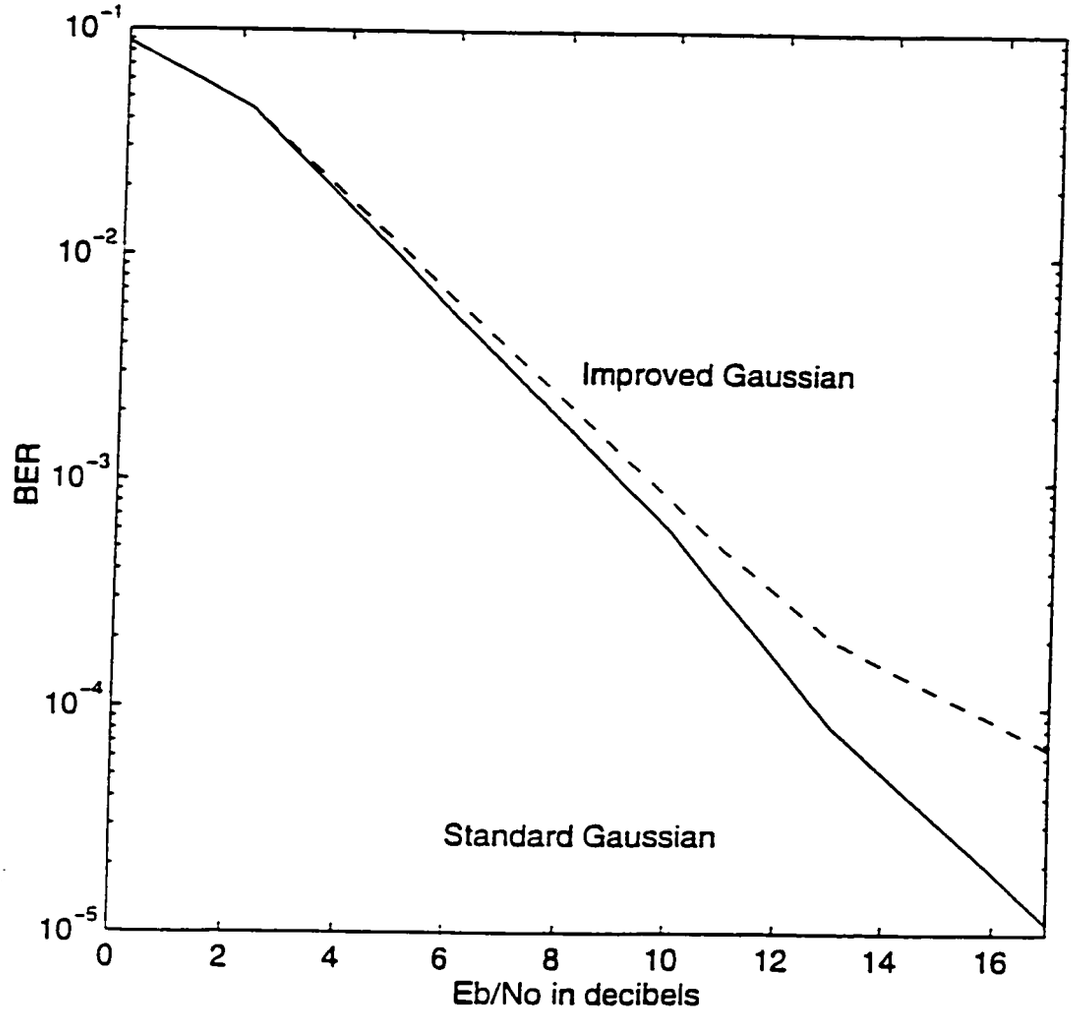

Figure 3.8 BER versus Eb/No for a correlator receiver. Perfect power control, spreading code phase estimation and carrier phase estimation; K = 8; $\bar{L} = 3$; $N = 127$.

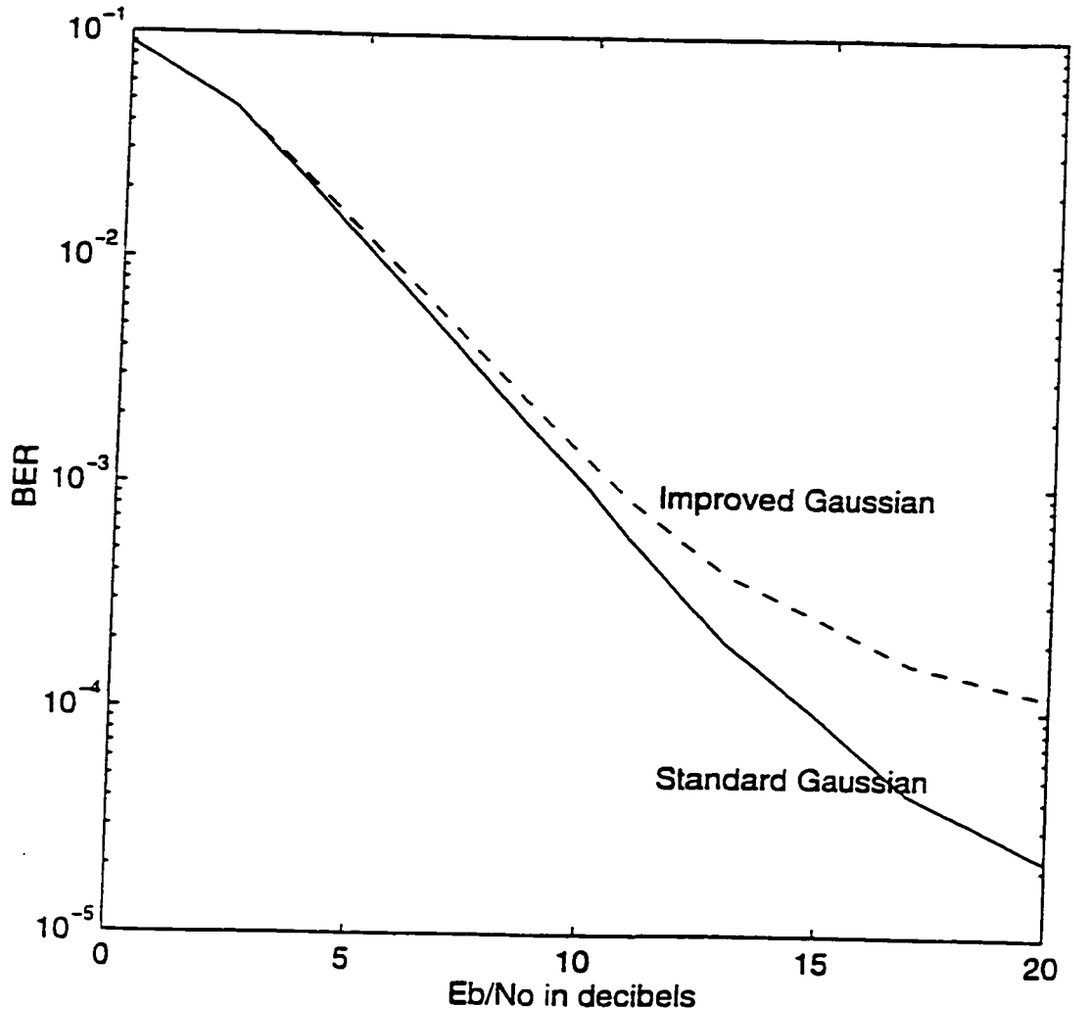

Figure 3.9 BER versus Eb/No for a correlator receiver. Perfect power control, spreading code phase estimation and carrier phase estimation; K = 3; $\bar{L} = 3$; $N = 31$.

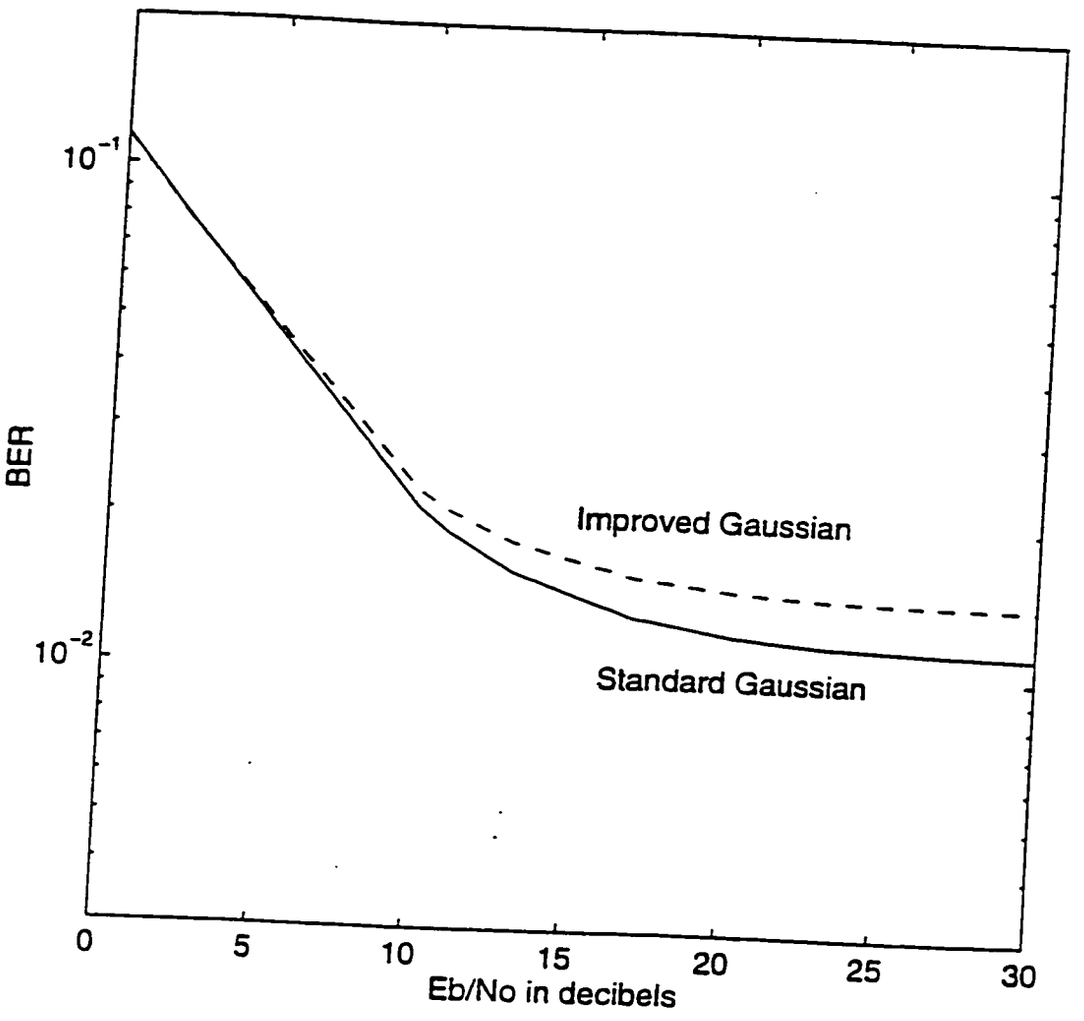

Figure 3.10 BER versus Eb/No for a correlator receiver. Perfect power control, spreading code phase estimation and carrier phase estimation; K = 8; $\bar{L} = 3$; $N = 31$.

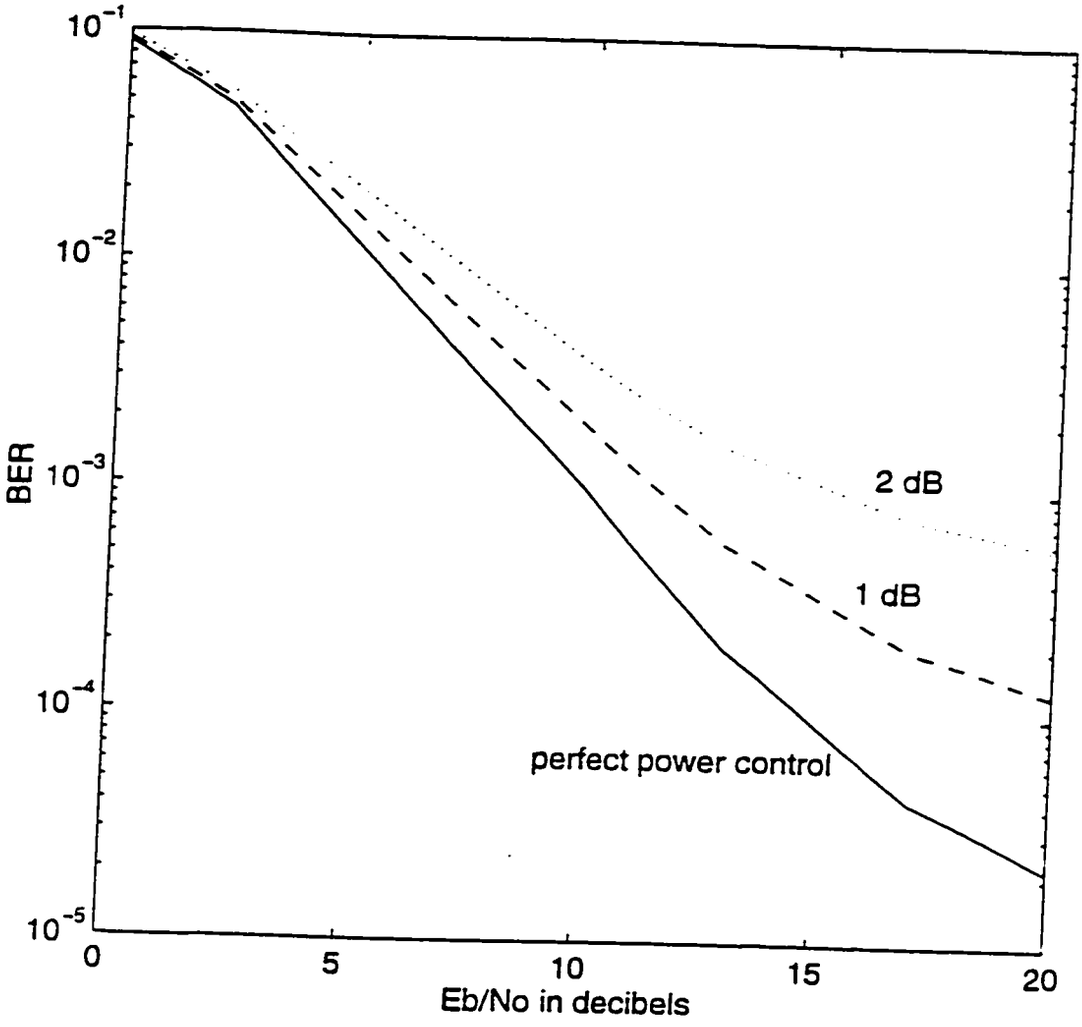

Figure 3.11 BER versus $\frac{E_b}{N_o}$ for a correlator receiver with different levels of imperfections in power control scheme. Perfect phase estimates; $K = 3$; $\bar{L} = 3$; $N = 31$.

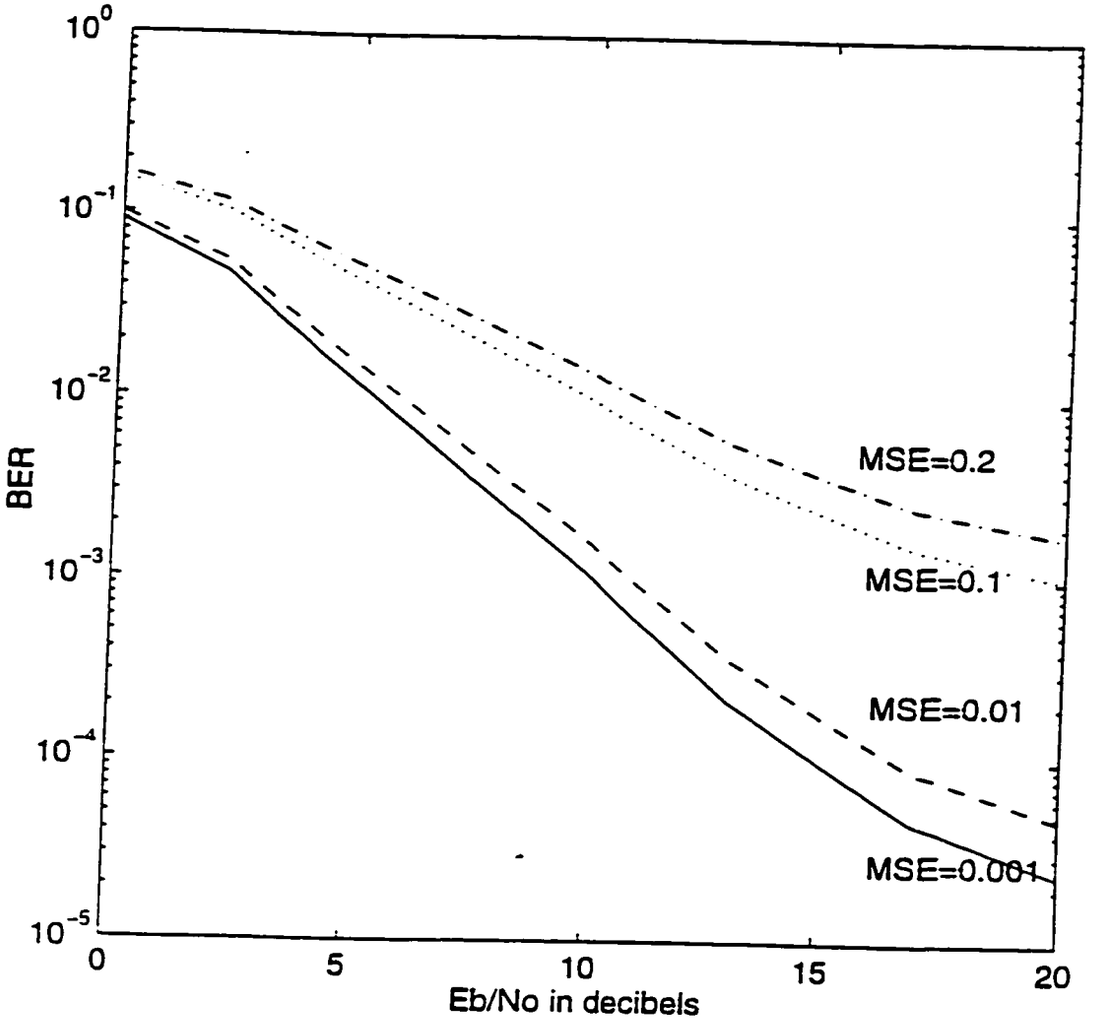

Figure 3.12 BER versus $\frac{E_b}{N_o}$ for a correlator receiver with different levels of imperfections in carrier phase estimation. Perfect power control and code phase estimation; $K = 3$; $\tilde{L} = 3$; $N = 31$.

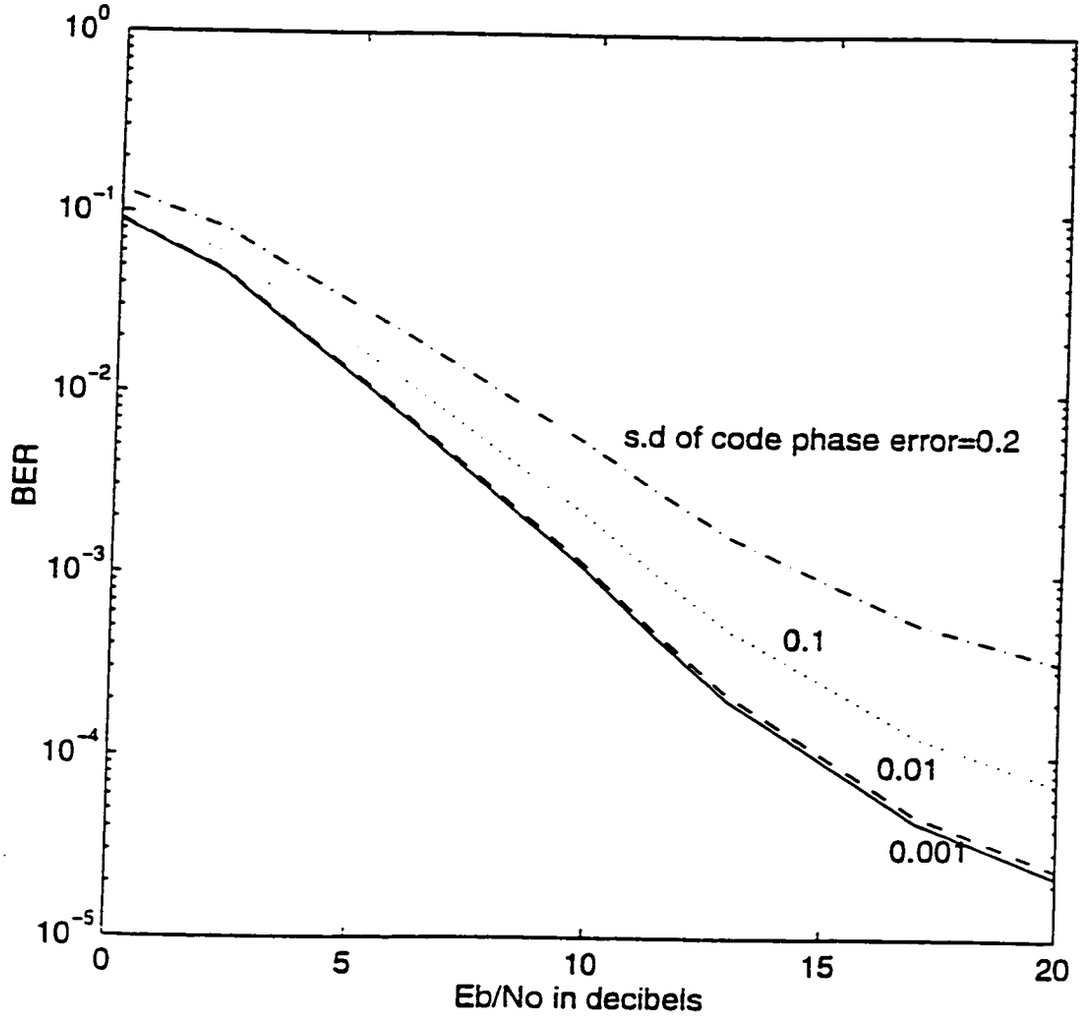

Figure 3.13 BER versus $\frac{E_b}{N_o}$ for a correlator receiver with different levels of imperfections in spreading code phase estimates. Perfect power control and carrier phase estimation; $K = 3$; $\bar{L} = 3$; $N = 31$.

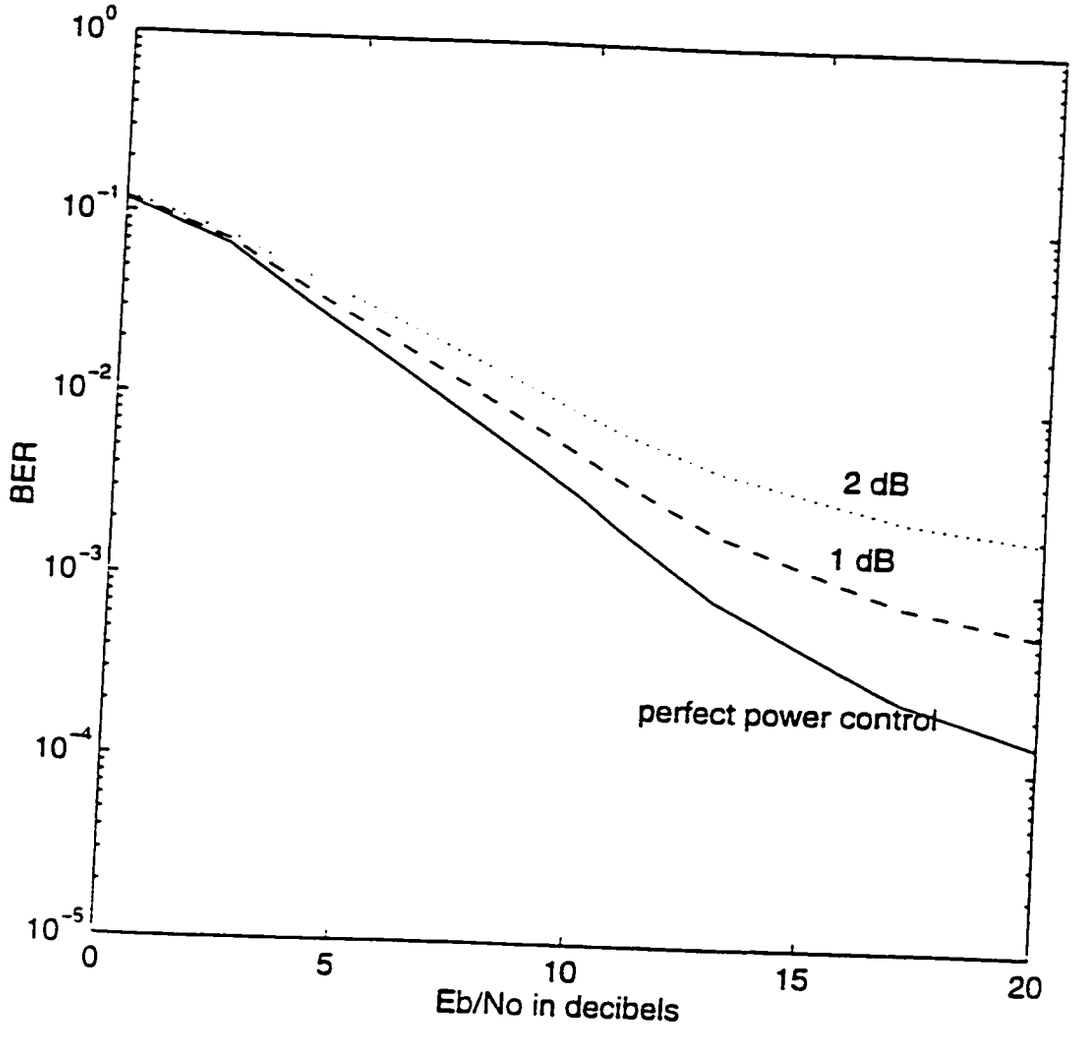

Figure 3.14 BER versus $\frac{E_b}{N_o}$, for a correlator receiver with imperfections in power control and phase estimates. MSE in carrier phase estimate = 0.01; standard deviation of normalized error in code phase estimate = 0.1; $K = 3$; $\bar{L} = 3$; $N = 31$.

Figure 3.11 is a plot of BER versus $\frac{E_b}{N_o}$ for different levels of imperfections in power control. It is assumed that there are no imperfections in synchronization of spreading code or carrier phase estimation. It may be seen in Figure 3.11 that, with perfect power control, a BER of 10^{-3} can be achieved at an $\frac{E_b}{N_o}$ of 10 dB whereas with an imperfection in power control resulting in 2 dB variance in normalized received signal power, the BER increases to $4X10^{-3}$.

As in Figure 3.12, the carrier phase estimation error also has a significant impact on the BER performance. At an $\frac{E_b}{N_o}$ value of 10 dB, BER values corresponding to MSE of 0.01, 0.1 and 0.2 are $1.5X10^{-3}$, 10^{-2} and $1.5X10^{-2}$ respectively. BER versus $\frac{E_b}{N_o}$ is shown in Figure 3.13 for different levels of imperfections in the synchronization of spreading code. It is assumed that there are no imperfections in power control or carrier phase estimation. As seen in Figure 3.13, the performance is not significantly degraded for a standard deviation of normalized code phase estimate error below 0.01, but any value of 0.1 or more has a detrimental effect on the BER performance. At an $\frac{E_b}{N_o}$ value of 10 dB, BER at standard deviation values of 0.01, 0.1 and 0.2 are 10^{-3}, $2.5X10^{-3}$ and $6X10^{-3}$ respectively. BER performance when all three imperfections are present is shown in Figure 3.14.

To bring out the effect of imperfect power control, imperfect carrier phase estimates and imperfect spreading code phase estimates individually, BER is plotted as functions of the variance of the normalized received power. MSE in carrier phase estimate and standard deviation of code phase estimate error in Figures 3.15, 3.16 and 3.17 respectively. Figures 3.15, 3.16 and 3.17 clearly illustrate the degree of

degradation in performance incurred by the correlator receiver at various values of these three imperfections. From Figure 3.15, it is seen that almost perfect power control is a necessity for CDMA systems with correlation receiver. Performance degrades rapidly as power control deteriorates. The MSE in carrier phase estimates must be below 0.01 to ensure acceptable BER performance as seen in Figure 3.16. If the standard deviation of the normalized code phase estimate error is more than 0.1, the system performance is significantly affected as seen in Figure 3.17.

As stated before, a correlation receiver is a simple CDMA receiver. A more complex receiver with better performance is the multipath combining RAKE receiver. The effect of system imperfections on such a receiver is analyzed in the next section.

3.3 Performance of Diversity Combining RAKE Receiver

The principle of the diversity combining RAKE receiver was discussed in Chapter 2. In a fading multipath mobile environment, multipath diversity combining receivers are known to achieve improvement over non-combining single path correlator receivers [15, 17, 56]. Such receivers are complex as they require channel parameter estimation and spreading code phase estimates of each path signal. The best performance of such a receiver is achieved under ideal conditions of operation, i.e. perfect power control, perfect channel parameter estimation and perfect spreading code phase estimation. In mobile multiple access communication systems, one or more of the above mentioned factors can be imperfect. In this section, the BER performance of an indoor CDMA system with a RAKE receiver is analyzed. In

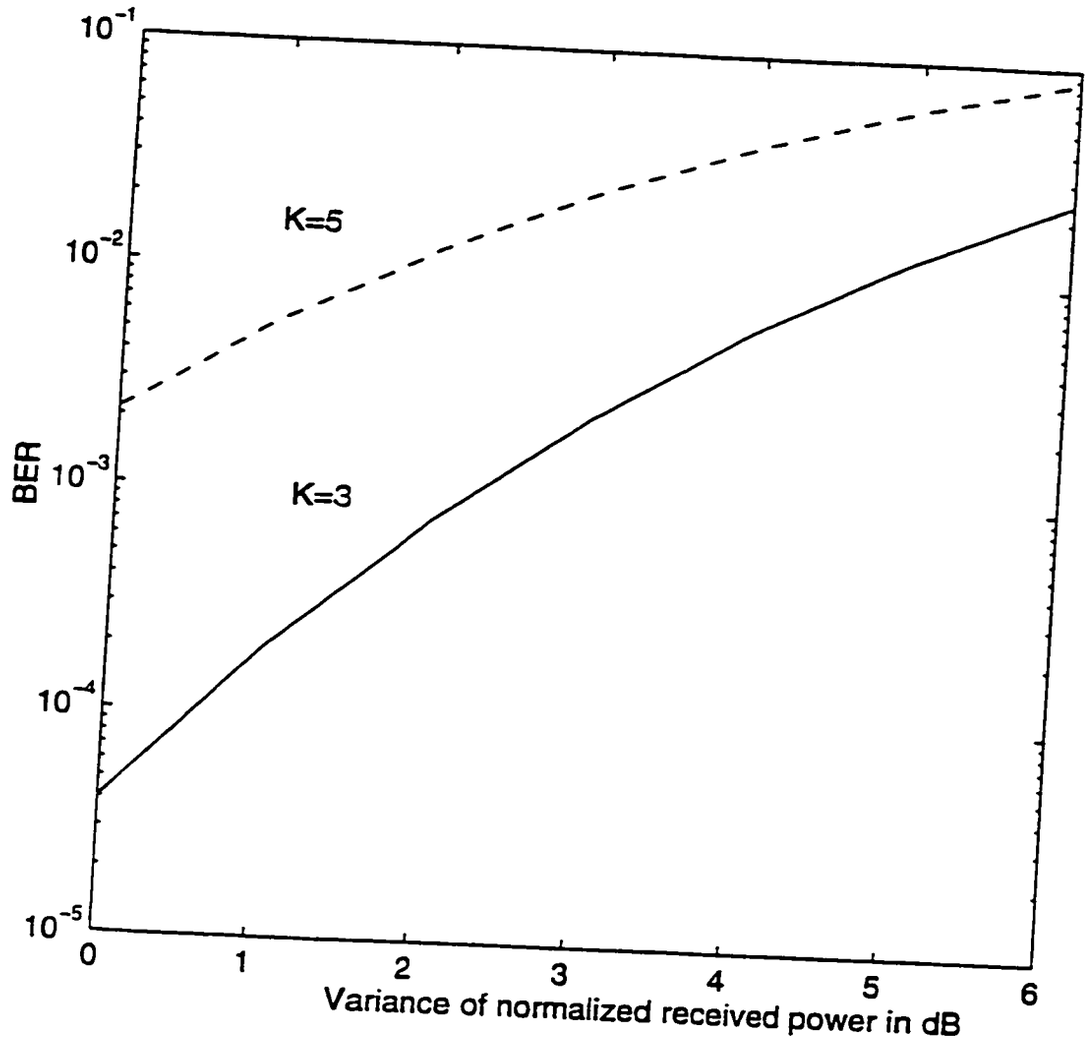

Figure 3.15 BER versus variance of normalized received power. Perfect carrier phase and code phase estimation; $\frac{E_b}{N_o} = 15$ dB; $\bar{L} = 3$; $N = 31$.

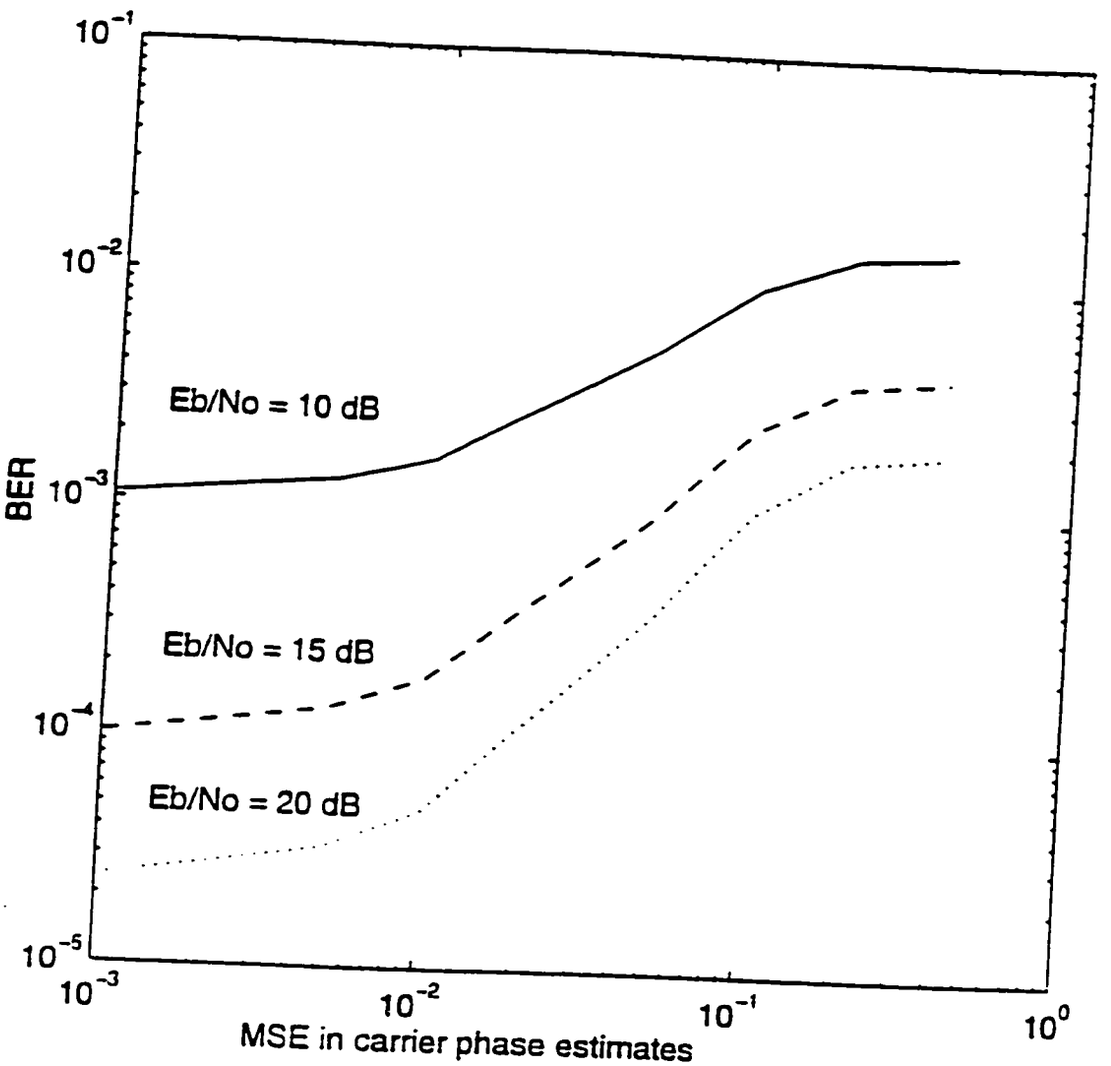

Figure 3.16 BER versus mean square of normalized error in carrier phase estimation. Perfect power control and spreading code phase estimation; number of users of the system, $K = 3$; $\bar{L} = 3$; $N = 31$.

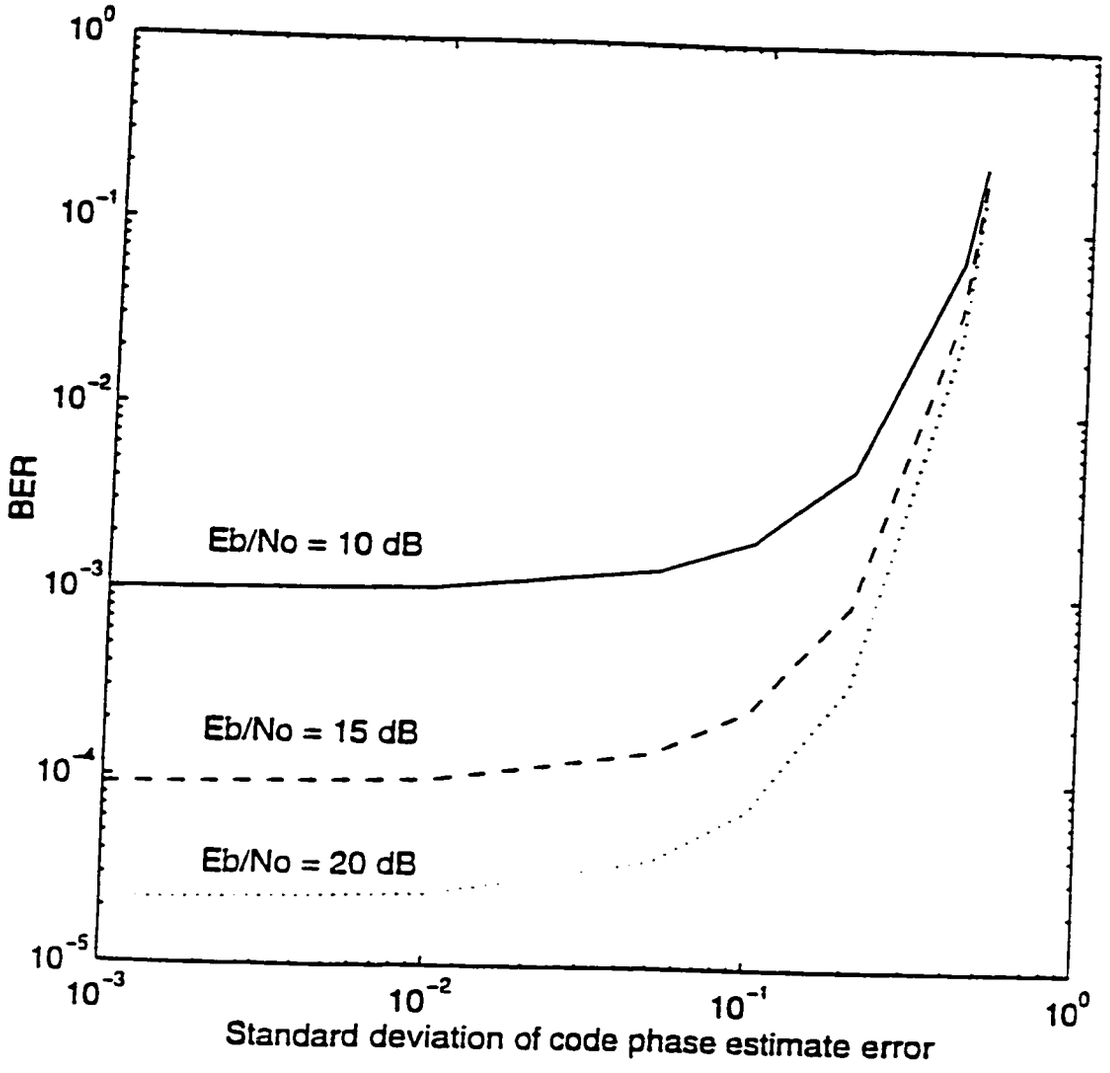

Figure 3.17 BER versus standard deviation of normalized error in code phase estimate. Perfect power control and carrier phase estimation; $K = 3$; $\bar{L} = 3$; $N = 31$.

particular, the effect of imperfections in power control, channel parameter estimates and spreading code phase estimates on the performance of such receivers is investigated. In Section 3.3.1, components of the received signal at the base station are examined and models to analyze the effect of system imperfections on the performance are developed. An equation for the data estimate is developed in Section 3.3.2. This is followed by BER analysis and numerical results in Sections 3.3.3 and 3.3.4 respectively.

3.3.1 Diversity Combining RAKE Receiver

The block diagram of the RAKE receiver is shown in Figure 3.18. The received signal at the input is the same as in Equation (3.13). The first step in the receiver is down conversion to the baseband in-phase (I) signal $r_I(t)$ and quadrature phase (Q) signal $r_Q(t)$ by multiplying $r(t)$ by $\cos\omega_c t$ and $\sin\omega_c t$, respectively as shown in Figure 3.18. The down converted and low-pass filtered in-phase signal for the desired user i, may be written as

$$\begin{aligned} r_I(t) &= \sqrt{\frac{P_i}{2}} \sum_{\lambda=1}^{L_i} g_I(i,\lambda) a_i(t-\tau_{i,\lambda}) b_i(t-\tau_{i,\lambda}) \\ &+ \sum_{k=1,k\neq i}^{K} \sum_{\lambda=1}^{L_k} \sqrt{\frac{P_k}{2}} g_I(k,\lambda) a_k(t-\tau_{k,\lambda}) b_k(t-\tau_{k,\lambda}) \\ &+ n_I(t). \end{aligned} \tag{3.63}$$

In Equation (3.63), the first term represents the multipath signals of the desired user. These signals are combined in a RAKE receiver using channel parameter estimates. The second term is the MAI signal due to other users of the CDMA system and

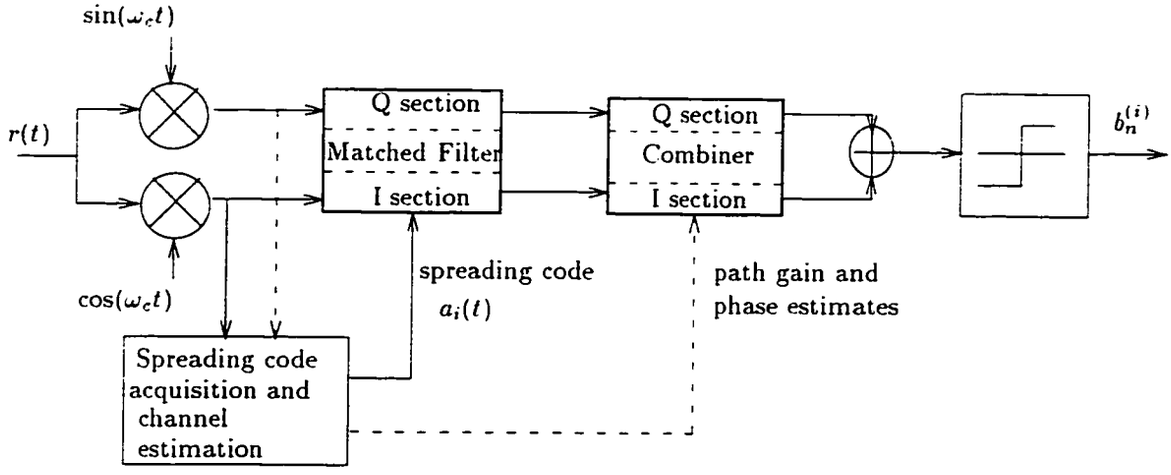

Figure 3.18 RAKE receiver with multipath combining.

the third term is the low-pass filtered thermal noise. The quadrature signal $r_Q(t)$ is obtained by setting I to Q in Equation (3.63). Quantities $g_I(k,\lambda) = g_{k,\lambda}\cos(\phi_{k,\lambda})$ and $g_Q(k,\lambda) = g_{k,\lambda}\sin(-\phi_{k,\lambda})$. The functional block diagram for the receiver shown in Figure 3.18 consists of two sections; a spreading code synchronization unit and a data demodulation unit. In the presence of multiple users, imperfections in code phase estimation will result in error $\Delta\tau_{i,\lambda}$, $1 \le \lambda \le L_i$ in path delay estimates such that

$$\hat{\tau}_{i,\lambda} = \tau_{i,\lambda} + \Delta\tau_{i,\lambda}. \tag{3.64}$$

where $\hat{\tau}_{i,\lambda}$ denotes the estimated delay of the λth path signal of the ith user. The code phase estimation error is modeled as a zero mean Gaussian random variable with a variance $\sigma^2_{\Delta\tau_{i,\lambda}}$.

In the data demodulation arm of the receiver, the baseband in-phase signal $r_I(t)$

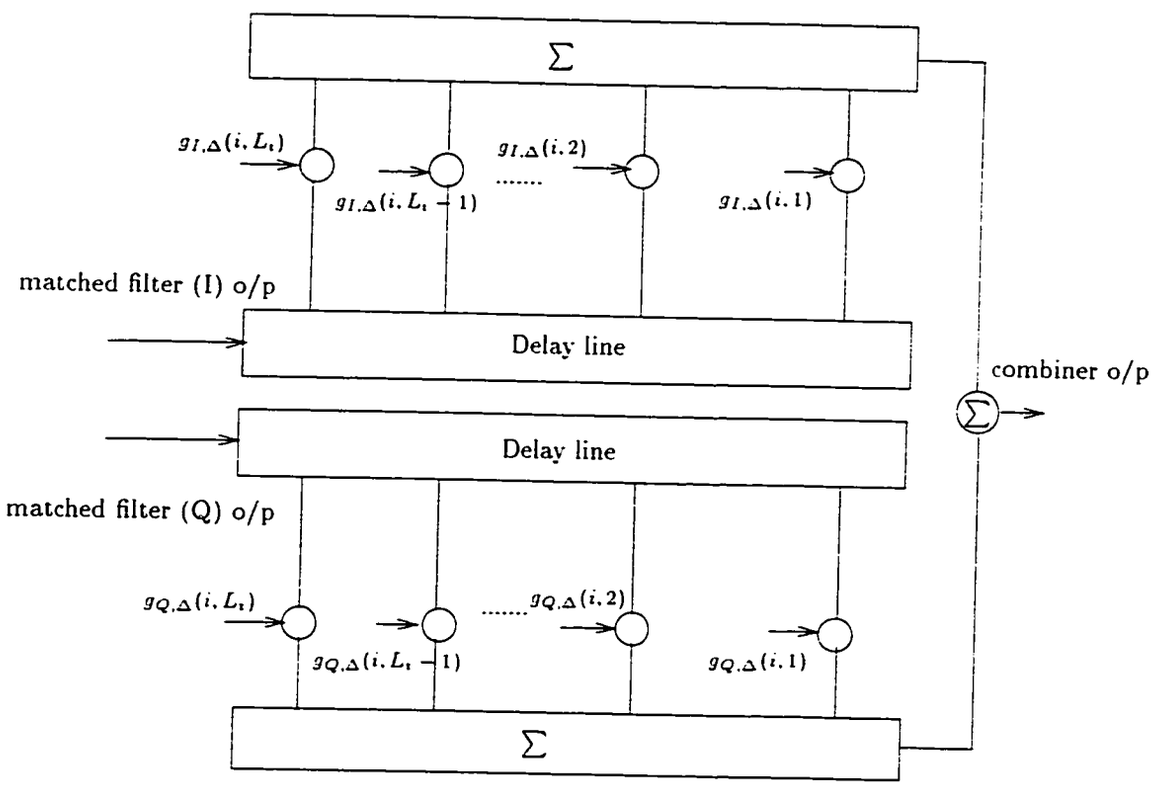

Figure 3.19 Transversal filter used for multipath combining.

and the quadrature signal $r_Q(t)$ for the desired user i are passed through separate but identical matched filters loaded with its spreading code $a_i(t)$ obtained from the synchronization unit. The two matched filter outputs are input to the RAKE combiner. This RAKE combiner consists of two separate transversal filters (I and Q) each with taps as shown in Figure 3.19. The time delays between taps and the tap weights are set by the channel estimator. The impulse response of the RAKE combiner is, in a way, the time reversal of the channel impulse response.

The path gain and phase estimates will not be perfect due to time variations in the mobile radio channel, multiple access interference, and imperfections of the estimation technique. If errors in amplitude estimates $\Delta g_{i,\lambda}$ and phase estimates, $\Delta\phi_{i,\lambda}$ are considered, then the estimates for amplitude and phase are given by

$$\hat{g}_{i,\lambda} = g_{i,\lambda} + \Delta g_{i,\lambda} \tag{3.65}$$

and

$$\hat{\phi}_{i,\lambda} = \phi_{i,\lambda} + \Delta\phi_{i,\lambda}, \tag{3.66}$$

respectively, for $1 \leq \lambda \leq L_i$. All of the estimation errors are modeled as i.i.d zero mean Gaussian random processes with variances $\sigma^2_{\Delta g_{i,\lambda}}$ and $\sigma^2_{\Delta\phi_{i,\lambda}}$ respectively. It is assumed that the sets $\{\Delta\tau_{i,\lambda}\}$, $\{\Delta g_{i,\lambda}\}$ and $\{\Delta\phi_{i,\lambda}\}$ are mutually independent and members within each set are i.i.d random processes for all λ.

3.3.2 Analysis of Data Estimates

The error in the spreading code phase estimate results in $a_i(t - \hat{\tau}_{i,\lambda})$. $1 \leq \lambda \leq L_i$. being fed to the matched filter. In the absence of estimation errors. the tap coefficients at the αth tap point are set to $g_I(i, \alpha)$ and $g_Q(i, \alpha)$ respectively for I and Q transversal filters. Because of the estimation errors. the tap co-efficients at tap point α are set to $g_{I,\Delta}(i, \alpha)$ and $g_{Q,\Delta}(i, \alpha)$ respectively for the I and Q transversal filters as shown in Figure 3.19. Quantities $g_{I,\Delta}(i, \lambda)$ and $g_{Q,\Delta}(i, \lambda)$ are given by

$$g_{I,\Delta}(i, \lambda) = (g_{i,\lambda} + \Delta g_{i,\lambda}) \cos(\phi_{i,\lambda} + \Delta\phi_{i,\lambda}) \tag{3.67}$$

and

$$g_{Q,\Delta}(i, \lambda) = (g_{i,\lambda} + \Delta g_{i,\lambda}) \sin(-\phi_{i,\lambda} - \Delta\phi_{i,\lambda}). \tag{3.68}$$

For notational simplicity, the following functions are introduced. The first function is given by

$$m(i, k, \alpha, \lambda) = m = \lfloor \frac{\hat{\tau}_{i,\alpha} - \tau_{k,\lambda}}{T_b} \rfloor, \tag{3.69}$$

where m indicates the number of bits $b_n^{(i)}$ lags behind $b_n^{(k)}$. Similarly the second function

$$\tau(i, k, \alpha, \lambda) = \tau = (\hat{\tau}_{i,\alpha} - \tau_{k,\lambda}) - mT_b \tag{3.70}$$

indicates the amount $b_n^{(i)}$ is delayed relative to $b_n^{(k)}$. It is to be noted that τ defined by Equation (3.70) ensures that it lies within 0 to T_b.

The combiner output for the nth symbol of user i. sampled at the appearance of

the last path's correlator peak at $t = (n+1)T_b + \hat{\tau}_{i,L_i}$, is given by

$$Y_{i,\Delta} = D_{i,\Delta} + F_{i,\Delta} + I_{i,\Delta} + N_{i,\Delta}. \tag{3.71}$$

where $D_{i,\Delta}$ is the combiner's output of the ith user's desired signal, $F_{i,\Delta}$ is the output which corresponds to ith user's paths not matched to combiner delays, $I_{i,\Delta}$ is the output due to MAI and $N_{i,\Delta}$ is the output noise signal. In Equation (3.71), $D_{i,\Delta}$, $F_{i,\Delta}$, $I_{i,\Delta}$ and $N_{i,\Delta}$ are given by

$$D_{i,\Delta} = \sum_{\alpha=1}^{L_i} y(i,i,\alpha,\alpha). \tag{3.72}$$

$$F_{i,\Delta} = \sum_{\alpha=1}^{L_i} \sum_{\lambda=1,\lambda\neq\alpha}^{L_i} y(i,i,\alpha,\lambda). \tag{3.73}$$

$$I_{i,\Delta} = \sum_{k=1,k\neq i}^{K} \sum_{\alpha=1}^{L_i} \sum_{\lambda=1}^{L_i} y(i,k,\alpha,\lambda) \tag{3.74}$$

and

$$\begin{aligned} N_{i,\Delta} \;=\; & \sum_{\alpha=1}^{L_i} \left\{ \int_{nT_b}^{(n+1)T_b} \Big[\hat{g}_{i,\alpha} \cos(\hat{\phi}_{i,\alpha}) n_I(t+\hat{\tau}_{i,\alpha}) + \right. \\ & \left. \hat{g}_{i,\alpha} \sin(-\hat{\phi}_{i,\alpha}) n_Q(t+\hat{\tau}_{i,\alpha}) \Big] a_i(t) dt \right\}. \end{aligned} \tag{3.75}$$

In Equations (3.72) - (3.74),

$$y(i,k,\alpha,\lambda) = \sqrt{\frac{P_k}{2}} g_{k,\lambda} \hat{g}_{i,\alpha} \cos(\phi_{k,\lambda} - \hat{\phi}_{i,\alpha}) [b_{n-m-1}^{(k)} R_{k,i}(\tau) + b_{n-m}^{(k)} \hat{R}_{k,i}(\tau)]. \tag{3.76}$$

where τ stands for $\tau(i,k,\alpha,\lambda)$. The time continuous partial correlation functions $R_{k,i}(\tau)$ and $\hat{R}_{k,i}(\tau)$ have been defined previously. A hard decision on the combiner output $Y_{i,\Delta}$ provides a data estimate of the ith user's nth symbol as

$$\hat{b}_n^{(i)} = \mathrm{sgn}(Y_{i,\Delta}). \tag{3.77}$$

This data estimate variable is used in the BER analysis reported in the next subsection.

3.3.3 BER Analysis

It has been shown in Section 3.2.4 that the standard Gaussian approximation is quite accurate with $N = 31$. To calculate the BER using this approximation, expressions for the expected desired signal strength and variances of interferences and thermal noise at the output of the receiver are derived. The SNR is found and it is used as the argument of the Q function to compute the BER.

From Equations (3.72) and (3.76), $D_{i,\Delta}$ may be written as

$$\begin{aligned} D_{i,\Delta} &= D_i + D_\Delta \\ &= \sum_{\alpha=1}^{L_i} \sqrt{\frac{P_i}{2}} g_{i,\alpha}^2 \cos(\Delta\phi_{i,\alpha}) b_n^{(i)} R_{i,i}(\Delta\tau_{i,\alpha}) \\ &+ \sum_{\alpha=1}^{L_i} \sqrt{\frac{P_i}{2}} g_{i,\alpha} \Delta g_{i,\alpha} \cos(\Delta\phi_{i,\alpha}) b_n^{(i)} R_{i,i}(\Delta\tau_{i,\alpha}). \end{aligned} \tag{3.78}$$

In Equation (3.78), D_i represents the desired signal and D_Δ is zero mean Gaussian noise due to estimation errors of channel parameters. By taking the expected value

of the mutually independent random variables in Equation (3.78), the average value of the desired signal strength and the variance of noise due to channel estimation errors are written as

$$E\left\{D_i^2\right\} = \frac{1}{2}E\{P_i\}E\{R_{i,i}^2(\Delta\tau)\}\bar{L}T_b^2G\cdot \left[G(1+\epsilon^{-2\sigma_{\Delta\phi}^2})+(\bar{L}-1)G\epsilon^{-\sigma_{\Delta\phi}^2}\right] \tag{3.79}$$

and

$$\mathrm{Var}(D_\Delta) = \frac{1}{4}E\{P_i\}E\{R_{i,i}^2(\Delta\tau)\}\bar{L}T_b^2G\sigma_{\Delta g}^2(1+\epsilon^{-2\sigma_{\Delta\phi}^2}). \tag{3.80}$$

where the fact that $E\left\{\left[b_n^{(i)}\right]^2\right\} = 1$ has been used. To derive Equations (3.79) and (3.80) it is assumed that $\sigma_{\Delta\tau_{i,\alpha}}^2 = \sigma_{\Delta\tau}^2$, $\sigma_{\Delta\phi_{i,\alpha}}^2 = \sigma_{\Delta\phi}^2$ and $\sigma_{\Delta g_{i,\alpha}}^2 = \sigma_{\Delta g}^2$ for $1 \le i \le K$, $1 \le \alpha \le L_k$. Also, $E\{g_{i,\alpha}^2\} = G_\alpha$ and $E\{g_{i,\alpha}^4\} = 2G_\alpha^2$ for the αth path of the ith user for $1 \le i \le K$. The average number of paths $\bar{L}_i$ is assumed to be $\bar{L}$ for all i. The average path power gain G is equal to $1/\bar{L}\sum_{\alpha=1}^{\bar{L}} G_\alpha$, where G_α is the mean square value of the αth path.

In Equations (3.79) and (3.80), $E\left\{R_{i,i}^2(\Delta\tau_{i,1})\right\}$ has to be evaluated. This is done as follows. In a practical synchronization system, most likely values of the error $\Delta\tau_{i,\alpha}$ lie between $+T_c$ and $-T_c$. During this interval the autocorrelation function of the spreading code may be written as

$$R_{i,i}(\Delta\tau_{i,\alpha}) = \begin{cases} 1-\frac{|\Delta\tau_{i,\alpha}|}{T_c}: & |\Delta\tau_{i,\alpha}| \le T_c \\ 0 & \text{otherwise.} \end{cases} \tag{3.81}$$

$E\left\{R_{i,i}^2(\Delta\tau)\right\}$ is derived as

$$E\left\{R_{i,i}^2(\Delta\tau)\right\} = 1 - \frac{2}{T_c}\sqrt{\frac{2}{\pi}}\sigma_{\Delta\tau} + \frac{1}{T_c^2}\sigma_{\Delta\tau}^2. \tag{3.82}$$

The variance of $F_{i,\Delta}$ may be obtained from Equation (3.73) as

$$\mathrm{Var}(F_{i,\Delta}) = \frac{1}{4}E\{P_i\}\bar{L}(\bar{L}-1)G(G+\sigma_{\Delta g}^2)E\left\{\left[R_{i,i}^2(\tau) + \hat{R}_{i,i}^2(\tau)\right]\right\}. \tag{3.83}$$

To evaluate Equation (3.83), the probability density function of $\tau(i,i,\alpha,\lambda)$ has to be obtained. For the case of perfect synchronization, the probability density function of $\tau(i,i,\alpha,\lambda)$ is given by

$$f_\tau(\tau) = \begin{cases} \frac{-|\tau|}{(\Delta-2T_c)^2} + \frac{\Delta-T_c}{(\Delta-2T_c)^2} & T_c \le |\tau| \le \Delta - T_c \\ 0 & \text{otherwise.} \end{cases} \tag{3.84}$$

where τ stands for $\tau(i,i,\alpha,\lambda)$. In the case of imperfect synchronization, the probability density function of $\tau(i,i,\alpha,\lambda)$ is obtained as the convolution of the density function given by Equation (3.84) and the Gaussian distributed error in path delay $\Delta\tau$. This density function is given by

$$\begin{aligned} f_\tau(\tau) &= \frac{1}{2}\left[\mathrm{erf}\left(\frac{|\tau|+T_c-\Delta}{\sqrt{2}\sigma_{\Delta\tau}}\right) - \mathrm{erf}\left(\frac{|\tau|-T_c}{\sqrt{2}\sigma_{\Delta\tau}}\right)\right]\left[\frac{|\tau|}{(\Delta-2T_c)^2} - \frac{\Delta-T_c}{(\Delta-2T_c)^2}\right] \\ &+ \frac{\sigma_{\Delta\tau}}{(\Delta-2T_c)^2\sqrt{2\pi}}\left[e^{-\left(\frac{|\tau|+T_c-\Delta}{\sqrt{2}\sigma_{\Delta\tau}}\right)^2} - e^{-\left(\frac{|\tau|-T_c}{\sqrt{2}\sigma_{\Delta\tau}}\right)^2}\right]. \end{aligned} \tag{3.85}$$

where erf(x) has been defined previously.

Similarly, $\mathrm{Var}(I_{i,\Delta})$ is obtained from Equation (3.74) as

$$\mathrm{Var}(I_{i,\Delta}) = \sum_{k=1,k\neq i}^{K} \frac{1}{4} E\{P_k\} \bar{L}^2 G(G + \sigma_{\Delta g}^2) E\left\{\left[R_{k,i}^2(\tau) + \hat{R}_{k,i}^2(\tau)\right]\right\}. \tag{3.86}$$

To evaluate Equation (3.86), the probability density function of $\tau(i,k,\alpha,\lambda)$ has to be obtained. As before, for the case of perfect synchronization, the probability density function of $\tau(i,k,\alpha,\lambda)$ is given by

$$f_\tau(\tau) = \begin{cases} \frac{1}{\Delta+T_b}[1 - \frac{|\tau|}{\Delta+T_b}] & 0 \leq |\tau| \leq \Delta + T_b \\ 0 & \text{otherwise.} \end{cases} \tag{3.87}$$

where τ stands for $\tau(i,k,\alpha,\lambda)$. In the case of imperfect synchronization, the probability density function of $\tau(i,k,\alpha,\lambda)$ is obtained as the convolution of the density function given by Equation (3.87) and the Gaussian distributed error in path delay $\Delta\tau$. This density function is given by

$$\begin{aligned} f_\tau(\tau) &= \frac{1}{2}\left[\mathrm{erf}(\frac{|\tau|}{\sqrt{2}\sigma_{\Delta\tau}}) - \mathrm{erf}(\frac{|\tau| - T_b - \Delta}{\sqrt{2}\sigma_{\Delta\tau}})\right]\left[\frac{1}{(\Delta+T_b)} - \frac{|\tau|}{(\Delta+T_b)^2}\right] \\ &+ \frac{\sigma_{\Delta\tau}}{\sqrt{2\pi}(\Delta+T_b)^2}\left[e^{-(\frac{|\tau|-T_b-\Delta}{\sqrt{2}\sigma_{\Delta\tau}})^2} - e^{-(\frac{|\tau|}{\sqrt{2}\sigma_{\Delta\tau}})^2}\right]. \end{aligned} \tag{3.88}$$

The time continuous partial cross-correlation functions $R_{k,i}$ and $\hat{R}_{k,i}$ are defined in terms of the discrete aperiodic cross-correlation function of the spreading codes as given in Section 3.2.2.

The terms $E\left\{R_{i,i}^2(\tau) + \hat{R}_{i,i}^2(\tau)\right\}$ and $E\left\{R_{k,i}^2(\tau) + \hat{R}_{k,i}^2(\tau)\right\}$ can be evaluated by

numerical integration. The variance of the thermal noise at the output of the combiner may be derived from Equation (3.75) as

$$\mathrm{Var}(N_{i,\Delta}) = \frac{N_o}{4} T_b \bar{L} (G + \sigma^2_{\Delta g}). \tag{3.89}$$

By using the Gaussian approximation to model the effect of interferences, the $SNR_{i,\Delta}$ of data estimates is obtained from Equations (3.79), (3.80), (3.83), (3.86) and (3.89) as

$$SNR_{i,\Delta} = \frac{E\{D_i^2\}}{\mathrm{Var}(D_\Delta) + \mathrm{Var}(F_{i,\Delta}) + \mathrm{Var}(I_{i,\Delta}) + \mathrm{Var}(N_{i,\Delta})}. \tag{3.90}$$

The bit error probability is then given by

$$p^{(i)}_{e,\Delta} = Q(\sqrt{SNR_{i,\Delta}}). \tag{3.91}$$

where the Q function has been defined in Section 3.2.3.

3.3.4 Numerical Results

The BER performance is computed using the system parameters given in Section 3.2.4. The effects of each system imperfection on BER performance are shown in Figures 3.20 - 3.22. The performance for a combination of all system imperfections is presented in Figure 3.23. In these figures, the spreading code sequence period, $N = 31$ and the number of users, $K = 9$. It is to be noted that with the correlator receiver, K was equal to 3. A value of $K = 9$ is possible with the RAKE receiver because of

the improved performance obtained by combining multipath signals. BER is plotted as a function of $\frac{E_r}{N_o}$. where E_r is the received energy from all paths of the desired user. E_r is written as $E_r = \bar{L}GE_b$. where E_b is the energy from one path signal. Figure 3.20 is a plot of BER versus $\frac{E_r}{N_o}$ for different levels of imperfections in power control. It is assumed that there are no imperfections in the estimation of spreading code phase and channel parameters. With imperfections in power control resulting in 2 dB variance in the normalized received signal power. the BER is five times the BER with perfect power control at an $\frac{E_r}{N_o}$ of 10 dB (Figure 3.20). The channel parameter estimation error also has a significant impact on the BER performance (Figure 3.21). It is assumed that there is perfect power control and spreading code phase estimation. It is seen in Figure 3.21 that at an $\frac{E_r}{N_o}$ of 10 dB. BER values corresponding to MSE in channel estimates of 0.001. 0.01. 0.1 and 0.2 are $7X10^{-4}$. 10^{-3}. $3X10^{-2}$ and $7X10^{-2}$ respectively. The effect of spreading code phase error on BER has been computed assuming no imperfections in power control and channel parameter estimation (Figure 3.22). The performance is not much affected for a standard deviation of normalized code phase estimate error below 0.01. but any value of 0.1 or more has a detrimental effect on the BER performance. At an $\frac{E_r}{N_o}$ value of 10 dB. BERs at standard deviation values of 0.01. 0.1 and 0.2 are $8X10^{-4}$. $2X10^{-3}$ and $5X10^{-3}$ respectively. The BER performance with a combination of all three imperfections is presented in Figure 3.23.

To bring out the effect of imperfections in power control. channel parameter estimation and spreading code phase estimations more clearly. the BER is plotted as

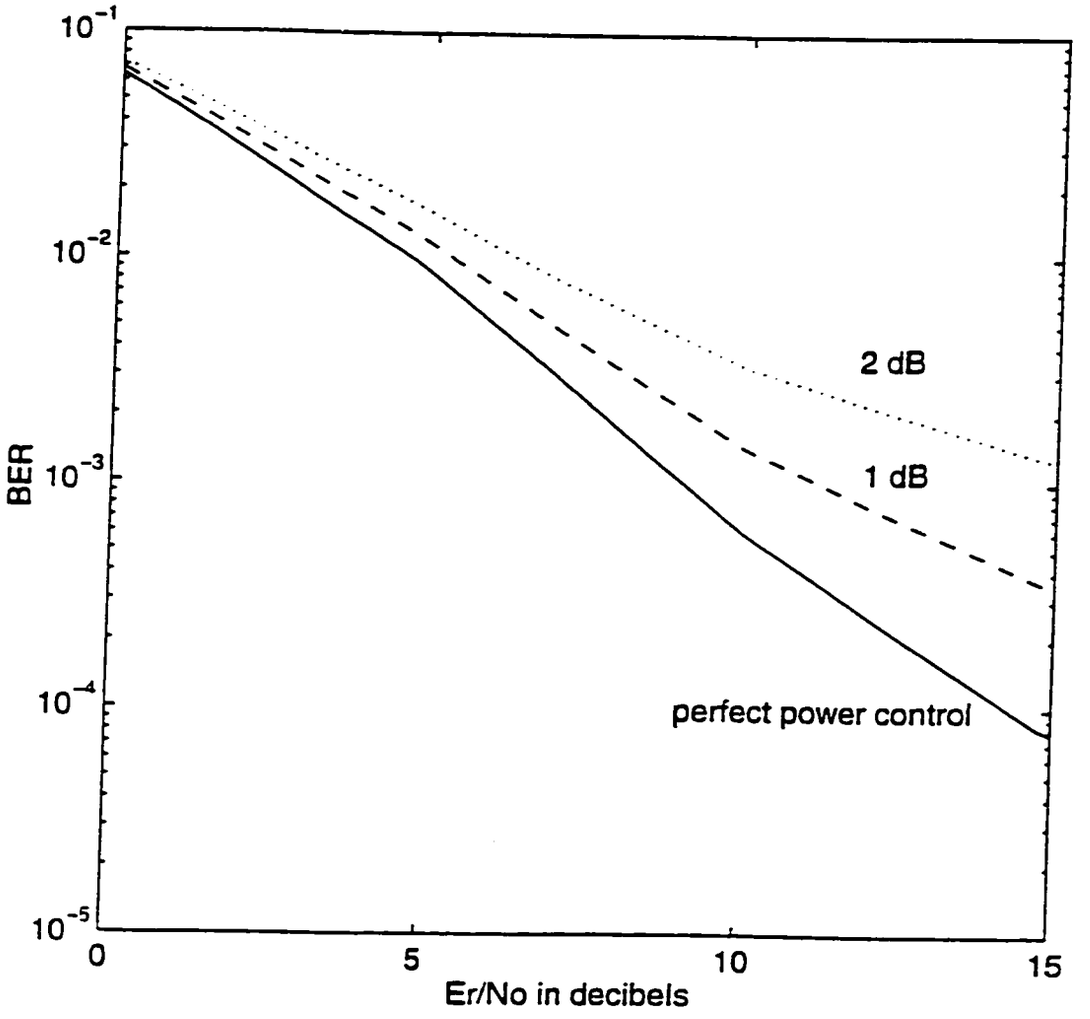

Figure 3.20 BER versus $\frac{E_r}{N_o}$ for a RAKE receiver with different levels of imperfections in power control scheme. Perfect phase estimates; $K = 9$; $\bar{L} = 3$; $N = 31$.

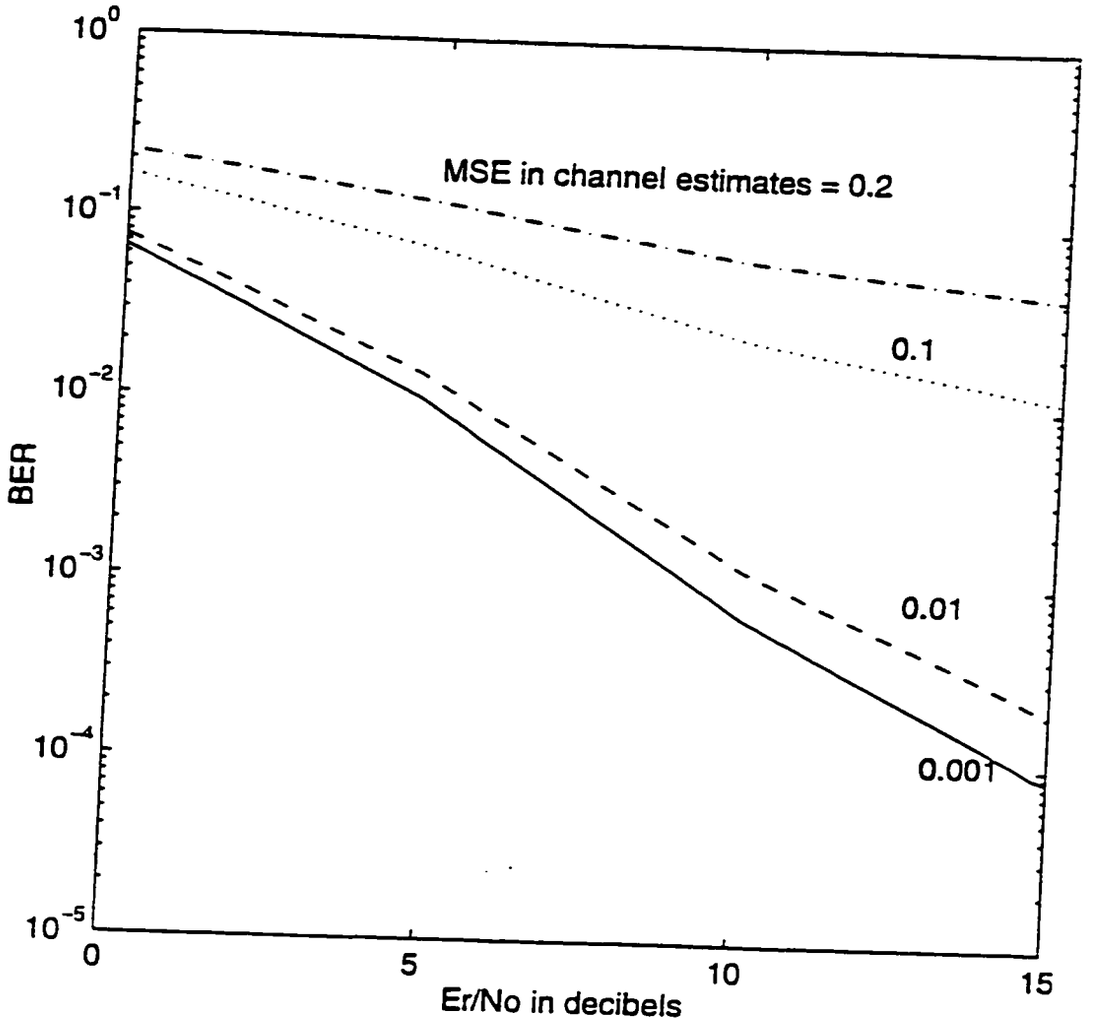

Figure 3.21 BER versus $\frac{E_r}{N_o}$ for a RAKE receiver with different levels of imperfections in channel parameter estimation. Perfect power control and code phase estimation; $K = 9$; $\bar{L} = 3$; $N = 31$.

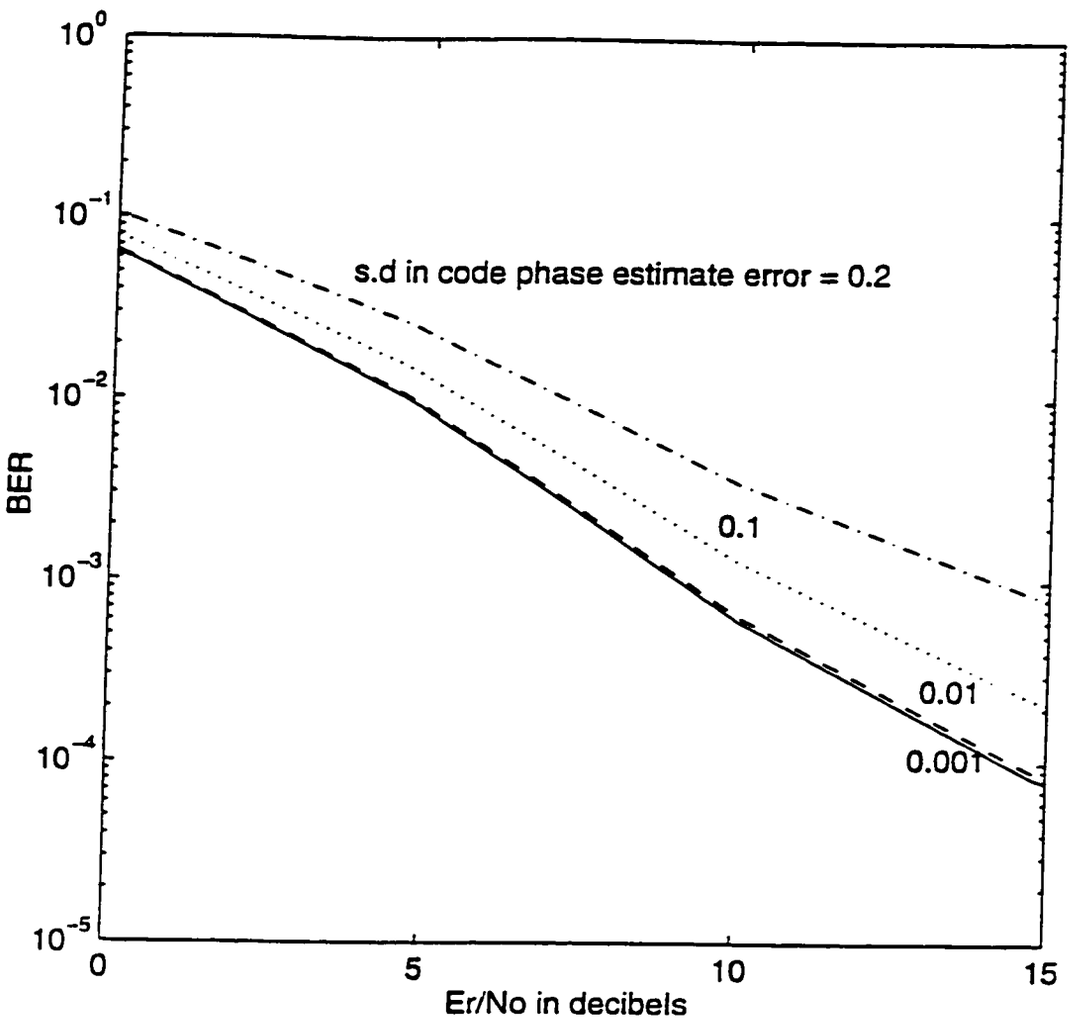

Figure 3.22 BER versus $\frac{E_r}{N_o}$ for a RAKE receiver with different levels of imperfections in spreading code phase estimates. Perfect power control and channel parameter estimation; $K = 9$; $\bar{L} = 3$; $N = 31$.

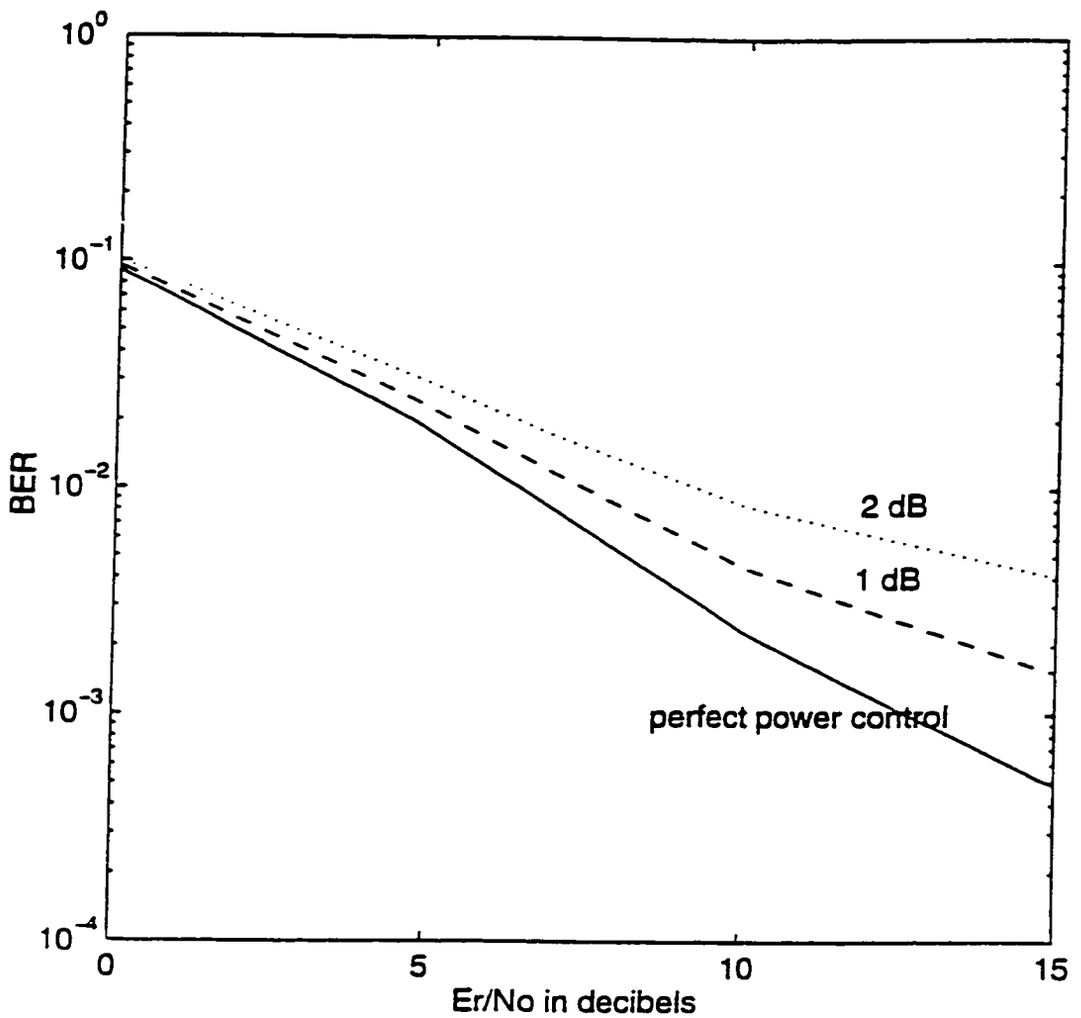

Figure 3.23 BER versus $\frac{E_r}{N_o}$, for a RAKE receiver with imperfections in power control and phase estimates. MSE in channel parameter estimate = 0.01 and standard deviation of normalized error in code phase estimate = 0.1; $K = 9$; $\bar{L} = 3$; $N = 31$.

functions of variance of normalized received power in dB. MSE in channel parameter estimation and standard deviation of normalized code phase error, respectively in Figures 3.24 - 3.26. These figures clearly illustrate the degree of performance degradation incurred by the receiver at various values of imperfections. From Figure 3.24 it is seen that the variance of received power should be less than 1-2 dB for acceptable BER performance. The fact that channel parameter estimation techniques should have a MSE less than 0.01 is illustrated in Figure 3.25. If the standard deviation of normalized code phase error is more than 0.1, the system performance is significantly degraded as seen in Figure 3.26.

3.4 Summary

Spread spectrum multi-access receivers with imperfections in power control, channel parameter estimation and spreading code phase estimation were analyzed. Two types of receivers - correlator and multipath diversity combining RAKE - were considered. Imperfection in power control was taken into account by modeling the received signal power as a log-normally distributed random variable whereas the estimate errors were modeled as zero mean Gaussian random variables. These imperfections are of particular concern in CDMA systems. The performance of such receivers degrades significantly when the variance of normalized received power is above 0 dB, or the MSE in channel parameter estimation is above 0.01 or the standard deviation of the normalized code phase error is above 0.1. It was also shown that the capacity of an indoor CDMA system that uses a correlator receiver is con-

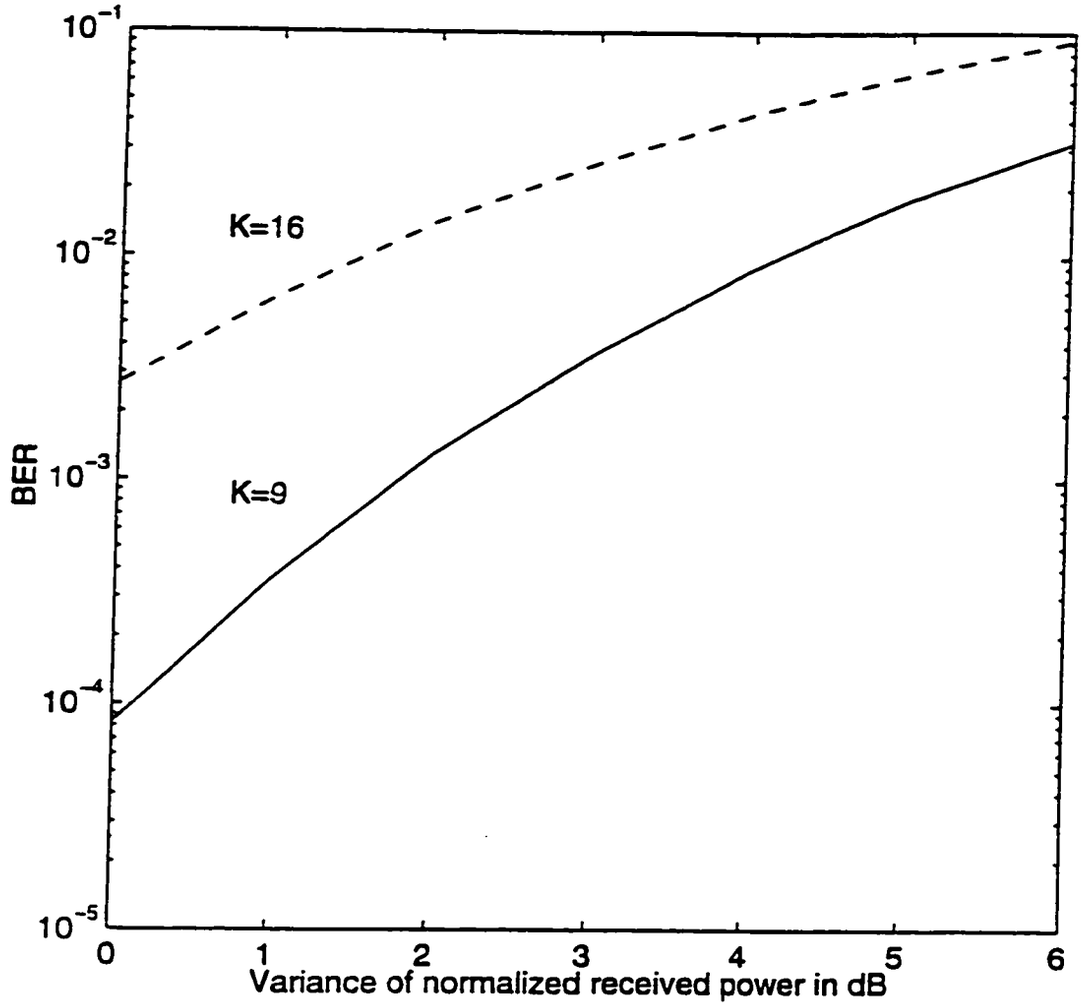

Figure 3.24 BER versus Variance of normalized received power. Perfect channel parameter estimation and code phase estimation; $\frac{E_r}{N_o} = 15dB$; $\bar{L} = 3$; $N = 31$.

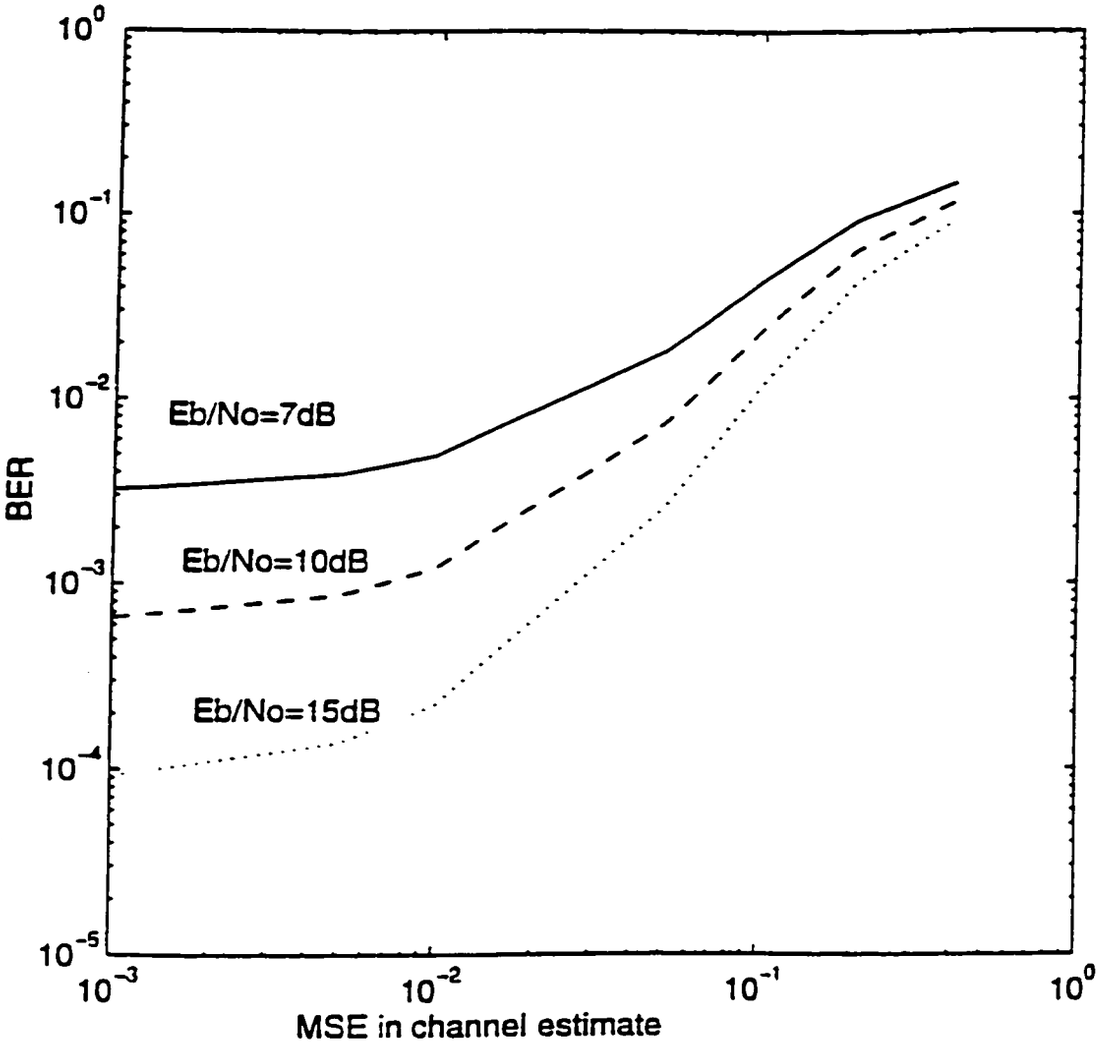

Figure 3.25 BER versus MSE in channel parameter estimation. Perfect power control and spreading code phase estimation; $K = 9$; $\bar{L} = 3$; $N = 31$.

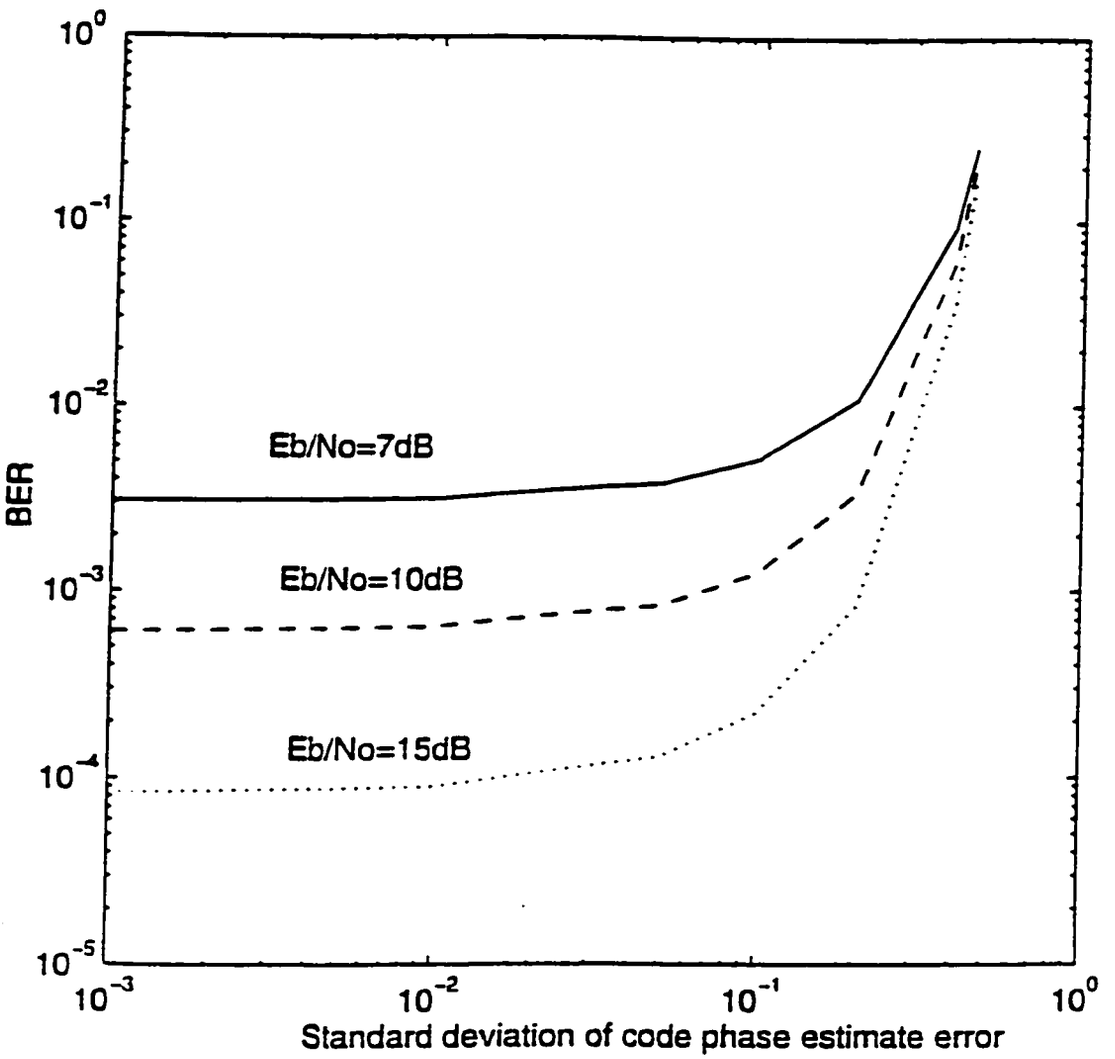

Figure 3.26 BER versus standard deviation of normalized code phase error. Perfect power control and channel parameter estimation; $K = 9$; $\bar{L} = 3$; $N = 31$.

siderably less than that of a system that uses a multipath diversity combining RAKE receiver. It is attractive to develop alternate rec

4. Effect of System Imperfections on the Performance of CDMA Correlator Receiver with CCI Cancellation

4.1 Introduction

As shown in Chapter 3 asynchronous CDMA systems using correlators or RAKE receivers have poor multiple access capacity. This is due to the lower bound on mean square cross-correlation levels among codes allocated to system subscribers. If this interference is accurately estimated it is possible to regenerate and subsequently cancel its effect from the received signal. Thus the effective signal to noise ratio for the desired channel can be increased. This process is referred to as CCI regeneration and cancellation. This, however, results in a complex receiver structure. This type of receiver is therefore more suited to the base station than to portable units. With increasing demand for personal communications and commercial use of available spectrum, the hardware complexity is becoming secondary to the spectral efficiency which results in higher capacity.

In this chapter, analysis is done on a DS CDMA correlator receiver that employs a cascade of CCI cancelers for communication over indoor multipath fading channels.

Such a receiver first coherently demodulates and de-spreads the received signal using a set of correlators, one for each active portable transmitter. These correlators use estimated values of carrier phases and spreading code phases to obtain initial data estimates. The CCI is regenerated by the cancellation scheme using the initial data estimates and the estimated channel parameters and spreading code phases. The regenerated CCI is subsequently subtracted from the down converted received signal. Assuming the channel estimates to be correct, as long as the majority of initial data estimates are correct, most of the CCI can be removed. The received signal from which CCI has been canceled is demodulated and de-spread using a second set of correlators. This yields improved data estimates. The process can be repeated one or more number of times to yield a cascade of CCI cancelers.

There are basically two ways of realizing CCI cancellation. In the first method, known as pre-correlation cancellation, CCI at the input of the correlator receiver is regenerated. This regenerated CCI is subtracted from the input of a second correlator stage resulting in better data estimates at the correlator output. This type of CCI cancellation is analyzed in this chapter. In the second method, a replica of the CCI at the output of the correlator is regenerated and subtracted from the output of the correlator [20]. This is referred to as post correlation cancellation of CCI. From a practical point of view, cancellation of interference from the received signal at the front end of the correlator has certain advantages:

- This permits improved detection of autocorrelation peaks of the weak signals at the second or the subsequent correlator receiver stages.

- The total cancellation of all known transmitted signals in the received signal helps the spreading code phase acquisition.

- This method of CCI cancellation alleviates, to some extent, the near-far problem. The near channels will be received at a higher signal strength with the result that they can be more accurately regenerated and canceled from the lower power far channel received signal.

Another major issue in CCI cancellation is whether the interference is canceled successively or in parallel. While successive interference cancellation can lead to a somewhat simpler receiver [22], it suffers from a large processing delay that varies with the number of active users. This could become a problem in many applications.

As opposed to this, parallel pre-correlation cancellation with not so stringent system power control is a better suited alternative in many applications. With rapid advances in Very Large Scale Integration (VLSI) technology, a small increase in complexity should not be a major problem. One pertinent question is the required accuracy for the power control so as to realize the capacity improvement in such a scheme. In this chapter, this question along with the effects of channel estimation and spreading code synchronization errors are addressed. The results of such an analysis allow the system designer to pick the right system parameters. In carrying out the analysis, system BER is used as the performance measure.

The transmitter and channel models used for the analysis are the same as those described in Chapter 3. More details on the implementation of parallel pre-correlation

cancellation are given in Section 4.2. Analysis of data estimates with imperfections in power control, channel estimates and spreading code phase estimates is given in Section 4.3. This is followed by a BER analysis in Section 4.4 and numerical results in Section 4.5. Results are summarized in Section 4.6.

4.2 CDMA Correlator Receiver with Parallel Pre-correlation Cancellation of CCI

The down converted and low-pass filtered signal for the desired user i, derived in Section 3.2.1, is given by

$$\begin{aligned} r_d^{(i)}(t) &= \sqrt{\frac{P_i}{2}} g_d(i,i,1) a_i(t-\tau_{i,1}) b_i(t-\tau_{i,1}) + \\ &\quad \sqrt{\frac{P_i}{2}} \sum_{\lambda=2}^{L_i} g_d(i,i,\lambda) a_i(t-\tau_{i,\lambda}) b_i(t-\tau_{i,1}) + \\ &\quad \sum_{k=1,k\neq i}^{K} \sum_{\lambda=1}^{L_k} \sqrt{\frac{P_k}{2}} g_d(i,k,\lambda) a_k(t-\tau_{k,\lambda}) b_k(t-\tau_{i,1}) + n_d^{(t)}(t) \\ &= D_d^{(i)}(t) + F_d^{(i)}(t) + I_d^{(i)}(t) + n_d^{(i)}(t). \end{aligned} \tag{4.1}$$

where $n_d^{(i)}(t)$ is the lowpass filtered noise. The basic idea of the canceler is to regenerate the replica of the CCI given by the second and third terms in Equation (4.1) and subtract them from the down converted received signal $r_d^{(i)}(t)$. This CCI is regenerated by using a preliminary set of data estimates, power level estimates, spreading code phase estimates and channel parameter estimates of all users.

The schematic to obtain preliminary channel and data estimates and to regenerate CCI is shown in Figure 4.1. Preliminary data estimates obtained using the correlator

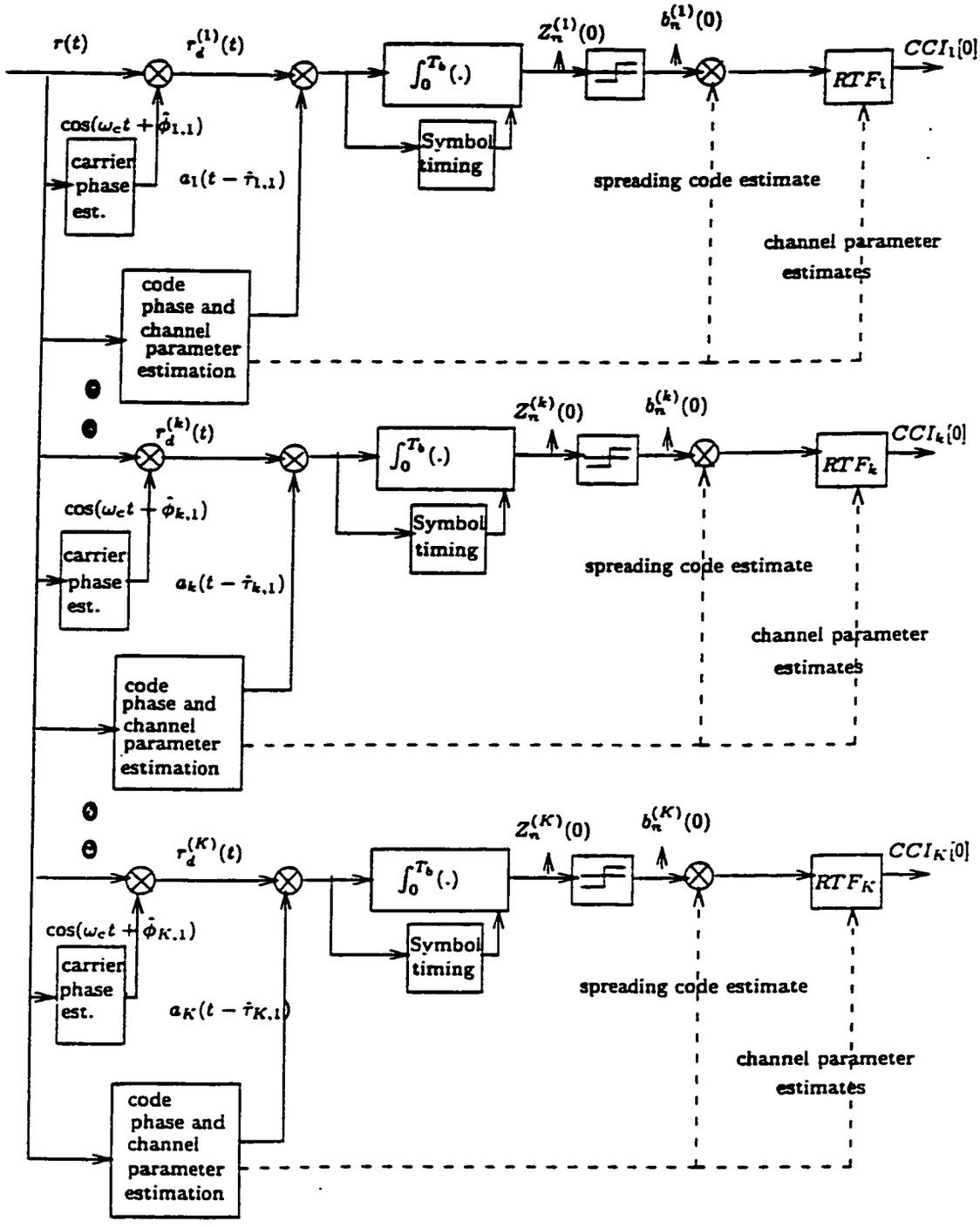

Figure 4.1 Data and channel estimation at the preliminary stage of CCI canceling receiver and subsequent interference regeneration using the estimates.

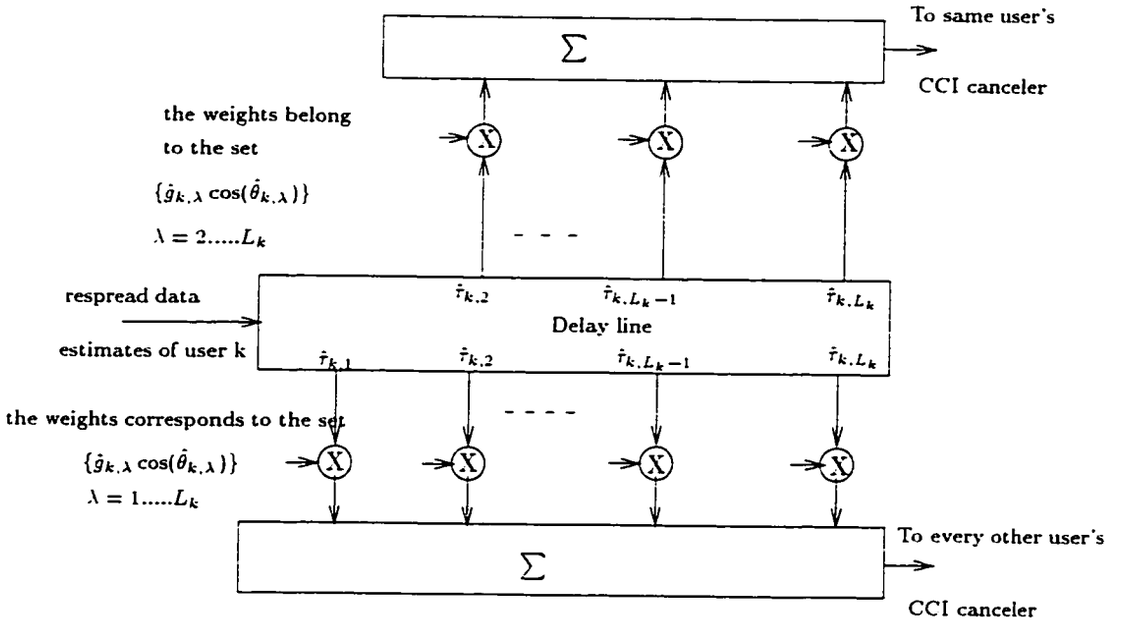

Figure 4.2 Multipath channel emulator using RTF.

receiver are spread using estimated spreading code phases. The spread signals are passed through a channel emulator realized using Regenerating Transversal Filter (RTF) shown in detail in Figure 4.2.

The impulse response of the RTF is the same as that of the channel. The regenerated interference components are summed up and then subtracted from a delayed version of the down converted signal as shown in Figure 4.3. The improved parameter estimates obtained from this CCI canceled signal can be used for better regeneration of CCI in a second CCI regenerator as shown in Figure 4.3. By repeating this operation, a cascade of CCI cancelers is derived as shown in Figure 4.4.

Channel parameter estimates and spreading code phase estimates are required

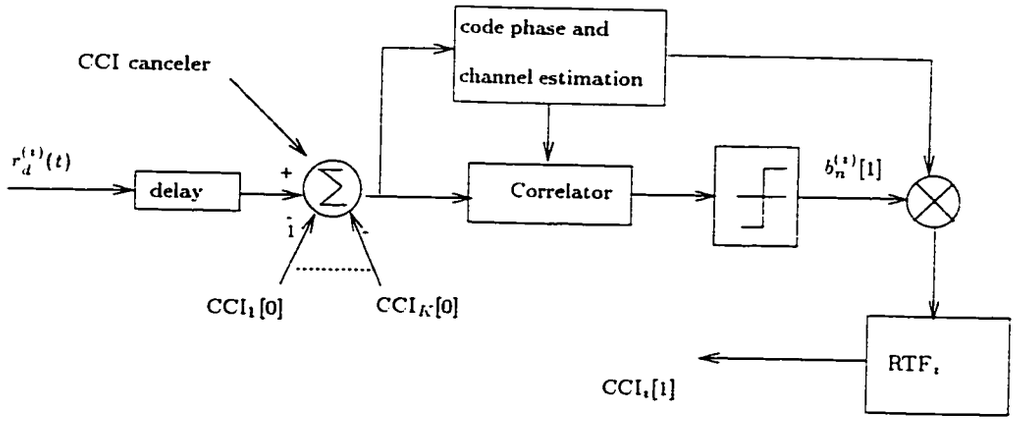

Figure 4.3 One stage of CCI cancellation.

to obtain preliminary data estimates and to regenerate CCI. Because of imperfect estimation, the error in the amplitude estimate $\Delta g_{k,\lambda}$, the error in the phase estimate $\Delta\phi_{k,\lambda}$, and the error in the delay estimates $\Delta\tau_{k,\lambda}$ have to be considered. The estimated values of these parameters and the error modeling were discussed in Chapter 3.

4.3 Analysis of Data Estimates

The first step in CCI regeneration and the cancellation process is to obtain data estimates, channel parameter estimates, spreading code phase estimates and incoming signal power level estimates. These steps are shown in Figure 4.1. A power level estimate is obtained from the autocorrelation peak at the correlator output. It is assumed that power levels are estimated without error. Using estimated carrier phase and spreading code phase, the correlator receiver of the kth user demodulates the signal. A hard decision on the correlator output $Z_n^{(k)}$ provides a data estimate

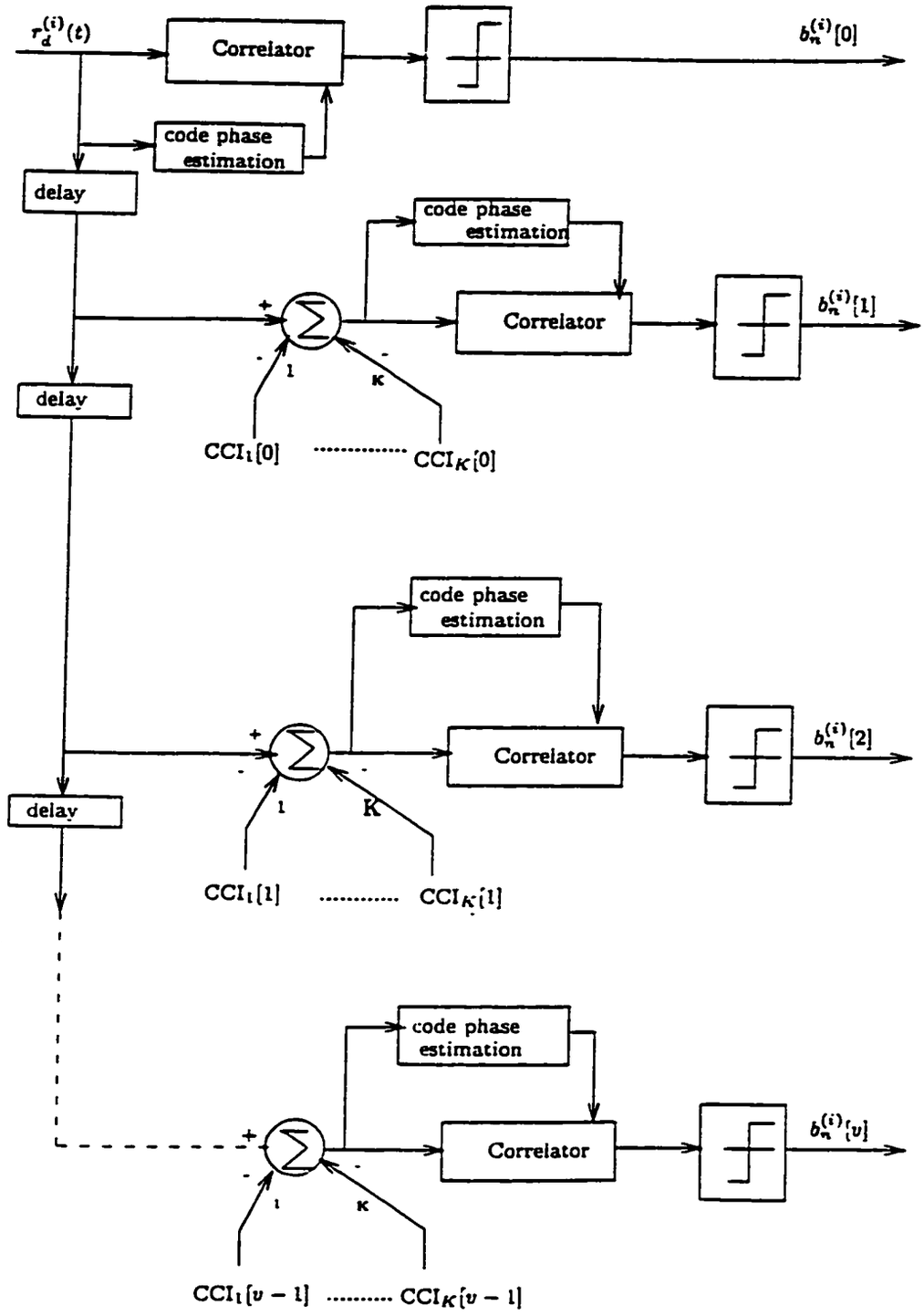

Figure 4.4 A correlator receiver with cascaded pre-correlation CCI canceler stages.

of the kth user's nth symbol as

$$b_n^{(k)}[0] = \mathrm{sgn}(Z_n^{(k)}). \tag{4.2}$$

This was derived in Section 3.2.2. The zero in the square bracket is to denote that the data estimate is from a stage before CCI cancellation.

Preliminary data estimates $\{b_n^{(k)}[0]\}$ for all users are obtained in a similar manner. These are then used to form the corresponding data signal set $\{b_n^{(k)}[0](t)\}$. Then for $k \neq i$ the preliminary data signal estimates are re-spread using estimated spreading codes. As shown in Figure 4.2, the spread signals are then passed through RTF_k which emulates the channel characteristics of the kth user. The method of regenerating the interference from paths other than the desired path, IDS for cancellation from the same user is also explained in Figure 4.2. In the presence of estimation errors, the tap weights of RTF_k are represented by $\hat{g}_{k,\lambda}\cos(\hat{\phi}_{k,\lambda})$. The error in the spreading code phase results in an error in path delay estimates. This results in tap positions at $\hat{\tau}_{k,\lambda}$ instead of at $\tau_{k,\lambda}$. Because of the asynchronous nature of user transmissions, for the nth symbol, the interfering symbols of other users are $n-1-m$ and $n-m$ where m can take on the values -1, 0, or 1. Thus, for regenerating and canceling the interference to the nth data signal of user i, the other user data estimates for $(n-2)$, $(n-1)$, n and $(n+1)$ data intervals must be available. It may be seen that, during the detection of the nth symbol, the CCI cancellation can be done on $l = (n-2)$th symbol only. The regenerated self interference component,

IDS in the ith user's $l = (n-2)$ th symbol at time t is given by

$$\hat{F}_d^{(i)}[0](t) = \sum_{\lambda=2}^{L_i} \sqrt{\frac{P_i}{2}} \hat{g}_d(i,i,\lambda) a_i(t - \hat{\tau}_{i,\lambda}) b_l^{(i)}[0](t - 2T_b - \hat{\tau}_{i,\lambda}). \tag{4.3}$$

Similarly, the regenerated MAI component is obtained as

$$\hat{I}_d^{(i)}[0](t) = \sum_{k=1,k\neq i}^{K} \sum_{\lambda=1}^{L_k} \sqrt{\frac{P_k}{2}} \hat{g}_d(i,k,\lambda) a_k(t - \hat{\tau}_{k,\lambda}) b_l^{(k)}[0](t - 2T_b - \hat{\tau}_{k,\lambda}). \tag{4.4}$$

In Equations (4.3) and (4.4), $\hat{g}_d(i,k,\lambda) = \hat{g}_{k,\lambda} \cos(\hat{\phi}_{k,\lambda} - \hat{\phi}_{i,1})$. The net values of IDS and MAI, denoted by $\tilde{F}_d^{(i)}[0](t)$ and $\tilde{I}_d^{(i)}[0](t)$ respectively, at the input to the correlator after the first canceler stage are obtained by subtracting the regenerated components given by Equations (4.3) and (4.4) from the two symbol delayed received components. These net values are given by

$$\tilde{F}_d^{(i)}[0](t) = F_d^{(i)}(t - 2T_b) - \hat{F}_d^{(i)}[0](t) \tag{4.5}$$

and

$$\tilde{I}_d^{(i)}[0](t) = I_d^{(i)}(t - 2T_b) - \hat{I}_d^{(i)}[0](t). \tag{4.6}$$

With these as inputs, the corresponding output components of the correlator for the lth bit of the ith user are given by

$$F_l^{(i)}[1] = \sum_{\lambda=2}^{L_i} \sqrt{\frac{P_i}{2}} \left\{ f(i,i,\lambda,l) - \hat{f}(i,i,\lambda,l,1) \right\} \tag{4.7}$$

and

$$I_l^{(i)}[1] = \sum_{k=1,k\neq i}^{K} \sum_{\lambda=1}^{L_k} \sqrt{\frac{P_k}{2}} \left\{ f(i,k,\lambda,l) - \hat{f}(i,k,\lambda,l,1) \right\}. \tag{4.8}$$

Once again, the number '1' in the brackets indicate the CCI canceler stage number. In Equations (4.7) and (4.8)

$$f(i,k,\lambda,l) = g_d(i,k,\lambda) \left\{ b_{l-m-1}^{(k)} R_{k,i}(\tau) + b_{l-m}^{(k)} \hat{R}_{k,i}(\tau) \right\} \tag{4.9}$$

and

$$\hat{f}(i,k,\lambda,l,1) = \hat{g}_d(i,k,\lambda) \left\{ b_{l-m'-1}^{(k)}[0] R_{k,i}(\tau') + b_{l-m'}^{(k)}[0] \hat{R}_{k,i}(\tau') \right\}. \tag{4.10}$$

The notations m and τ in Equation (4.9) were defined in Section 3.2.2 to denote the relative number of bit shifts and time delays. The new notations m' and τ' are introduced in Equation (4.10). This is done to include the effect of estimation errors and are given by

$$m' = m'(i,k,\lambda) = \lfloor \frac{\hat{\tau}_{k,\lambda} - \hat{\tau}_{i,1}}{T_b} \rfloor \tag{4.11}$$

and

$$\tau' = \tau'(i,k,\lambda) = (\hat{\tau}_{k,\lambda} - \hat{\tau}_{i,1}) - m' T_b. \tag{4.12}$$

The output of the correlator after the first CCI canceler stage is given by

$$Z_l^{(i)}[1] = D_l^{(i)} + F_l^{(i)}[1] + I_l^{(i)}[1] + \zeta_l^{(i)}. \tag{4.13}$$

It is to be noted that $D_l^{(i)}$ and $\zeta_l^{(i)}$ are not changed by CCI cancellation. The hard decision data estimate after one stage of CCI cancellation is then given by

$$b_l^{(i)}[1] = \mathrm{sgn}(Z_l^{(i)}[1]). \tag{4.14}$$

Using a similar procedure, one can obtain the contributions of the net IDS and MAI at the correlator output of the vth canceler stage, corresponding to $l = (n - v - 1)$th symbol, as

$$F_l^{(i)}[v] = \sum_{\lambda=2}^{L_i} \sqrt{\frac{P_i}{2}} \left\{ f(i, i, \lambda, l) - \hat{f}(i, i, \lambda, l, v) \right\} \tag{4.15}$$

and

$$I_l^{(i)}[v] = \sum_{k=1, k\neq i}^{K} \sum_{\lambda=1}^{L_k} \sqrt{\frac{P_k}{2}} \left\{ f(i, k, \lambda, l) - \hat{f}(i, k, \lambda, l, v) \right\}. \tag{4.16}$$

In Equations (4.15) and (4.16),

$$\hat{f}(i, k, \lambda, l, v) = \hat{g}_d(i, k, \lambda) \left\{ b_{l-m'-1}^{(k)}[v-1] R_{k,i}(\tau') + b_{l-m'}^{(k)}[v-1] \hat{R}_{k,i}(\tau') \right\}. \tag{4.17}$$

The output of the correlator after the vth CCI canceler stage is then written as

$$Z_l^{(i)}[v] = D_l^{(i)} + F_l^{(i)}[v] + I_l^{(i)}[v] + \zeta_l^{(i)}. \tag{4.18}$$

The hard decision data estimate after v stages of CCI cancelers is then

$$b_l^{(i)}[v] = \mathrm{sgn}(Z_l^{(i)}[v]). \tag{4.19}$$

The BER of the data estimates obtained after CCI cancellation is next derived using the standard Gaussian approximation.

4.4 BER Analysis

The probability of bit error $p_e^{(i)}$ for the ith user's preliminary data estimate was derived in Section 3.3. For a single stage of CCI cancellation, the signal output of the correlator, $Z_l^{(i)}[1]$ is given in Equation (4.13). It may be noted that $Z_l^{(i)}[1]$ differs from the pre-cancellation correlator output $Z_n^{(i)}$ given in Equation (3.17) only in the IDS term $F_n^{(i)}$ and the MAI term $I_n^{(i)}$. It is easy to see that $F_l^{(i)}[1]$ and $I_l^{(i)}[1]$ are zero mean random variables. With considerable manipulations, the expected value of the square of each term in $F_l^{(i)}[1]$ and $I_l^{(i)}[1]$ are obtained. Then, by rearranging and simplifying the terms, the variances of $F_l^{(i)}[1]$ and $I_l^{(i)}[1]$ are obtained as

$$\begin{aligned}\mathrm{Var}\left(F_l^{(i)}[1]\right) &= \frac{1}{2}(\bar{L}_i - 1)E\{P_i\}\left[\frac{G}{2}E\left\{R_{i,i}^2(\tau) + \hat{R}_{i,i}^2(\tau)\right\} + \right. \\ &\quad \frac{(G+\sigma_{\Delta g}^2)}{2}E\left\{R_{i,i}^2(\tau') + \hat{R}_{i,i}^2(\tau')\right\} - (1 - 2p_e^{(i)}[0]). \\ &\quad \left. \exp(-\frac{\sigma_{\Delta\phi}^2}{2})E\left\{R_{i,i}(\tau)R_{i,i}(\tau') + \hat{R}_{i,i}(\tau)\hat{R}_{i,i}(\tau')\right\}\right] \qquad (4.20)\end{aligned}$$

and

$$\begin{aligned}\mathrm{Var}\left(I_l^{(i)}[1]\right) &= \sum_{k=1,k\neq i}^{K}\frac{1}{2}\bar{L}_k E\{P_k\}\left[\frac{G}{2}E\left\{R_{k,i}^2(\tau) + \hat{R}_{k,i}^2(\tau)\right\} + \right. \\ &\quad \frac{(G+\sigma_{\Delta g}^2)}{2}E\left\{R_{k,i}^2(\tau') + \hat{R}_{k,i}^2(\tau')\right\} - (1 - 2p_e^{(k)}[0]). \\ &\quad \left. \exp(-\frac{\sigma_{\Delta\phi}^2}{2})E\left\{R_{k,i}(\tau)R_{k,i}(\tau') + \hat{R}_{k,i}(\tau)\hat{R}_{k,i}(\tau')\right\}\right]. \qquad (4.21)\end{aligned}$$

For the sake of clarity in notations, in Equations (4.20) and (4.21), τ represents $\tau(i,i,\lambda)$ and $\tau(i,k,\lambda)$ respectively. This is possible because τ does not depend on k in Equation (4.20). Similarly, in Equations (4.20) and (4.21), τ' stands for $\tau'(i,i,\lambda)$ and $\tau'(i,k,\lambda)$ respectively. The fact that $E\{b_l^{(k)}b_l^{(k)}[0]\} = 1 - 2p_e^{(k)}[0]$, $1 \leq k \leq K$, where $p_e^{(k)}[0]$ is the kth user's error probability before CCI cancellation, has been utilized in Equations (4.20) and (4.21). G and $\bar{L}_k$ have been defined previously. $E\left\{R_{k,i}^2(\tau') + \hat{R}_{k,i}^2(\tau')\right\}$ has to be obtained to evaluate Equations (4.20) and (4.21). For this the density function of τ' has to be calculated. A close examination of Equations (3.25) and (4.12) reveals that the density function of τ' is the same as that of τ, but with different variance. This is because τ is the sum of a uniformly distributed random variable and a Gaussian distributed estimation error. τ' is the sum of a uniformly distributed random variable and two Gaussian distributed estimation errors. For $\sigma_{\Delta\tau_{k,\lambda}}^2 = \sigma_{\Delta\tau}^2$ for all values of k and λ, the density function of $\tau'(i,i,\lambda)$ and $\tau'(i,k,\lambda)$ are given by Equations (3.38) and (3.41) respectively, with $\sigma_{\Delta\tau}$ replaced by $\sqrt{2}\sigma_{\Delta\tau}$.

In order to evaluate $E\left\{R_{k,i}(\tau)R_{k,i}(\tau') + \hat{R}_{k,i}(\tau)\hat{R}_{k,i}(\tau')\right\}$, the joint density function has to be obtained. Using the method of obtaining the joint density function of two functions of two randon variables [64], this joint density function may be written as

$$f_{\tau',\tau}(\tau',\tau) = f_\tau(\tau) f_{\Delta\tau_{k,\lambda}}(\Delta\tau_{k,\lambda}). \tag{4.22}$$

The density function of τ has already been derived in Equation (3.41). The path delay estimation errors $\{\Delta\tau_{k,\lambda}, 1 \leq k \leq K, 1 \leq \lambda \leq L_k\}$ are zero mean Gaussian

variables with equal variance of $\sigma_{\Delta\tau}$. The joint density function can thus be obtained. All the expected values in Equations (4.20) and (4.21) are evaluated using numerical integration.

The ith user's signal to noise ratio after one stage of CCI cancellation is given by

$$SNR_l^{(i)}[1] = \frac{E\{[D_l^{(i)}]^2\}}{\mathrm{Var}(F_l^{(i)}[1]) + \mathrm{Var}(I_l^{(i)}[1]) + \mathrm{Var}(\zeta_l^{(i)})}. \tag{4.23}$$

As before, the probability of bit error $p_e^{(i)}[1]$ after one stage CCI cancellation may be computed from

$$p_e^{(i)}[1] = Q\left(\sqrt{SNR_l^{(i)}[1]}\right), \tag{4.24}$$

where the Q function has been defined previously.

With v stages of CCI cancelers and data decisions, the variances of the IDS term and the MAI term may be obtained by recursive calculation at each stage. These are given by

$$\begin{aligned}\mathrm{Var}\left(F_l^{(i)}[v]\right) = \; & \frac{1}{2}(\bar{L}_i - 1)E\{P_i\}\left[\frac{G}{2}E\left\{R_{i,i}^2(\tau) + \hat{R}_{i,i}^2(\tau)\right\} + \right. \\ & \frac{(G+\sigma_{\Delta g}^2)}{2}E\left\{R_{i,i}^2(\tau') + \hat{R}_{i,i}^2(\tau')\right\} - (1 - 2p_e^{(i)}[v-1]). \\ & \left. \exp(-\frac{\sigma_{\Delta\phi}^2}{2})E\left\{R_{i,i}(\tau)R_{i,i}(\tau') + \hat{R}_{i,i}(\tau)\hat{R}_{i,i}(\tau')\right\}\right] \end{aligned} \tag{4.25}$$

and

$$\mathrm{Var}\left(I_l^{(i)}[v]\right) = \sum_{k=1,k\neq i}^{K} \frac{1}{2}\bar{L}_k E\{P_k\}\left[\frac{G}{2}E\left\{R_{k,i}^2(\tau) + \hat{R}_{k,i}^2(\tau)\right\} + \right.$$

$$\frac{(G+\sigma_{\Delta g}^2)}{2}E\left\{R_{k,i}^2(\tau')+\hat{R}_{k,i}^2(\tau')\right\}-(1-2p_e^{(k)}[v-1]).$$
$$\exp(-\frac{\sigma_{\Delta\phi}^2}{2})E\left\{R_{k,i}(\tau)R_{k,i}(\tau')+\hat{R}_{k,i}(\tau)\hat{R}_{k,i}(\tau')\right\}\Big]. \qquad (4.26)$$

Signal to noise ratio after v stages of CCI cancelers is obtained by substituting Var $\left(F_l^{(i)}[v]\right)$ and Var $\left(I_l^{(i)}[v]\right)$ in place of Var $\left(F_l^{(i)}[1]\right)$ and Var $\left(I_l^{(i)}[1]\right)$ in Equation (4.23) and recalculating the expression. The bit error probability $p_e^{(i)}[v]$ after v stages of CCI cancelers is obtained by recomputing Equation (4.24) with this new value of SNR.

Because of the pre-correlation CCI cancellation, the error variance of the channel estimates and the code phase estimates decreases in the subsequent correlator receiver stages. It has been reported that the error variance is inversely related to the number of co-users [65]. A correct data estimate results in accurate regeneration and cancellation of one co-user signal. An approximate way, therefore, to model the improvement in the accuracy of estimates after j, $1 \leq j \leq v$ stages of interference cancellation is to multiply the estimate error variances by $2p_e^{(k)}[j]$; $p_e^{(k)}[j]$ being the BER after the jth cancellation. This is a reasonable assumption as the cancellation at the $(j+1)$ th stage reduces the CCI from $(1-p_e^{(k)}[j])$ users. The factor 2 occurs because the cancellation of the CCI generated from incorrect data signal estimates doubles the corresponding CCI.

4.5 Numerical Results

Performance results are computed for a system with parameter values described in Section 3.2.4. Results are presented for various combinations of factors. The BER performance with perfect conditions is shown in Figure 4.5. The individual effect of various system imperfections on BER performance is shown in Figures 4.6 - 4.10. Next, the combined effect of imperfections is presented in Figures 4.11 and 4.12. In all these figures, the spreading code period, $N = 31$ and the number of users, $K = 16$. Because of the possible capacity improvements due to CCI cancellation, the number of users, K considered is 16 as compared to $K = 3$ in the last chapter. Under ideal conditions of operation, the single user BER performance can be achieved with 3 stages of CCI cancellation (Figure 4.5). Another important observation is that most of the performance improvement is realized with 2 stages of cancellation. Figure 4.6 is a plot of BER versus $\frac{E_b}{N_o}$ for up to four stages of CCI cancellation when there is power control imperfection resulting in 2 dB variance in the normalized received power. The channel estimate errors and spreading code phase estimate errors were assumed to be zero in this figure. It may be seen that single user BER performance is obtained with four stages of interference cancellation.

The effect of channel estimate error on BER performance is shown in Figures 4.7 and 4.8. Perfect power control and spreading code phase estimation are assumed in both cases. For computing the results shown in Figure 4.7, the MSE in channel estimation was assumed to be constant at 0.01 at all stages of CCI cancellation. This is the situation when the initial channel estimates are used in all subsequent

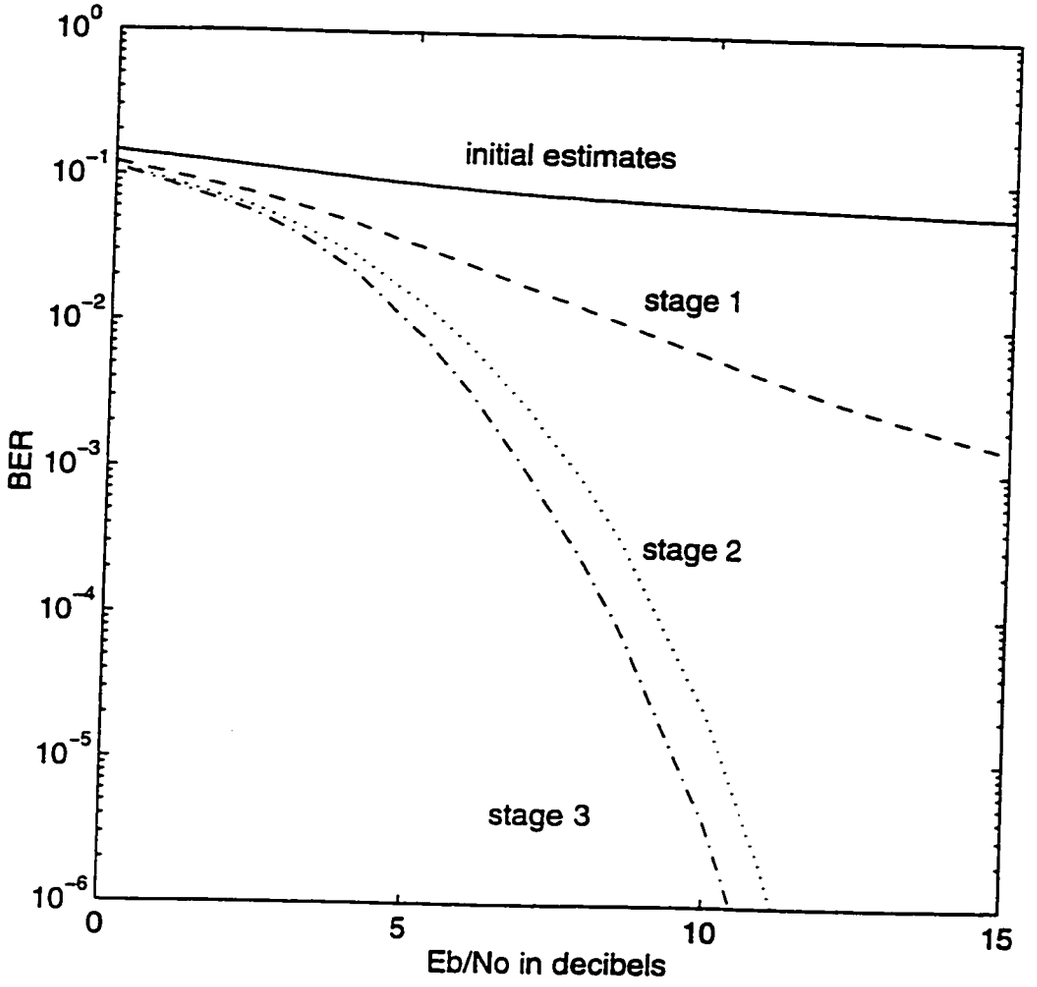

Figure 4.5 BER versus $\frac{E_b}{No}$ for a CCI canceling CDMA correlator receiver. Perfect conditions; $K = 16$; $\bar{L} = 3$; $N = 31$.

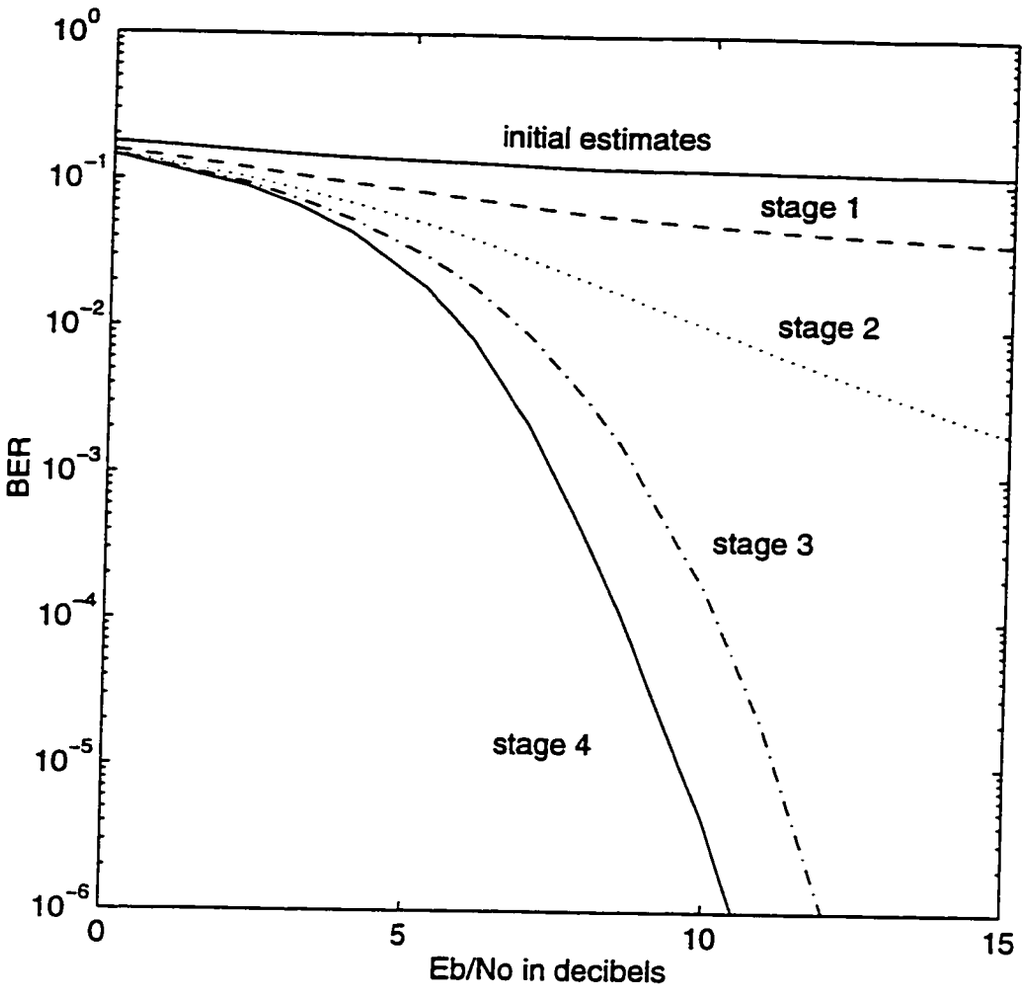

Figure 4.6 BER versus $\frac{E_b}{No}$ for a CCI canceling CDMA correlator receiver. 2 dB variance in normalized received power; no code phase estimate error; no channel estimation error; $K = 16$; $\bar{L} = 3$; $N = 31$.

stages of CCI regeneration without an attempt to re-estimate the channel parameters after each stage of CCI cancellation. The channel estimation error raises the noise floor level, limiting BER performance. Single user BER performance cannot be realized by adding more stages of cancelers (Figure 4.7). The effect of decreased error variance at successive stages of CCI cancellation is considered in Figure 4.8. To obtain this BER performance, channel estimation is repeated after each stage of interference cancellation. An initial MSE of 0.01 is assumed in the preliminary stage. A MSE in channel estimate of 0.01 in the preliminary stage can be tolerated by such receivers when there are no errors in power control or spreading code phase estimates and with channel estimation after each stage of cancellation (Figure 4.8). In this case single user BER performance can be obtained with 4 stages of CCI cancellation.

The effect of spreading code phase estimate error on BER performance is shown in Figures 4.9 and 4.10. In both cases perfect power control and channel estimation are assumed. The performance with a standard deviation of normalized error in code phase estimation of 0.1 at all stages of the receiver is shown in Figure 4.9. This is the situation when code phase estimates obtained at the preliminary stage are used at following stages of the receiver for CCI regeneration and subsequent de-spreading. This results in poor BER performance (Figures 4.9). This is not surprising because the noise due to errors in the code phase estimate in the preliminary stage is maintained in successive CCI regeneration and cancellation stages. The BER performance with code phase estimation performed after each stage of CCI

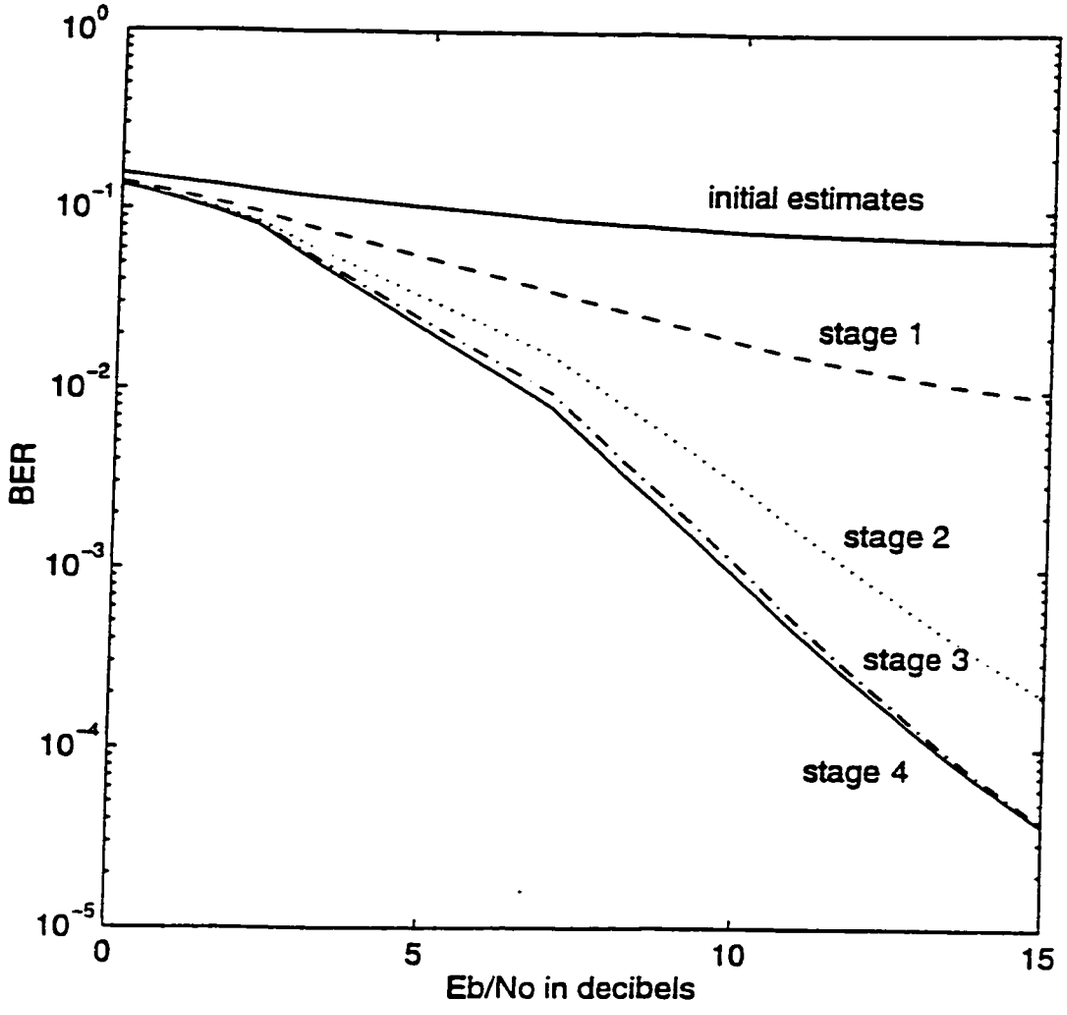

Figure 4.7 BER versus $\frac{E_b}{No}$ for a CCI canceling CDMA correlator receiver. Perfect power control scheme; no code phase estimate error; MSE in channel estimation of 0.01 at all stages; $K = 16$; $\bar{L} = 3$; $N = 31$.

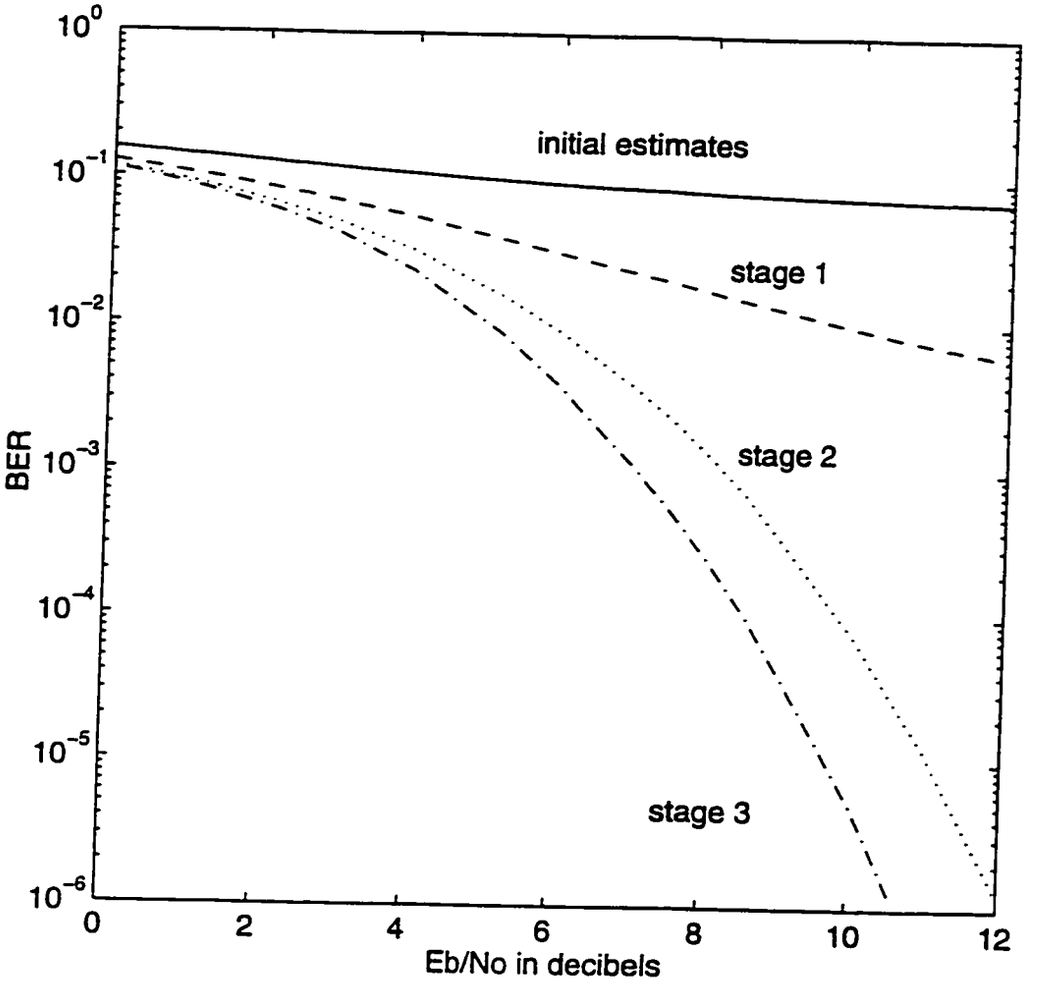

Figure 4.8 BER versus $\frac{E_b}{No}$ for a CCI canceling CDMA correlator receiver. Perfect power control scheme; no code phase estimate error; MSE in channel estimation of 0.1 at preliminary stage, decreases proportional to BER of previous stage in successive cancellation stages ; $K = 16$; $\bar{L} = 3$; $N = 31$.

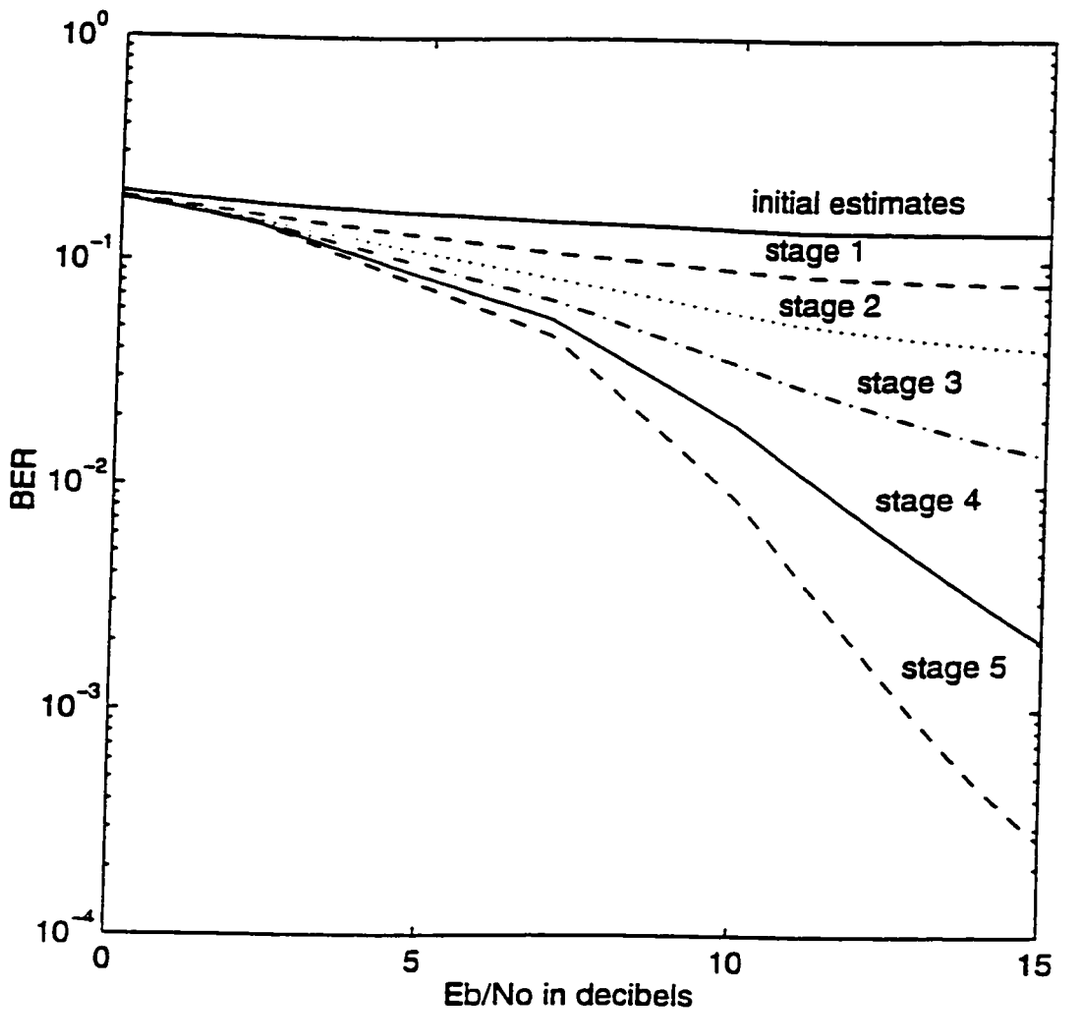

Figure 4.9 BER versus $\frac{E_b}{N_o}$ for a CCI canceling CDMA correlator receiver. Perfect power control scheme; no channel estimation error; standard deviation of normalized error in code phase estimate of 0.1 at all stages; $K = 16$; $\bar{L} = 3$; $N = 31$.

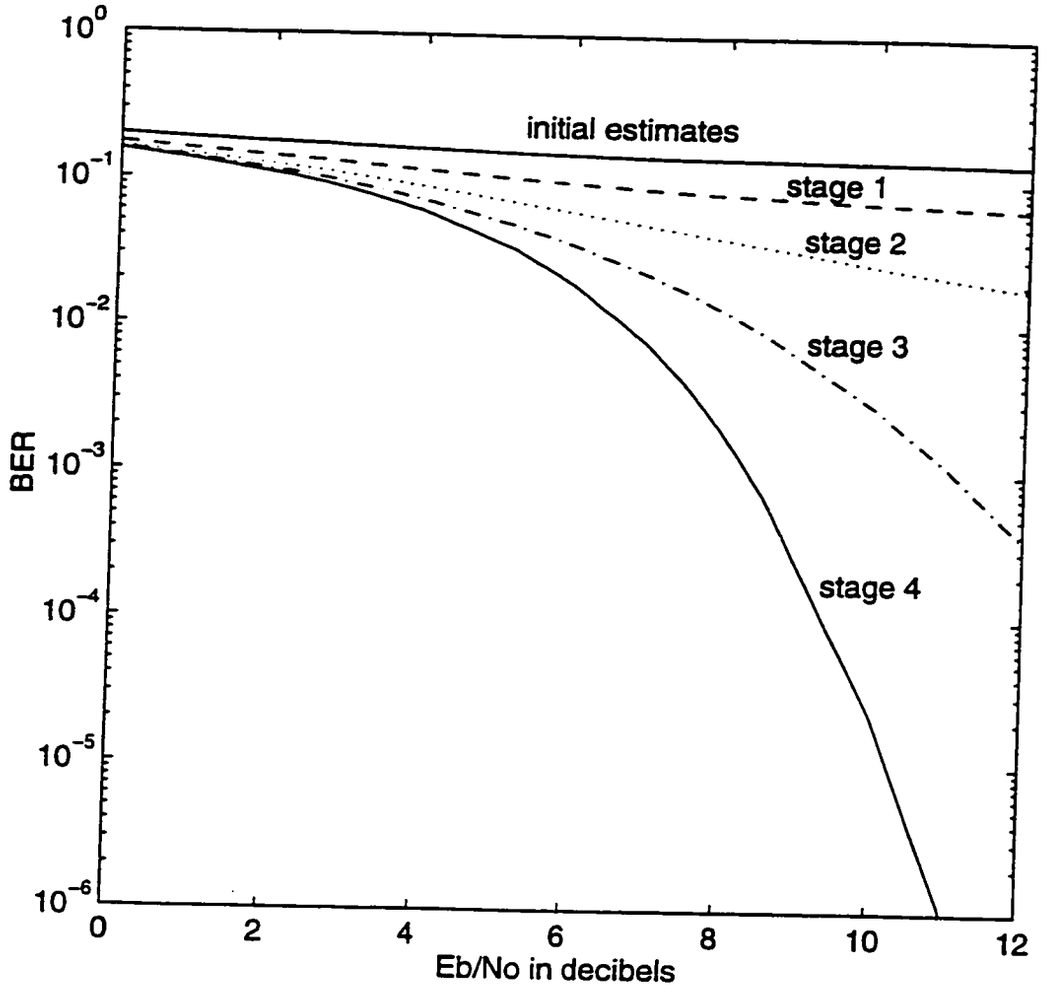

Figure 4.10 BER versus $\frac{E_b}{No}$ for a CCI canceling CDMA correlator receiver. Perfect power control scheme; no channel estimation error; standard deviation of normalized error in code phase estimate of 0.1 at preliminary stage, decreases proportional to BER of previous stage in successive cancellation stages; $K = 16$; $\bar{L} = 3$; $N = 31$.

cancellation is shown in Figure 4.10. An initial standard deviation in normalized code phase estimate error of 0.1 is assumed in the preliminary stage. When there are no errors in power control or channel estimates, and with code phase estimation performed after each canceler stage, the standard deviation in normalized code phase error of 0.1 in the preliminary stage can be tolerated by such receivers (Figure 4.10).

The BER performance with a combination of imperfections is shown in Figures 4.11 and 4.12. The effect of a combination of errors in channel estimation and code phase estimation is considered in Figure 4.11. Perfect power control is assumed in this case. The effect of a combination of all three system imperfections is considered in Figure 4.12. Improvement in the BER performance is limited in the presence of a combination of these imperfections. However, the BER performance can be improved by performing channel estimation and code phase estimation after each stage of CCI cancellation. This, however, results in increased receiver complexity.

4.6 Summary

Analysis was done on the BER performance of a parallel CCI canceling CDMA correlator receiver with imperfections in power control, spreading code phase and channel estimation. Under perfect conditions, CCI cancellation method can significantly improve the BER and the system capacity with three stages of cancelers. Such a receiver can tolerate up to 2 dB variance in the normalized received power or a MSE of 0.01 in channel estimates or a standard deviation of 0.1 in normalized

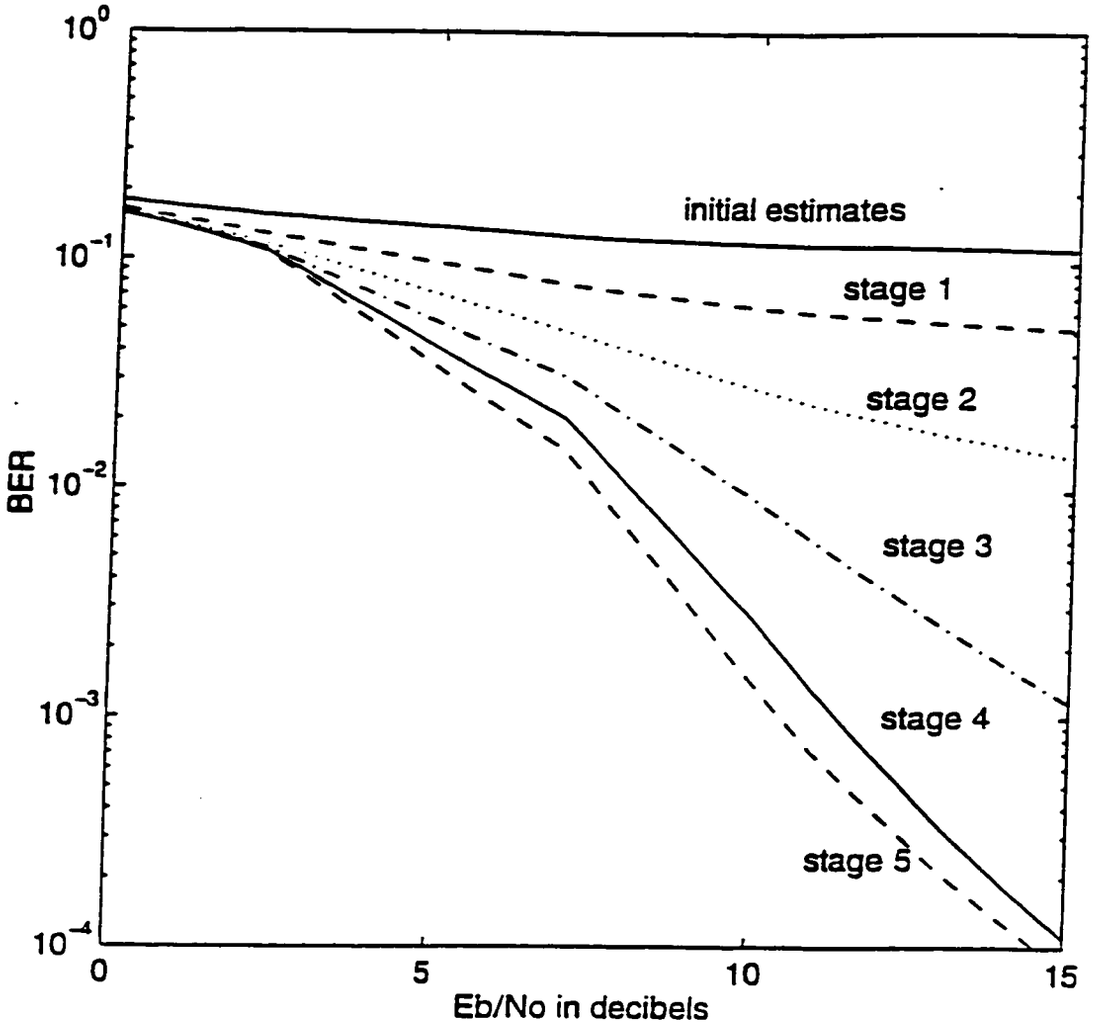

Figure 4.11 BER versus $\frac{E_b}{No}$ for a CCI canceling CDMA correlator receiver. Perfect power control scheme; MSE in channel estimation = 0.001 and standard deviation of normalized error in code phase estimate = 0.01 at all stages; $K = 16$; $\bar{L} = 3$; $N = 31$.

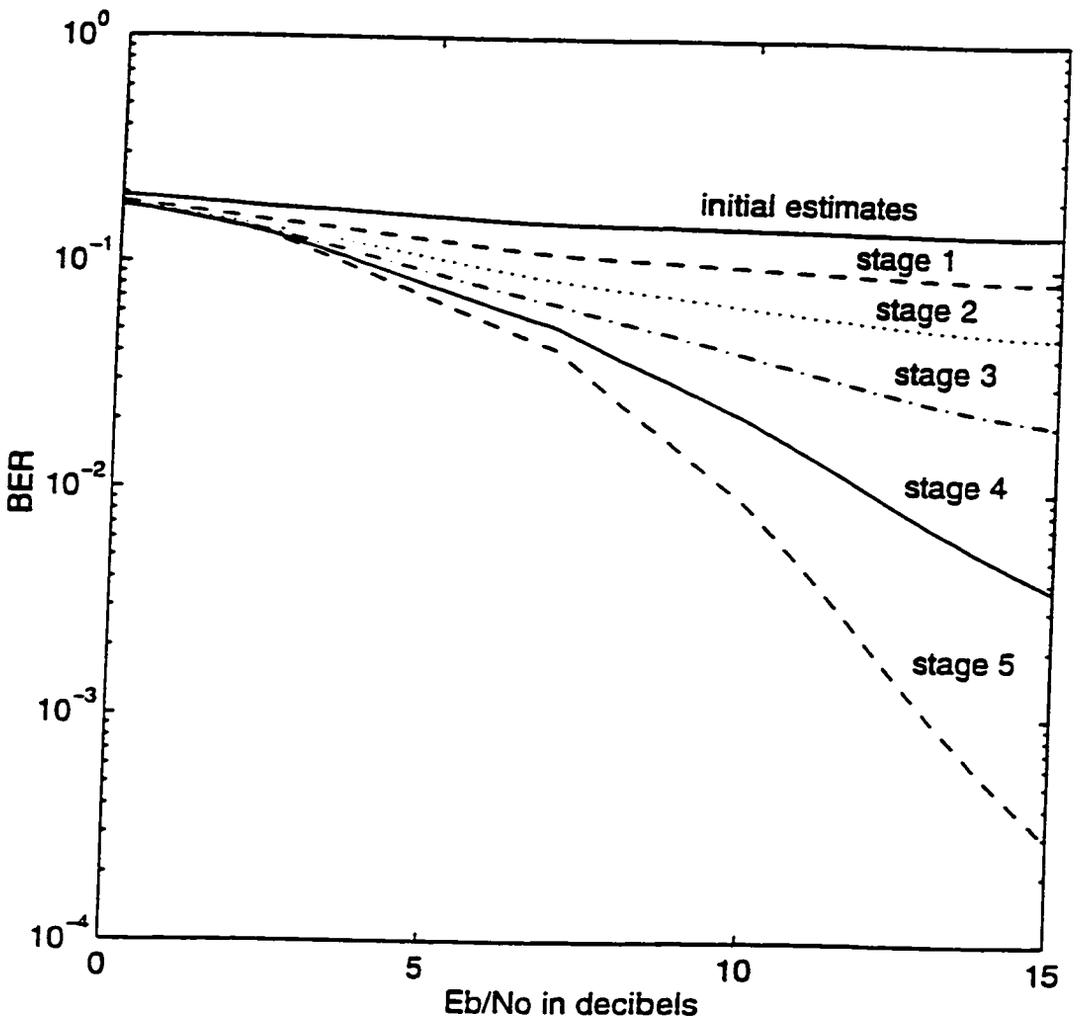

Figure 4.12 BER versus $\frac{E_b}{N_o}$ for a CCI canceling CDMA correlator receiver. Imperfect power control scheme resulting in 1 dB variance in normalized received power; MSE in channel estimation = 0.001 and standard deviation of normalized error in code phase estimate of 0.01 at all stages; $K = 16$; $\bar{L} = 3$; $N = 31$.

code phase estimate error. To keep the performance within acceptable limits, in the presence of a combination of these imperfections, the channel estimation and the code phase estimation have to be repeated after each stage of CCI cancellation.

5. Effect of System Imperfections on the Performance of a CDMA Receiver with CCI Cancellation and Multipath Diversity Combining

5.1 Introduction

As stated in Chapter 3, a multipath combining RAKE receiver has better performance than a single path correlator receiver in an indoor multipath environment. CCI regeneration and cancellation can be used to improve performance of the RAKE receiver even further. The CCI cancellation method is specially suited to multipath combining receivers because channel parameter estimation is used even for a single stage RAKE receiver. These channel and spreading code phase estimates can be used to regenerate CCI which is subsequently canceled from the received signal.

In this chapter, analysis is done on the BER performance of a multipath combining CDMA receiver that employs a cascade of CCI cancelers. The transmitter and channel model used for the analysis is the same as that described in Chapter 3. The principle of the CCI canceling RAKE receiver is explained in Section 5.2. Analysis of data estimates with imperfections in power control, channel estimates and spreading code phase estimates is presented in Section 5.3. It is followed by BER

analysis in Section 5.4 and numerical results in Section 5.5. Results are summarized in Section 5.6.

5.2 Multipath Combining CDMA Receiver with CCI Cancellation

The in-phase and quadrature down converted, and low-pass filtered signals for the desired user i were derived in Section 3.3.1. The equation for in-phase component is repeated below.

$$\begin{aligned} r_I(t) &= \sqrt{\frac{P_i}{2}} \sum_{\lambda=1}^{L_i} g_I(i,\lambda) u_i(t-\tau_{i,\lambda}) + \\ &\quad \sum_{k=1,k\neq i}^{K} \sum_{\lambda=1}^{L_k} \sqrt{\frac{P_k}{2}} g_I(k,\lambda) u_k(t-\tau_{k,\lambda}) + n_I(t). \end{aligned} \tag{5.1}$$

The quantities, $g_I(k,\lambda)$ and $n_I(t)$ have been defined previously. The quadrature signal $r_Q(t)$ is obtained by setting I to Q in Equation (5.1). The first term in (5.1) is the desired signal for the ith user. As before, the second term in Equation (5.1) corresponds to the multiple access interference and the third term is due to the additive white Gaussian noise. The canceler creates a replica of the CCI to user i represented by the second term of Equation (5.1). This is done using initial estimates of data, channel parameters and spreading code phases of all interfering users and then subtracting them from the down converted received signals $r_I(t)$ and $r_Q(t)$ continuously in time. The schematic for obtaining initial data estimates for each user and CCI regeneration is shown in Figure 5.1. The initial data estimate is obtained in a similar manner as described in Section 3.3.1 using Matched Filter

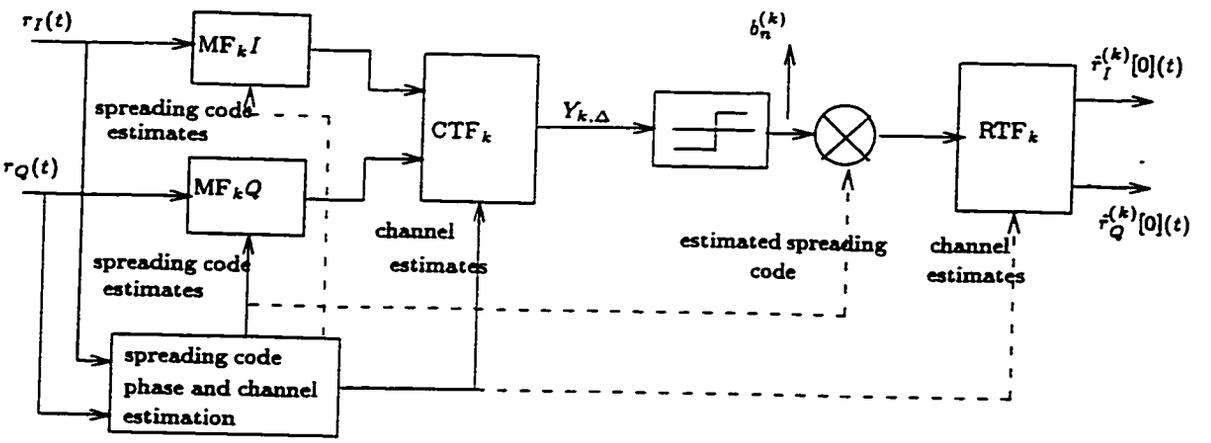

Figure 5.1 The data demodulation and CCI regeneration in the preliminary stage of a CCI canceling RAKE receiver. A similar unit is required for all the users of CDMA system.

(MF) and Combining Transversal filter (CTF) as shown in Figure 5.1. This data estimate is re-spread using the estimated spreading code. The channel emulation required for CCI regeneration is realized by using a Regenerating Transversal Filter (RTF), shown in detail in Figure 5.2. The impulse response of the RTF is the same as that of the channel. The regenerated interference components are summed up and then subtracted from a delayed version of the down converted received signals $r_I(t)$ and $r_Q(t)$ continuously in time (Figure 5.3). By repeating this operation, a cascade of CCI cancelers and diversity combiners is derived (Figure 5.4).

In the next section, analysis is done on the effect of imperfect power control, channel estimation and spreading code phase estimation on the data estimates of a diversity combining receiver with CCI cancellation. The modeling of these imper-

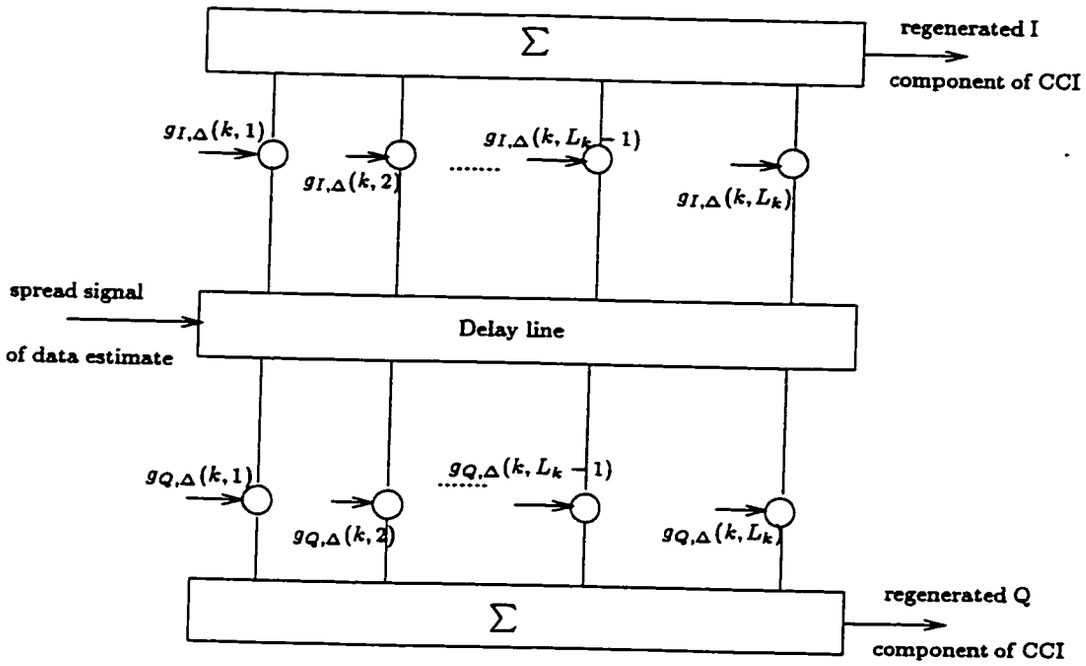

Figure 5.2 Multipath channel emulator using RTF.

fections are the same as described previously in Section 3.3.1.

5.3 Analysis of Data Estimates

The data estimate of the ith user's nth symbol in the preliminary data decision stage has been derived in Section 3.3.2 as

$$b_n^{(i)}[0] = \text{sgn}(Y_{i,\Delta}). \tag{5.2}$$

where $Y_{i,\Delta}$ is the pre-cancellation combiner output. As in Chapter 4, the zero in the square bracket indicates that the data estimate is from a stage before CCI cancellation. Initial data estimates $\{b_n^{(k)}[0]\}$ for all users can be obtained in a similar

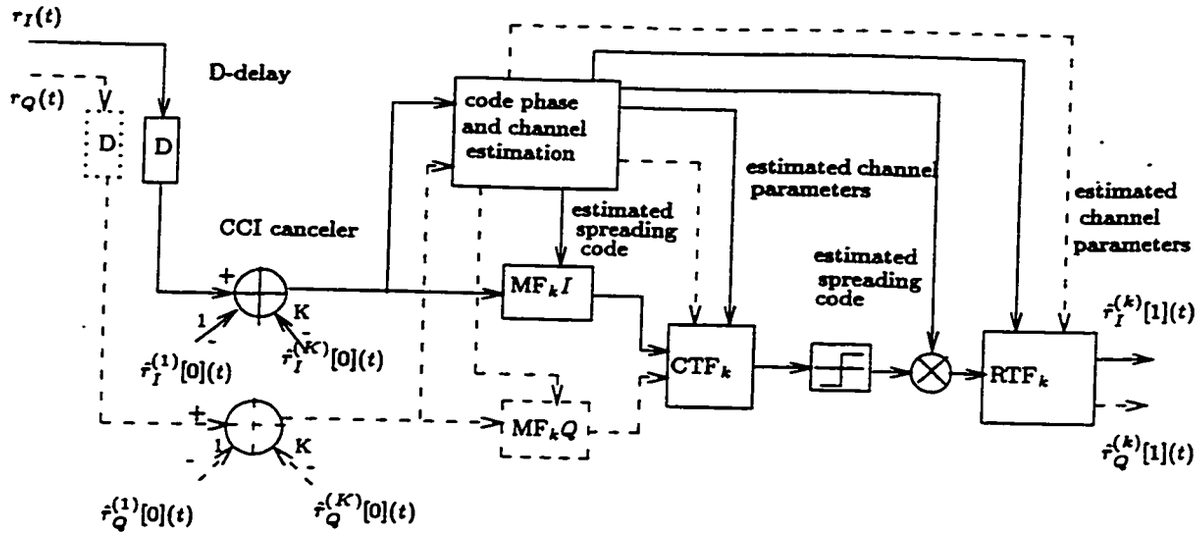

Figure 5.3 First stage of CCI cancellation and subsequent regeneration of CCI using improved data and channel estimates.

manner. These are then used to form their corresponding data signal set $\{\hat{b}_n^{(k)}[0](t)\}$. Then for $k \neq i$, the initial data estimates are re-spread using estimated spreading codes. These spread data estimates are passed through RTF_k which emulates the channel characteristics of the kth user as shown in Figure 5.2. In the presence of estimation errors, the tap weights of RTF_k are represented by $g_{I,\Delta}(k,\lambda) = (g_{k,\lambda} + \Delta g_{k,\lambda})\cos(\phi_{k,\lambda} + \Delta\phi_{k,\lambda})$ and $g_{Q,\Delta}(k,\lambda) = (g_{k,\lambda} + \Delta g_{k,\lambda})\sin(-\phi_{k,\lambda} - \Delta\phi_{k,\lambda})$ respectively for the I and Q parts. The error in the spreading code phase results in an error in path delay estimates. This results in tap positions at $\hat{\tau}_{k,\lambda}$ instead of at $\tau_{k,\lambda}$. As explained in Chapter 4, during the detection of the nth symbol, the CCI cancellation can be done on the $l = (n-2)$th symbol only due to the asynchronous nature of user transmissions. By adding all the interfering signals of the other $K-1$

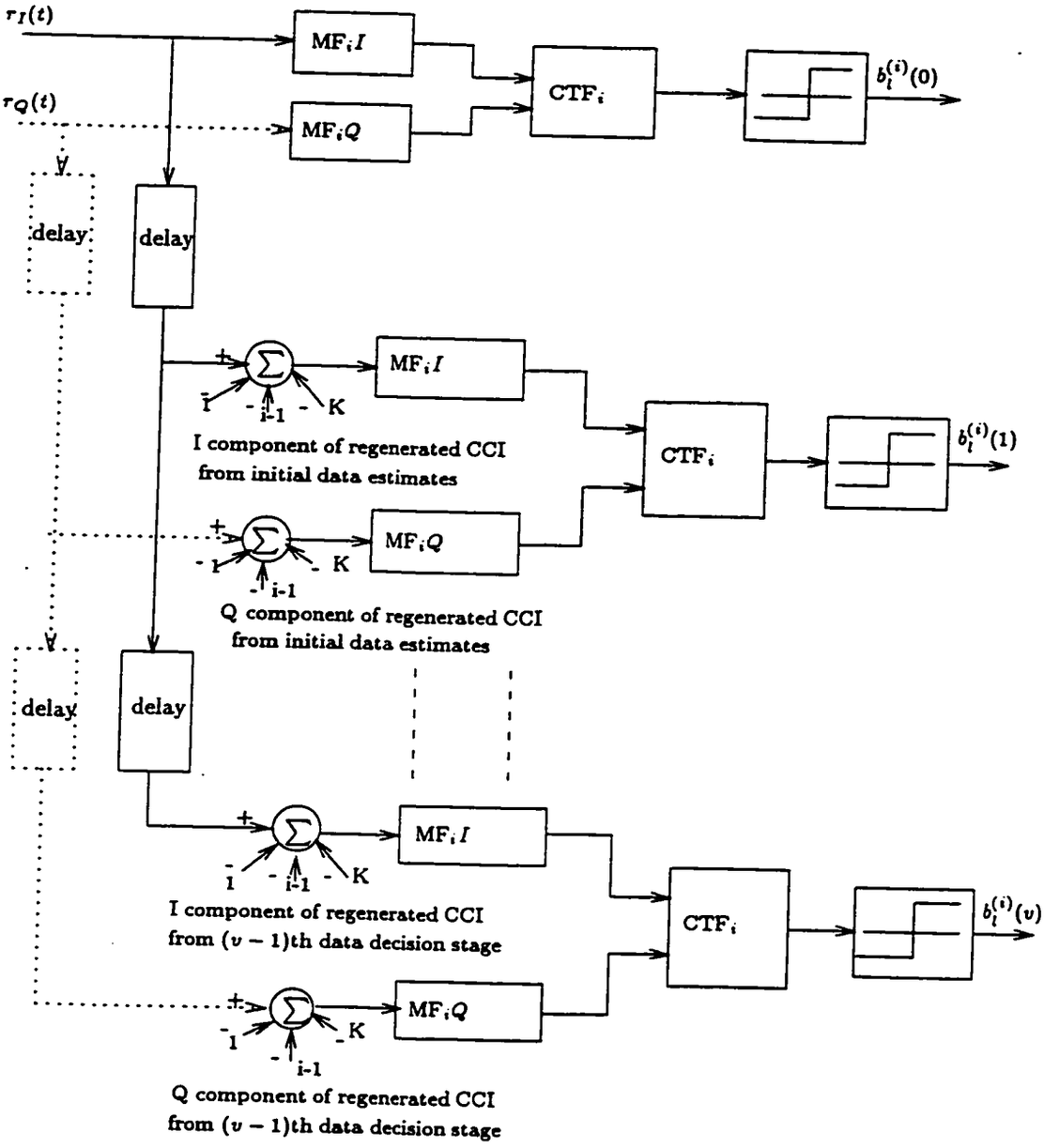

Figure 5.4 Multipath combining RAKE receiver with cascaded CCI canceler stages.

users, a replica of user i's in-phase CCI that occurred $2T_b$ earlier can be obtained as

$$\hat{r}_I^{(i)}[0](t) = \sum_{k=1,k\neq i}^{K} \sum_{\lambda=1}^{L_k} \sqrt{\frac{P_k}{2}} g_{I,\Delta}(k,\lambda) b_k[0](t - 2T_b - \hat{\tau}_{k,\lambda}) a_k(t - \hat{\tau}_{k,\lambda}). \tag{5.3}$$

Similarly, the Q component can be obtained from Equation (5.3) by replacing I with Q. The spreading signal being periodic with a period of T_b, $a_k(t+nT_b) = a_k(t)$. This regenerated CCI is subtracted from a two symbol delayed, down converted received signal. The I component of the CCI canceled received signal after the first stage of cancellation is given by

$$\begin{aligned}
\tilde{r}_I^{(i)}[1](t) &= r_I(t - 2T_b) - \hat{r}_I^{(i)}[0](t) \\
&= \sqrt{\frac{P_i}{2}} \sum_{\lambda=1}^{L_i} g_I(i,\lambda) b_i(t - 2T_b - \tau_{i,\lambda}) a_i(t - \tau_{i,\lambda}) + \\
&\quad \sum_{k=1,k\neq i}^{K} \sum_{\lambda=1}^{L_k} \sqrt{\frac{P_k}{2}} g_I(k,\lambda) b_k(t - 2T_b - \tau_{k,\lambda}) a_k(t - \tau_{k,\lambda}) - \\
&\quad \sum_{k=1,k\neq i}^{K} \sum_{\lambda=1}^{L_k} \sqrt{\frac{P_k}{2}} g_{I,\Delta}(k,\lambda) b_k[0](t - 2T_b - \hat{\tau}_{k,\lambda}) a_k(t - \hat{\tau}_{k,\lambda}) + \\
&\quad n_I(t - 2T_b).
\end{aligned} \tag{5.4}$$

The corresponding $\tilde{r}_Q^{(i)}[1](t)$ can be obtained by setting I to Q in Equation (5.4). These signals are passed through the second set of matched filters. The CTF output is obtained by convolution of the matched filter output with the impulse response of the second multipath combiner. This combiner output is given by

$$Y_{i,\Delta}[1] = D_i + D_\Delta + F_{i,\Delta} + I_{i,\Delta}[1] + N_{i,\Delta}. \tag{5.5}$$

A comparison of Equation (5.5) with the pre-cancellation combiner output, $Y_{i,\Delta}$ in Equation (3.71) shows that the multi-user interference term, $I_{i,\Delta}$ is different. The multi-user interference term after one stage of interference cancellation, $I_{i,\Delta}[1]$, in Equation (5.5) may be written as

$$I_{i,\Delta}[1] = \sum_{k=1,k\neq i}^{K} \sum_{\alpha=1}^{L_i} \sum_{\lambda=1}^{L_k} \{y(i,k,\alpha,\lambda) - \hat{y}(i,k,\alpha,\lambda,1)\}. \tag{5.6}$$

The notations, $y(i,k,\alpha,\lambda)$ and $\hat{y}(i,k,\alpha,\lambda,1)$ used in Equation (5.6) are given by

$$y(i,k,\alpha,\lambda) = \sqrt{\frac{P_k}{2}} g_{k,\lambda}\hat{g}_{i,\alpha}\cos(\phi_{k,\lambda} - \hat{\phi}_{i,\alpha})[b^{(k)}_{n-m-1}R_{k,i}(\tau) + b^{(k)}_{n-m}\hat{R}_{k,i}(\tau)] \tag{5.7}$$

and

$$\hat{y}(i,k,\alpha,\lambda,1) = \sqrt{\frac{P_k}{2}}\hat{g}_{k,\lambda}\hat{g}_{i,\alpha}\cos(\hat{\phi}_{k,\lambda} - \hat{\phi}_{i,\alpha})\left[b^{(k)}_{n-m'-1}[0]R_{k,i}(\tau') + b^{(k)}_{n-m'}[0]\hat{R}_{k,i}(\tau')\right]. \tag{5.8}$$

The quantities m and τ in Equation (5.7) are used to define the relative number of bit shifts and delay respectively, as previously discussed in Section 3.3.2. The new notations, m' and τ' have been introduced in Equation (5.8). This is done to include the effect of path delay estimation errors. They are given by

$$m' = m'(i,k,\alpha,\lambda) = \lfloor \frac{\hat{\tau}_{i,\alpha} - \hat{\tau}_{k,\lambda}}{T_b} \rfloor \tag{5.9}$$

and

$$\tau' = \tau'(i,k,\alpha,\lambda) = (\hat{\tau}_{i,\alpha} - \hat{\tau}_{k,\lambda}) - m'T_b. \tag{5.10}$$

A hard decision on the combiner output $Y_{i,\Delta}[1]$ provides a data estimate of ith user's nth symbol as

$$b_n^{(i)}[1] = \mathrm{sgn}(Y_{i,\Delta}[1]). \tag{5.11}$$

Extending the analysis to the case of v stages of CCI cancellation is fairly straightforward. The signal at the output of the CTF corresponding to the $l = (n-v-1)$th symbol after v stages of CCI cancellation can be written as

$$Y_{i,\Delta}[v] = D_i + D_\Delta + F_{i,\Delta} + I_{i,\Delta}[v] + N_{i,\Delta}. \tag{5.12}$$

The fourth component of Equation (5.12) is the only new term and is given by

$$I_{i,\Delta}[v] = \sum_{k=1,k\neq i}^{K} \sum_{\alpha=1}^{L_i} \sum_{\lambda=1}^{L_i} \left\{ y(i,k,\alpha,\lambda) - \hat{y}(i,k,\alpha,\lambda,v) \right\}, \tag{5.13}$$

where

$$\begin{aligned} \hat{y}(i,k,\alpha,\lambda,v) &= \sqrt{\frac{P_k}{2}} \hat{g}_{k,\lambda} \hat{g}_{i,\alpha} \cos(\hat{\phi}_{k,\lambda} - \hat{\phi}_{i,\alpha}). \\ &\quad \left[b_{n-m'-1}^{(k)}[v-1]\, R_{k,i}(\tau') + b_{n-m'}^{(k)}[v-1]\, \hat{R}_{k,i}(\tau') \right]. \end{aligned} \tag{5.14}$$

A hard decision on the combiner output $Y_{i,\Delta}[v]$ provides a data estimate of the ith user's nth symbol as

$$b_n^{(i)}[v] = \mathrm{sgn}(Y_{i,\Delta}[v]). \tag{5.15}$$

The BER of the data estimates obtained after CCI cancellation is next derived using a standard Gaussian approximation.

5.4 BER Analysis

The method for BER analysis of pre-cancellation data estimates has already been developed in Section 3.3.3. With CCI cancellation, only the variance of the CCI component of the output decision variable is changed. For a single stage of CCI cancellation, the output of the combiner, $Y_{i,\Delta}[1]$ is given in Equation (5.5). It may be noted that $Y_{i,\Delta}[1]$ differs from the pre-cancellation combiner output $Y_{i,\Delta}$ only in the CCI term $I_{i,\Delta}$. It is also seen that $I_{i,\Delta}[1]$ is a zero mean random variable. Therefore, by taking the expectation of the square of the terms in Equation (5.6) and using the fact that the random variables involved in the expectation are mutually independent, the variance of the CCI term $I_{i,\Delta}[1]$ can be determined as

$$\begin{aligned}\mathrm{Var}\left(I_{i,\Delta}[1]\right) = & \sum_{k=1,k\neq i}^{K} \frac{1}{4}\bar{L}_k^2 E\left\{P_k\right\}\Big[G(G+\sigma_{\Delta_g}^2)E\left\{R_{k,i}^2(\tau)+\hat{R}_{k,i}^2(\tau)\right\}+ \\ & (G+\sigma_{\Delta_g}^2)^2 E\left\{R_{k,i}^2(\tau')+\hat{R}_{k,i}^2(\tau')\right\}- \\ & 2G(G+\sigma_{\Delta_g}^2)\exp(\frac{-\sigma_{\Delta_\phi}^2}{2})(1-2p_{e,\Delta}^{(k)}[0]). \\ & E\left\{R_{k,i}(\tau)R_{k,i}(\tau')+\hat{R}_{k,i}(\tau)\hat{R}_{k,i}(\tau')\right\}\Big]. \end{aligned} \tag{5.16}$$

The facts that $E\{[b_l^{(k)}]^2\}=1$, and $E\{b_l^{(k)}b_l^{(k)}[0]\}=1-2p_e^{(k)}[0]$, where $p_e^{(k)}[0]$ is the kth user's error probability before CCI cancellation, were used to obtain Equation (5.16). Variances $\sigma_{\Delta_{g_{k,\lambda}}}^2=\sigma_{\Delta_g}^2$, $\sigma_{\Delta_{\phi_{k,\lambda}}}^2=\sigma_{\Delta_\phi}^2$ and $E\{g_{k,\lambda}^2\}=G$ for all k and λ. All

the expectation operations in Equation (5.16) can be evaluated by using a procedure similar to that developed in Section 4.4.

The ith user's signal to noise ratio after one stage of CCI cancellation is thus obtained as

$$SNR_{i,\Delta}[1] = \frac{E\{D_i^2\}}{\mathrm{Var}(D_\Delta) + \mathrm{Var}(F_{i,\Delta}) + \mathrm{Var}(I_{i,\Delta}[1]) + \mathrm{Var}(N_{i,\Delta})}. \tag{5.17}$$

The probability of bit error $p_e^{(i)}[1]$ after one stage CCI cancellation may be computed from

$$p_e^{(i)}[1] = Q\left(\sqrt{SNR_{i,\Delta}}[1]\right), \tag{5.18}$$

where the Q function has been defined previously.

With v stages of CCI cancelers and data decisions, the variance of the CCI term $I_{i,\Delta}[v]$ is obtained by recalculating the variance repetitively. This variance is given by

$$\begin{aligned}
\mathrm{Var}\left(I_{i,\Delta}[v]\right) \;=\; & \sum_{k=1,k\neq i}^{K} \frac{1}{4}\bar{L}_k^2 E\{P_k\}\left[G(G+\sigma_{\Delta g}^2)E\left\{R_{k,i}^2(\tau)+\hat{R}_{k,i}^2(\tau)\right\}+\right. \\
& (G+\sigma_{\Delta g}^2)^2 E\left\{R_{k,i}^2(\tau')+\hat{R}_{k,i}^2(\tau')\right\}- \\
& 2G(G+\sigma_{\Delta g}^2)\exp(\frac{-\sigma_{\Delta\phi}^2}{2})(1-2p_{e,\Delta}^{(k)}[v-1]). \\
& \left. E\left\{R_{k,i}(\tau)R_{k,i}(\tau')+\hat{R}_{k,i}(\tau)\hat{R}_{k,i}(\tau')\right\}\right],
\end{aligned} \tag{5.19}$$

where $p_{e,\Delta}^{(k)}[v-1]$ is the BER of the kth user after $(v-1)$ stages of CCI cancellation. The signal to noise ratio after v stages of CCI cancelers can be obtained by substi-

tuting Var $(I_{i,\Delta}[v])$ in place of Var $(I_{i,\Delta}[1])$ in Equation (5.17) and recalculating the expression. The bit error probability $p_e^{(i)}[v]$ after v stages of CCI cancelers can be obtained by recomputing Equation (5.18) with this new value of SNR.

As mentioned in Chapter 4, the error variance of the channel estimates and the code phase estimates decreases in the subsequent RAKE receiver stages because of CCI cancellation. To obtain this variance reduction, channel estimation and code phase estimation must be performed after each stage of CCI cancellation. It is reasonable to assume that interference cancellation at the $(j+1)$ th stage reduces the CCI from $(1-p_e^{(k)}[j])$ times the number of users, $p_e^{(k)}[j]$ being the BER after the jth cancellation stage. One way to calculate the reduction in the variance of estimate errors after j, $1 \leq j \leq v$ stages of CCI cancellation is to multiply the variances by $2p_e^{(k)}[j]$. The factor 2 is used because the cancellation of the CCI generated from incorrect data signal estimates doubles the corresponding CCI.

5.5 Numerical Results

Performance results are computed for an indoor CDMA system with parameter values described in Section 3.2.4. Results are presented for various combinations of factors. The BER performance under perfect conditions is given in Figure 5.5. The individual effect of various system imperfections on BER performance is shown in Figures 5.6 - 5.9. Their combined effect is presented in Figure 5.10. In these figures the spreading code period, $N = 31$ and the number of users, $K = 16$. Under perfect conditions, approximately single user BER performance can be obtained using one

stage of CCI cancellation (Figure 5.5). This improvement is much the same as that reported in [24]. This implies significant savings in hardware compared to the use of a CCI canceling correlator receiver. Figure 5.6 is a plot of BER versus $\frac{E_T}{N_o}$ for up to two stages of CCI cancellation in the presence of power control imperfections resulting in 2 dB variance in the normalized received power. It is assumed that there are no channel estimate errors and spreading code phase estimate errors. As shown in Figure 5.6, the single user BER performance is obtained with two stages of cancellation.

The effect of channel estimate error on BER performance is shown in Figures 5.7 and 5.8. It is assumed in both cases that there are perfect power control and spreading code phase estimations. The BER performance when MSE in channel estimates is constant at 0.01 at all stages is shown in Figure 5.7. Single user BER performance cannot be realized by increasing the number of canceler stages. This is due to the increase in the noise floor level because of channel estimation error. The BER performance with channel estimation repeated after each CCI cancellation stage is shown in Figure 5.8. A MSE of 0.1 is assumed in the preliminary stage of the receiver. In this situation, single user BER performance can be achieved with two stages of CCI cancelers. The effect of the spreading code phase estimate error on the BER performance is illustrated in Figure 5.9. To arrive at this result, perfect power control and channel estimation are assumed. The standard deviation of the normalized code phase estimate error is constant at 0.1 in all stages of the receiver. When there are no errors in power control and channel estimates, a standard

deviation value of 0.1 can be tolerated by such receivers (Figure 5.9).

The BER performance when all three imperfections are present is shown in Figure 5.10. It is shown in this figure that CCI cancellation does not improve BER appreciably when the variance of the normalized received power is 2 dB, MSE in channel estimates is 0.01, and standard deviation of normalized error in spreading code phase estimates is 0.1. For CCI cancellation to be effective when a combination of system imperfections is present, the power control imperfections and estimates imperfections must be minimized below these values. An alternate method is to repeat channel estimation and code phase estimation after each stage of CCI cancellation.

5.6 Summary

Analysis was done on the performance of a CCI canceling spread spectrum multiaccess RAKE receiver with imperfections in power control, spreading code phase, and channel estimation. It is clear from the analysis and numerical results presented in this chapter that with perfect conditions the CCI cancellation technique employed with RAKE receivers can provide significant improvement in BER and capacity with just one stage of CCI canceler. Such receivers can tolerate 2 dB variance in the normalized received power, or 0.01 MSE in the channel estimates, or 0.1 standard deviation in the normalized code phase estimates error. The BER performance degrades significantly when a combination of estimate errors is present with 2 dB imperfections in power control. To keep the performance of such receivers within an

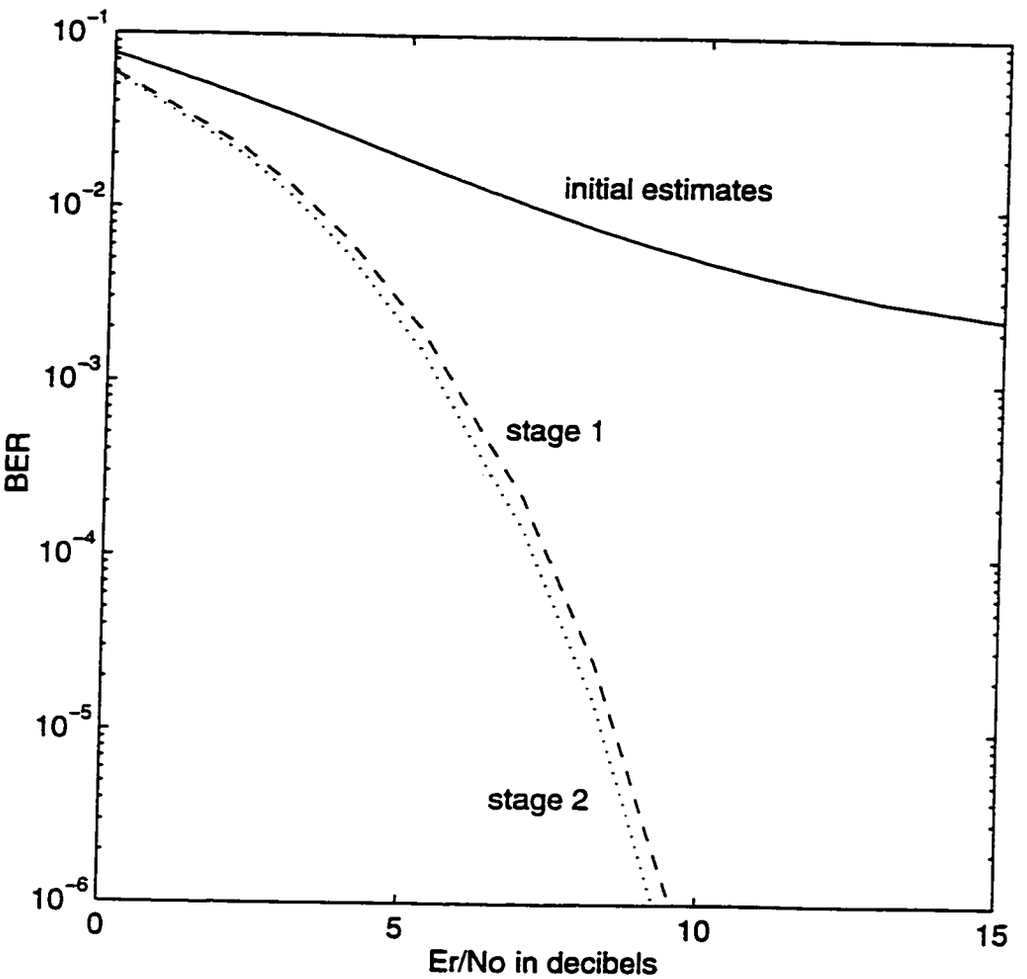

Figure 5.5 BER versus $\frac{E_r}{No}$ for a CCI canceling CDMA RAKE receiver. Perfect conditions; $K = 16$; $\bar{L} = 3$; $N = 31$.

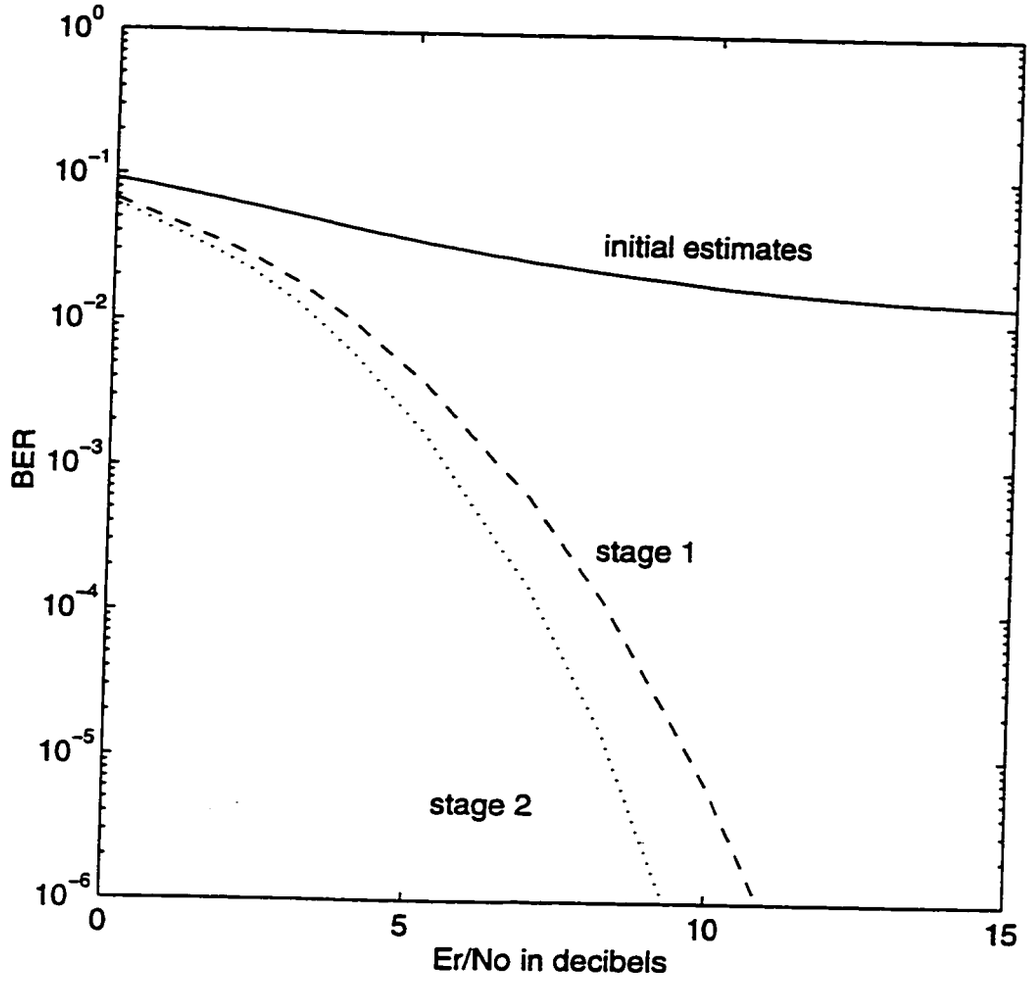

Figure 5.6 BER versus $\frac{E_r}{No}$ for a CCI canceling CDMA RAKE receiver. 2 dB variance in normalized received power; no channel parameter estimation error; no spreading phase error; $K = 16$; $\bar{L} = 3$; $N = 31$.

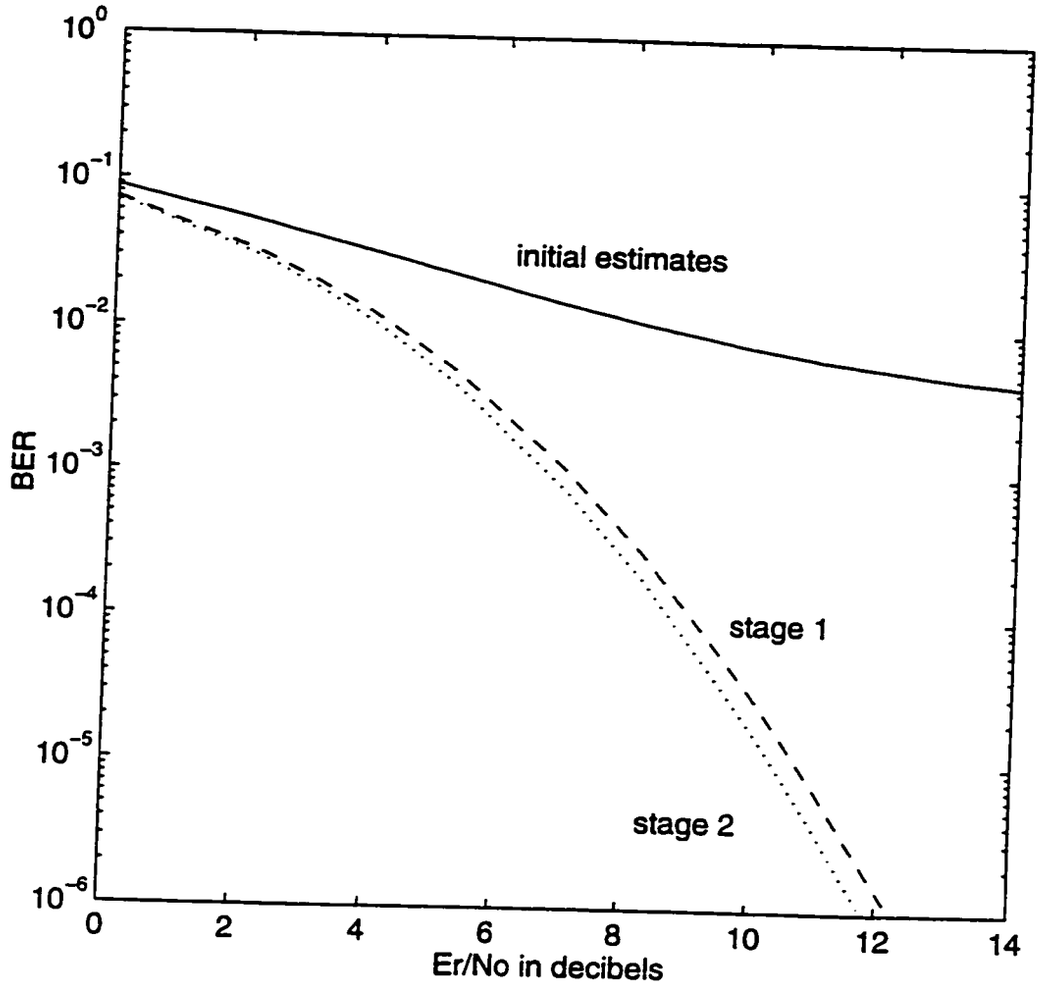

Figure 5.7 BER versus $\frac{E_r}{No}$ for a CCI canceling CDMA RAKE receiver. Perfect power control scheme; no spreading code phase error; MSE in channel estimation of 0.01 at all stages of the receiver; $K = 16$; $\bar{L} = 3$; $N = 31$.

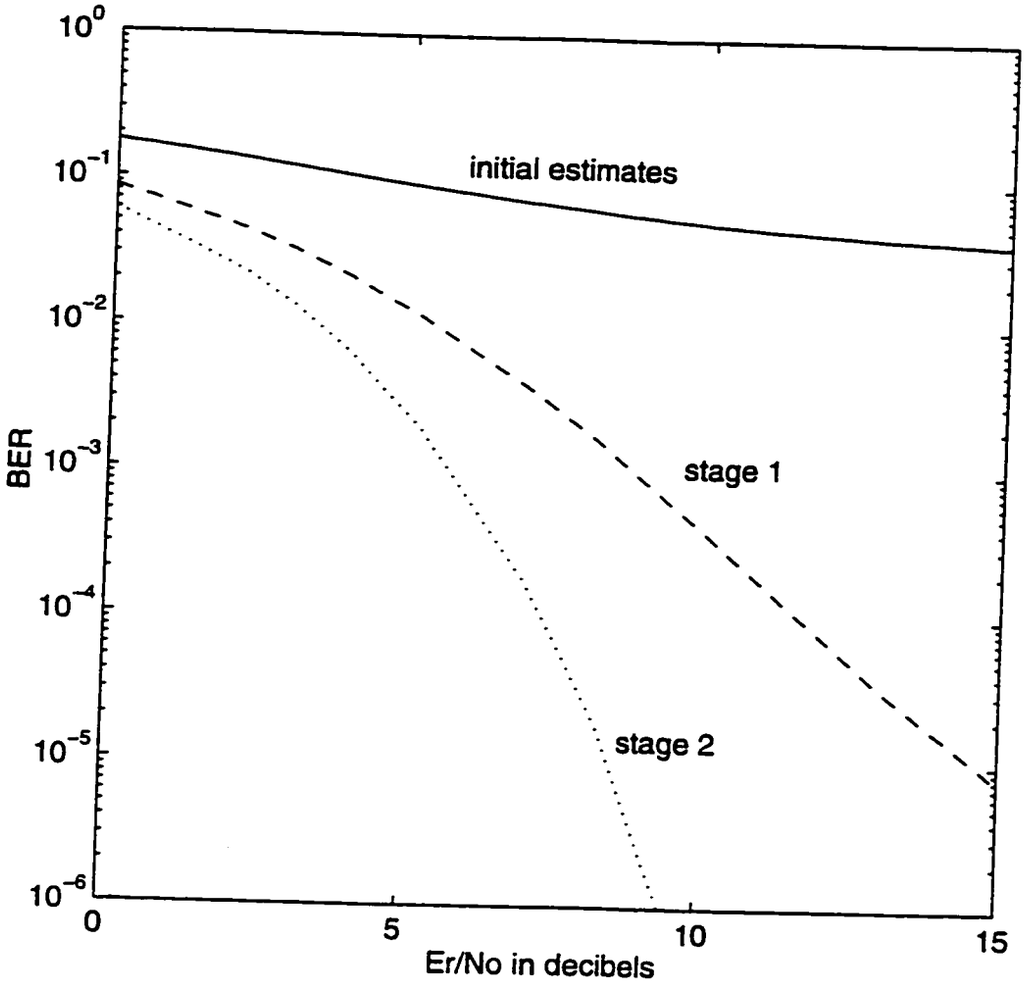

Figure 5.8 BER versus $\frac{E_r}{No}$ for a CCI canceling CDMA RAKE receiver. Perfect power control scheme; no spreading code phase error; MSE in channel estimation of 0.1 at initial stage, decreasing proportional to BER of previous stage in the successive cancellation stages; $K = 16$; $\bar{L} = 3$; $N = 31$.

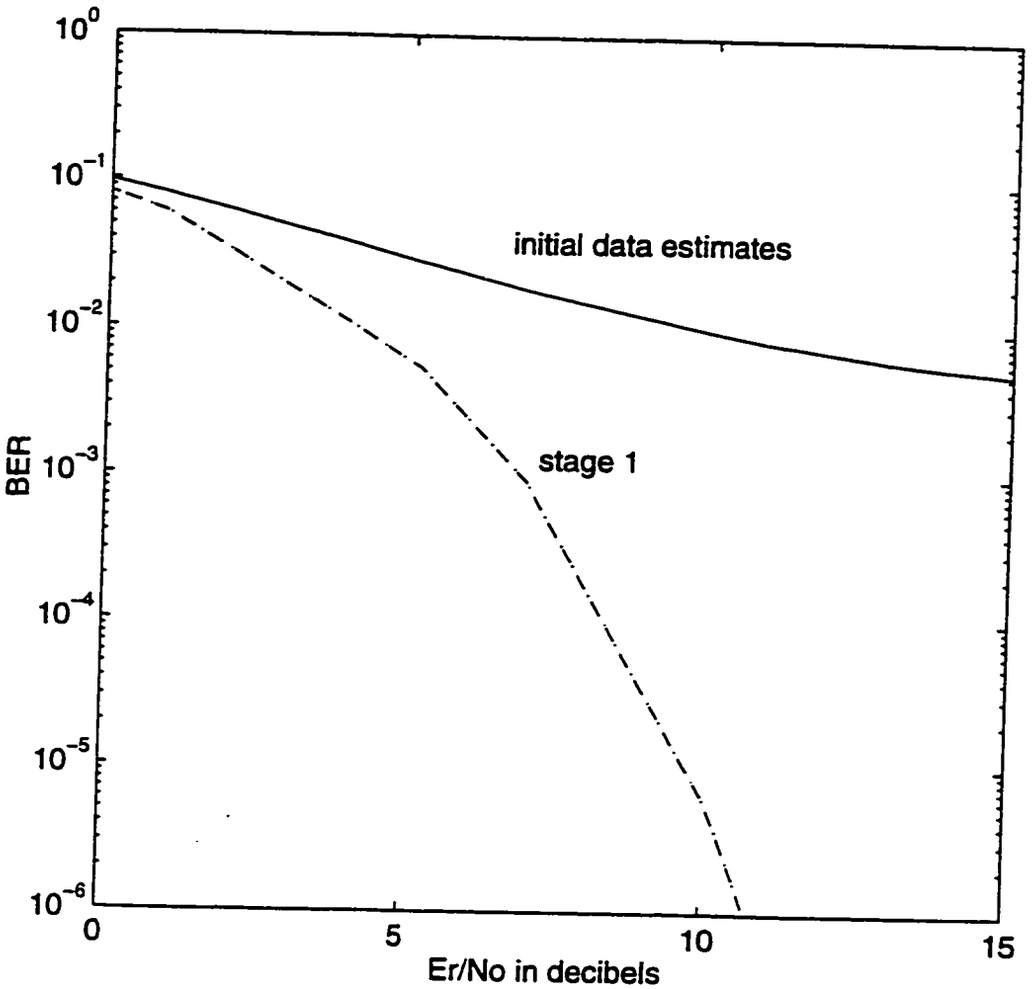

Figure 5.9 BER versus $\frac{E_r}{No}$ for a CCI canceling CDMA RAKE receiver. Perfect power control scheme; no channel estimation error; standard deviation of normalized error in code phase estimates is 0.01 at all stages; $K = 16$; $\bar{L} = 3$; $N = 31$.

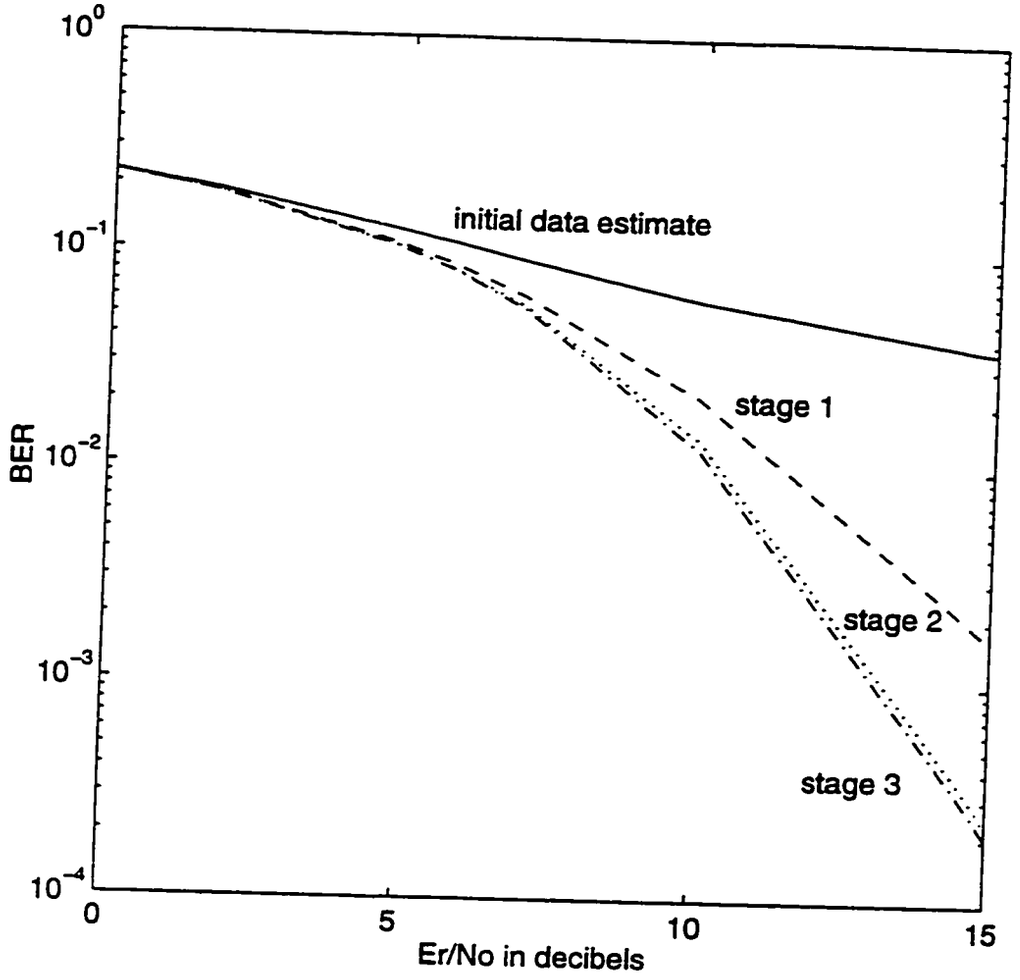

Figure 5.10 BER versus $\frac{E_r}{No}$ for a CCI canceling CDMA RAKE receiver. Imperfect power control scheme resulting in 2 dB variance in normalized received power; MSE in channel estimation = 0.01 and standard deviation of normalized error in code phase estimates is 0.1 at all stages; $K = 16$; $\bar{L} = 3$; $N = 31$.

acceptable limit in the presence of this level of power control imperfections, channel estimation and code phase estimation has to be repeated after each stage of CCI cancellation. This results in a reduction of MSE in estimates in succeeding stages of cancelers. This restores the effectiveness of CCI cancellation.

6. BER Performance Simulation

Analytical techniques used to predict the BER performance (Chapters 3-5) have the advantage of being computationally efficient. However, approximations were made in the analysis to arrive at closed form expressions. For example, the Gaussian approximation was used to model multiple access interference. It is a common practice to evaluate performance by computer simulation. Simulation techniques allow one to accurately model complex systems and channels although this results in high computational complexity.

In this chapter, time-domain simulation programs that model and simulate the baseband indoor CDMA system are developed using MATLAB simulation software. These programs are used to predict the BER performance of CDMA receiver structures analyzed theoretically and reported in previous chapters. The system imperfections are appropriately modeled and included in the simulation program for performance evaluation. Simulation results are then compared to analytical results and the validity of approximations used in the analysis is examined.

6.1 Methods of BER Estimation in Simulation

A number of distinct techniques are commonly used to estimate BER in simulation [25]-[31]. Two techniques used for BER estimate of indoor CDMA receivers are

the Monte Carlo (MC) method and the modified MC based on Importance Sampling (IS). A brief introduction to these techniques is given below.

In AWGN channels, when equally likely binary symbols are transmitted, the symbol error probability p is given by

$$p = \int_{V_T}^{\infty} f(v)dv, \tag{6.1}$$

where $f(v)$ is the conditional density function of the decision variable given -1 was transmitted, and V_T is the threshold level for symbol decision. Equation (6.1) may be rewritten as

$$\begin{aligned} p &= \int_{-\infty}^{\infty} h(v)f(v)dv \\ &= E\{h(v)\}, \end{aligned} \tag{6.2}$$

where

$$h(v) = \begin{cases} 1 & v \geq V_T \\ 0 & v < V_T. \end{cases} \tag{6.3}$$

A natural MC estimator, $\hat{p}_{MC}$ of p given by Equation (6.2) is the sample mean

$$\hat{p}_{MC} = \frac{1}{N_{MC}} \sum_{i=1}^{N_{MC}} h(v_i), \tag{6.4}$$

where, $v_i = v(t_i)$ and t_i are the symbol spaced instants at which decisions are made. It is clear that $h(v)$ is an error detector and the summation is in effect an error

counter. Equation (6.4) suggests that a suitable empirical basis for estimating BER is to process N_{MC} symbols through the system, to count the number of errors n and obtain an estimate of BER as the sample mean; thus

$$\hat{p}_{MC} = \frac{n}{N_{MC}}. \tag{6.5}$$

In the limit as $N_{MC} \rightarrow \infty$, the estimate $\hat{p}_{MC}$ converges to p. This is referred to as the conventional Monte Carlo (MC) method.

In the case of finite N_{MC}, reliability of the estimator is quantified in terms of confidence intervals. Two numbers h_1 and h_2 which are functions of $\hat{p}_{MC}$ are chosen with the interval $h_1 - h_2$ as small as possible, so that with high probability, $h_2 \leq p \leq h_1$. Specifically

$$\text{Prob}[h_2 \leq p \leq h_1] = 1 - \alpha, \tag{6.6}$$

where, $h_1 - h_2$ is the confidence interval and $1 - \alpha$ is the confidence level. Two other qualities of the BER estimator are its bias and variance. The BER estimator is unbiased if $E\{\hat{p}_{MC}\} = p$. The MC estimate of BER is unbiased and $\sigma^2(\hat{p}_{MC}) = \frac{p(1-p)}{N_{MC}}$, where $\sigma^2(\hat{p}_{MC})$ is its variance [25].

At 0.95 confidence level, a symbol size $N_{MC} = \frac{10}{p}$ provides a confidence interval of $[1.8\ \hat{p}_{MC}, 0.55\ \hat{p}_{MC}]$ which has an uncertainity factor of approximately 2 in the BER. If $N_{MC} = \frac{100}{p}$, then at a confidence level of 0.95, the confidence interval is narrower in $[1.25\ \hat{p}_{MC}, 0.8\ \hat{p}_{MC}]$. This implies processing of 10^8 symbols to obtain a BER of

10^{-6}. Thus there is a trade-off between run time and the statistical variability.

6.1.1 Importance Sampling

The MC method is inefficient at very low values of BER. In a modified version of MC simulation, realized through importance sampling (IS), the "important" events in BER simulation (creation of symbol errors) are generated frequently. This is often done through a deliberate distortion, called biasing, of the statistics of the underlying error creation processes [25]-[29]. Finally the error count is properly unbiased.

The idea behind IS may be illustrated by rewriting Equation (6.2) in an equivalent form

$$\begin{aligned} p &= \int_{-\infty}^{\infty} h(v)\frac{f(v)}{f^*(v)}f^*(v)dv \\ &= \int_{-\infty}^{\infty} h^*(v)f^*(v)dv \\ &= E_*\{h^*(v)\}, \end{aligned} \tag{6.7}$$

where $f^*(v)$ is the biased density function such that the variance of the BER estimator is reduced. Symbol E_* is used to indicate that the expectation is with respect to $f^*(v)$. The ratio $\frac{f(v)}{f^*(v)} = W(v)$ is called the weight and the inverse $B(v) = W^{-1}(v)$ is the bias at v. As mentioned before, a natural estimator of the expectation is the

sample mean defined as

$$\begin{aligned} \hat{p}_{IS} &= \frac{1}{N_{IS}} \sum_{i=1}^{N_{IS}} h^*(v_i) \\ &= \frac{1}{N_{IS}} \sum_{i=1}^{N_{IS}} H(v_i) W(v_i). \end{aligned} \tag{6.8}$$

The functions of $H(v_i)$ and $h(v)$ are identical, but $H(v_i)$ is the error detector with $f^*(v)$ the governing density function. The quantity $W(v_i)$ is the weight of the noise sample in the ith symbol duration.

The IS BER estimator $\hat{p}_{IS}$ is unbiased and the variance $\sigma^2(\hat{p}_{IS})$ of the IS estimator is given by [25]

$$\sigma^2(\hat{p}_{IS}) = \frac{1}{N_{IS}} \int_{V_T}^{\infty} f(v)[W(v) - p]dv, \tag{6.9}$$

where V_T is the threshold voltage of symbol decision. From Equation (6.9) it is seen that the variance of the IS estimator $\sigma^2(\hat{p}_{IS})$ can be reduced to zero if $W(v) = p$ for $v \geq V_T$. In practice, this is not possible because p is an unknown quantity. The MC estimator variance is given by [25]

$$\begin{aligned} \sigma^2(\hat{p}_{MC}) &= \frac{p(1-p)}{N_{MC}} \\ &= \frac{1}{N_{MC}} \int_{V_T}^{\infty} f(v)[1-p]dv. \end{aligned} \tag{6.10}$$

A comparison of Equations (6.9) and (6.10) shows that any weighting $[W(v) - p]$ which is less than $(1-p) \approx 1$ (for $v \geq V_T$) will reduce the value of the integral in Equation (6.9), so that for $N_{MC} = N_{IS}$, the IS estimator variance will be reduced.

Putting this in a different perspective, for a given estimator variance, the ratio $\frac{N_{MC}}{N_{IS}}$ denotes savings in computation.

The fundamental objective of IS is to select $f^*(v)$ so as to minimize the variance of $\hat{p}_{IS}$ and thus the overall computation burden. It turns out that the optimal sampling density $f^*(v)$ is proportional to $f(v)$. It may be easily shown that $\mathrm{Var}(\hat{p}_{IS}) = 0$ if the normalization $f^*(v) = f(v)h(v)/p$ is used. Unfortunately, this unconstrained optimal solution is not practical because it assumes knowledge of the unknown parameter, p. However, it indicates features necessary for good IS densities. A good biasing density should concentrate its probability mass where more errors occur.

The method of choosing an appropriate IS density function for BER simulation of CDMA receivers is illustrated below. The bit error event, important in BER simulation, is created mostly by the CCI component of the total noise. A close examination of the equations for the CCI terms derived in Chapters 3 - 5 reveals the magnitude of the CCI terms to be dependent on $\cos\phi$, where ϕ is uniformly distributed in $[0, 2\pi]$ or equivalently, in $[-\pi, \pi]$. The CCI attains its maximum value when ϕ is close to zero. For proper operation, the maximum value of CCI should be less than the desired signal magnitude. A good sampling methodology should force ϕ more often close to zero. This can be achieved, for example, by selecting a biasing model in which ϕ has a Gaussian or Laplacian distribution that is truncated to $[-\pi, \pi]$. As the Gaussian distributed random variable can be easily generated using MATLAB, it was selected as the biasing density for ϕ.

When there are a number of error contributors, as in the case of an indoor CDMA

system, it is important to know whether a given error contributor is to be biased or not. Another issue is biasing of various processes so as to reduce the variance of the BER estimate. Although no optimal solution for this biasing problem has been reported in the literature, not biasing a significant error contributor greatly increases the variance of the estimator [29]. It is also shown that it is better not to bias an error contributor which is not significant.

A combination of MC and IS techniques is used to obtain the BER estimates reported in this chapter. For BER greater than 10^{-3}, MC simulation was used. For lower BER, the IS technique was the preferred method. In some cases, the results obtained by the IS technique were verified by time consuming MC simulations.

6.2 Simulation of Indoor CDMA System with Single Stage Receiver

To simulate an indoor CDMA system, the system constituents have to be simulated. These constituents are multiple DS SS transmitters, indoor channel, and receiver. The low-pass equivalent representation of the system is used in the simulation. The block diagram of the system simulated is shown in Figure 6.1. The system model consists of models for transmitter, channel, and receiver. Simulation is based on picking samples from various probability distributions that model the random processes in a DS/CDMA indoor radio system. This is performed a number of times to obtain BER estimates within a specified confidence interval. In most simulations four samples per spreading code chip are used. However, higher sampling rates are

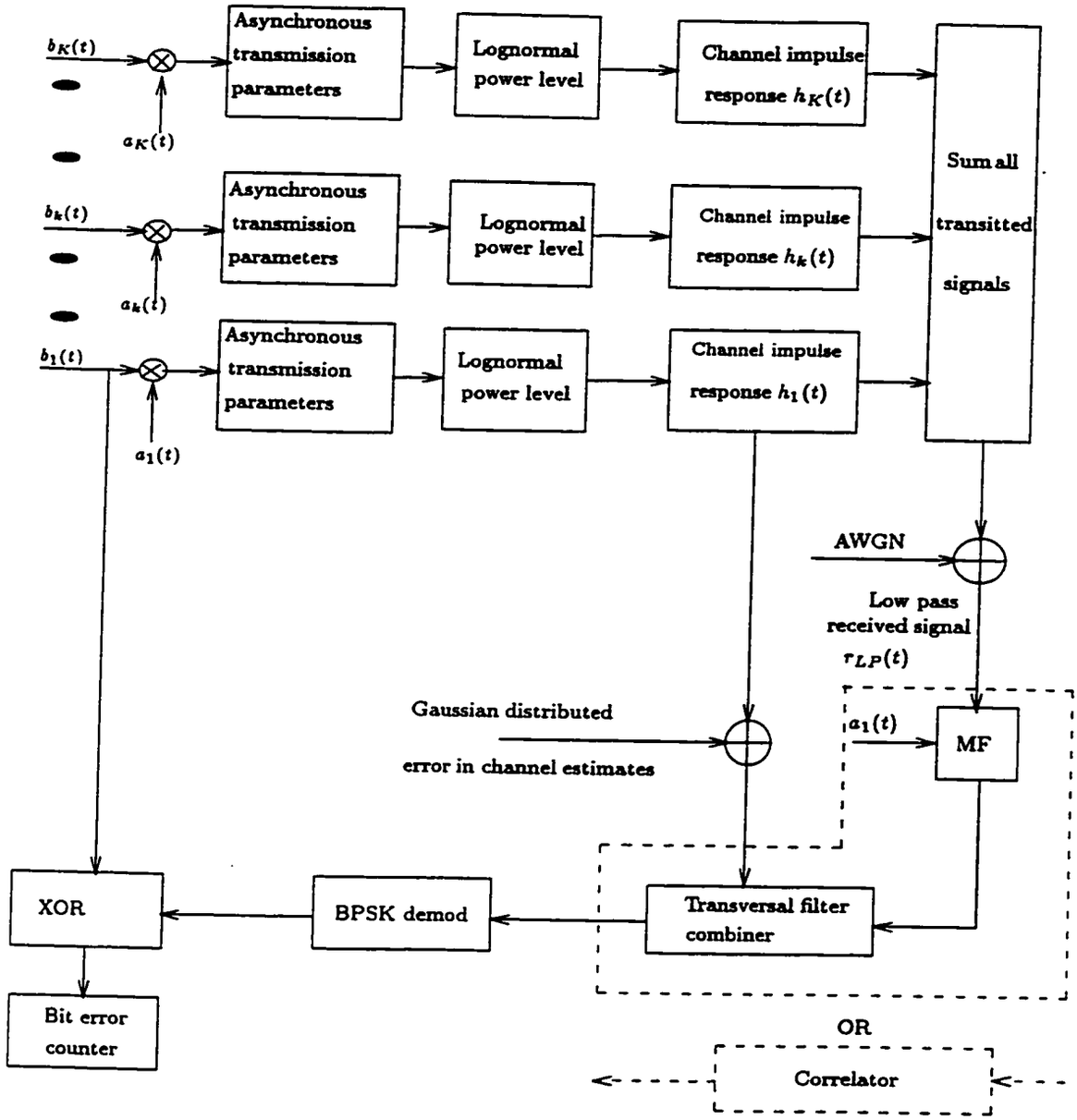

Figure 6.1 Low-pass equivalent of the indoor CDMA system simulated to obtain the BER performance of a single stage CDMA correlator and RAKE receivers.

used to evaluate the effect of spreading code phase estimation error.

6.2.1 System Models for Simulation

In developing the system models for simulation, the following assumptions are made.

- The data bits of the different users are independent.
- The different user transmissions are asynchronous in $[0, T_b]$, where T_b is the data bit duration.
- The multipath amplitudes are uncorrelated Rayleigh random variables and the phases are uniform in $[-\pi, +\pi]$.
- The number of multipaths is three for all users and these paths occupy the first three bins. (This will reduce complexity in the software that tracks the multipaths).
- The multipath amplitudes and phases remain constant for a frame interval of 256 data bits.

Transmitter model

In simulation, the transmitter functions are represented by models for data source, spreading code, asynchronous transmission and power control imperfections. The

data waveform and spreading code waveform of a particular user k, are denoted as

$$b_k(t) = \sum_j b_k^j P_{T_b}(t - jT_b); b_k^j \in \{\pm 1\} \tag{6.11}$$

and

$$a_k(t) = \sum_i a_k^i P_{T_c}(t - iT_c); a_k^i \in \{\pm 1\}, \tag{6.12}$$

respectively; where P_T is a rectangular pulse of unit height and duration T, b_k^j is the jth bit of user k, and a_k^i is the ith chip of the spreading sequence of user k. Each user is assigned a unique spreading code sequence from a family of Gold code sequences of length 31 generated using two maximal length shift register (MLSR) sequences. These MLSR sequences were obtained using two primitive polynomials represented by 45 and 75 in octal. The data bit duration T_b and the spreading code chip duration T_c are related as $T_b = NT_c$, where N is the period of the spreading code. To reduce the simulation time, $N = 31$ was used for all simulation programs. The data transmission rate is 1Mbps, resulting in $T_b = 1$ microsecond. A random variable T_k, uniformly distributed in $\{0, T_b\}$ is used to represent the transmitter delay of the kth user. The MATLAB software has built in functions to generate uniformly distributed and Gaussian distributed random variables. Random variables with other distributions are obtained using other techniques. The imperfection in power control is taken into account by a log-normal distributed random variable to represent the received power level. The term e^X has a log-normal distribution where X is a Gaussian distributed random variable. As the variance of the normalized

received power is specified in dB scale, log-normal distributed variable to base 10 is obtained as 10^X, where X is a Gaussian random variable.

Channel model

The complex low-pass equivalent impulse response of the bandpass channel for the link between the kth user and the base station is written as

$$h_k(t) = \sum_{\lambda=1}^{L} g_{k,\lambda}\delta(t - t_{k,\lambda})e^{j\theta_{k,\lambda}} \tag{6.13}$$

where $g_{k,\lambda}, t_{k,\lambda}$ and $\theta_{k,\lambda}$ are the path amplitude, time delay and phase of the kth user's λth path respectively. Quantity $g_{k,\lambda}$ is a Rayleigh distributed random variable. Quantities $t_{k,\lambda}$, $\theta_{k,\lambda}$ are uniformly distributed in $\{0, \Delta\}$ and $\{0, 2\pi\}$ respectively, where Δ is the delay spread. The Rayleigh distributed path amplitude is generated by the following method.

Let X be a uniformly distributed {0, 1} random variable. An exponentially distributed random variable can be generated as

$$Y = -\ln(X). \tag{6.14}$$

The probability distribution function of Y is then

$$f_Y(y) = \frac{1}{2\sigma^2}\exp(-\frac{y}{2\sigma^2}). \tag{6.15}$$

By taking the square root of Y, a Rayleigh distributed random variable can be generated. Therefore

$$Z = \sqrt{Y} \tag{6.16}$$

has a distribution given as

$$f_Z(z) = \frac{z}{\sigma^2} \exp(-\frac{z^2}{2\sigma^2}), \tag{6.17}$$

with a variance $\sigma^2 = \frac{1}{2}$. This random variable is used to represent the path amplitude.

The number of paths L, is assumed to be the same for all users and is given by

$$L = \lfloor \frac{\Delta}{T_c} \rfloor. \tag{6.18}$$

Channel parameters are changed in every data frame to take into account the time varying nature of the channel.

Receiver models

For a correlator receiver, the low-pass equivalent representation includes a correlator and a data decision stage. The function of the correlator is implemented in the simulation by multiplying the low-pass received signal with a spreading code aligned with the first path signal. This is followed by a summation which is equivalent to integration. The hard decision stage takes a decision on the binary symbol by considering the polarity of the real part of the correlator output signal. This process is

equivalent to BPSK demodulation.

The multipath diversity combining RAKE receiver consists of a filter matched to the specific user's spreading code, a diversity combiner, and a BPSK demodulator. The matched filter is implemented as a bank of correlators with each correlator aligned to a particular path signal. The diversity combiner is implemented as a transversal filter with a number of taps equal to the number of significant paths of the user. Maximal ratio combining is realized by providing weights that are equal to the corresponding path amplitudes at each tap point and then summing the weighted outputs. This is followed by data decision on the combiner output.

To evaluate the performance of the receiver in the presence of imperfections, Gaussian distributed error signals with zero mean are generated. These are added to the path delay, amplitude and phase parameters in the simulation. The variance of the Gaussian distributed error is changed to obtain different levels of imperfections.

6.2.2 Program Structure

Program construction is straightforward and it is shown in the flow chart in Figure 6.2. Initialization procedures are necessary first to generate user spreading codes and then for arrays and all other variables. Initialization includes frame length definition in number of bits, the number of frames to be processed for obtaining BER estimates with sufficient confidence, etc. The spreading codes are the same set of Gold codes with period 31 that were used for BER analysis. In the second step, a loop is repeated for a sufficient number of times. This loop consists of a

transmitter section, a channel section, and a receiver section. An error detector and counter stage after the receiver section counts the number of bits in error. For MC simulations, the estimate of the BER is calculated by dividing the number of errors by the number of bits processed. In cases where the IS technique is used, the weight of the biased density function is calculated and then used to unbias the error count.

For each iteration of the loop, the transmitter section generates frames of sampled random data bits, one frame each for all K users. The sampled data frame of each user is multiplied by the corresponding sampled spreading code frame. The asynchronous nature of the user transmissions is taken into account by shifting the frames by an amount equal to their corresponding transmitter delay. The imperfections in power control are taken into account by multiplying the transmitted frame of each user by a log-normal random variable.

In the channel section, the uniformly distributed path delays, Rayleigh distributed path amplitudes and uniformly distributed path phases for all L resolvable paths of all K users are generated. In the reverse link, these channel parameters are independent among users. White noise is also generated and added to the sum of the K user signals to obtain the total received signal at the base station.

In the receiver section, the received signal is passed through a correlator or a RAKE receiver. For a correlator receiver, de-spreading is done with the desired spreading code aligned with the first path signal. This is followed by summation and data decision. In a RAKE receiver, the path signals at the matched filter output are maximal ratio combined using a transversal filter combiner which is provided

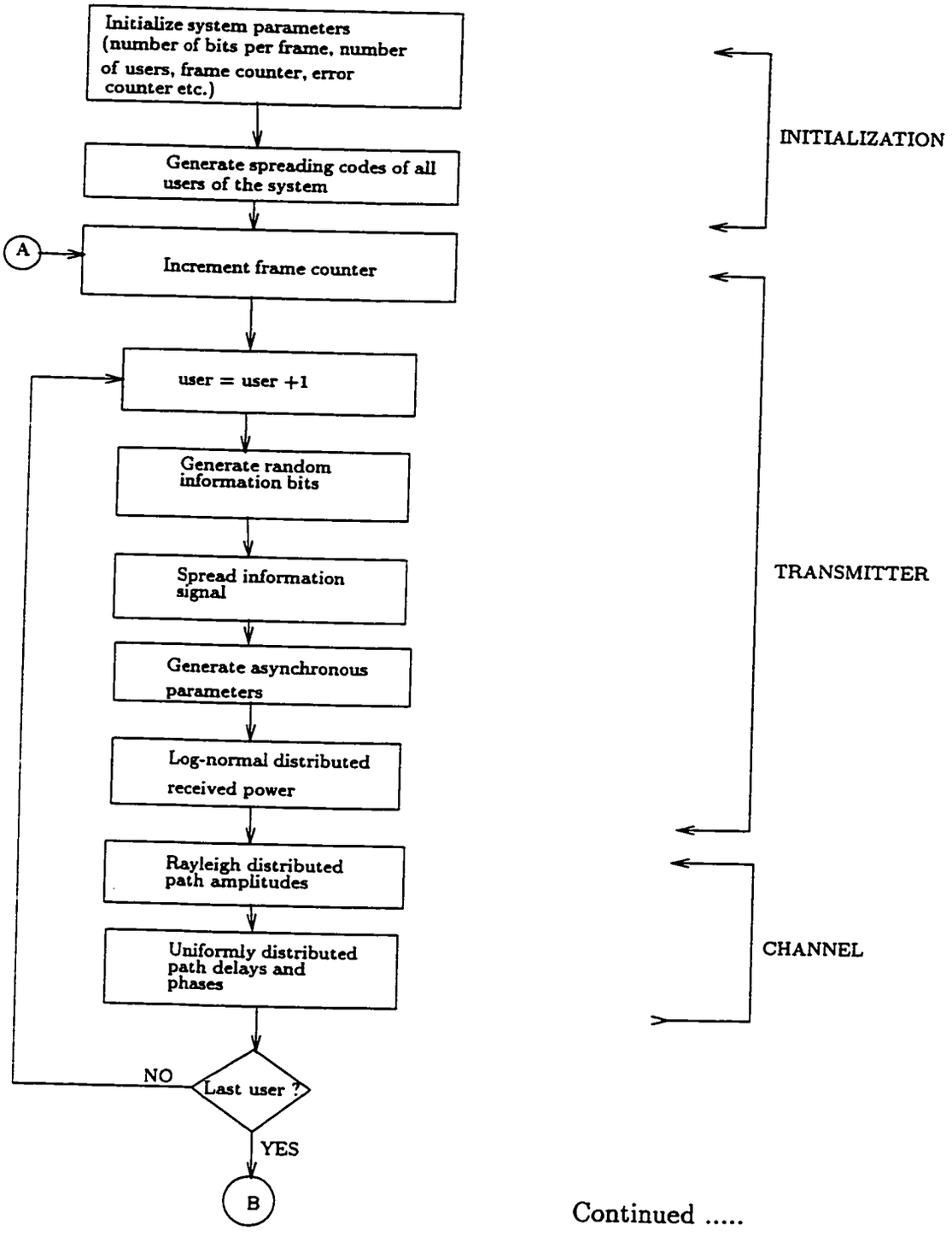
Initialize system parameters (number of bits per frame, number of users, frame counter, error counter etc.)
Generate spreading codes of all users of the system
A
Increment frame counter
user = user +1
Generate random information bits
Spread information signal
Generate asynchronous parameters
Log-normal distributed received power
Rayleigh distributed path amplitudes
Uniformly distributed path delays and phases
NO
Last user ?
YES
B
INITIALIZATION
TRANSMITTER
CHANNEL

Continued .....

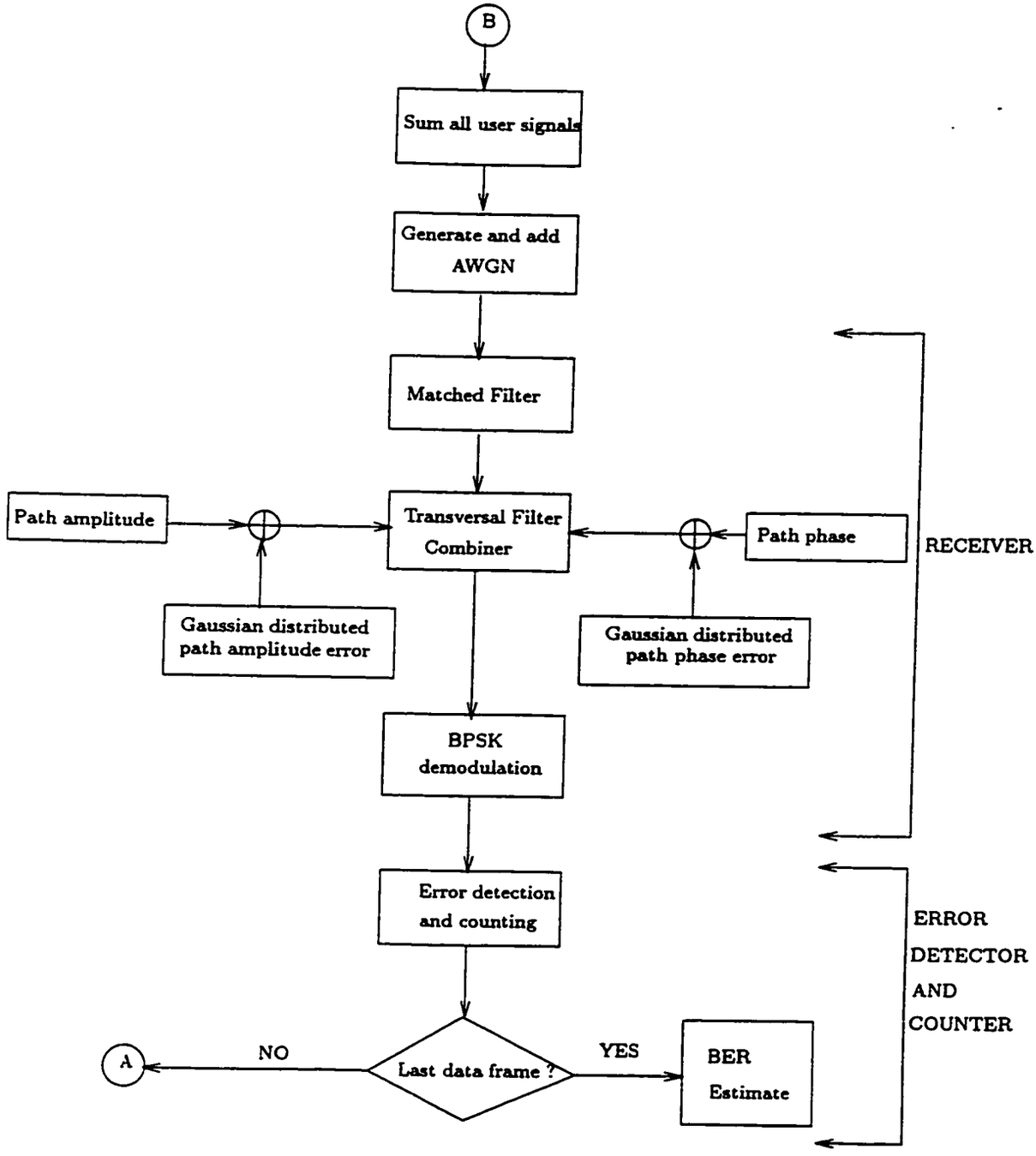

Figure 6.2 Flow chart of the simulation program for BER performance evaluation of a CDMA receiver in indoor radio channel.

with estimates of path amplitudes and phases. The error in channel estimates is accounted by generating zero mean Gaussian random variables with different variances. The variance of the amplitude error is $E\{\Delta g_{k,\lambda}^2\} = \text{MSE}$ and the variance of phase error is obtained as $E\{\Delta \phi_{k,\lambda}^2\} = \pi^2 \text{MSE}$, where MSE is the mean square of the normalized error. The combiner output is then BPSK demodulated using a hard decision stage. Hard decision stage decides in favor of a bit '1' if the real part of the correlator or combiner output is positive and decides in favor of a bit '0' if the real part of the correlator or combiner output is negative.

6.2.3 Simulation Results

The complete indoor CDMA system is simulated and the BER performance is evaluated under different conditions using MC and IS techniques. The MC simulation is used to obtain BER up to 10^{-3}. A symbol size of $\frac{10}{p}$, where p is the BER to be estimated, is selected for this. As stated previously, this symbol size provides a BER estimate in the confidence interval $[1.8p, 0.55p]$ at a confidence level of 0.95. Simulation based on IS sampling is used to obtain BER in the $10^{-3} - 10^{-6}$ range. An approximate symbol size required for the $[1.8p, 0.55p]$ confidence interval at 0.95 confidence level is specified in [27]. This symbol size is obtained by comparing the BER obtained by IS simulation by time consuming MC simulation. To gain confidence in the required symbol size, BER performance of a single user spread spectrum system with BPSK carrier modulation is simulated using the IS technique. The set of symbol sizes needed to get the analytical BER for $\frac{E_b}{N_o}$ in the 0 - 10 dB range is derived using extensive simulations. To obtain BER estimates within the previously

specified confidence interval, a symbol size of 1,000 - 10,000 is found to be sufficient in the $10^{-3} - 10^{-6}$ range.

For a CDMA correlator receiver, the simulated BER versus $\frac{E_b}{N_o}$ performance results are shown in Figures 6.3 - 6.5 for various values of N and K. The BER obtained using standard Gaussian and improved Gaussian approximations are included for comparison. As evident in these figures, the standard Gaussian approximation provides accurate BER for $\frac{E_b}{N_o}$ values up to 10 - 12 dB. This is especially true for $N = 31$, even with a small number of users, K. At low values of BER, standard Gaussian approximation provides optimistic BER and improved Gaussian approximation provides pessimistic BER compared to the simulated BER. The agreement between the simulated and the analytical results becomes poor at larger values of the processing gain N. The agreement also gets poor as the number of users K becomes fewer. This may be attributed to the fact that, when the delays and phases of user transmissions are random, the number of users K has to be large for the Gaussian approximation to be accurate. Similarly, for large values of processing gain N, multiple access interference may be accurately approximated by a Gaussian random variable only at fixed values of phases and delays of user transmissions [54].

The BER performance results for a CDMA RAKE receiver using MC simulation are shown in Figures 6.6 - 6.9. Perfect conditions are simulated for the result shown in Figure 6.6 whereas the effect of power control imperfections, channel parameter estimation imperfections, and spreading code phase estimate imperfections are considered in Figures 6.7, 6.8 and 6.9 respectively. For simulation results, the confidence

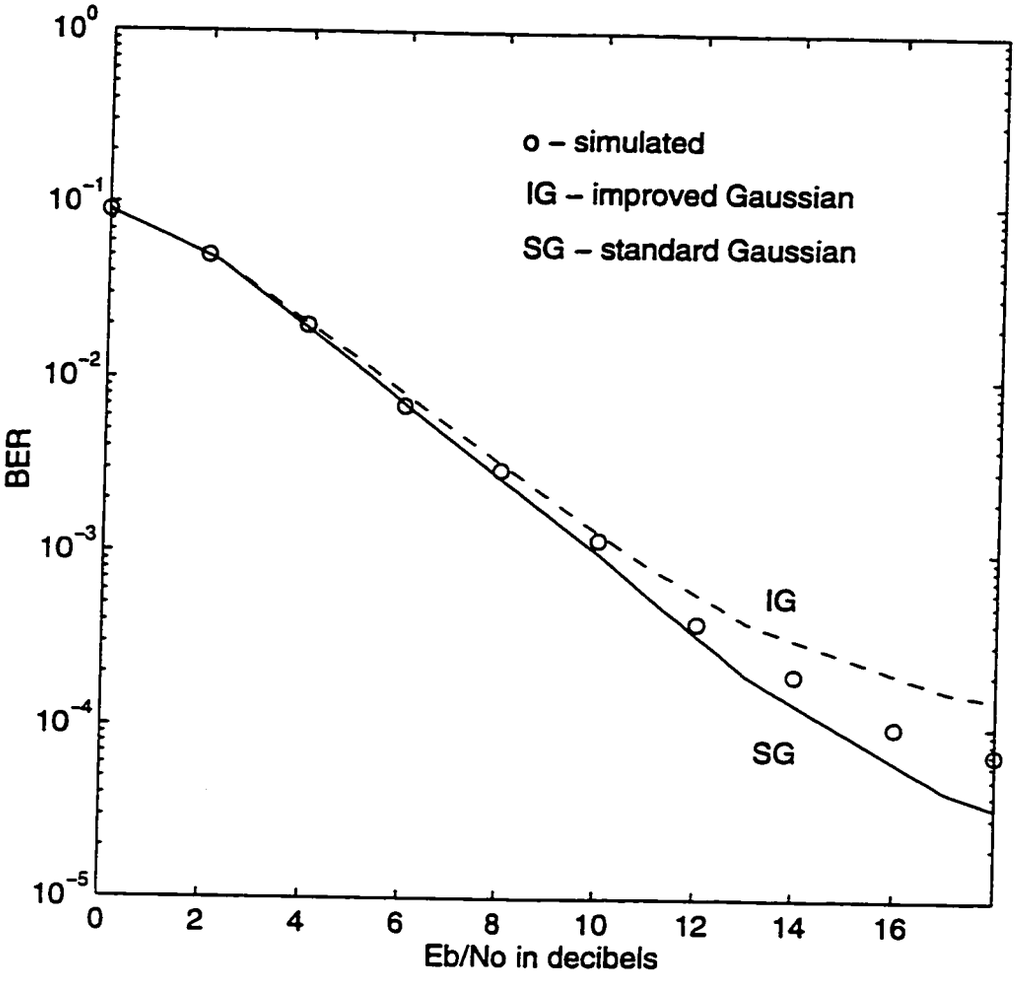

Figure 6.3 BER versus $\frac{E_b}{No}$ results (analytical and simulation) for a CDMA correlator receiver. Perfect conditions, average number of paths per user, $\bar{L} = 3$; $N = 31$; $K = 3$.

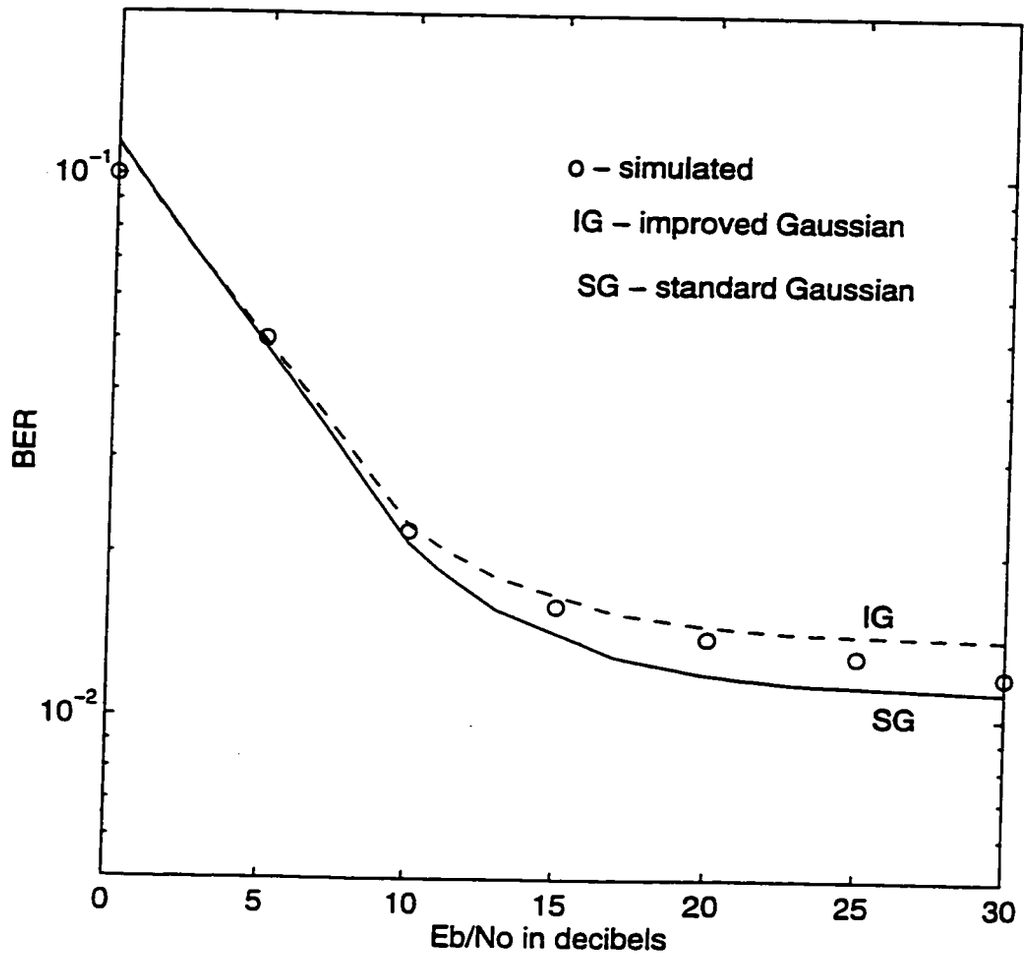

Figure 6.4 BER versus $\frac{E_b}{No}$ results (analytical and simulation) for a CDMA correlator receiver. Perfect conditions, average number of paths per user, $\bar{L} = 3$; $N = 31$, $K = 8$.

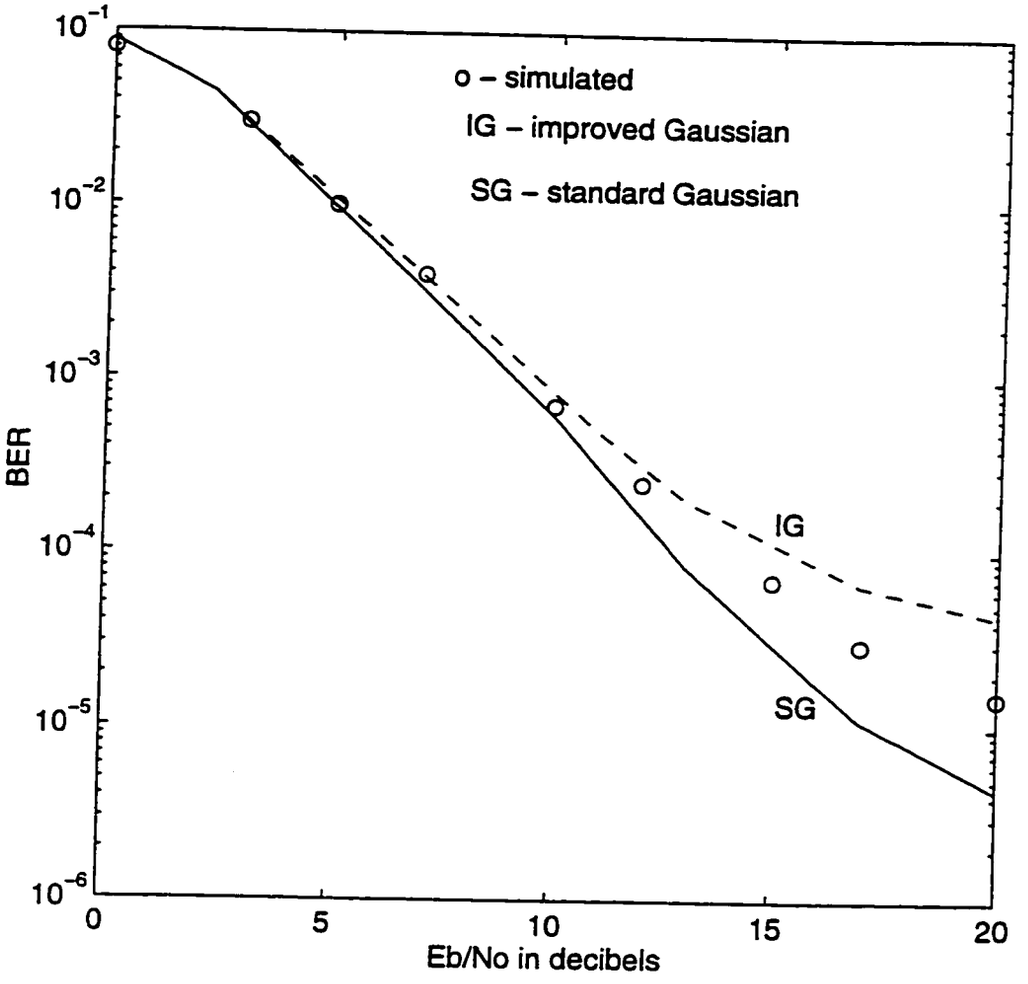

Figure 6.5 BER versus $\frac{E_b}{No}$ results (analytical and simulation) for a CDMA correlator receiver. Perfect conditions, average number of paths per user, $\bar{L} = 3$; $N = 127$, $K = 8$.

intervals (at 0.95 confidence level) are also shown. Results obtained by analysis in Chapter 3 are also included in these figures. The BER obtained using the standard Gaussian approximation lies within the confidence interval of the simulated BER estimate (Figures 6.6 - 6.9). This agreement between the simulated and analytical result justifies the approximations used in the analysis. As stated before, the computational effort required for analytical methods is considerably less. For example, the numerical computation of analytical expression for BER takes only a few minutes of computer time whereas MC simulation of BER performance of an indoor CDMA system with RAKE receiver takes approximately two days of computer time.

6.3 Simulation of Indoor CDMA System with CCI Canceling Receivers

The program structure for simulating the BER performance of a CCI canceling receiver is similar but more elaborate than that described in Section 6.2. There is a receiver section for each user of the system. To simulate the above program a computer system with large memory is required. The data estimates and channel parameter estimates of each user are stored and they are used to regenerate its contribution of CCI. Regenerated CCI of each user is subtracted from the received signal and a second set of receivers is used to demodulate the CCI-canceled signal. This has to be performed for each user of the CDMA system.

The block diagram of the system simulated for one stage CCI regeneration and cancellation, and subsequent data demodulation is shown in Figure 6.10. This pro-

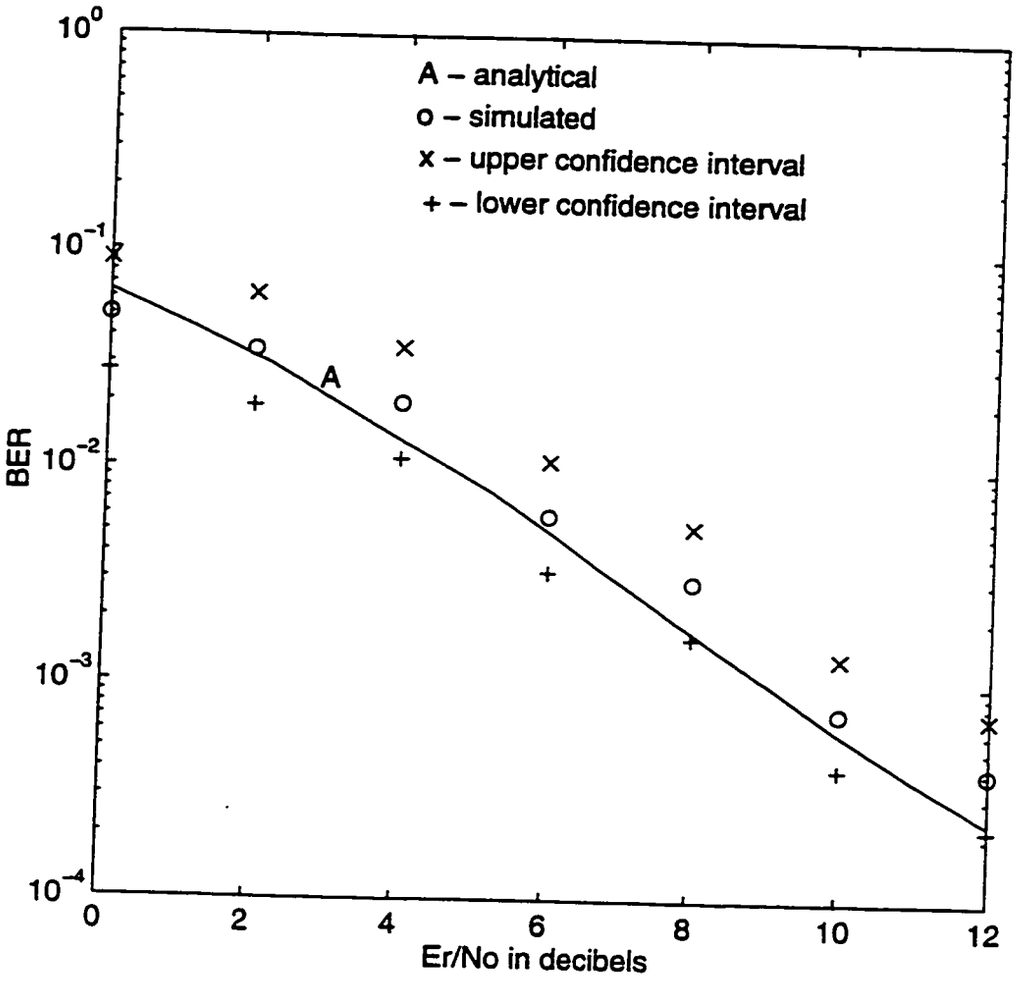

Figure 6.6 BER performance results by analysis and simulation for a CDMA RAKE receiver. Perfect conditions; $\bar{L} = 3$; $N = 31$; $K = 9$. The confidence intervals of the simulated BER results at a confidence level of 0.95 are also shown.

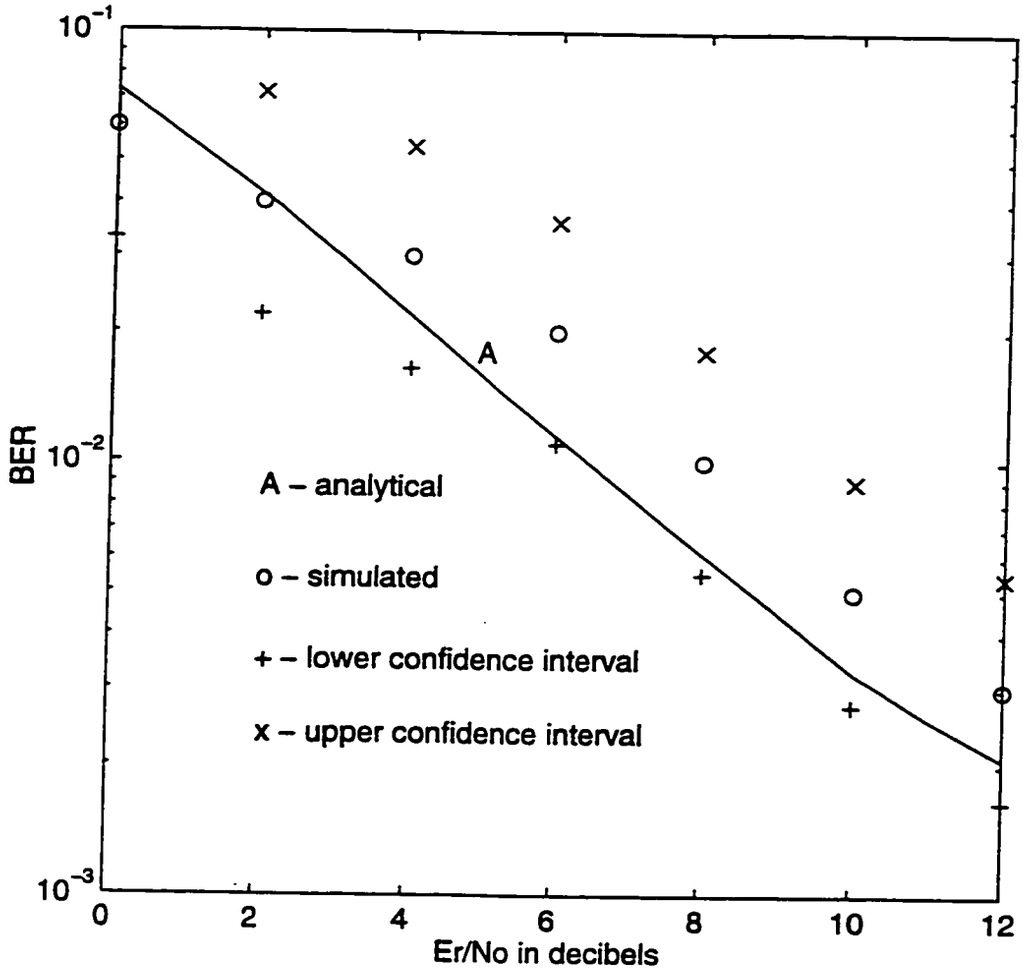

Figure 6.7 BER performance results by analysis and simulation for a CDMA RAKE receiver. Variance of normalized received power = 2dB; perfect channel parameter estimation and code phase estimation; $\bar{L} = 3$; $N = 31$; $K = 9$. The confidence intervals of the simulated BER results at a confidence level of 0.95 are also shown.

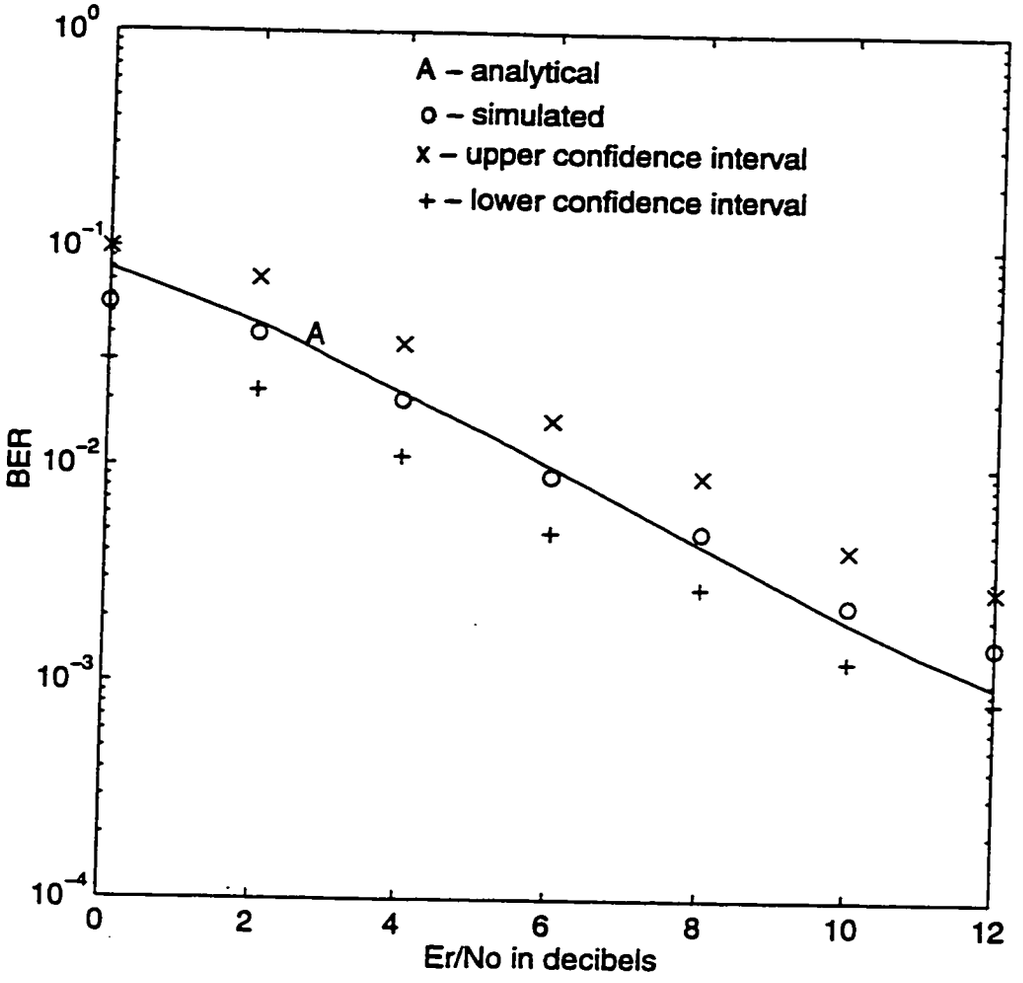

Figure 6.8 BER performance results by analysis and simulation for a CDMA RAKE receiver. MSE in channel parameter estimation = 0.01; perfect power control and code phase estimation; $\bar{L} = 3$; $N = 31$; $K = 9$. The confidence intervals of the simulated BER results at a confidence level of 0.95 are also shown.

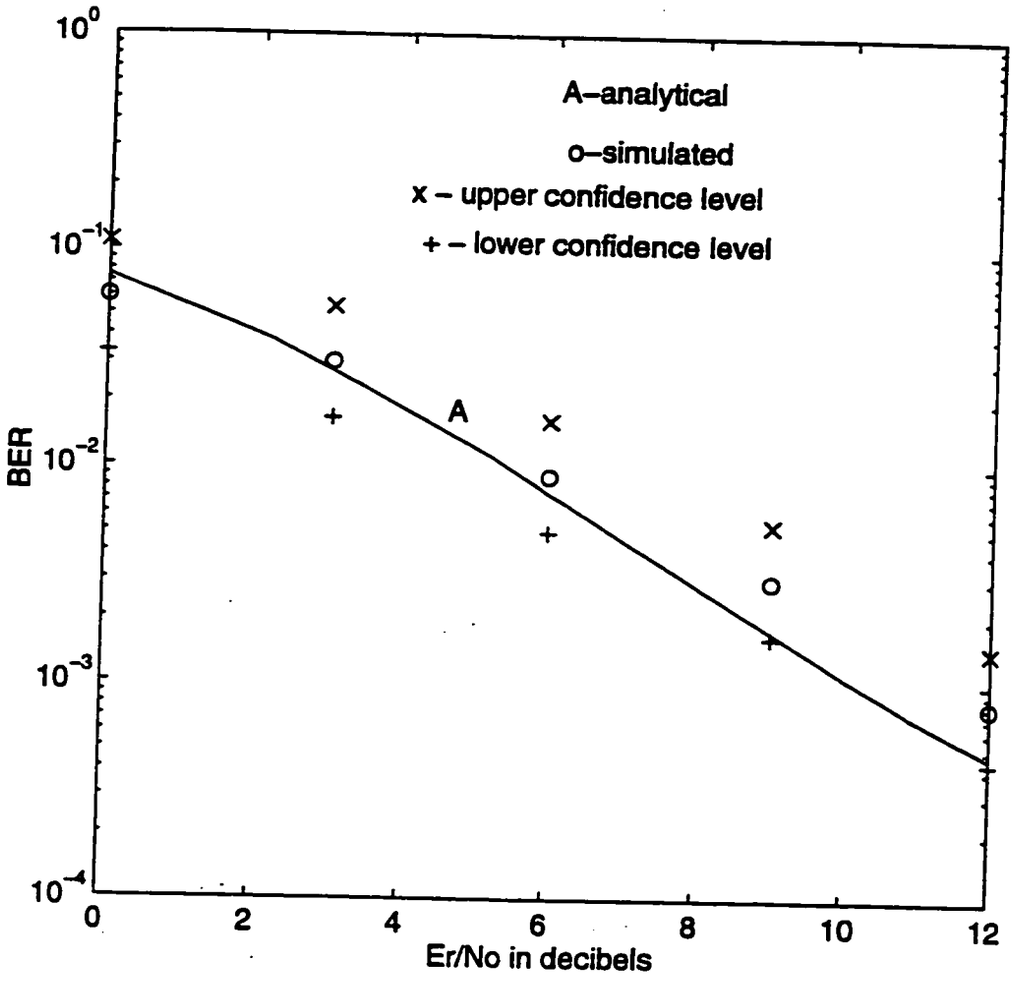

Figure 6.9 BER performance results by analysis and simulation for a CDMA RAKE receiver. Standard deviation of code phase error = 0.1; perfect power control and channel estimation; $\bar{L} = 3$; $N = 31$; $K = 9$. The confidence intervals of the simulated BER results at a confidence level of 0.95 are also shown.

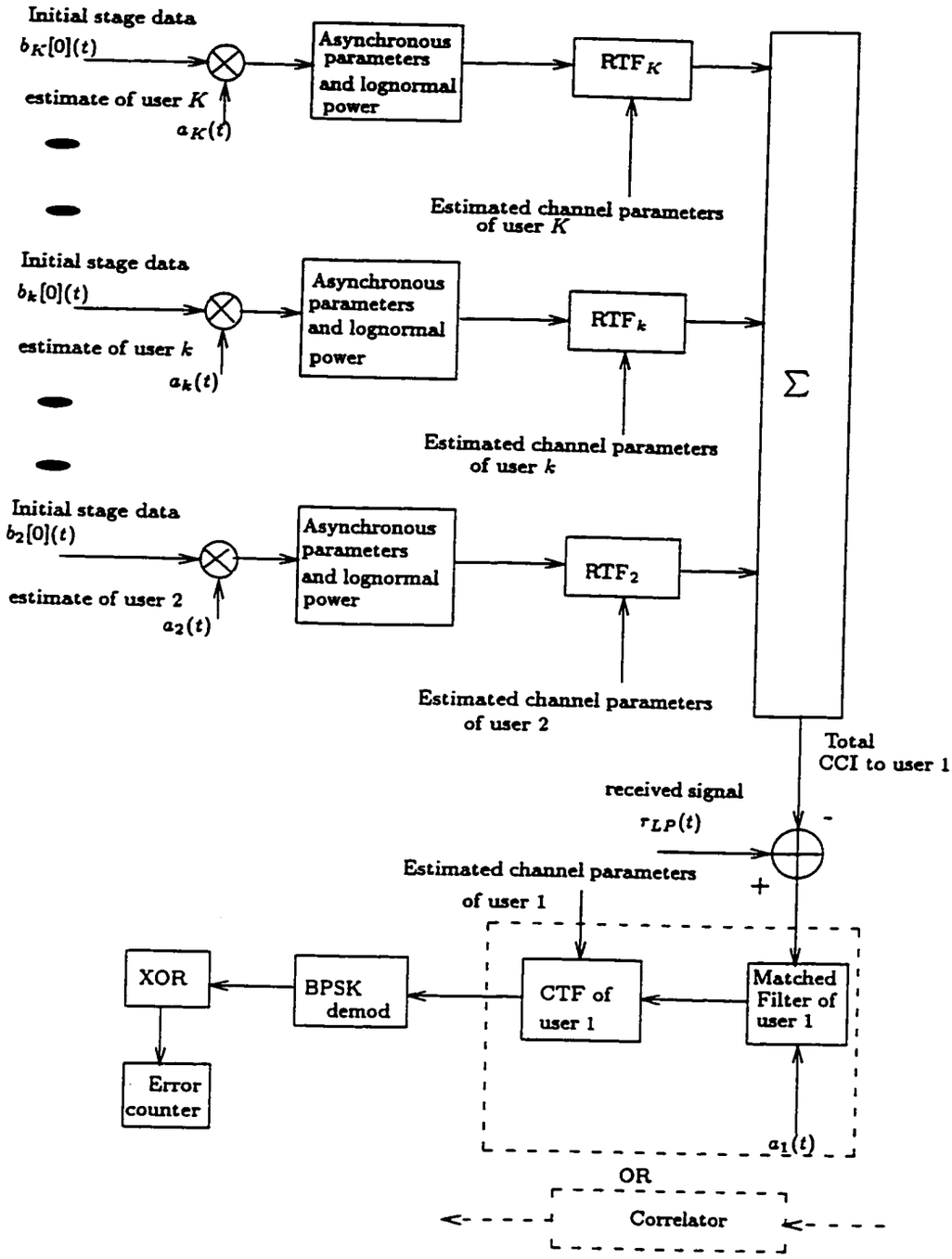

Figure 6.10 Low-pass equivalent of the indoor CDMA system simulated to obtain the BER performance of CDMA receivers with one stage of CCI cancellation. The block schematics shown is w.r.t the user 1.

cess of regeneration, CCI cancellation, and demodulation of data signal is repeated one or more number of times by logical extension of the procedure illustrated in Figure 6.10.

The effect of power control imperfections and channel parameter estimates imperfections on the performance of the receiver is also simulated by a procedure similar to that described in Section 6.2. One additional feature of the procedure is the inclusion of the effect of error in channel estimates in the CCI regeneration for every user. The flow chart illustrating the simulation procedure for one stage of CCI regeneration and cancellation is shown in Figure 6.11. Two or more stages of CCI regeneration and cancellation can be simulated by repeating the operations depicted in this flow chart.

6.3.1 Simulation Results

Elaborate simulations using MC and IS techniques are performed to evaluate BER performance of CCI canceling CDMA receivers. Simulations are performed for correlator and diversity combining RAKE receivers with CCI cancellation. The effect of each system imperfection is simulated separately to study its effect on BER. A combination of system imperfection is also simulated to examine its combined effect on the receiver performance.

The BER performance results for a CCI canceling correlator receiver are presented in Figures 6.12 - 6.14. Results in Figure 6.12 are obtained assuming perfect conditions. Imperfect power control is assumed in obtaining results presented in

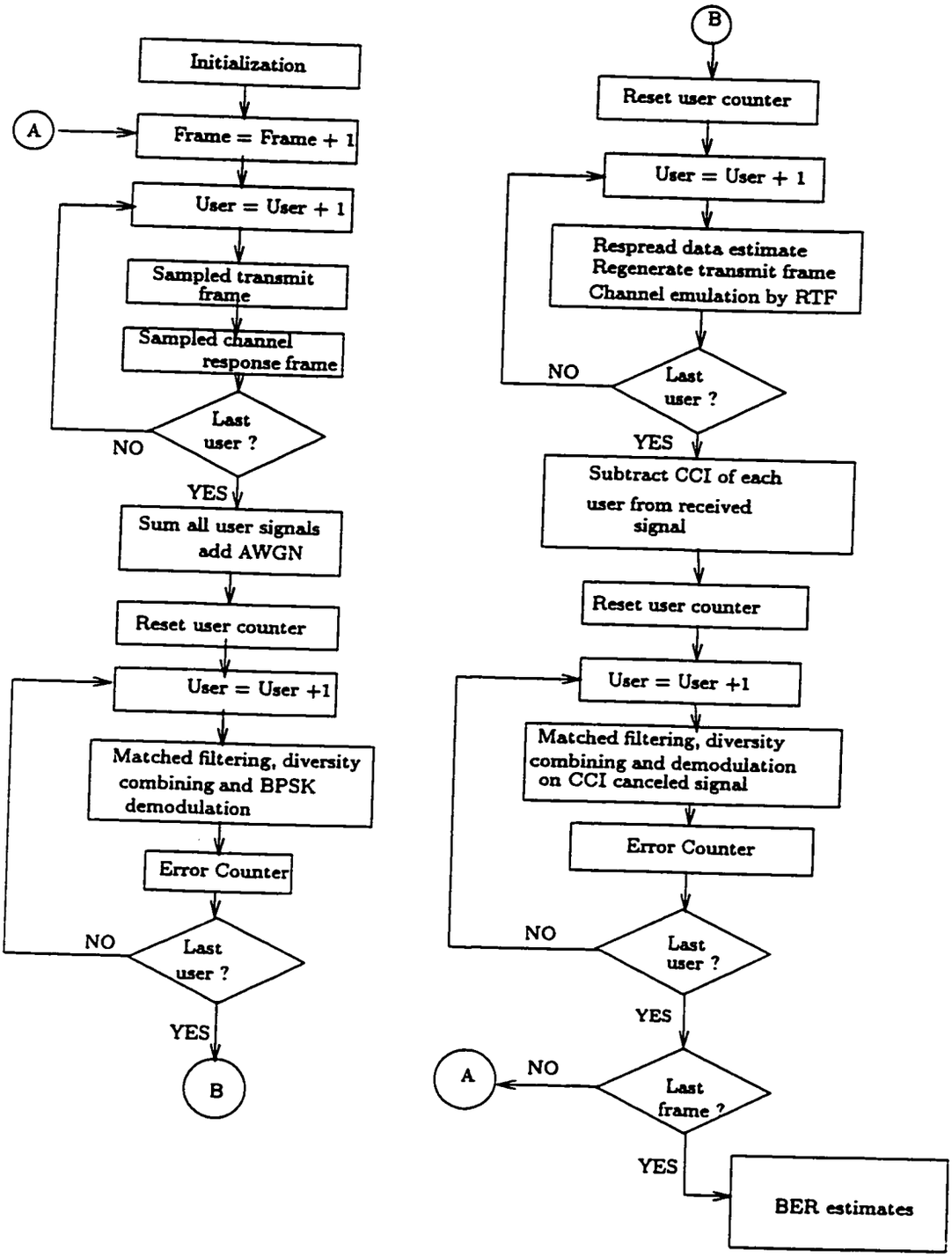

Figure 6.11 Flow chart of the simulation program for BER performance evaluation of CCI canceling CDMA receivers.

Figure 6.13 whereas to arrive at the results shown in Figure 6.14 imperfect channel estimates are assumed. Similarly the simulated BER performance of a CCI canceling RAKE receiver for various combination of factors are shown in Figures 6.15 - 6.19. In all cases the analyzed BER performance is also shown for comparison.

For initial stages of CCI cancelers, simulated and analytical results are almost in agreement (Figures 6.12 - 6.19). However, with an increasing number of canceler stages, theoretical curves become optimistic in comparison with simulation curves. This can be attributed to the removal of CCI by the cancellation scheme. Reduced CCI is equivalent to fewer transmitting users and this is equivalent to lower values of K. As shown in previous cases, optimistic BER results are provided by the standard Gaussian approximation when K is small. Up to a BER of 10^{-4} the Gaussian approximation is reasonably accurate. The Gaussian approximation has resulted in an SNR difference of 1 to 1.5 dB lower for a given value of BER in the range of 10^{-4} to 10^{-6}.

6.4 Summary

The BER performance of correlator and diversity combining RAKE receivers was evaluated with and without CCI cancellation. Imperfections in power control, channel estimates and spreading code phase estimates were incorporated in the simulation model. Computational burden was reduced by using IS techniques to evaluate low values of BER. The simulated bit error rate results were compared with those obtained using analytical approximations. For the correlator receiver, results

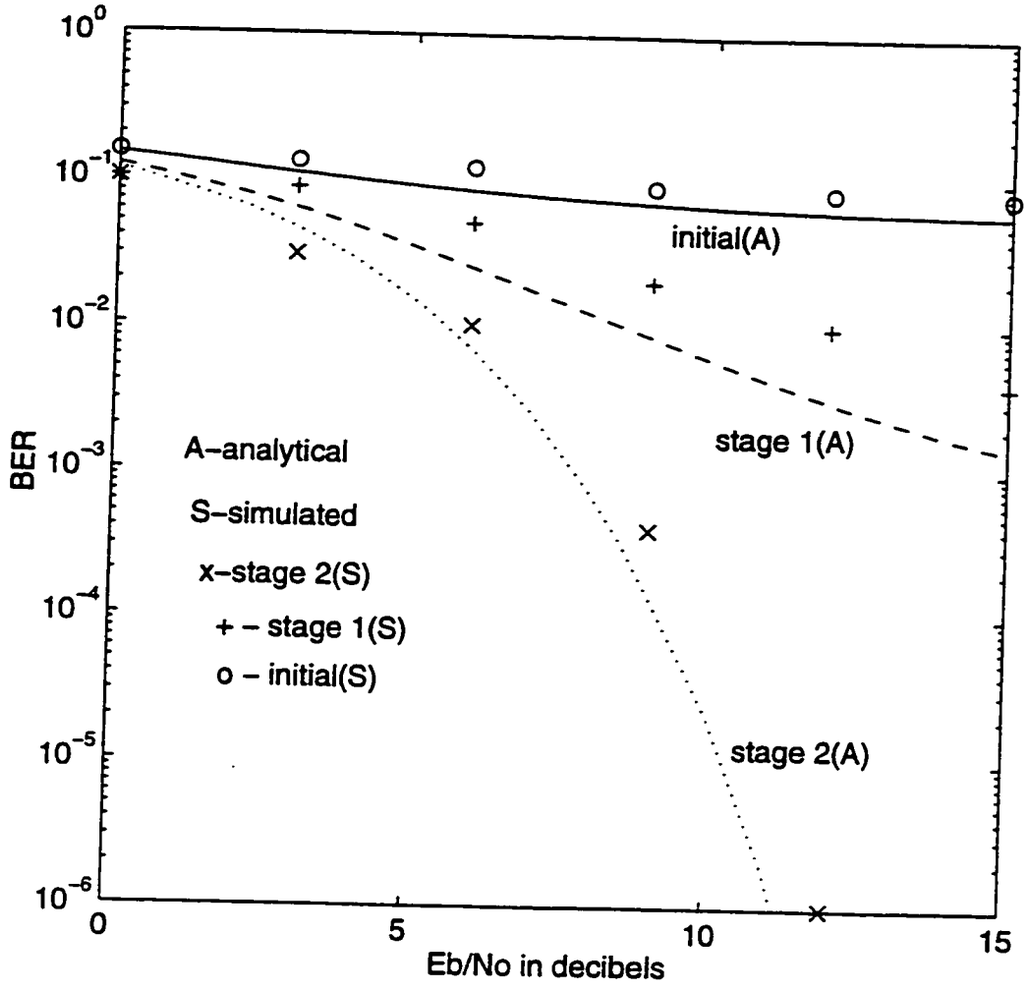

Figure 6.12 BER performance results by analysis and simulation for a CCI canceling CDMA correlator receiver. Perfect conditions; $\bar{L} = 3$; $N = 31$; $K = 16$.

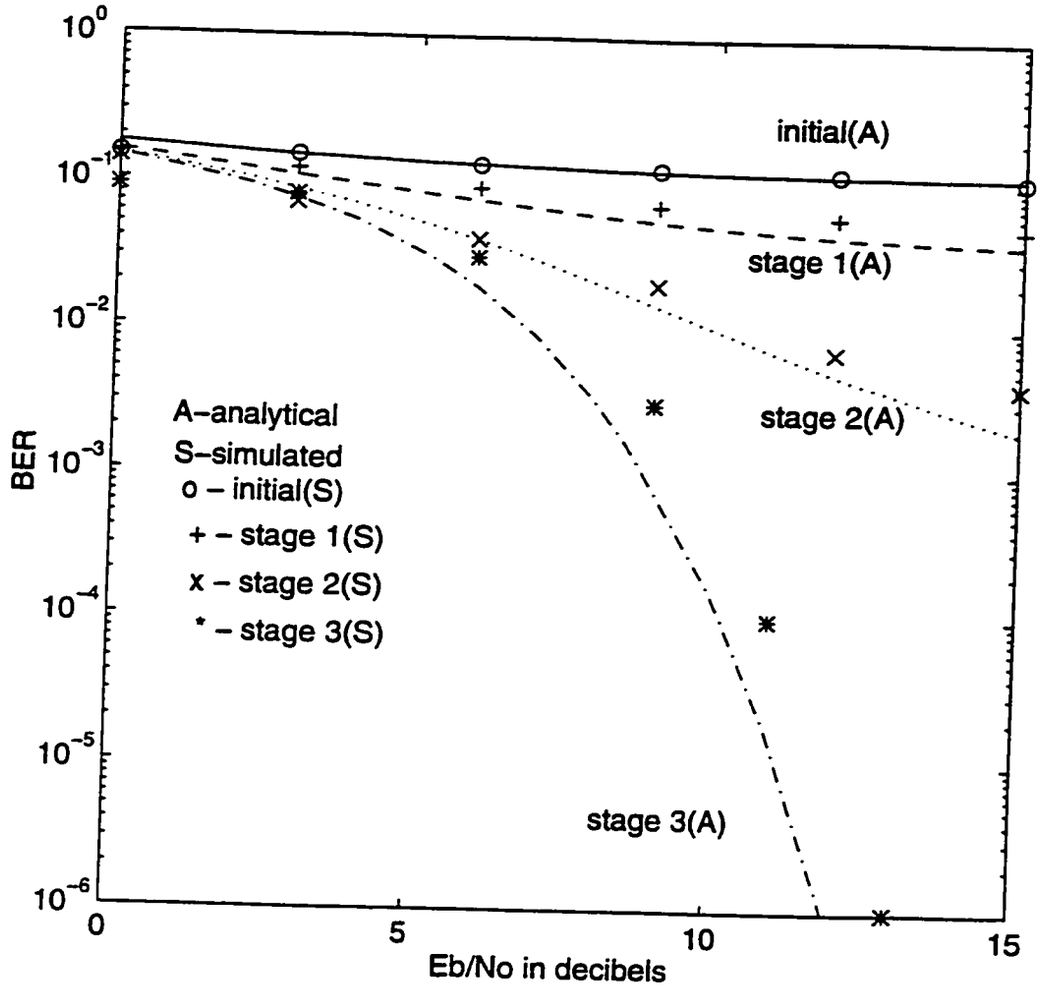

Figure 6.13 BER performance results by analysis and simulation for a CCI canceling CDMA correlator receiver. Variance of received power = 2dB; perfect channel parameter estimation and code phase estimation; $\bar{L} = 3$; $N = 31$; $K = 16$.

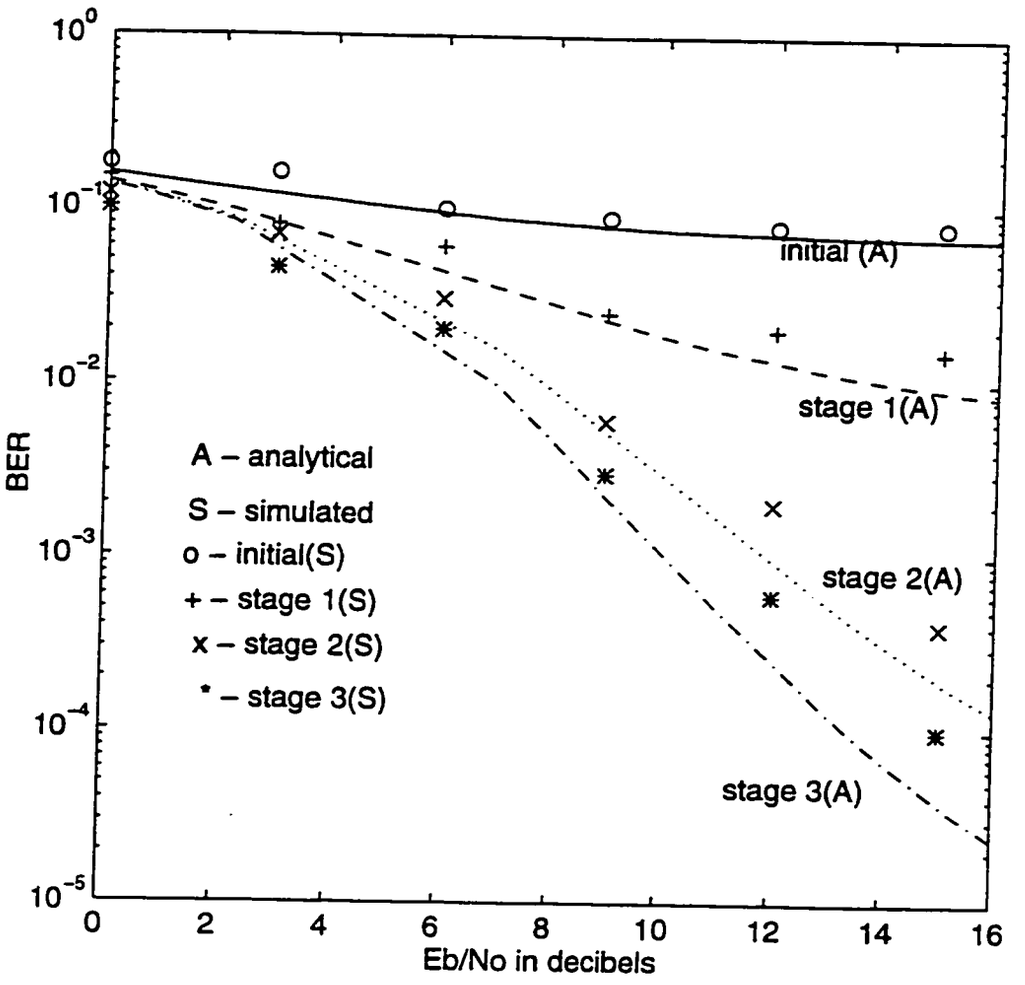

Figure 6.14 BER performance results by analysis and simulation for a CCI canceling CDMA correlator receiver. MSE in channel parameter estimation = 0.01; perfect power control and code phase acquisition; $\bar{L} = 3$; $N = 31$; $K = 16$.

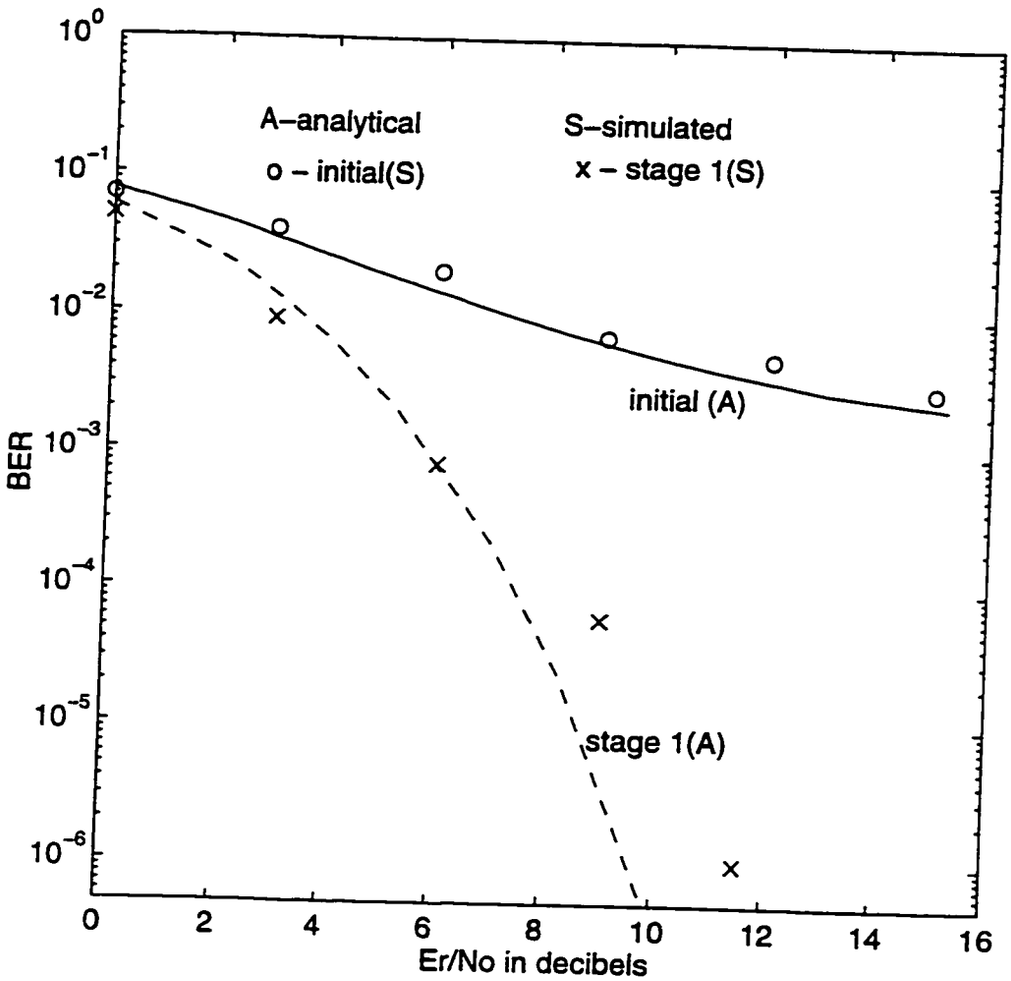

Figure 6.15 BER performance results by analysis and simulation for a CCI canceling CDMA RAKE receiver. Perfect conditions; $\bar{L} = 3$; $N = 31$; $K = 16$.

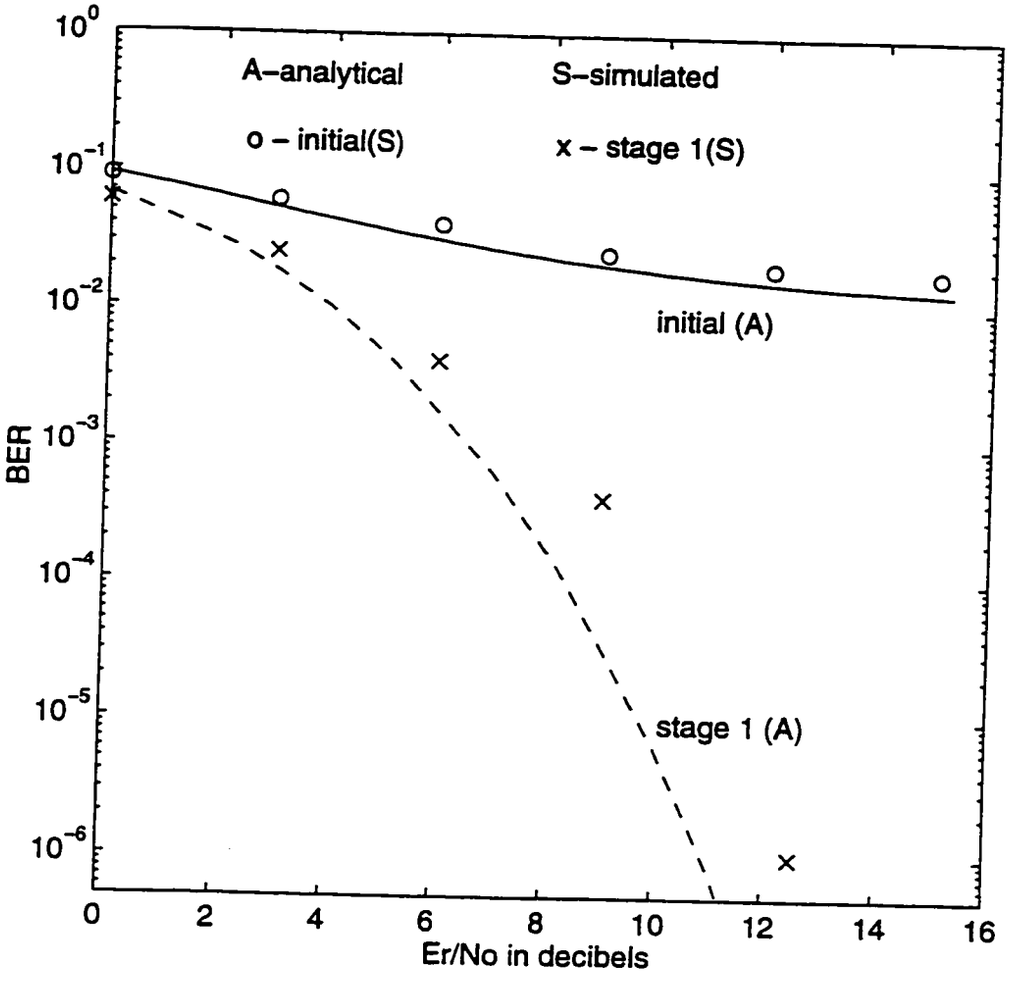

Figure 6.16 BER performance results by analysis and simulation for a CCI canceling CDMA RAKE receiver. Variance of received power = 2dB; perfect channel parameter estimation and code phase estimation; average number of paths per user, $\bar{L} = 3$; $N = 31$; $K = 16$.

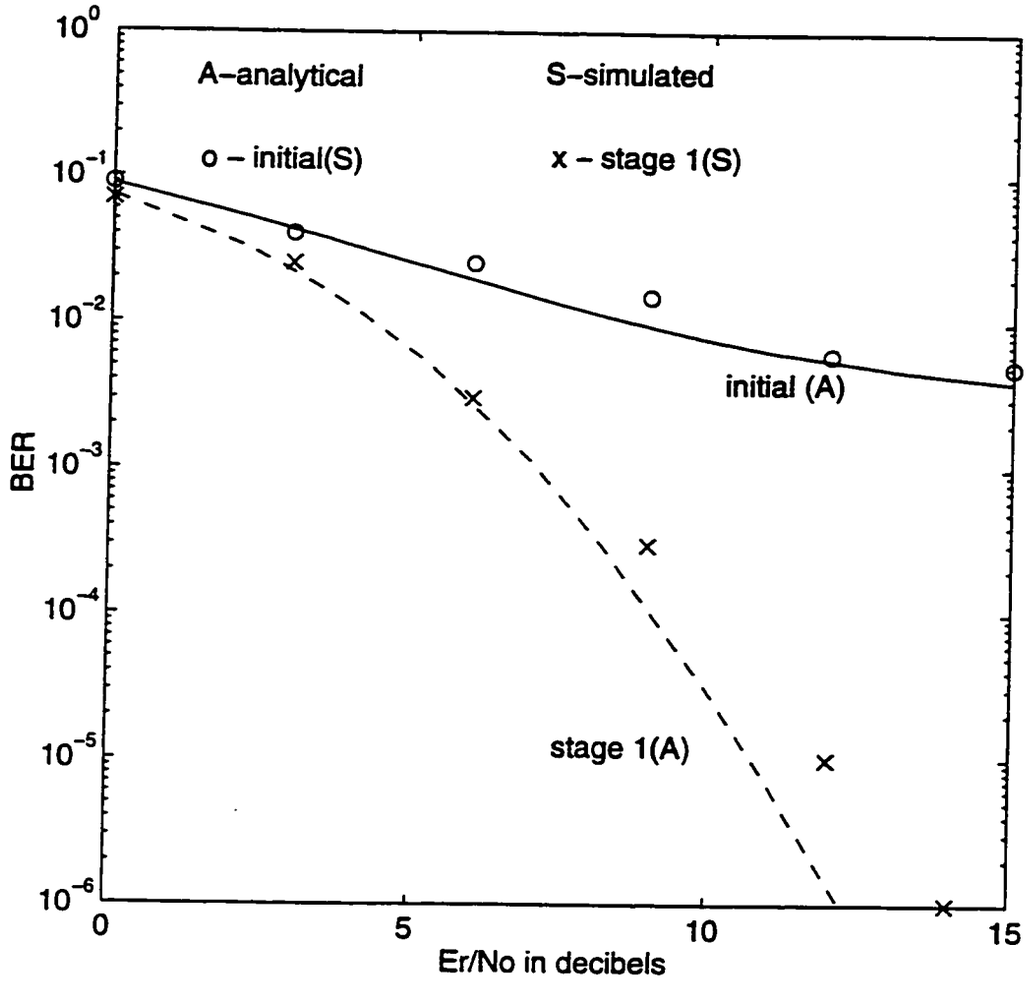

Figure 6.17 BER performance results by analysis and simulation for a CCI canceling CDMA RAKE receiver. MSE in channel parameter estimation = 0.01; perfect power control and code phase acquisition; $\bar{L} = 3$; $N = 31$; $K = 16$.

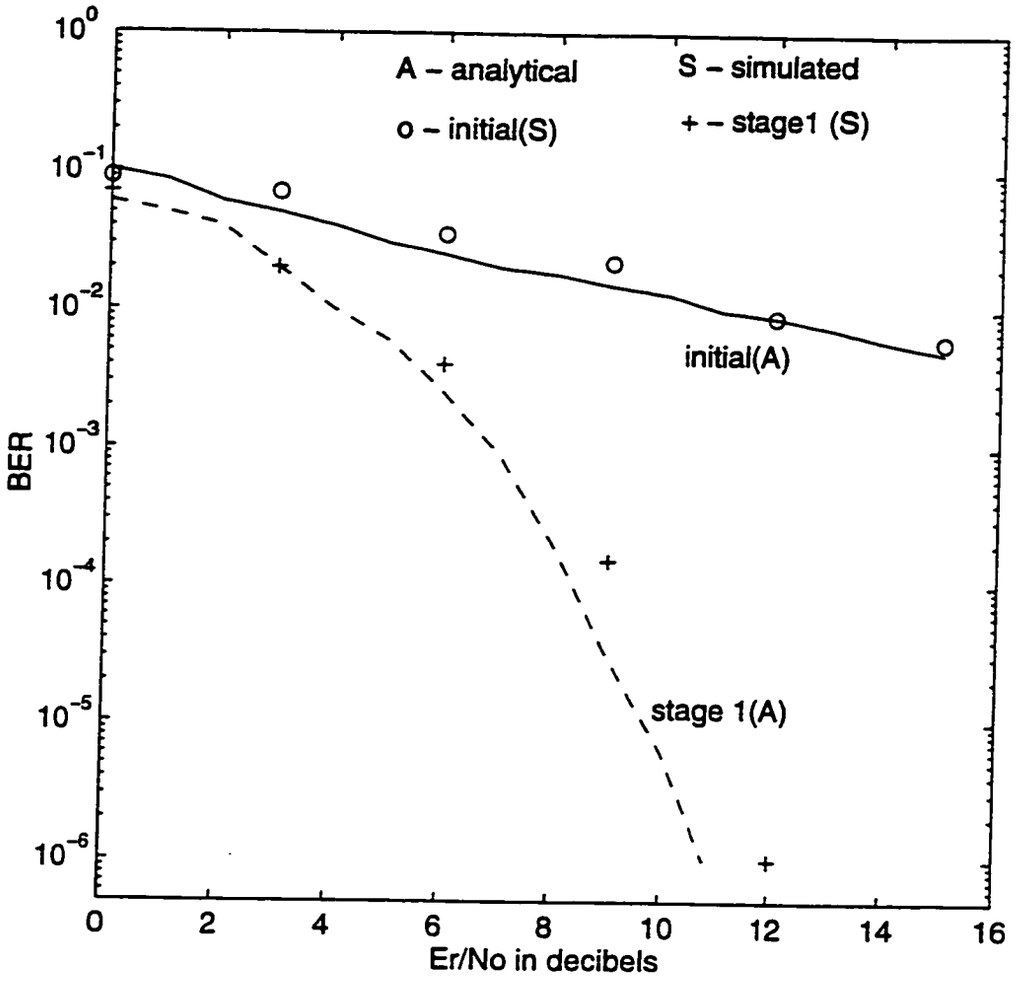

Figure 6.18 BER performance results by analysis and simulation for a CCI canceling CDMA RAKE receiver. Standard deviation of normalized error in code phase estimate = 0.1; perfect power control and channel parameter estimation; $\bar{L} = 3$; $N = 31$; $K = 16$.

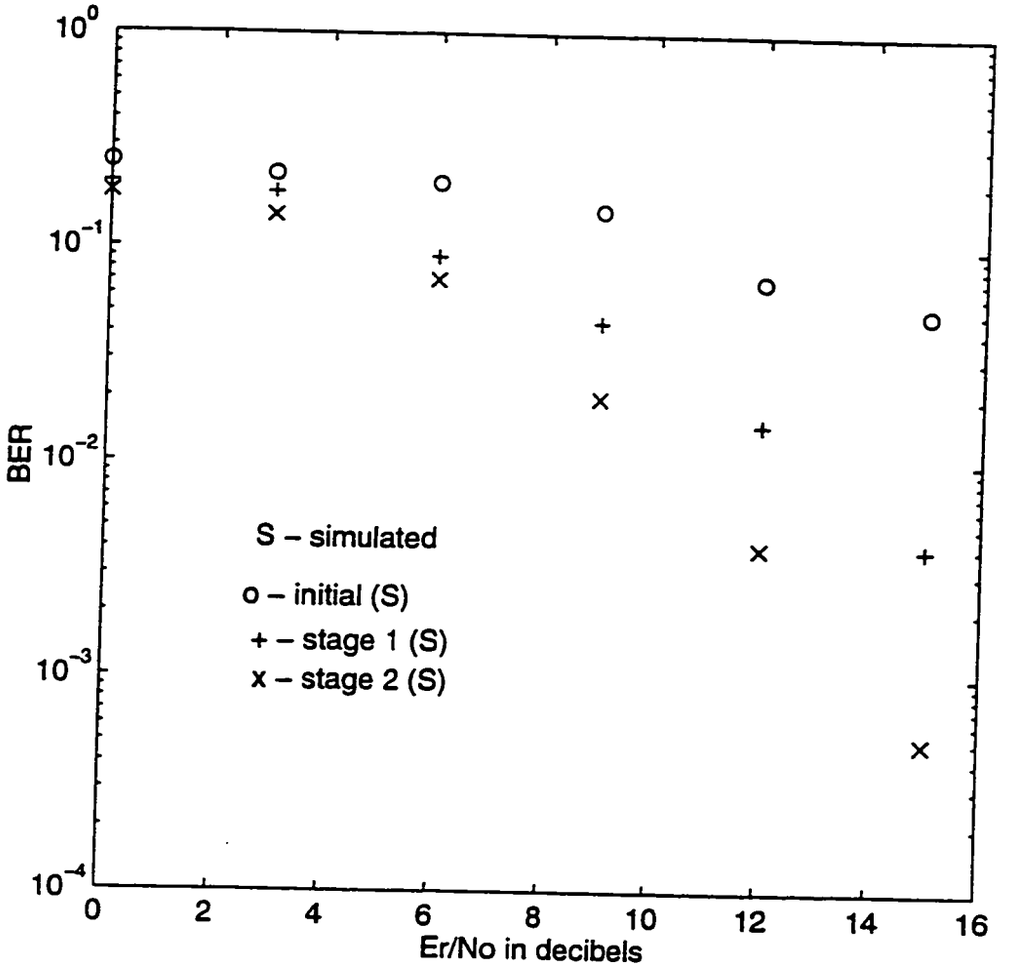

Figure 6.19 BER performance results by simulation for a CCI canceling CDMA RAKE receiver. MSE in channel parameter estimation = 0.01; standard deviation of normalized error in code phase estimation = 0.1; variance of normalized received power = 2dB; $\bar{L} = 3$; $N = 31$; $K = 16$.

using the standard Gaussian approximation method and the improved Gaussian method are the same as those using simulation, for an $\frac{E_b}{N_o}$ below 10-12 dB. However, at higher values of an $\frac{E_b}{N_o}$, standard Gaussian approximation provides optimistic BER and improved Gaussian approximation provides pessimistic BER values compared to the simulation results. For diversity combining receivers, it is shown that analytical results lie within the confidence interval of the simulated BER estimates. For a CCI canceling receiver, the analytical and simulation results are in agreement in the preliminary stages of the receiver. However, analytical BER results are optimistic in the CCI cancellation stages, especially at higher values of SNR. As stated before, this is due to the reduction in the effective number of users, K, with more stages of CCI cancellation.

7. Conclusions and Future Work

The following objectives of the research were stated in Chapter 1:

1. Analyze the effect of imperfections in transmitter power control, carrier phase estimate and spreading code phase estimate on the BER performance of a CDMA correlator receiver in a frequency selective slow Rayleigh fading indoor channel.

2. Analyze the effect of the above imperfections on the BER performance of a multipath diversity combining CDMA receiver in the same indoor mobile channel environment.

3. Develop analysis for the BER performance of a parallel pre-correlation CCI canceling CDMA correlator receiver with the same imperfections and for the same channel.

4. Analyze the effect of imperfections on the BER performance of a CCI canceling multipath diversity combining CDMA receiver in the indoor mobile radio channel.

5. Develop programs to simulate indoor CDMA system with correlator and multipath combining receivers with and without CCI cancellation and verify the analytical results.

7.1 Conclusions

The work presented in this thesis shows that the above five objectives have been realized. The overall conclusions are summarized as follows:

1. An expression for the probability of bit error of a CDMA correlator receiver was derived. The effect of system imperfections was included in the derivation. The BER was numerically computed for various combinations of factors. The individual effect of various system imperfections on BER performance as well as their combined effect were presented in Chapter 3. It is concluded that the spectral efficiency of such systems is approximately 0.1 bits/sec/Hz at a BER of 10^{-4} under perfect operating conditions. As expected, the spectral efficiency decreases with system imperfections. The performance of such receivers degrades significantly when the variance of the normalized received power is above 0 dB, or the mean square error in the normalized carrier phase estimate is above 0.01 or the standard deviation of the normalized code phase error is above 0.1.

2. An expression for the probability of bit error of a CDMA RAKE receiver was derived taking into account the effect of imperfections. Numerical computation of the BER was done for various combinations of factors. The individual effect of various system imperfections on the BER performance and their combined effect were presented in Chapter 3. It is shown that the spectral efficiency of such systems is 0.25 bits/sec/Hz at a BER of 10^{-3} under perfect

operating conditions. It is demonstrated that imperfections in power control, path amplitude and phase estimation, and spreading code phase estimation are of particular concern. The performance of these receivers degrades when the variance of received power is above 0 dB, or the mean square error of the normalized path amplitude and phase estimate is above 0.01 or the standard deviation of the normalized code phase error is above 0.1. The need for receiver structures which can provide better spectral efficiency by using new signal processing such as regeneration and cancellation of co-channel interference at the receiver, is emphasized in Chapter 3.

3. An analysis was developed for the BER performance of a parallel pre-correlation CCI canceling CDMA receiver in a frequency selective slow Rayleigh fading indoor channel. This analysis included the effect of system imperfections. Numerical computations of the BER of a multi-stage CCI cancellation receiver was done for various combinations of system imperfections. The individual and combined effects of various system imperfections on the BER performance were presented in Chapter 4. It is concluded that a spectral efficiency of 0.5 bits/sec/Hz at BER of 10^{-6} is possible under perfect conditions, with three stages of CCI regeneration and cancellation. For the cancellation scheme to be effective, only a limited margin of error in channel estimation and spreading code phase estimation can be tolerated.

4. An analysis that included the effect of system imperfections was performed for the BER performance of a CCI canceling CDMA diversity combining RAKE

receiver in a frequency selective slow Rayleigh fading indoor channel (Chapter 5). It is concluded from the numerical results that a spectral efficiency of 0.5 bits/sec/Hz at BER of 10^{-6} is possible under perfect conditions, with one stage of CCI regeneration and cancellation. This implies that there is considerable saving of hardware compared to the use of a CCI canceling correlator receiver. It is also shown that the performance of these receivers degrades significantly when the variance of the normalized received power is above 2 dB, or the mean square of normalized error in path amplitude and phase estimate is above 0.01 or the standard deviation of the normalized code phase error is above 0.1. For CCI cancellation to be effective, channel and spreading code phase estimation have to be repeated after each canceler stage when a combination of these imperfections is present.

5. Simulation programs were developed to verify the analytical results obtained for an indoor CDMA system with correlator and multipath combining RAKE receivers with and without CCI cancellation (Chapter 6). The BER estimate was obtained by employing the Monte Carlo and importance sampling techniques. In the case of BER performance, modeling the CCI using the Gaussian approximation is quite accurate with spreading gain, $N = 31$ and number of users, $K = 3 - 8$. The BER with Gaussian approximation is in reasonable agreement with the simulated BER estimates for lower values of SNR and with a large number of users. However, for BER in the range of 10^{-4} to 10^{-6}, the Gaussian approximation results in an SNR difference of about 1 - 1.5 dB lower

for a given value of BER.

7.2 Contributions of this Research Work

- A new analysis of the effect of combined imperfections in power control, channel estimation and spreading code phase estimation on the BER performance of correlator and diversity combining RAKE receiver has been developed.

- The effect of system imperfections on the BER performance of CDMA receivers in a frequency selective Rayleigh fading channel has been simulated.

- A new analysis for the BER performance of the parallel pre-correlation CCI canceling CDMA correlator receiver has been developed. The effect of combined imperfections in power control, channel estimation and spreading code phase estimation on the BER performance of CCI canceling CDMA correlator and diversity combining receiver has also been theoretically analyzed.

- A new strategy for the application of importance sampling to simulate indoor CDMA system has been proposed. Confidence in the new strategy has been established by extensive indoor CDMA system simulations.

7.3 Future Work

The analytical work reported in this thesis uses a Gaussian distribution to model estimate errors. A challenging extension to this analysis is to consider specific schemes for channel estimation and spreading code phase estimation in an indoor channel and to evaluate the distribution of the error in estimates and to use these

distributions to analyze the BER performance of CCI canceling receivers. From the work reported in this thesis. it is seen that CCI regeneration and cancellation can result in substantial increase in system capacity. Because of the complexity of such receivers. their use in a base station is more practical. Many of the subsystems required for this kind of receivers can be shared by different user receivers at the base station. Developing receiver architecture that time shares various subsystems. thereby reducing complexity, seems to be a challenging area that requires further work. Developing precise signal processing techniques for channel estimation and spreading code phase estimation is another major hurdle to be overcome before the capacity improvements with CCI cancellation can be realized. A trade off study among complexity - performance - capacity issues is necessary before deployment of such receivers in future personal communication systems.

References

[1] R. Schneiderman, *Wireless Personal Communications*, IEEE Press, Piscataway, New Jersey, 1994.

[2] J. Williamson, " The Wireless Industry erupts worldwide," *Telephony*, August 1992, pp. 26-32.

[3] T.S. Rappaport, "Indoor radio communications for factories of the future," *IEEE Commun. Magazine.*, Vol. 27, No.5, May 1989, pp. 15-24.

[4] D.L. Schilling, L.B. Milstein, R.L. Pickholtz, M. Kullback, and F. Miller, " Spread spectrum for commercial communications," *IEEE Commun. Magazine.*, Vol. 29, No.4, April 1991, pp. 66-79.

[5] K.S. Gilhousen, I.M. Jacobs, R. Padovani, A. Viterbi, L.A. Weaver, Jr., and C.E. Wheatley III, " On the capacity of a cellular CDMA system," *IEEE Trans. Veh. Technol.*, Vol. 40, No.2, May 1991, pp. 303-312.

[6] E.A Geraniotis, and M.B Pursley, "Performance of noncoherent direct sequence spread spectrum communication over specular multipath fading channels," *IEEE Trans. Commun.*, Vol. COM-34, No.3, March 1986, pp. 219-226.

[7] G.L. Turin, " Introduction to spread spectrum antimultipath techniques and their application to urban digital radio," *Proc. IEEE*, Vol. 68, March 1980, pp. 328-353.

[8] W.C.Y Lee, " Overview of cellular CDMA," *IEEE Trans. Veh. Technolo.*, Vol. 40, No.2, May 1991, pp. 291-301.

[9] Qualcomm Inc., "Proposed EIA/TIA wide-band spread spectrum standard".

[10] A.J. Viterbi, and R. Padovani, " Implications of mobile cellular CDMA," *IEEE Commun. Magazine*, Vol. 30, No.12, December 1992, pp. 38-41.

[11] R. Gold, "Optimal binary sequences for spread spectrum multiplexing," *IEEE Trans. on Inform. Theory*, Vol. IT-13, October 1967, pp. 619-621.

[12] T. Kasami, "Weight distribution of Bose-Chaudhuri-Hocquenghem codes," *Combinatorial Mathematics and its applications*, University of North Carolina Press, 1969.

[13] M.B. Pursley, "Performance Evaluation for Phase-Coded Spread Spectrum Multiple Access Communication - Part I: System Analysis," *IEEE Trans. Commun.*, Vol. COM-25, No.8, August 1977, pp. 795-799.

[14] D.V. Sarwate, and M.B. Pursley, " Performance Evaluation for Phase-Coded Spread Spectrum Multiple Access Communication - Part II: Code Sequence Analysis," *IEEE Trans. Commun.*, Vol. COM-25, No.8, August 1977, pp. 800-803.

[15] G.L. Turin, " The effect of multipath and fading on the performance of direct-sequence, CDMA systems," *IEEE Journal on Selected Areas in Commun.*, Vol. SAC-68, No.4, July 1984, pp. 597-603.

[16] J.S. Lehnert, and M.B. Pursley, "Error probabilities for binary direct-sequence spread-spectrum communications with random signature sequences," *IEEE Trans. Commun.*, Vol. COM-35, No.1, January 1987, pp. 87-98.

[17] J.S. Lehnert, and M.B. Pursley, "Multipath diversity reception of spread-spectrum multiple-access communications," *IEEE Trans. Commun.*, Vol. COM-35, No.11, November 1987, pp. 1189-1198.

[18] M. Chase, and K. Pahlavan, "Direct sequence spread spectrum over measured indoor radio channels," *IEICE Trans. on Commun.*, Vol. E76-B. No.8 August 1993, pp. 835-840.

[19] R.S. Mowbray, R.D. Pringle, and P.M. Grant, "Increased CDMA system capacity through adaptive cochannel Interference regeneration and cancellation," *IEE Proceedings-I*, Vol. 139, No.5, October 1992, pp. 515-524.

[20] C.Y. Yoon, R. Kohno, and H. Imai, "A Spread-Spectrum Multiaccess System with Co-channel Interference Cancellation for Multipath Fading Channels," *IEEE Journal on Selected Areas in Commun.*, Vol. 11, No. 7, September 1993, pp. 1067-1075.

[21] A. Kaul, and B.D. Woerner, "Analytic limits on performance of adaptive multistage interference cancellation for CDMA," *Electronic Letters*, Vol. 30, No.25, December 1994, pp. 2093-2095.

[22] P. Patel, and J. Holtzman, "Analysis of a Simple Successive Interference Cancellation in a DS/CDMA System," *IEEE Journal on Selected Areas in Commun.*, Vol. 12, No.5, June 1994, pp. 796-807.

[23] M. Everbring, B. Gudmundson, G. Larson, and P. Teder, "CDMA with Interference Cancellation : A Technique for High Capacity Wireless Systems," *Proceedings of ICC'93*, May 23-26, Geneva, Switzerland, pp. 1901-1906.

[24] R. Kohno, C.Y. Yoon, and H. Imai, "Cascaded Co-Channel Interference Cancelling and Diversity Combining for Spread-Spectrum Multi-access over Multipath Fading Channels," *IEICE Trans. on Commun.*, Vol. E76-B. No.2 February 1993, pp. 163-168.

[25] M.C. Jeruchim, "Techniques for estimating the bit error rate in the simulation of digital communication systems," *IEEE Journal on Selected Areas in Commun.*, Vol. SAC-2, No.1, January 1984, pp. 153-170

[26] W.H. Tranter, and K.L. Kosbar, " Simulation of communication systems," *IEEE Commun. Magazine*, Vol. 32, No.7, July 1994, pp. 26-35.

[27] K.S. Shanmugam, and P. Balban, " A modified Monte-Carlo simulation technique for the evaluation of error rate in digital communication systems," *IEEE Trans. on Commun.*, Vol. COM-28, No.11, November 1980, pp. 1916-1924.

[28] D. Lu, and K. Yao, "Improved importance sampling technique for efficient simulation of digital communication systems," *IEEE Journal on Selected Areas in Commun.*, Vol. 6, No.1, January 1988, pp. 67-75

[29] P.M. Hahn, and M.C. Jeruchim, "Developments in the theory and application of importance sampling," *IEEE Trans. on Commun.*, Vol. COM-35, No.7, July 1987, pp. 706-714.

[30] B.D. Woerner, J.H. Reed, and T.S. Rappaport, "Simulation issues for future wireless modems," *IEEE Commun. Magazine*, Vol. 32, No.7, July 1994, pp. 42-53.

[31] H.S. Misser, A. Kegel, and R. Prasad, "Monte Carlo simulation of direct sequence spread spectrum for indoor radio communication in a Rician fading channel," *IEE Proceedings-I*,Vol. 139, No. 6, December 1992, pp. 620-624.

[32] R.E. Ziemer, and R.L. Peterson, *Digital Communication and Spread Spectrum Systems*, Macmillan Publishing Company, New York, 1985.

[33] G.R. Cooper, and C.D. McGillem, *Modern Communications and Spread Spectrum*, MacGraw-Hill Book Company,1986.

[34] M.K. Simon, J.K. Omura, R.A. Scholtz, and B.K. Levitt, *Spread Spectrum Communications*, Vol. I, II, and III, Computer Press, Maryland, U.S.,1985.

[35] R.L. Pickholtz, D.L. Schilling, and L.B. Milstein,"Theory of spread spectrum communication - A Tutorial," *IEEE Trans. on Commun.* Vol. COM-30, No.5, May 1982, pp. 855-884.

[36] B. Sklar, *Digital Communication fundamentals and Applications* , Prentice-Hill, Englewood cliffs, New Jersey 1988.

[37] F.J. MacWilliams, and N.J.A. Sloane, "Pseudorandom sequences and arrays," *Proceedings of IEEE* , Vol. 64, No.12, December 1976, pp. 1715-1729.

[38] L.R Welch, "Lower bounds on the maximum cross-correlation of signals," *IEEE Trans. on Inform. Theory.*, Vol. IT-30, May 1974, pp. 397-399.

[39] M.B. Pursley, and H.F.A. Roefs, "Numerical evaluation of correlation parameters for optimal phases of binary shift register sequences," *IEEE Trans. Commun.*, Vol. COM-27, No.10, October 1979, pp. 1597-1604.

[40] H. Hashemi, "The indoor radio propagation channel," *Proceedings of IEEE*, Vol. 81, No.7, July 1993, pp. 943-967.

[41] H. Hashemi, "Impulse response modeling of indoor radio propagation channels," *IEEE Journal on Selected Areas in Commun.*, Vol. 11, Vo.7, September 1993, pp. 967-977.

[42] R.J.C. Bultitude, "Measurement, characterization and modeling of indoor 800/900 MHz radio channels for digital communications," *IEEE Commun. Magazine*, Vol. 25, No.6, June 1987, pp. 5-12.

[43] R.J.C. Bultitude, S.A. Mahmoud, and W.A. Sullivan, "A comparison of indoor radio propagation characteristics at 910 MHz and 1.75 GHz," *IEEE Journal on Selected Areas in Commun.*, Vol.SAC-7, No.1, January 1989, pp. 20-30.

[44] D.M.J. Devasirvatham, "Multipath time delay spread in digital portable radio environment," *IEEE Commun. Magazine*, Vol. 25, No.6, June 1987, pp. 13-21.

[45] T.S. Rappaport, and C.D. McGillem, "UHF fading in factories," *IEEE Journal on Selected Areas in Commun.*, Vol. SAC-7, No.1, January 1987, pp. 40-48.

[46] S.E. Alexander, "Radio propagation within buildings at 900MHz," *Electronics Letters*, Vol. 18, No.21, October 1982, pp. 913-914.

[47] R. Ganesh, and K. Pahlavan, "Statistical modeling and computer simulation of indoor radio channel," *IEE Proceedings-I*, Vol. 138, No.3, June 1991, pp. 153-161.

[48] P. Yegani, and C.D. McGillem, "A statistical model for the factory radio channel," *IEEE Trans. Commun.*, Vol. COM-39, October 1991, pp. 1445-1453.

[49] A.A.M. Saleh, and R.A. Valenzuela, "A Statistical Model for Indoor Multipath Propagation," *IEEE Journal on Selected Areas in Commun.*, Vol. SAC-5, No.2, February 1987, pp. 128-137.

[50] J.G. Proakis, *Digital Communications*, McGraw-Hill, NewYork, 1989.

[51] P. Jung, P.W. Baier, and A. Steil, "Advantages of CDMA and Spread Spectrum Techniques over FDMA and TDMA in Cellular Mobile Radio Applications," *IEEE Trans. Veh. Technol.*, Vol. 42, No.3, August 1993, pp. 357-364.

[52] H. Xiang, "Binary code division multiple access systems operating in multipath fading, noisy channels," *IEEE Trans. Commun.*, Vol. COM-33, No.8, August 1985, pp. 775-784.

[53] J.S. Lehnert, "An efficient technique for evaluating direct sequence spread spectrum multiple-access communications," *IEEE Trans. Commun.*, Vol. 37, No.8, August 1989, pp. 851-858.

[54] R.K. Morrow, and J.S. Lehnert, "Bit-to-bit error dependence in slotted DS/SSMA packet systems with random signature sequences," *IEEE Trans. Commun.*, Vol. 37, No.10, October 1989, pp. 1052-1061.

[55] J.S. Holtzman, "A simple accurate method to calculate spread-spectrum multiple access error probabilities," *IEEE Trans. Commun.*, Vol. 40, No.3, March 1992, pp. 461-464.

[56] C. Kchao, and G.L. Stuber, "Analysis of a direct-sequence spread spectrum cellular radio system," *IEEE Trans. Commun.*, Vol. 41, No.10, October 1993, pp. 1507-1516.

[57] D.C. Cox, "Universal digital portable radio communications," *Proceedings of IEEE*, Vol. 75, No.4, April 1987, pp. 436-477.

[58] L.B. Milstein, T.S. Rappaport, and R. Barghouti, "Performance evaluation of CDMA," *IEEE Journal on Selected Areas in Commun.*, Vol. 10, No.9, May 1992, pp. 680-689.

[59] C.L Weber, G.K Huth, and B.H Batson, "Performance considerations of CDMA systems," *IEEE Trans. Veh. Technol.*, Vol. VT-30, No.1, February 1981, pp. 3-9.

[60] F. Simpson, and J.M. Holtzman, "Direct-sequence CDMA power control, interleaving and coding" *IEEE Journal on Selected Areas in Commun.*, Vol. 11, No.7, September 1993, pp. 1085-1095.

[61] A.J. Viterbi, A.M. Viterbi, and E. Zehavi, "Performance of power controlled wide-band terrestrial digital communication," *IEEE Trans. Commun.*, Vol. 41, No.4, April 1993, pp. 559-569.

[62] D.V. Sarwate, and M.B. Pursley, "Cross correlation properties of pseudo-random and related sequences," *Proceedings of IEEE* , Vol. 68, No.5, May 1980, pp. 593-619.

[63] H. Kaufmann, R. King, and U. Fawar, "Digital spread spectrum multipath diversity receiver for indoor communications, " *Proceedings of IEEE Veh. Techno. Conference, VT'92* Denver, May 1992, pp. 1038-1041.

[64] A. Paupolis, *Probability, Random Variables, and Stochastic Processes*, McGraw-Hill Inc., NewYork, 1991.

[65] A.S. Mekkoth, S. Kumar, and E.J. Salt, " Effect of PN-code acquisition on the capacity of an indoor direct sequence spread spectrum system," *Proceedings of WIRELES-94*, Calgary, July 1994, Vol. 2, pp. 597-605

[66] Y. Sanada, A. Kajiwara, and M. Nakagawa, " Adaptive RAKE receiver for mobile communications," *IEICE Trans. on Commun.*,Vol. E76-B, No.8, August 1993, pp. 1002-1007.